The University of Southern Mississippi

## The Aquila Digital Community

Dissertations

Fall 12-2009

# Investigation of Novel Thiol "Click" Reactions

Justin William Chan
*University of Southern Mississippi*

Follow this and additional works at: https://aquila.usm.edu/dissertations

Part of the Materials Chemistry Commons, and the Polymer Chemistry Commons

### Recommended Citation

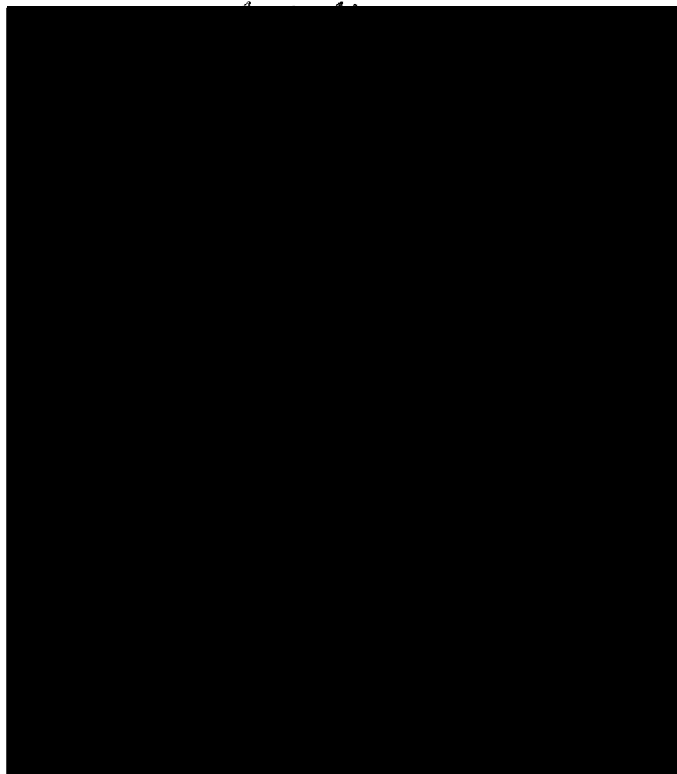The University of Southern Mississippi


INVESTIGATION OF NOVEL THIOL "CLICK" REACTIONS


by

Justin William Chan


A Dissertation
Submitted to the Graduate School
of The University of Southern Mississippi
in Partial Fulfillment of the Requirements
for the Degree of Doctor of Philosophy


Approved:


December 2009

The University of Southern Mississippi

# INVESTIGATION OF NOVEL THIOL "CLICK" REACTIONS

by

Justin William Chan

Abstract of a Dissertation
Submitted to the Graduate School
of The University of Southern Mississippi
in Partial Fulfillment of the Requirements
for the Degree of Doctor of Philosophy

December 2009

ABSTRACT

INVESTIGATION OF NOVEL THIOL "CLICK" REACTIONS

by Justin William Chan

December 2009

The thio-Michael addition reaction is traditionally considered a base catalyzed

reaction which involves high catalyst concentrations and long reaction times. This

reaction utilizes potent, simple nucleophiles to catalyze the reaction, decreases the

catalyst concentration and greatly increases the reaction times. The free radical mediated

thiol-ene click reaction uses light or heat and an initiator to catalyze the rapid and

quantitative addition of thiols to most electron rich enes without the formation of side

products and in the absence of solvent. Recently, the thiol-ene click reaction has been

exploited for these reasons in materials science and organic synthesis. The research

herein describes the nucleophile catalyzed thio-Michael addition to electron poor enes as

a integral reaction in the canon of thiol-ene click reactions. This dissertation includes

chapters of the kinetics and spectroscopic evaluation of the nucleophile catalyzed thio-

Michael addition reaction and resulting products; the use of nucleophile catalyzed thio-

Michael addition for the rapid synthesis of star polymers; and the physical and

mechanical properties of networks prepared with a combination of the photo-cured and

nucleophile cured reactions of multi-acrylates with multi-functional thiols.

This dissertation also discusses the less researched thiol-yne reaction, which

provides the addition of two thiol groups to one alkyne group. Mechanistically, a thiyl

radical adds to an alkyne group creating a very reactive thio vinyl radical, which, in turn,

abstracts a hydrogen from another thiol creating a new thiyl radical. The resulting thio

vinyl group, which shows higher reactivity than the initial alkyne, reacts rapidly with a second thiyl group. Additional chapters in this dissertation will discuss the formation of multi-functional materials (16 > functionality > 8) in a sequential nucleophile catalyzed thio-Michael addition followed by the thiol-yne reaction; the mechanical and physical properties of films prepared with multi-functional alkynes and multi-functional thiols; and the linear relationship of refractive index and sulfur content in polysulfide networks made possible by the thiol-yne reaction.

The first fundamental study discusses a proposed anionic chain mechanism for the nucleophile catalyzed thio-Michael addition to electron poor alkenes. Traditional base catalyzed mechanisms show the deprotonation of the thiol by a weak base such as triethyl amine. Results show that nucleophilic amines, such as hexyl amine, with similar pKa values as the weak bases have faster rates of reaction, indicating that base strength alone is not responsible for the apparent increase in rates. Results demonstrate that the effect of nucleophilicity has a greater role than basicity (pKa) in the rates of reaction. An anionic chain mechanism is proposed involving the initiation of the thio-Michael reaction by an initial attack of a nucleophile onto an electron poor double bond creating a super-strong enolate anion which carries out the subsequent base catalyzed thio-Michael addition.

The second study reports the facile formation of star polymers using the nucleophile catalyzed thio-Michael addition reaction of polymers prepared by reversible addition-fragmentation chain transfer (RAFT) polymerization and a tri-acrylate monomer. The nucleophilic catalyst employed for the thio-Michael addition reaction has shown to have a dual purpose: to catalyze the Michael addition and to prevent the disulfide formation commonly seen in the reduction step of the RAFT end group.

Acrylates are commonly used for the preparation of polymer networks due to their wide commercial availability, tunable mechanical properties, and sensitivity to photopolymerization. Photo-cured multi-acrylate systems produce films with inhomogeneous micro-structures leading to broad glass transition temperatures ($T_g$). Incorporation of thiols into these systems narrows the $T_g$s but quantitative addition (1 to 1) of thiol to acrylate does not occur due to the competitive acrylate homopolymerization. The nucleophile catalyzed thio-Michael addition reaction promotes the quantitative addition of thiols to acrylates resulting in very narrow $T_g$s. The third study discusses the use of sequential thio-Michael reaction followed by the photo-cured reaction. This process allows tunability of mechanical and physical properties of resulting films.

In the fourth study, the nucleophile catalyzed thio-Michael addition reaction is used for preparation of multi-functional alkynes. Alkynes, like alkenes, react rapidly and quantitatively with thiols in a photocured system in a 1:2 ratio. A series of poly-functional branched materials was prepared by clicking two thiol groups to one terminal alkyne proceeded quantitatively, in the absence of solvent, rapidly and with no evidence of side products.

The fifth study demonstrates the preparation of a series of multi-functional alkyne monomers (f=4,6,8) that were subsequently photopolymerized with a series of multi-functional thiols (f=2,3,4). Mechanical and physical properties showed an increasing correlation between gel point and functionality. Additionally, this study demonstrated the utility of tailoring the $T_g$ values by increasing the functionality of starting monomers.

High sulfur content materials have shown to have high refractive index values. In the final study, networks were prepared from commercially available dialkyne and dithiols, consisting only of sulfur and hydrocarbon. Sulfur content in some films reached

nearly 50% and, as a result, refractive index values were determined to be greater than

1.65. Data from this study shows a linear relationship between the weight% sulfur and

the refractive index in sulfur containing crosslinked hydrocarbon networks.

# DEDICATION

To a great mentor and scientist, Professor Charles E. Hoyle (1948-2009).

This work is dedicated to him and those who embody and embrace his ethics in the lab

and morals in life.


To my wife.


AMDG

# ACKNOWLEDGEMENTS

# TABLE OF CONTENTS

          Abstract
          Introduction
          Experimental
          Results and Discussion
          Summary and Conclusions
          References

          Abstract
          Introduction
          Experimental
          Results and Discussion
          Summary and Conclusions
          Acknowledgments
          References

LIST OF CHARTS AND SCHEMES

Chart

Scheme

# LIST OF ILLUSTRATIONS

CHAPTER I

INTRODUCTION

Photopolymerization is a synthetic method that converts low molecular weight

monomers into high molecular weight polymers or polymeric networks via a light

induced chain reaction. Some typical advantages to this technique are rapid cure rate,

low VOC emissions, spatial and temporal control of polymerization, and versatility of

applications.[1-2] Some of these applications include protective coatings, adhesives,

inks, electronics, and optical materials.[3-4] A typical photopolymerization formulation

may have monomers, photoinitiators (free radical or cationic), oligomers,

prepolymers, and viscosity modifiers. Understanding the role of each component

within a formulation allows for tailoring of end use properties such as adhesion,

flexibility, surface hardness, weatherability, solvent resistance, and abrasion

resistance.[1,5] Additionally, the source, intensity, wavelength, and dose of light

determine the rate of polymerization which can affect final film properties.

Acrylates and methacrylates are widely used due to their reactivity to UV

light, multifunctionality, cost, and versatility, i.e. increasing formulation viscosity can

be achieved by increasing monomer functionality. Additionally the UV cured film

properties of photopolymerized acrylates can be easily tuned by varying amounts of

multi-functional components.[6] **Scheme 1.1.** illustrates the typical polymerization

scheme of acrylates. An initiator decomposes into radical species by way of some

chemical process (photoinitiator with light or thermal initiator with heat) which can

subsequently initiate polymerization of reactive components in a free radical chain

growth process.

*Initiation*

$$PI \xrightarrow{h\nu} PI^* \longrightarrow P\bullet + I\bullet$$

$$P\bullet + M \longrightarrow P\text{-}M\bullet$$

*Propagation*

$$P\text{-}M\bullet + nM \longrightarrow PM_n\bullet$$

*Termination*

$$PM_n\bullet + PM_m \longrightarrow PM_{n+m}$$
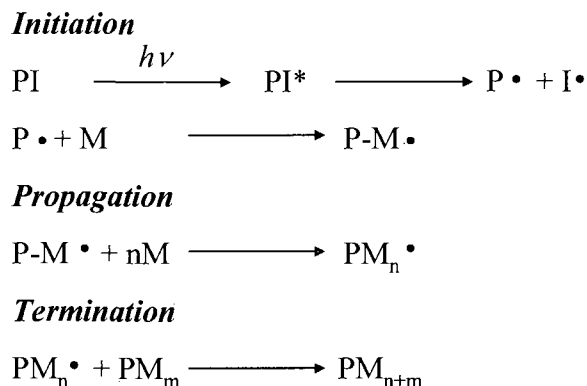
**Scheme 1.1.** Schematic of a traditional chain-growth polymerization mechanism.

In the case of multifunctional acrylates, the ene undergoes this rapid chain growth process to produce highly crosslinked macromolecular materials. The result of this rapid step growth is gelation within the initial stages of conversion which subsequently leads to vitirification and inhomogeneous network formation.[6-12] This inhomogeneity in network structure leads to unreacted acrylate species and broad glass transitions temperatures, which decreases the ability to tune final network structures and, hence, mechanical and physical properties. [11-14] Additionally, systems based on multifunctional acrylates demonstrate inhibition by oxygen and polymerization shrinkage stress.[15,16]

*Thiol-Ene Photopolymerization*

Thiol-ene photopolymerization chemistry utilized the highly useful and efficient addition of thiols across unsaturated carbon-carbon double bonds for network formation, polymer modification, and small molecule synthesis. The basic radical mediated thiol-ene step growth process shows advantages over basic chain growth processes in various synthetic techniques.[1,2,13-19] **Scheme 1.2.** shows the typical reaction mechanism of the addition of thiols to electron rich alkenes. Within

this mechanism, a thiol undergoes a chemical reaction with a photoinitiator in the

presence of UV light to generate a thiyl radical. This thiyl radical adds across an

electron rich double bond forming a carbon centered radical. This carbon centered

radical subsequently abstracts a hydrogen from another thiol generating another thiyl

radical. Because of the inherent behavior of the thiol within these systems, a free

radical step growth reaction occurs.

*Initiation*

R-SH + PI $\xrightarrow{h\nu}$ R-S •

*Propagation*

R-S • + [alkene with R'] $\longrightarrow$ [RS—CH₂—CH•—R']

*Chain Transfer*

[RS—CH₂—CH•—R'] + R-SH $\longrightarrow$ [RS—CH₂—CH(H)—R'] + R-S •
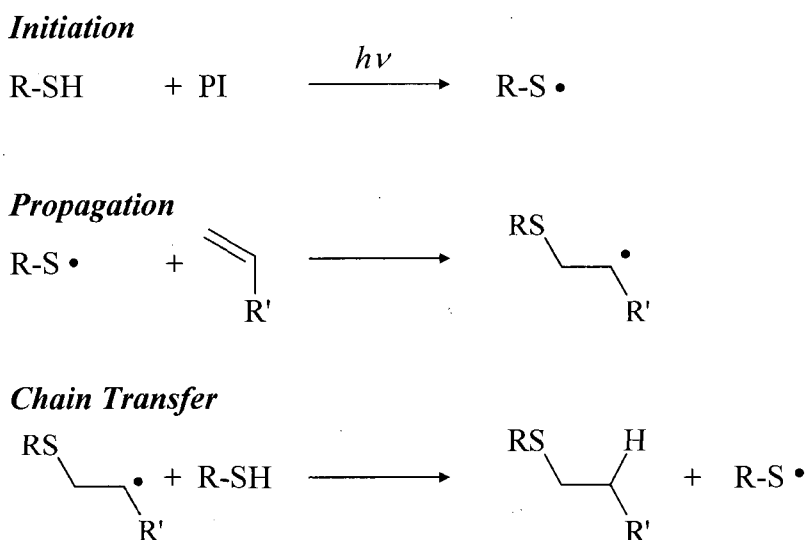
**Scheme 1.2.** Schematic of the typical radical mediated thiol-ene photoinitiated reaction.

The addition of thiols to unsaturated carbon-carbon bonds is a well known

reaction and has been studied for over 100 years.[28] Interest in the thiol-ene

mechanism for photocuring and other free radical reactions was developed later at

W.R. Grace by Morgan, Ketley, and coworkers.[17,29-34] Within this work, most of the

fundamental knowledge of thiol-ene systems as evaluated, which laid the foundation

for future research. For example, kinetic rate constants for the addition of various

thiols to unsaturated carbon-carbon bonds were established.[17] The use of thiol-ene

systems was overshadowed in the 1970's with the increasing usage of more cost

effective acrylate systems that exhibited excellent physical and mechanical properties. However the work established at W.R. Grace culminated in a resurgence within the last decade. This work has highlighted the physical and mechanical properties of model thiol-ene systems, yielded rates of polymerization in various conditions, and demonstrated the unequivocal control over network structure in most thiol-ene networks. **Figure 1.1.** illustrates typical electron rich carbon-carbon double bonds that have been employed in reactions within photoinitiated thiol-ene systems, whereby, the rate of addition of a given thiol across an electron rich carbon-carbon double bond is determined by the electron density of the carbon-carbon double bond.[17,30]
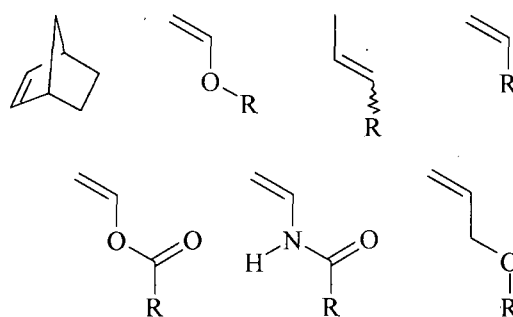
**Figure 1.1.** Structures of typical electron rich enes used in thiol-ene photopolymerized systems.

Recently the thiol-ene reaction has been exploited for its efficient utility and has been termed a "click" reaction.[35-38] The term "click" was coined by Sharpless and coworkers in 2001 and is applied to a list of chemical reactions that obey certain criteria:[39]

1) be modular,

2) be wide in scope,

3) give very high yields,

4) generate only inoffensive byproducts that can be removed by non chromatographic methods,

5) and be stereospecific (but not necessarily enantio-selective).

Sharpless and coworkers required that the reactions have simple reaction conditions, be not sensitive to oxygen and water, use readily available starting materials, use benign solvent or no solvent, and be isolatable by non-chromatographic methods. Some common examples of typical "click" reactions are cycloadditions of unsaturated species, including the Diels Alder reactions; nucleophilic substitution reactions, such as ring opening reactions of strained electrophilic heterocycles; non-aldol type carbonyl chemistry, including formation of thioureas, ureas, and aromatic heterocycles; and additions to carbon-carbon multiple bonds including Michael additions with Nu-H reactants.

The typical radical mediated reaction of thiols to electron rich alkenes exhibits the five main criteria, as well as, the other requirements, which makes this reaction exceptional for materials, polymer, and small molecule modification. In particular, most small molecule thiols do not have a high propensity for hydrogen bonding and are low viscosity liquids at room temperature, which reduces the need for solvents in many systems. In addition, many functionalized thiols and enes are widely commercially available and both classes of compounded show good stability over time. And finally, since many thiol-ene systems do not require the use of photoinitiator, reactions can proceed very simply under facile conditions; thiol-ene click reactions are initiated just by placing in UV light and, depending on light intensity and sample thickness, mainly, the reactions proceed to quantitative conversions within seconds.

Killops and coworkers report the preparation of dendrimers conveniently using the thiol-ene click reaction.[37] Triallyl triazine trione (trifunctional alkene) was reacted with thioglycerol to produce a 6 functional alcohol that subsequently was reacted in a transesterification reaction to produce a 6 functional alkene, which was then reacted with thioglycerol to produce a 12 functional alcohol. By alternating thiol-ene "click" and transesterification steps, a 48 functional alcohol was prepared at greater than 90% yields isolated in one simple precipitation step.

Networks can be prepared from a multifunctional thiol and multifunctional electron rich ene if one or both of the multifunctional monomers has a functionality greater than 2. Within these systems, thiols react with electron rich alkenes rapidly to produce highly crosslinked uniform networks.[17] Network formation of these systems exhibits a delay in gelation due to the apparent step growth mechanism, shown in **Scheme 1.2.**, which usually obey the predicted gel point equation:

$$p_c = \sqrt{\frac{1}{r(1 - f_1)(1 - f_2)}}$$

where r is the molar ratio of component 1 to component 2, here thiol and ene; $p_c$ is the gel point, and $f_1$ is the functionality of the alkene and $f_2$ is the functionality of the thiol. [15-17, 21-23] In some cases, however, when the functionality of component 1 or component 2 is greater than 4, which is not uncommon in typical thiol-ene formulations, systems do not obey the gel point theory. Further discussion of this topic will be addressed in Chapter VII.

In comparison to photopolymerized multifunctional acrylate systems, thiol-enes have some desirable advantages. Atmospheric oxygen does not inhibit the photopolymerization of thiol-ene networks.[25-27] In a thiol-ene system, a peroxy radical produced from atmospheric oxygen can easily undergo a chain transfer reaction with a thiol to produce a thiyl radical, nearly unaffecting the rate of the thiol-ene polymerization. Also, networks can form with a decrease in network stress build-up due to the unique kinetics of thiol-ene systems.[17,24] And finally, thiol-ene networks, prepared with multifunctional electron rich enes produce uniform, highly dense networks characterized by narrow glass transition temperatures, $T_g$, in particular narrow full width half maximum (FWHM) values by dynamic mechanical analysis (DMA).

Crosslinked multifunctional acrylate systems exhibit broad $T_g$s that can span over 100°C above and below room temperature. This feature can be desirable for many applications; however in tailoring systems for transitions for exact application temperatures, $T_g$s of crosslinked multifunctional acrylate systems can be difficult to tune. Reports of thiol-ene/acrylate systems demonstrate the broadening of $T_g$s due to the incorporation of photopolymerized multi-functional acrylates within a thiol-ene system.[13,14] As the amount of thiol-ene/acrylate ratio decreased, the $T_g$s of resulting networks increased and broadened demonstrating the loss of homogeneity. This is a result of the inhomogeneous formation of the acrylate networks. Many crosslinked multifunction acrylate systems have been shown to form areas of high crosslink density in early stages of polymerization, followed by gelation and vitrification at very low conversions of double bond.[6,7]

*Thio-Michael Addition*

The thio-Michael addition reaction is employed for the addition of thiols with electron deficient carbon-carbon double bonds.[17,41-59] Some examples of species containing electron deficient carbon-carbon double bonds are illustrated in **Figure 1.2.** The thio-Michael addition reaction is just one example of the many types of conjugate addition reactions that have been utilized for centuries as a useful and efficient synthetic tool. The Michael addition reaction refers to the addition of a nucleophile, or a Michael donor, across an activated (electron deficient) carbon-carbon multiple bond, or a Michael acceptor.[41-43] Traditionally, the Michael donor is an enolate, in the classical Michael reaction, alcohol, in the oxa-Michael reaction, amine, in the aza-Michael reaction, or a thiol, in the thio-Michael reaction.[41-43] Sir Arthur Michael discovered the classical addition of acetoacetate to methyl methacrylate in the late 1800's. Since then many have investigated this powerful tool for the preparation of small molecules, polymers, and, recently, polymeric networks for a wide range of applications.
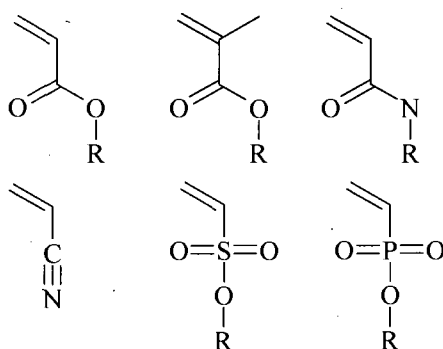


**Figure 1.2.** Structures of typical electron deficient enes used in thio-Michael addition reactions.

The thio-Michael addition reaction has been well investigated for its potential applications in many sulfur rich biological systems. There are many examples of the *base catalyzed* thio-Michael addition.[28,43-53] The reaction mechanism is shown in **Scheme 1.3.** This mechanism illustrates the formation of the thiolate anion in the thermodynamically controlled deprotonation of a thiol by a base, (B). Typically, tertiary amines are employed to deprotonate the thiol and catalyst quantities can be as high as 20 wt%.[44,51] Upon deprotonation of the thiol acid, the thiolate nucleophile attacks the electron poor double bond resulting in the formation of an enolate intermediate, see **Scheme 1.3.** The resulting enolate, then, abstracts a proton; however, few researchers agree on the source of that proton. If the reaction is carried out in a polar protic solvent, such as water or an alcohol, many hypothesize that the well solvated conjugate base (of the base catalyst) quickly donates a proton to the highly reactive enolate ($pK_a = \sim 25$) and the base catalyst is regenerated to initiate another propagation reaction. If the reaction is carried out in an aprotic solvent, the ion pair is well shielded and the thiolate has been hypothesized to attack as part of an ion pair.[52,53]

Interestingly, simple nucleophilic catalysts have been shown to catalyze the thio-Michael reaction with exceptional rates and decreased catalyst concentrations producing quantitative yields.[54-59] Others have demonstrated the efficiency of nucleophilic catalysis in the carbon and oxa- Michael additions, as well.[60-62] The reaction proceeds in an anion chain mechanism, shown in **Scheme 1.4,** whereby a strong nucleophile, such as a tertiary phosphine or primary amine, initially attacks an electron deficient carbon-carbon double bond forming a strong enolate base.

*Initiation*



*Propagation (polar solvent)*
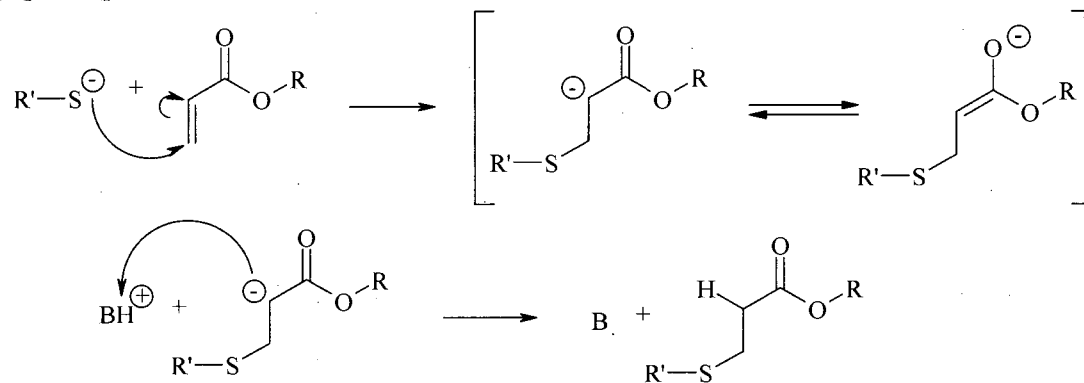


*Propagation (non-polar solvent)*
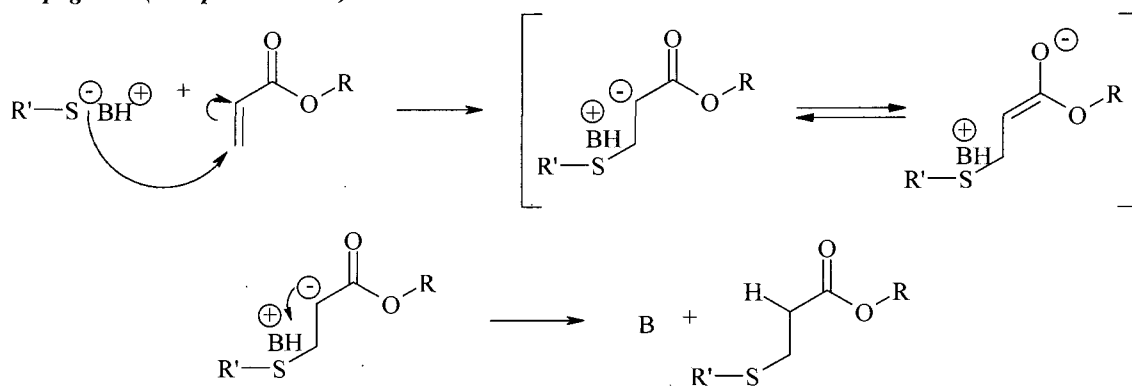


**Scheme 1.3.** Schematic of the base catalyzed thio-Michael addition reaction.

Subsequently, the enolate base deprotonates a thiol and forms a thiolate anion that propagates the thio-Michael reaction. Chapter III discusses the differences in mechanisms between the base and nucleophile catalyzed thio-Michael reactions in greater detail.

*Initiation*
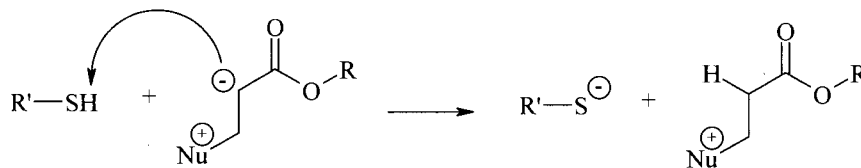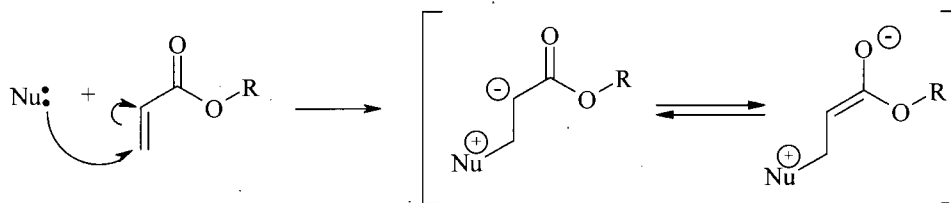


*Propagation*
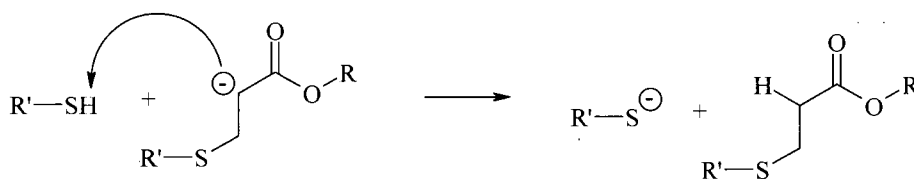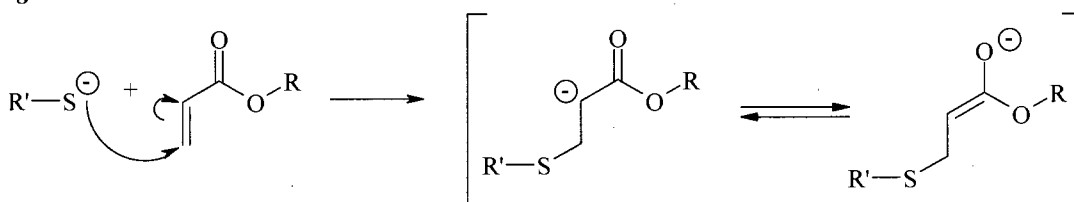


**Scheme 1.4.** Proposed nucleophile catalyzed thio-Michael addition reaction.

*Radical-Mediated Thiol-yne Reaction*

It has been reported in the past that small molecule monofunctional thiols in solution undergo a two-step sequential reaction with alkynes producing dithioethers in high yields.[17,63,64] These reports, reported over 50 years ago, are unclear of the kinetics and yields produced under the conditions employed.[63-65] The reaction mechanism is similar to that of the thiol-ene reaction. **Scheme 1.5.** illustrates the highly efficient thiol-yne reaction mechanism. In the photoinitiation step, a thiyl radical is produced, which adds across a terminal electron rich carbon-carbon triple

bond. Subsequently, a thio-vinyl ether carbon centered radical is formed which

undergoes chain transfer with another thiol group to form the thio vinyl ether.

Another thiyl radical formed in either the initiation step or a chain transfer step adds

across the thio vinyl ether group forming a carbon centered radical. This radical then

undergoes a chain transfer step to produce the 1,2-dithioether. Some reports have

shown that formation of the mono-addition product or the 1,1-dithioether is possible

in cases where either phenylacetylene or benzene thiol are the starting reagents.[17,28]

**Initiation**

$$R\text{—}SH \quad + \quad PI \quad \xrightarrow{\ hv\ } \quad R\text{—}S\bullet$$

**Propagation I**



**Chain Transfer I**



**Propagation II**



**Chain Transfer II**
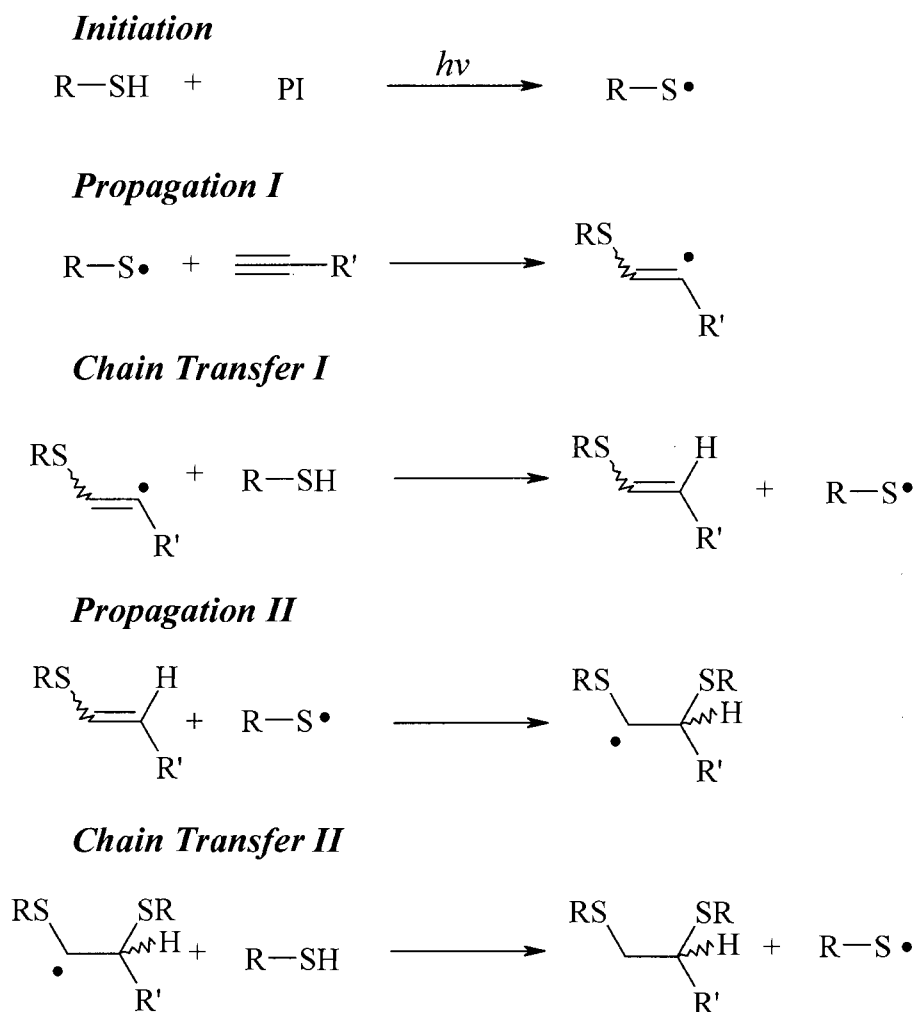


**Scheme 1.5.** Schematic of the radical-mediated thiol-yne photoinitiated reaction.

Few reports have demonstrated the thiol-yne reaction for the preparation of novel materials.[54,58,66,67] Fairbanks and coworkers recently showed that a tetrafunctional thiol readily polymerizes with dialkynes via a radical mediated step growth process nearly identical to that for traditional thiol-enes.[66] The reaction was reported to proceed at fast rates under ambient conditions to high conversion of both thiol and alkyne. Additionally, in this study it was reported that using alkynes in place of alkenes with the reaction of thiols, the $T_g$ of resulting networks was considerably higher (accompanied by broader FWHM values) for the networks prepared with alkynes. Also in this report, Fairbanks reported that the addition of a thiol to an alkyne was considerably slower than the addition of a thiol with the subsequently formed thio-vinyl ether, by a factor of 1/3.

*Summary*

Photopolymerization via a light induced chain reaction process is an efficient method of preparing polymeric networks, as well as, other general chemical modifications. Monomers containing acrylate moieties are widely used due to their reactivity to UV light, availability, cost, and versatility. In the case of multifunctional acrylates, the acrylate moiety undergoes a rapid chain growth process to produce highly crosslinked macromolecular materials, exhibiting broad glass transition temperatures, reaction inhibition to oxygen, and vitrification at low conversion of functional groups, which can change network properties over time. Photopolymerized thiol-ene systems utilize a highly efficient reaction in which thiols react across unsaturated carbon-carbon double bonds for network formation, polymer modification, and small molecule synthesis.

The addition of thiols to unsaturated carbon-carbon bonds is a well known reaction and has been investigated for nearly a century. However, recently the thiol-ene reaction has been canonized in the "click" chemistry list of reaction noting its vast utility, application, and exceptional efficiency. The radical mediated reaction of thiols to electron rich alkenes follows the general criteria as a "click" reaction, making it exceptional for small molecule modification, materials, and polymeric thiol-ene networks. Thiol-ene networks are prepared through the reaction of multifunctional thiols and multifunctional electron rich enes, given that one or both of the monomers has functionality greater than 2. Thiol-ene networks have some considerable advantages over photopolymerized acrylate systems, such as efficiency in the presence of oxygen, delayed gelation, and uniform network, which allows tailorability of physical and mechanical properties. Because of the high reactivity of electron poor carbon-carbon double bonds in radical mediated reactions, competitive reactions between thiol-acrylate, for example, and acrylate-acrylate reactions inhibit the thiol-acrylate reaction from producing quantitative conversion of thiol to ene.

Quantitative conversion of thiol and electron deficient enes can be achieved with the thio-Michael addition reaction given proper reaction conditions. Traditionally, the thio-Michael reaction is base catalyzed and reactions can be sluggish and produce non quantitative yields even in high concentration of base catalyst. Interestingly, simple nucleophiles catalyze the thio-Michael addition reaction with exceptional rates at low catalyst concentrations, and these reactions produce near quantitative yields. Finally, even though there have been literature reports of the radical mediated two step reaction of thiols with alkynes, few have utilized the thiol-yne reaction for the preparation of novel polymeric materials.

References

1. Jacobine, A. F. In *Radiation Curing in Polymer Science and Technology*; Fouassier, J. P., Rabek, J. F., Eds.; Elsevier Applied Science: London, 1993; Vol. III, pp 219–268.

2. Woods, J. G. In *Radiation Curing: Science and Technology*; Pappas, S. P., Ed.; Plenum Press: New York, 1992; pp 333–398.

3. Hoyle, C.E.; Cole, M.; Bachemin, M.; Kuang, W.; Viswanathan, K.; Jonsson, S. ACS Symposium Series **2003**; 847; (Photoinitiated Polymerization): 52-64.

4. Cole M.C.; Bachemin M.; Nguyen, C.K.; Viswanathan, K.; Hoyle, C.E.; Jonsson, S.; Hall, H.K. Experience the World of UV/EB RadTech 2000: The Premier UV/EB Conference & Exhibition Technical Conference Proceedings Baltimore MD, United States Apr 9-12, 2000:211-220.

5. Roffery, C.G. *Photopolymerization of Surface Coatings*. Wiley Interscience: New York, 1982.

6. Kloosterboer, J.G. *Imag. Sci,* **1986**, 30, 177.

7. Kloosterboer, J.G. *Advances in Polymer Science* **1988**, 84, 1.

8. Kloosterboer, J.G.; Van de Hei, G.M.; Boots, H.M. *J. Polym. Commun.* **1984**, 25(12), 354.

9. Roffey, C.G. *Photogeneration of Reactive Species for UV Curing*. John Wiley and Sons: New York, 1997.

10. Bowman, C.N.; Okay, O.; Redy S. *Macromolecules* **2005**; 38: 4501-4511.

11. Bowman, C.N.; Anseth, K.S.; *Chem. Eng. Sci.* **1994**; 48(14): 2207-2217.

12. Peppas N.; et al. *Polym. Bull.* **1993**; 31: 229-233.

13. Senyurt, A.F.; Wei, H.; Phillips, B.; Cole, M.; Nazarenko, S.I.; Hoyle, C.E.; Piland, S.G.; Gould, T.E. *Macromolecules* **2006**, 39(19), 6315-6317.

14. Wei, H.; Senyurt, A.F.; Jonsson, S.; Hoyle, C.E.; *J. Polym. Sci., Part A: Polym. Chem.* **2007**, 45(5), 822-829.

15. Carioscia, J. A.; Lu, H.; Stansbury, J. W.; Bowman, C. N. *Dent. Mater.* **2005**, 21, 1137-1143.

16. Lu, H., Carioscia, J.A.; Stansbury, J.W., Bowman, CN. *Dent. Mater.* **2005**, 21, 1129-1136.

17. Hoyle, C.E.; Lee, T.Y.; Roper, T. *J. Polym. Sci., Part A: Polym. Chem.* **2004**, 42, 5301-5338.

18. Natarajan, L.V.; Shepherd, C.K.; Brandelik, D.M.; Sutherland, R.L.; Chandra, S.; Tondiglia, V.P.; Tomlin, D.; Bunning, T. *J.; Chem. Mater.* **2003**, 15, 2477-2484.

19. Hagberg, E.C.; Malkoch, M.; Ling, Y.; Hawker, C.J.; Carter, K.R. *Nano Lett.* **2007**, 7, 233-237.

20. Jacobine, A.F.; Glaser, D.M.; Grabek, P.J.; Mancini, D.; Masterson, M.; Nakos, S.T.; Rakas. M.A.; Woods, J.G. *J. Appl. Polym. Sci.*, **1992**, 45, 471.

21. Hiemenz Book

22. Odian Book

23. Clark, T.; Kwisnek, L.; Hoyle, C.E.; Nazarenko, S. *J. Polym. Sci., Part A: Polym. Chem.* **2008**, 47(1), 14-24.

24. Kloxin, C.J.; Scott, T.F.; Bowman, C.N. *Macromolecules*, **2009**, 42(7), 2551–2556.

25. Hoyle, C.E.; Hensel, R.D; Grubb, M.B.; *Polym. Photochem.* **1984**, 4, 69.

26. Hoyle, C.E.; Hensel, R.D.; Grubb, M.B. *J. Polym. Sci. Polym. Chem. Ed.* **1984**, 22, 1865.

27. Cramer, N.B.; Scott. J.P.; Bowman, C.N. *Macromolecules* **2002**, 35, 5361.

28. Patai, S. *The Chemistry of the Thiol Group, Parts 1-2*, John Wiley and Sons, Inc., New York, 1974.

29. Morgan, C.R.; Ketley, A.D. *J. Radiat. Cur.* **1980**, 7(10), 7.

30. Morgan, C. R.; Magnotta, F.; Ketley, A. D. *J. Polym. Sci. Polym. Chem. Ed.* **1977**, 15, 627.

31. Gush, D. P.; Ketley, A.D. *Mod. Paint. Coat.* **1978**, 58.

32. Bush, R.W.; Ketley, A.D.; Morgan, C.R.; Whitt, D.G. *J. Radiat. Cur.* **1980**, 20.

33. Morgan, C.R.; Ketley, A.D. *J. Polym. Sci. Polym. Lett. Ed.* **1978**, 16, 75.

34. Morgan, C. R. U.S. Patent 3,784,524, 1974.

35. Dondoni, A. *Angew. Chem. Int. Ed.* **2008**, 47, 2–5.

36. Gress, A.; Volkel, A.; Schlaad, H. *Macromolecules* **2007**, 40, 7928..

37. Killops, K.L.; Campos, L.M.; Hawker C.J. *J. Am. Chem. Soc.* **2008**, 130(15), 5062–5064.

38. Campos, L.M.; Meinel, I.; Guino, R.G.; Schierhorn, M.; Gupta, N.; Stucky, G.D.; Hawker, C.J. *Adv. Mater.* **2008**, 20, 3728–3733.

39. Kolb, H.C.; M. G. Finn, M.G.; Sharpless, K.B. *Angew. Chem. Int. Ed.* **2001**, 40, 2004-2021.

40. Lecamp, L.; Houllier, F.; Youssef, B.; Bunel, C. *Polymer* **2001**, 42, 2727.

41. Bruice, P.Y. *Organic Chemistry, 3$^{rd}$ Ed.*, Prentice Hall, Upper Saddle River, NJ, USA, 2001.

42. Smith, M.B.; March, J. *March's Advanced Organic Chemistry: Reactions, Mechanisms, Structure, 5th Ed.*, John Wiley and Sons, Inc., New York, 2001.

43. Mather, B. D.; Viswanathan, K.; Miller, K.M.; Long, T.E. *Prog. Polym. Sci.* **2006**, 31, 487-531.

44. Kilambi, H.; Stansbury, J.W.; Bowman, C.N. *J. Polym. Sci., Part A: Polym. Chem.* **2008**, 46, 3452–3458.

45. White, J.E. *Ind. Eng. Chem. Prod. Res. Dev.* **1986**, 25, 395-400.

46. Dmuchovsky, B.; Bineyard, B.D.; Zienty, F.B. *J. Am. Chem. Soc.* **1964**, 86, 2874-2877.

47. Li. M.; De, P.; Gondi, S.R; Sumerlin, B.S. *J. Polym. Sci., Part A: Polym. Chem.* **2008**, 46, 5093-5100.

48. Bae, J.W.; Lee, E.; Park, K.M.; Park, K.D. *Macromolecules* **2009**, 42(10), 3437–3442.

49. Menow-Garw, D. *J. Org. Chem.* **1972**, 37(24), 3797-3803.

50. Nebioglu, A.; Leon, J.A.; Khudyakov, I.V. *Ind. Eng. Chem. Res.* **2008**, 47, 2155-2159.

51. Dmuchovsky, B.; Bineyard, B.D.; Zienty, F.B. *J. Am. Chem. Soc.* **1964**, 86, 2874-2877.

52. Ignatov, V.A.; et. al. *Izvestiya Vysshikh Uchebnykh Zavedenii, Khimiya I Khimicheskaya Tekhnologiya* **1980**, 23(11), 1350-1355.

53. Hurd, C.D.; Gershbein, L.L. *J. Am. Chem. Soc.* **1947**, 69, 2328-35.

54. Chan, J.W.; Hoyle, C.E.; Lowe, A.B. *J. Am. Chem. Soc.* **2009**, 131 (16), 5751–5753.

55. Chan, J.W.; Yu, B.; Hoyle, C.E.; Lowe, A.B. *Chem. Commun.* **2008**, 4959-4961.

56. Shin, J.; Matsushima, H.; Chan, J.W.; Hoyle, C.E *Macromolecules* **2009**, 42(9), 3294-3301.

57. Nurmiab, L.; Lindqvistb, J.; Randevb, R.; Syrettb, J.; Haddleton, D.H. *Chem. Commun.* **2009**, 2727-2729.

58. Yu, B.; Chan, J.W.; Hoyle, C.E.; Lowe, A.B. *J. Polym. Sci., Part A: Polym. Chem.* **2009**, 47(14), 3544-3557.

59. Becer, C.R.; Hoogenboom, R.; Schubert, U.S. *Angew. Chem. Int. Ed.* **2009**, 48(27), 4900-4908.

60. Stewart, I.C.; Bergman, R.G.; Toste, F.D. *J. Am. Chem. Soc.* **2003**, 125, 8696-8697.

61. Nising, C.F.; Bräse, S. *Chem. Soc. Rev.* **2008**, 37, 1218–1228.

62. Gimbert, C.; Lumbierres, M.; Marchi, C.; Moreno-Mañas, M.; Sebastián, R.M.; Vallribera, A. *Tetrahedron* **2005,** 61, 8598–8605.

63. Blomquist, A. T.; Wolinsky, J. *J. Org. Chem.* **1958**, *23*, 551.

64. Behringer, H. *Annalen* **1949**, *564*, 219.

65. Griesbaum, *Angew. Chem. Int. Ed.* **1965**, *9*, 273.

66. Fairbanks, B. D.; Scott, T. F.; Kloxin, C. J.; Anseth, K. S.;  Bowman, C. N. *Macromolecules* **2008**, 42, 211.

67. Chan, J.W.; Zhou, H.; Hoyle, C.E.; Lowe, A.B. *Chem. Mater.* **2009**, 21(8), 1579-1585.

# CHAPTER II

## OBJECTIVES

As stated in the Introduction section, it is important to study novel reactions for more efficient methods of preparing materials. This research is focused on the nucleophile catalyzed thio-Michael addition reaction and the thiol-yne reactions to understand the basic chemical synthetic pathways and structure property relationships of various novel polymeric networks. Specifically, the goals of this work are stated below:

1. Elucidate the nucleophile catalyzed thio-Michael addition reaction using various catalysts, thiols, and electron deficient alkenes.

2. Examine the kinetics, mechanical, and physical properties of networks prepared by the controlled incorporation of multi-functional thiols into multi-acrylate networks.

3. Investigate the utility of the nucleophile catalyzed thio-Michael addition reaction in a one-pot synthesis of star polymers.

4. Demonstrate the efficiency of the thiol-alkyne reaction through the preparation of poly-functional materials in a two-step one-pot thio-Michael / thio-yne sequential reaction.

5. Establish the relationship of crosslink density and mechanical properties of thiol-yne systems with monomer of functionality greater than 4.

6. Correlate the effect of sulfur content on refractive index of crosslinked hydrocarbon networks prepared through the thiol-yne reaction.

The first objective will elucidate the mechanism of the nucleophile-catalyzed thio-Michael addition and demonstrates its usefulness as an effective synthetic approach to modifying materials. This reaction will further be utilized in preparing novel materials and increasing the efficiency of modifying polymer structures.

The second objective will investigate the differences of formulations that are cured by either pre-reacting thiol groups into matrices using the nucleophile-catalyzed thio-Michael addition reaction or photocuring the thiols into the matrices. The former matrices are expected to have no unreacted thiols due to the highly efficient nucleophile catalyzed thio-Michael addition reaction; whereas, the latter is expected to have unreacted thiols due to the competing acrylate homopolymerization reaction. Physical and mechanical properties of these matrices will vary and this study will determine those variations.

The third objective will utilize the nucleophile-catalyzed thio-Michael addition reaction for the preparation of star polymers via a convergent approach. This technique will demonstrate the efficiency of the reaction without isolation, purification, and modification of starting materials.

The fourth objective will examine the conditions necessary for preparing materials via the sequential thio-Michael and thiol-yne reactions for the generation of polyfunctional materials.

Finally, the fifth and sixth objectives will demonstrate the high-throughput nature of preparing networks for determining structure property relationships using the thiol-yne reaction. Probing networks prepared with novel monomers of high functionality will demonstrate the dependence of monomer functionality and crosslink density on tuning

mechanical properties. Additionally, the linear relationship between sulfur content and refractive index in highly crosslinked networks will be determine prepared by the thiol-yne reaction.

CHAPTER III

# THE KINETICS OF THE NUCLEOPHILE CATALYZED THIO-MICHAEL

# ADDITION REACTION

## Abstract

The addition of thiols to electron deficient alkenes was investigated in the presence of nucleophilic catalysts such as primary amines and tertiary phosphines. The conjugate addition of hexanethiol and hexyl acrylate was utilized as a model system. Kinetics were determined by real-time Fourier transform infrared (RTIR) spectroscopy. A typically used Brønsted base catalyst, triethylamine (pk$_a$= 10.75), was used as a reference for comparison. The conjugate addition of hexanethiol and hexyl acrylate the presence of 0.4 M hexyl amine (pK$_a$= 10.6) was monitored by RTIR and results indicate an increase in rate of reaction greater than 3 orders of magnitude in comparison to triethylamine and near quantitative yields (>95%) in 500 seconds. These results indicated that a catalyst with more nucleophilic character increased reaction rates. Other Brønsted base catalysts showed similar results to triethylamine. To further investigate our hypothesis of a nucleophilic catalyst based mechanism, tertiary phosphines were employed in catalytic amounts and results confirmed the increased rates of the conjugate addition. Additionally, the thio-Michael conjugate addition showed even exceptional reactivity in lower concentrations of the phosphine catalysts than the amines. In addition other thiols and electron deficient carbon-carbon double bonds demonstrated exceptional rates of reactivity and final yields. Finally, an anion chain mechanism is proposed for the nucleophile catalyzed thio-Michael addition.

## Introduction

The thiol-ene "click" reaction has recently drawn a great deal of attention given its exceptional utility in organic synthesis, polymer functionalization and network modification.[1-3] The well known radical-mediated thiol-ene "click" reaction involves hydrothiolation of α,β-unsaturated alkenes and has been studied for decades.[1-7] Such reactions can be initiated thermally or photochemically (with or without added photoinitiator) and proceed via thiyl radical addition to the C=C bond followed by a chain transfer reaction affording the corresponding thioether in essentially quantitative yield. Recently, the thiol-ene reaction has been widely investigated for its general applicability in a wide range of fields, including, but not limited to, biocompatible network materials,[8] dendrimer synthesis,[9,10] nano-imprinting and lithography,[11-16] liquid crystal and holographic materials,[17-20] and protein immobilization.[21] One drawback of the radical-mediated reaction is the non-quantitative formation of thioether with α,β-unsaturated *electron poor* alkenes, such as acrylates and acrylamides which are widely given their ready availability.[3] Acrylates, for example, react with both thiols and other acrylates (via radical polymerization) giving a mixture of products in a photo or thermal initiated system. As such, the radical mediated thiol-ene "click" reaction is best performed with *electron rich* double bonds for quantitative formation of thioether.[3-5, 22, 23]

The base catalyzed conjugate addition of thiolate anions to electron deficient carbon-carbon double bonds has been investigated extensively for small molecule synthesis,[20,24,25] polymer modification,[25-27] step-growth polymerizations,[28] and in other applications with various activated substrates including maleimides,[26,28-30] (meth)acrylates, acrylamides,[20,24,31-36] and other α,β-unsaturated species.[27,37] The base

catalyzed thio-Michael addition affords relatively high yields of thioether product by optimizing conditions such as catalyst, solvent, and reactant choices.[3,25,29,32-36] For example, the work of Hubbell and coworkers in the preparation of peptide (cysteine containing) modified hydrogels in tissue engineering applications, highlights the facile nature of the thio-Michael addition of cysteine to various electron poor enes and is typically achieved by tuning the pH of the buffered aqueous systems to slightly above neutral pH ( ~ 8).[32-36] Many base catalyzed systems, however, result in less than quantitative conversion, require lengthy reaction times, highly polar, low volatile solvents, higher catalyst concentrations, and elevated reaction temperatures.

Less is known about the *nucleophile catalyzed* thio-Michael addition reaction. Evidence of primary amine catalyzed reaction of thiols with $\alpha,\beta$-unsaturated electron poor enes was presented over 40 years ago when Ogata and coworkers studied the increased catalytic activity of ethanolamine and other primary amines.[ref] In contrast to the base catalyzed reaction, the nucleophile catalyzed thio-Michael reaction exhibits qualities of a typical radical-mediated thiol-ene "click" reaction, i.e. it facilitates the modular, orthogonal addition of thiols to electron poor alkenes in a quantitative fashion with minimal amounts of simple commercially available catalysts. Most reactions can be performed in the absence of solvent, without heat or light, and reach quantitative conversions often within a few hundred seconds.[38-42] Chan, Hoyle, and Lowe recently reported the modification of a tetra-functional pentaerythritol-based thiol and the quantitative formation of polyfunctional materials in a two step, one-pot technique employing, first, the phosphine catalyzed thio-Michael addition of propargyl acrylate, followed by the photo-initiated double addition of various thiols to the non-activated

carbon-carbon triple bond producing material with 16-functional groups.[38] Lowe and coworkers also reported the formation of 3-arm star RAFT-prepared polymers through the phosphine catalyzed thio-Michael addition of the polymer chain end with a tri-acrylate core.[39] Indeed, the use of phosphines as organocatalysts in organic synthesis is well documented.[68-71] For example, the efficiency of tertiary phosphines to catalyze Michael addition reactions was reported by Bergman, Toste, and coworkers with the addition of methanol to $\alpha,\beta$-unsaturated ketones resulting in exceptionally high enantio-selective yields.[68]

Herein, we report the kinetics of the nucleophile catalyzed thio-Michael reaction of hexanethiol to hexyl acrylate as a model system. The use of primary amines and tertiary phosphines will be the main focus of catalytic analysis. The use of other thiols and substrates is also described. In comparison to the traditionally used amine base catalyst, this work demonstrates the superior activity of primary amines and trialkyl phosphines as catalysts for thio-Michael addition reactions. Finally, we present an anion mediated chain reaction mechanism for such nucleophile catalyzed reactions.

<div align="center">Experimental</div>

*Materials*

All reactions were carried out at room temperature. All chemicals, solvents, and reagents were purchased from Sigma Aldrich Chemical Co. at the highest available purity and used without further purification. Nuclear magnetic resonance (NMR) spectra were recorded using a Bruker 300MHz spectrometer. $^1$H NMR samples were prepared in CDCl$_3$ at 15% (v/v%). Chemical shifts are reported in parts per million relative to TMS.

Thiol and acrylate conversions were monitored by real-time Fourier transform infrared (RTIR) spectroscopy using a modified Bruker 88 spectrometer. Reactions were conducted in a cell prepared by sandwiching samples between two sodium chloride plates at a thickness of 250 μm. IR absorption spectra were obtained at a scan rate of 5 scans per second. The characteristic IR absorbance bands used to monitor the disappearance of the reactant and monomer during the photoreactions were acrylate: 812 cm$^{-1}$ and thiol: 2570 cm$^{-1}$. The reactant conversions were calculated by integrating the peak areas as a function of time.

*Synthesis and Characterization*

*Hexylamine catalyzed thio-Michael addition reaction of hexanethiol with hexyl acrylate.* 0.600g (5mmoles) hexanethiol was mixed with 10μL (0.05M) of hexylamine in a 20 mL glass scintillation vial. To this was added 0.781g (5mmoles) hexyl acrylate and the mixture was quickly agitated.

$^1$H NMR of equimolar mixture of hexanethiol and hexyl acrylate in the presence of 0.05M hexylamine. (yield $^1$H NMR > 99%) (a) δ 4.074-4.030 ppm (t,2H); (b) δ 2.766-2.716 ppm (t, 2H); (c) δ 2.581-2.463 ppm (m, 4H); (d) δ 1.636-1.493 ppm (m, 4H); (e) δ 1.386-1.270 ppm (broad m, (14+)H, hexyl amine region); (f) δ 0.871-0.830 ppm (broad t, 6H); $^{13}$C NMR (a) δ 171.972 ppm; (b) δ 64.717 ppm; (c) δ 34.874 ppm (d) δ 32.042 ppm; (e) δ 31.325 ppm; (f) δ 29.431 ppm; (g) δ 28.454 ppm; (h) δ 26.925 ppm; (i) δ 25.476 ppm; (j) δ 22.449-22.473 ppm; (k) δ 13.924-13.890 ppm; (neat; 3 hours.; RT).

*Hexylamine catalyzed thio-Michael addition reaction of methyl 3-mercaptopropionate with hexyl acrylate.* 0.600g (5mmoles) methyl 3-mercaptopropionate was mixed with 10μL (0.05M) of hexylamine in a 20 mL glass scintillation vial. To this was added 0.781g (5mmoles) hexyl acrylate and the mixture was quickly agitated.

$^1$H NMR of equimolar mixture of methyl 3-mercaptopropionate and hexyl acrylate in the presence of 0.43M hexylamine. (yield $^1$H NMR > 99%) (a) δ 4.059-4.005 ppm (m,4H); (b) δ 2.767-2.719 ppm (t, 4H); (c) δ 2.568-2.519 ppm (t, 4H); (d) δ 1.601-1.508 ppm (m, 4H); (e) δ 1.404-1.246 ppm (broad m, (8+)H hexyl amine region); (f) δ 0.896-0.807 ppm (broad m 6+H); (neat; 6 hrs.; RT); $^{13}$C NMR (a) δ 171.683 ppm; (b) δ 64.707 ppm; (c) δ 64.404 ppm; (d) δ 34.634 ppm; (e) δ 31.242 ppm; (f) δ 30.454 ppm; (g) δ 28.375 ppm; (h) δ 26.839 ppm; (i) δ 25.387 ppm; (j) δ 22.360 ppm; (k) δ 18.853 ppm (l) δ 13.824 ppm (m) δ13.523 ppm; (neat; 6 hrs.; RT).

*Hexylamine catalyzed thio-Michael addition reaction of ethyl thioglycolate with hexyl acrylate.* 0.600g (5mmoles) ethyl thioglycolate was mixed with 10μL (0.05M) of hexylamine in a 20 mL glass scintillation vial. To this was added 0.781g (5mmoles) hexyl acrylate and the mixture was quickly agitated.

$^1$H NMR of equimolar mixture of ethylthioglycolate and hexyl acrylate in the presence of 0.43M hexylamine. (yield $^1$H NMR > 99%) (a) δ 4.172-4.101 (q,2H); (b) δ 4.066-4.011 ppm (t,2H); (c) δ 3.184 ppm (s, 2H); (d) δ 2.881-2.832 ppm (t, 2H); (e) δ 2.612-2.564 ppm (t, 2H); (f) δ 1.592-1.522 ppm (m, 2H); (g) δ 1.313-1.209 ppm (broad m, (10+)H hexyl amine region); (h) δ 0.853-0.810 ppm (broad m, 3H); $^{13}$C NMR (a) δ 171.538 ppm; (b) δ 170.106 ppm; (c) δ 64.760 ppm; (d) δ 61.225 ppm; (e) δ 34.175 ppm;

(f) δ 33.480 ppm; (g) δ 31.245 ppm; (h) δ 28.376 ppm; (i) δ 27.408 ppm; (j) δ 25.398 ppm; (k) δ 22.388 ppm; (l) δ 13.991 ppm; (m) δ13.835 ppm; (neat; 3 hours.; RT).

*Tripropylphosphine catalyzed thio-Michael addition reaction of hexanethiol with hexyl acrylate.* 0.591g (5mmoles) hexanethiol was mixed with 0.85μL (0.003M) of tripropylphosphine in a 20 mL glass scintillation vial. To this was added 0.781g (5mmoles) hexyl acrylate and the mixture was quickly agitated.

$^1$H NMR of equimolar mixture of hexanethiol and hexyl acrylate in the presence of 0.004M dimethylphenylphosphine. (yield $^1$H NMR > 99%) (a) δ 4.078-4.034 ppm (t,2H); (b) δ 2.770-2.720 ppm (t, 2H); (c) δ 2.586-2.467 ppm (m, 4H); (d) δ 1.619-1.496 ppm (hept, 4H); (e) δ 1.367-1.241 ppm (broad m, (14+)H, hexyl amine region); (f) δ 0.875-0.833 ppm (broad t, 6H); $^{13}$C NMR (a) δ 171.983 ppm; (b) δ 64.726 ppm; (c) δ 34.879 ppm (d) δ 32.047 ppm; (e) δ 31.334 ppm; (f) δ 29.438 ppm; (g) δ 28.462 ppm; (h) δ 26.930 ppm; (i) δ 25.484 ppm; (j) δ 22.459-22.446 ppm; (k) δ 13.936-13.901 ppm; (neat; 3 hours.; RT).

*Dimethylphenylphosphine catalyzed thio-Michael addition reaction of hexanethiol with hexyl acrylate.* 0.591g (5mmoles) hexanethiol was mixed with 0.6μL (0.003M) of dimethylphenylphosphine in a 20 mL glass scintillation vial. To this was added 0.781g (5mmoles) hexyl acrylate and the mixture was quickly agitated.

$^1$H NMR of equimolar mixture of hexanethiol and hexyl acrylate in the presence of 0.004M tripropylphosphine. (yield $^1$H NMR > 99%) (a) δ 4.077-4.032 ppm (t,2H); (b) δ 2.768-2.718 ppm (t, 2H); (c) δ 2.583-2.465 ppm (m, 4H); (d) δ 1.617-1.494 ppm (hept, 4H); (e) δ 1.388-1.239 ppm (broad m, (14+)H, hexyl amine region); (f) δ 0.873-0.830 ppm (broad t, 6H); $^{13}$C NMR (a) δ 171.974 ppm; (b) δ 64.717 ppm; (c) δ 34.871 ppm (d)

δ 32.039 ppm; (e) δ 31.327 ppm; (f) δ 29.430 ppm; (g) δ 28.455 ppm; (h) δ 26.922 ppm;

(i) δ 25.477 ppm; (j) δ 22.452-22.473 ppm; (k) δ 13.928-13.893 ppm; (neat; 3 hours.;

RT).

*Methyldiphenylphosphine catalyzed thio-Michael addition reaction of hexanethiol with hexyl acrylate.* 0.591g (5mmoles) hexanethiol was mixed with 0.75μL (0.003M) of methyldiphenylphosphine in a 20 mL glass scintillation vial. To this was added 0.781g (5mmoles) hexyl acrylate and the mixture was quickly agitated.

$^1$H NMR of equimolar mixture of hexanethiol and hexyl acrylate in the presence of 0.004M methyldiphenylphosphine. (yield $^1$H NMR ~ 90%) (a) δ 4.059-4.015 ppm (t,2H); (b) δ 2.750-2.700 ppm (t, 2H); (c) δ 2.565-2.447 ppm (m, 4H); (d) δ 1.600-1.477 ppm (hept, 4H); (e) δ 1.298-1.222 ppm (broad m, (14+)H, hexyl amine region); (f) δ 0.857-0.816 ppm (broad t, 6H); $^{13}$C NMR (a) δ 171.893 ppm; (b) δ 64.646 ppm; (c) δ 34.825 ppm (d) δ 31.997 ppm; (e) δ 31.297 ppm; (f) δ 29.399 ppm; (g) δ 28.410 ppm; (h) δ 26.876 ppm; (i) δ 25.447 ppm; (j) δ 22.409-22.395 ppm; (k) δ 13.876-13.841 ppm; (neat; 3 hours.; RT).

*DBN catalyzed thio-Michael addition reaction of hexanethiol with hexyl acrylate.* 0.591g (5mmoles) hexanethiol was mixed with 0.60μL (0.004M) of DBN in a 20 mL glass scintillation vial. To this was added 0.781g (5mmoles) hexyl acrylate and the mixture was quickly agitated.

$^1$H NMR of equimolar mixture of hexanethiol and hexyl acrylate in the presence of 0.003M DBN. (yield $^1$H NMR > 99%) (a) δ 4.077-4.032 ppm (t,2H); (b) δ 2.769-2.719 ppm (t, 2H); (c) δ 2.585-2.466 ppm (m, 4H); (d) δ 1.616-1.521 ppm (hept, 4H); (e) δ 1.363-1.272 ppm (broad m, (14+)H, hexyl amine region); (f) δ 0.872-0.833 ppm (broad t,

6H); ^{13}C NMR (a) δ 171.970 ppm; (b) δ 64.714 ppm; (c) δ 34.858 ppm (d) δ 32.027 ppm; (e) δ 31.324 ppm; (f) δ 29.423 ppm; (g) δ 28.452 ppm; (h) δ 26.908 ppm; (i) δ 25.475 ppm; (j) δ 22.475-22.443 ppm; (k) δ 13.933-13.900 ppm; (neat; 3 hours.; RT).

*DBU catalyzed thio-Michael addition reaction of hexanethiol with hexyl acrylate.* 0.591g (5mmoles) hexanethiol was mixed with 0.75μL (0.004M) of DBU in a 20 mL glass scintillation vial. To this was added 0.781g (5mmoles) hexyl acrylate and the mixture was quickly agitated.

^{1}H NMR of equimolar mixture of hexanethiol and hexyl acrylate in the presence of 0.003M DBU. (yield ^{1}H NMR > 99%) (a) δ 4.076-4.036 ppm (t,2H); (b) δ 2.772-2.708 ppm (t, 2H); (c) δ 2.553-2.447 ppm (m, 4H); (d) δ 1.600-1.526 ppm (hept, 4H); (e) δ 1.353-1.253 ppm (broad m, (14+)H, hexyl amine region); (f) δ 0.872-0.833 ppm (broad t, 6H); ^{13}C NMR (a) δ 171.972 ppm; (b) δ 64.669 ppm; (c) δ 34.824 ppm (d) δ 32.989 ppm; (e) δ 31.293 ppm; (f) δ 29.391 ppm; (g) δ 28.420 ppm; (h) δ 26.893 ppm; (i) δ 25.444 ppm; (j) δ 22.414 ppm; (k) δ 13.893-13.862 ppm; (neat; 3 hours.; RT).

*Hexylamine catalyzed thio-Michael addition reaction of hexanethiol with acrylonitrile.* 0.591g (5mmoles) hexanethiol was mixed with 22μL (2.0M) of hexylamine in a 20 mL glass scintillation vial. To this was added 0.250g (5mmoles) acrylonitrile and the mixture was quickly agitated.

^{1}H NMR of equimolar mixture of hexanethiol and acrylonitrile in the presence of 0.2 M hexylamine. (yield ^{1}H NMR > 99%) (a) δ 2.750-2.699 ppm (t, 2H); (b) δ 2.608-2.506 ppm (m, 4H); (c) δ 1.581-1.484 ppm (m, 4H); (d) δ 1.411-1.265 ppm (m, 6H); (e) δ 0.855-0.810 (t, 3H); ^{13}C NMR (a) δ 118.235 ppm; (b) δ 31.988 ppm; (c) δ 31.117 ppm;

(d) δ 29.163 ppm; (e) δ 28.189 ppm; (f) δ 27.353 ppm; (g) δ 22.280 ppm; (h) δ 18.888 ppm; (i) δ 13.783 ppm; (neat; 3 hours.; RT).

*Hexylamine catalyzed thio-Michael addition reaction of hexanethiol with N,N-dimethylacrylamide.* 0.591g (5mmoles) hexanethiol was mixed with 29μL (2.0M) of hexylamine in a 20 mL glass scintillation vial. To this was added 0.495g (5mmoles) *N,N-*dimethyl acrylamide and the mixture was quickly agitated.

$^1$H NMR of equimolar mixture of hexanethiol and *N,N*-dimethylacrylamide in the presence of 0.2 M hexylamine. (yield $^1_{H\,NMR}$ > 99%) (a) δ 2.800 ppm (s, 3H); (b) δ 2.832 ppm (2, 3H); (c) δ 2.719-2.668 ppm (t, 2H); (d) δ 2.501-2.450 ppm (t, 2H); (e) δ 2.441-2.391 (t, 2H); (f) δ 1.514-1.416 ppm (m, 2H); (g) δ 1.303-1.116 ppm (m, 6H); (h) 1.118-0.739 ppm (t, 3H); $^{13}$C NMR (a) δ 170.918 ppm; (b) δ 36.821 ppm; (c) δ 35.086 ppm; (d) δ 33.544 ppm; (e) δ 32.173 ppm; (f) δ 31.118 ppm; (g) δ 29.310 ppm; (h) δ 28.235 ppm; (i) δ 27.123 ppm; (j) δ 22.228 ppm; (k) δ 13.723 ppm; (neat; 3 hours.; RT).

*Hexylamine catalyzed thio-Michael addition reaction of hexanethiol with ethylcrotonate.* 0.591g (5mmoles) hexanethiol was mixed with 31μL (2.0M) of hexylamine in a 20 mL glass scintillation vial. To this was added 0.570g (5mmoles) ethylcrotonate and the mixture was quickly agitated.

$^1$H NMR of equimolar mixture of hexanethiol and ethylcrotonate in the presence of 0.2 M hexylamine. (yield $^1_{H\,NMR}$ > 95%) (a) δ 4.124-4.054 ppm (quart, 2H); (b) δ 3.187-3.072 ppm (m, 1H); (c) δ 2.615-2.313 ppm (m, 4H); (d) δ 1.561-1.414 ppm (m, 2H); (e) δ 1.360-1.161 (m, 12H); (f) δ 0.842-0.800 ppm (t, 3H); $^{13}$C NMR (a) δ 171.350 ppm; (b) δ 60.332 ppm; (c) δ 42.231 ppm; (d) δ 35.969 ppm; (e) δ 31.277 ppm; (f) δ

30.474 ppm; (g) δ 29.504 ppm; (h) δ 28.507 ppm; (i) δ 22.397 ppm; (j) δ 21.269 ppm; (k) δ 14.065 ppm; (l) δ 13.875 ppm; (neat; 12 hours.; RT).

*Hexylamine catalyzed thio-Michael addition reaction of hexanethiol with ethyl methacrylate.* 0.591g (5mmoles) hexanethiol was mixed with 31μL (2.0M) of hexylamine in a 20 mL glass scintillation vial. To this was added 0.570g (5mmoles) ethyl methacrylate and the mixture was quickly agitated.

$^1$H NMR of equimolar mixture of hexanethiol and ethyl methacrylate in the presence of 0.2 M hexylamine. (yield $^1$H NMR ~ 25%) (a) δ 4.201-4.130 ppm (quart, 2H); (b) δ 2.827-2.616 ppm (m, 3H); (c) δ 2.497-2.448 ppm (t, 2H); (d) δ 1.617-1.507 ppm (m, 2H); (e) δ 1.394-1.196 (m, 12H); (f) δ 0.874-0.828 ppm (t, 3H); $^{13}$C NMR (a) δ 175.143 ppm; (b) δ 60.425 ppm; (c) δ 40.166 ppm; (d) δ 35.410 ppm; (e) δ 32.551 ppm; (f) δ 31.338 ppm; (g) δ 29.488 ppm; (h) δ 28.446 ppm; (i) δ 24.550 ppm; (j) δ 16.734 ppm; (k) δ 14.106 ppm; (l) δ 13.823 ppm; (neat; 12 hours.; RT).

*Hexylamine catalyzed thio-Michael addition reaction of hexanethiol with ethylcinnamate.* 0.591g (5mmoles) hexanethiol was mixed with 39μL (2.0M) of hexylamine in a 20 mL glass scintillation vial. To this was added 0.890g (5mmoles) ethyl trans-cinnamate and the mixture was quickly agitated.

$^1$H NMR of equimolar mixture of hexanethiol and ethylcinnamate in the presence of 0.2 M hexylamine. (yield $^1$H NMR ~ 80%) (a) δ 7.352-7.216 ppm (m, 5H); (b) δ 4.292-4.243 ppm (t, 1H); (c) δ 4.068-4.021 ppm (quart, 2H); (d) δ 2.922-2.233 ppm (m, 4H); (e) δ 1.608-1.402 (m, 2H); (f) δ 1.375-1.121 ppm (m, 9H); (f) δ 0.867-0.825 ppm (m, 3H); $^{13}$C NMR (a) δ 175.143 ppm; (b) δ 60.425 ppm; (c) δ 40.166 ppm; (d) δ 35.410 ppm; (e)

δ 32.551 ppm; (f) δ 31.338 ppm; (g) δ 29.488 ppm; (h) δ 28.446 ppm; (i) δ 24.550 ppm; (j) δ 16.734 ppm; (k) δ 14.106 ppm; (l) δ 13.823 ppm; (neat; 12 hours; RT).

*Hexylamine catalyzed thio-Michael addition reaction of hexanethiol with N-propylmaleimide.* 0.591g (5mmoles) hexanethiol was mixed with 34μL (2.0M) of hexylamine in a 20 mL glass scintillation vial. To this was added 0.695g (5mmoles) *N*-propylmaleimide and the mixture was quickly agitated.

¹H NMR of equimolar mixture of hexanethiol and *N*-propylmaleimide in the presence of 0.2 M hexylamine. (yield ¹H NMR > 99%) (a) δ 3.700-3.658 ppm (m, 1H); (b) δ 3.472-3.423 ppm (t, 2H); (c) δ 3.138-3.046 and 2.540-2.446 ppm (m, 2H); (d) δ 2.882-2.666 ppm (m, 2H); (e) δ 1.680-1.495 (m, 4H); (f) δ 1.412-1.317 ppm (m, 2H); (g) δ 1.282-1.234 ppm (m, 4H); (h) δ 0.902-0.817 ppm (m, 6H); ¹³C NMR (a) δ 176.643 ppm; (b) δ 174.811 ppm; (c) δ 40.469 ppm; (d) δ 38.912 ppm; (e) δ 36.004 ppm; (f) δ 31.581 ppm; (g) δ 31.235 ppm; (h) δ 28.880 ppm; (i) δ 28.374 ppm; (j) δ 22.422 ppm; (k) δ 20.867 ppm; (l) δ 13.933 ppm; (m) δ 11.124 ppm (neat; 3 hours; RT).

*Hexylamine catalyzed thio-Michael addition reaction of hexanethiol with diethylfumarate.* 0.591g (5mmoles) hexanethiol was mixed with 39μL (2.0M) of hexylamine in a 20 mL glass scintillation vial. To this was added 0.860g (5mmoles) diethylfumarate and the mixture was quickly agitated.

¹H NMR of equimolar mixture of hexanethiol and diethylfumarate in the presence of 0.2 M hexylamine. (yield ¹H NMR > 99%) (a) δ 4.219-4.079 ppm (m, 4H); (b) δ 3.637-3.585 ppm (m, 1H); (c) δ 2.996-2.547 ppm (m, 4H); (d) δ 1.610-1.454 ppm (m, 2H); (e) δ 1.382-1.179 (m, 12H); (f) δ 0.873-0.828 ppm (t, 3H); ¹³C NMR (a) δ 171.724 ppm; (b) δ 170.637 ppm; (c) δ 61.226 ppm; (d) δ 60.829 ppm; (e) δ 41.413 ppm; (f) δ 36.465 ppm;

(g) δ 31.384 ppm; (h) δ 31.250 ppm; (i) δ 29.079 ppm; (j) δ 28.386 ppm; (k) δ 22.426 ppm; (l) δ 14.044 ppm; (m) δ 13.926 ppm (neat; 3 hours; RT).

*Hexylamine catalyzed thio-Michael addition reaction of hexanethiol with diethylmaleate.* 0.591g (5mmoles) hexanethiol was mixed with 39µL (2.0M) of hexylamine in a 20 mL glass scintillation vial. To this was added 0.860g (5mmoles) diethylmaleate and the mixture was quickly agitated.

$^1$H NMR of equimolar mixture of hexanethiol and diethylmaleate in the presence of 0.2 M hexylamine. (yield $^1$H NMR > 99%) (a) δ 4.206-4.066 ppm (m, 4H); (b) δ 3.624-3.572 ppm (m, 1H); (c) δ 2.983-2.535 ppm (m, 4H); (d) δ 1.599-1.443 ppm (m, 2H); (e) δ 1.349-1.185 (m, 12H); (f) δ 0.861-0.816 ppm (t, 3H); $^{13}$C NMR (a) δ 171.680 ppm; (b) δ 170.591 ppm; (c) δ 61.181 ppm; (d) δ 60.785 ppm; (e) δ 41.375 ppm; (f) δ 36.429 ppm; (g) δ 31.346 ppm; (h) δ 31.220 ppm; (i) δ 29.048 ppm; (j) δ 28.352 ppm; (k) δ 22.394 ppm; (l) δ 14.011 ppm; (m) δ 13.892 ppm (neat; 3 hours; RT).

*Kinetic Study*

Thiol was mixed with amine (or phosphine) catalyst in a 20 mL glass scintillation vial in the presence or absence of solvent. To this mixture, the substrate (ene) was quickly added at room temperature. The solution was sandwiched between NaCl salt plates with 250 micron glass spacers and sealed around the edges with grease to ensure constant sample thickness and minimal sample evaporation, respectively. Thiol (2570 cm$^{-1}$, -S-H stretch) and alkene (~1640 cm$^{-1}$,-C=C- stretch, or ~810 cm$^{-1}$, =C-H bend) peak intensities were collected and applied to Eq. 1 to generate conversion vs. time plots.

$$\text{Fractional conversion} = \frac{I_t - I^0}{I_t} \qquad \text{(Eq. 1)}$$

Eq. 1 describes the method for determining the fractional conversion of a reactive group at any time (t). $I^0$ represents the initial absorbance intensity produced from an IR scan of material of a certain thickness. $I_t$ represents the absorbance intensity produced at a given time (t). $k_{app}$ constants were calculated by assuming first order concentrations of both thiol and ene and taken from 0-30% conversion of thiol, unless otherwise noted.

## Results and Discussions

The well established base catalyzed Michael addition of thiols to electron deficient enes has been widely investigated for nearly a century. There is no dispute that in a given system, a thiol (-SH) can behave as a Brønsted acid and easily donate a proton to a stronger Brønsted base (catalyst), such as a tertiary amine ($NR_3$). The subsequently formed thiolate anion is known to be a strong nucleophile and can easily add across an electron deficient double bond resulting in high product yields depending on the nature of the substrate, thiol, and catalyst. However, the thiolate anion is not completely free to react in every given system, and reactivity depends on factors such as base strength and solvent polarity. [19,20,24,25,29,30,43-45]

Formation of an acid-base pair is thermodynamically controlled and essentially spontaneous; however the conjugate addition of a thiolate anion to an electron poor double bond is kinetically controlled and depends on other factors, such as the degree of solvation of the thiolate anion and its sterics. **Scheme 3.1.** shows the mechanism for the base-catalyzed thio-Michael addition reaction of a thiol, R'-SH, across an electron

deficient acrylic double bond.[29,44] The initial step is the formation of the thiolate anion, or ion pair, which strongly depends on the $pK_a$ values of both the thiol and the base catalyst. Depending on solvation of the ion pair and the base strength, a given number of free anions will be produced. Solvated thiolate anions can attack the electron deficient vinyl groups at the favorable $\beta$-position forming a carbon centered anion, or enolate in the case of the acrylic substrate shown. The $pK_a$ of the subsequently formed enolate ester ($pK_a$ ~25)[46] is greater than that of other potential bases in the system including the tertiary amine catalyst ($pK_a$ ~11), or the thiol ($pK_a$ ~ 7-11).[41]

The final step in the reaction is the protonation of the enolate anion at the $\alpha$-carbon of the vinyl group. As a very strong base, the enolate species can deprotonate any and all of the acidic species in the medium including the protonated base catalyst, unreacted thiol, or protic solvent (if present).[46] If water ($pK_a$=15.7) or alcohol (ethanol $pK_a$=16.0) is used as a solvent, it is plausible that the enolate anion could abstract a proton from the solvent molecule, even when the thiol or protonated base is present.[29, 46, 47] In a solvent-free, or aprotic solvent system, however, a proton can only be abstracted from 2 sources: the conjugate acid, $BH^+$, or thiol.

Simple nucleophilic catalysts have been used to catalyze the addition of a thiol across electron deficient carbon-carbon double bonds.[39-42] Nucleophilic catalysts show enhanced activity over bases with comparable or lower $pK_a$ values. By understanding the efficiency of nucleophilic catalysts in these types of Michael addition reactions, we have proposed the mechanism in **Scheme 3.2.**, whereby a nucleophile initiates the thiol-Michael addition leading to an anionic chain process. Albeit unique to the thio-Michael addition reaction, a similar nucleophile catalyzed chain mechanism has previously been

reported by Bergman, Toste, and coworkers for the oxa-Michael addition reaction. Addition of a nucleophilic catalyst, such as a *primary* amine or a tertiary phosphine, initiates the reaction by forming an electronically unfavorable, very reactive enolate-based zwitterion that begins a series of proton abstractions from the most readily available acid in the system, the thiol.[68] Klemarczyk and coworkers reported the isolation and spectroscopic analysis of the zwitterionic species formed between dimethylphenylphosphine and ethyl 2-cyanoacrylate, similar to the initiating species shown in **Scheme 3.2.**[71] The nucleophile catalyzed anionic chain mechanism, which is similar to the radical-mediated thiol-ene "click" chain mechanism, shows exceptionally increased kinetic profiles, quantitative conversion within minutes, little to no side products, can be performed in the absence of solvents, and orthogonality and should be considered essential within the canon of "click" reactions for materials modification and organic compound synthesis.

The conjugate addition of hexanethiol to hexyl acrylate is used as a model reaction to demonstrate the nature of the nucleophile catalyzed anionic chain mechanism. However, other experiments detailed within this report will highlight the applicability of various other thiols and electron deficient substrates that may be of interest to the broad audience of readers. **Figure 3.1.A.** shows the reaction progress vs. time of hexanethiol ($pK_a = 10.3$)[48] addition to hexyl acrylate with a catalytic amount (0.4 M) of triethylamine ($pK_a = 10.75$).[49] The rate of reaction is relatively slow and quantitative conversion is only achieved at prolonged (>12 hours) reaction time. In contrast, **Figures 3.1.B. and C.** show that as the catalyst nucleophilicity increases, the rate of conjugate addition increases significantly in the order: primary amine > secondary amine > tertiary amine.

There is a clear evident increase in the reaction rate with a secondary amine (di-*n*-propyl amine, $pK_a$ =11.00)[49] and further with a primary amine (hexylamine, $pK_a$ = 10.6)[50] in these reactions when compared to triethylamine, by ~3 orders of magnitude, see **Table 3.1.** for apparent rate constants. Considering that the $pK_a$ values of all 3 amines are nearly identical, the rates should not be as greatly affected if the reaction was proceeding by a purely base-catalyzed process. These data alone strongly suggest the existence of a nucleophile-based reaction mechanism.

Amines have a lone pair of electrons that can directly add into the double bond, and the reaction requires no initiation step; however, the initial attack of the amine on the double bond forces an energetically unfavorable transition state with the double bond.[43] In this case, the *soft* double bond has poor affinity for the *hard* amine.[58] The thiolate anion, a *soft* base, will add to the electron deficient double bond significantly faster than a nucleophilic, *hard*, amine given the delocalization of the electrons of a sulfur atom.[43] Bernasconi and coworkers determined that the $k_{observed}$ of the conjugate addition of thiolate species toward nitrostilbenes was 2 to 3 orders of magnitude higher than the same reaction, in buffered aqueous solution, with an amine of similar $pK_a$ explaining the increase in rate in terms of hard/soft base theory.[58] Similarly, Friedman and coworkers reported the $k_{RS}$/$k_{RNH_2}$ ratios at constant pH were 2.75 X 10$^2$ for acrylonitrile, 1.45 X 10$^2$ for methyl acrylate, and 1.78 X 10$^2$ for acrylamide.[43] Since primary amines were determined to be the most effective catalysts in the series of substituted amines for the thio-Michael addition, rate dependence on catalyst concentration was analyzed, and the data are shown in **Figure 3.2.** Results from this study indicate that the thiol alone will not undergo direct nucleophilic attack on the double bond, because formation of the

thiolate anion is a key step in the conjugate addition reaction.[29] Additionally in the presence of a weak base, like triethylamine, only a slight increase in the rate of conjugate addition occurs and is comparable to a non-catalyzed system. However, with the addition of catalytic amounts of hexylamine, the rates greatly increase. Again, since the $pK_a$ values of the amines are similar, in multiple solvents,[51-52] it is fair to conclude that the formation of $RS^-NR^1_3H^+$ is not a strong rate affecting factor in the nucleophile catalyzed reaction. Theoretically, the order of reactivity of amines in proton transfer usually increases in the order $NR_3 > NR_2H_1 > NRH_2$ according to the increased solvation of $NR_3H^+ < NR_2H_2^+ < NRH_3^+$.[53-57] A base catalyzed thio-Michael conjugate addition would, then, increase from $NR_3 > NR_2H > NRH_2$ based on the assumption that the protonated tertiary amine is more easily deprotonated. However, this trend is opposite of that in **Figure 3.1.** Therefore, one must conclude that in the presence of hexylamine, the thiolate anion is more readily formed, and the protonation of the subsequent enolate anion is not dependant on proton transfer from the protonated catalyst in a nucleophile catalyzed system, given that the $pK_a$ of $NR_3H^+$ (~10.6 for triethylamine) in most cases is greater than RSH (~10.3 for hexanethiol).

*Dependence of Nucleophilic Character of Amine Bases*

Examining other amine base/nucleophilic catalysts, 0.4M of 1,5-diazabicyclo[4.3.0]non-5-ene (DBN) and 1,8-diazabicyclo[5.4.0]undec-7-ene (DBU), shown in **Chart 3.1.**, were used to catalyze the reaction of hexanethiol to hexyl acrylate; however, the reaction profiles were too fast to be measured by RTIR, indicating that near quantitative conversion occurred in less than 10 seconds. DBN and DBU are catalysts used in various *base catalyzed* applications, such as the traditional carbon-Michael

reaction and dehydrohalogenation.[59-64] Reports suggest that these nitrogen rich

heterocyclic compounds have unusually strong nucleophilic character, as well.[60-63] The

data in **Table 3.2.** shows the kinetic profile of the conjugate addition of hexane thiol to

hexyl acrylate catalyzed by either DBN ($pK_a$ = 13.5) or DBU ($pK_a$ = 11.6) at

(0.004M).[62,64] These catalysts greatly increased the rates of reactions, as expected by the

increase in Brønsted basicity and nucleophilicity as compared to hexylamine and triethyl

amine.

To confirm that the apparent rate of conjugate addition was independent of

conjugate base pKa, 1,8-bis(dimethylamino) naphthalene [Proton Sponge (PS)] ($pK_a$ =

12.1)[63,67] was utilized as a well-known non-nucleophilic base to compare results of

nucleophilic catalysts with similar $pK_a$ values, such as DBN and DBU. Data in **Table**

**3.2.** indicate similar kinetic behavior of the thio-acrylate Michael addition of hexane thiol

($pK_a$ = 10.3) to hexyl acrylate catalyzed by (0.4M) PS to the system catalyzed by triethyl

amine, or no catalyst – little to no reactivity.

*Phosphines as Nucleophilic Catalysts*

Understanding that basicity of the catalyst had little effect on the reaction kinetics

at low catalyst concentrations (< 2 mol%), other nucleophilic species were examined to

verify the hypothesis of the nucleophile based process. Some of the most commonly

studied nucleophilic catalysts are tertiary phosphines, $PR_3$, where R is commonly an alkyl

or phenyl group. Indeed, trialkyl phosphines are known to catalyze the oxa-Michael and

traditional carbon-Michael addition reactions to electron deficient double bonds.[68-71]

Trialkyl phosphines have been reported to form conjugate addition products with acrylate

containing molecules.[71] Within this study, primary, secondary and tertiary amines were

used as initiating species and were all found to initiate anionic polymerization of ethyl 2-cyanoacrylate. Dimethylphenylphosphine, however, was confirmed by IR and NMR analysis to produce a stable zwitterionic compound with ethyl 2-cyanoacrylate. Additionally, Toste and coworkers demonstrated the efficient conjugate addition of methanol ($pK_a = 15.5$)[71] and other alcohols- with $\alpha,\beta$-unsaturated species in the presence of tertiary alkyl phosphines such as $PMe_3$ and $PBu_3$.[46,68] Vallribera and co-workers investigated the traditional carbon-Michael addition catalyzed with triphenylphosphine and tributylphosphine using various enes as substrates and malonates as donors. Similar to the study performed by Klemarczyk, a proposed mechanism indicates the initial attack of the phosphine on the $\beta$-position of the electron deficient double bond.

Four different tertiary phosphines were evaluated as catalysts in the reaction of hexanethiol with hexyl acrylate, see **Chart 3.2.** for structures. Similar to the study with DBU and DBN, 0.4M of tripropylphosphine (P($n$-Pr)$_3$), for example, was used to catalyze the reaction of hexanethiol with hexyl acrylate, and the reaction kinetics were too fast to be measured by RTIR. The data in **Figure 3.3.** and **Table 3.3.** shows the kinetic profiles of the thio-Michael addition in the presence of 0.003M of each phosphine with increasing reaction rates with increasing nucleophilicity of the phosphine catalyst.[68-75] (These reactions were also analyzed in solution and reactions showed similar kinetic behavior.) It is apparent that the sterics and electronic effects with lone pair delocalization around phosphorous, and hence the nucleophilicity, have a major impact on the rate of this reaction with reactivity following the order P($n$-Pr)$_3$>PMe$_2$Ph>>PMePh$_2$>PPh$_3$.[70-77] RTIR data shows >92% conversion of both thiol (2570 cm$^{-1}$) and acrylate (810 cm$^{-1}$) within 100 seconds in the presence of 0.003M P($n$-Pr)$_3$!

Phosphines, like amines, have a lone pair of electrons that are available for nucleophilic attack on an electron deficient carbon-carbon double bond. Phosphines however, have increased nucleophilic potential in comparison to amines with similar structures, because of increased polarizability of the phosphorous atom.[46] Additionally, phosphines are weaker bases than amines of similar structure, and the increased kinetics demonstrated in **Figure 3.3.** are, indeed, a result of the superior nucleophilic character of phosphines.[70-77] Consequently, phosphines, are similar to thiolate ions and have a large radius of delocalized electrons, which are more available than the lone pair of electrons of amines and which can easily overlap with the carbon-carbon double bond to initiate the nucleophilic attack. Therefore, phosphorous is a *soft* species, much like sulfur is a *soft* species, and more easily associates with the *soft* alkene, than does the *hard* nitrogen. This difference in polarizability explains the increase in rate with the phosphorous based catalysts over the nitrogen based ones.

*Effect of Thiol pK$_a$ on Apparent Reaction Rate*

The kinetics of the conjugate addition of thiols with increasing pK$_a$ to hexyl acrylate in the presence of 0.05M hexylamine were monitored in systems with no added solvent to determine a general kinetic trend with respect to thiol pK$_a$. Results of this study indicate that as the thiol pK$_a$ increased the apparent rate of reaction decreased. This data is inconsistent with what is expected from previous investigations. Bernasconi and coworkers describe the conjugate addition of thiols with increasing pK$_a$ toward nitrostilbenes under pH conditions that maintained a constant theoretical number of thiolate species in comparable experiments.[58] Kinetic data in this investigation showed that as the thiol pK$_a$ increased, the rate of addition of the thiolate to the carbon-carbon

double bond increased. These findings describe that a thiol with a higher $pK_a$ value (stronger Brønsted base), indeed, produces a more nucleophilic thiolate anion, given that in comparable experiments the number of thiolate species, the substrate, and the source of the proton being transferred ([acid]) remain constant; therefore, in the study by Bernasconi and coworkers, the apparent rate of the Michael addition of a thiol with a higher $pK_a$ value proceeds faster than the reaction of a thiol with a lower $pK_a$ value.[46, 57] Dmuchovsky and coworkers describe the base catalyzed addition of thiols to maleic anhydride showing that the reaction of the thiolate addition to the substrate increased with increasing $pK_a$ of the thiol. Additionally, it was reported that sterically hindered thiolate nucleophiles had decreased rates of reaction in this study and the dissociation constants, or $pK_a$, generally determined the rate of addition.[77] However, our data suggests that the order according to $pK_a$ of thiolate addition to hexyl acrylate is *reversed* and, hence, thiols with lower $pK_a$ values show faster apparent rates of reaction. With this data, we hypothesize that in the nucleophile catalyzed reactions in the absence of solvent or the presence of aprotic polar solvents (1) the chain transfer step, or the hydrogen abstraction by the enolate anion, in **Scheme 3.2.**, is highly affected by the $pK_a$ of the thiol, and (2) the most probable proton source for the chain transfer step is another thiol in solution, contrary to the accepted conjugate acid being the proton source in the base catalyzed reaction, see **Scheme 3.1.**

To further illustrate this concept in solvated systems, the apparent rates of addition of 2.0M of ethyl thioglycolate ($pK_a$ = 7.95)[48] with 2.0M hexyl acrylate was compared to the reaction of 2M methyl 3-mercaptopropionate ($pK_a$ = 9.33)[76] with 2.0M hexyl acrylate in the presence of 0.05M hexylamine as catalyst, see **Chart 3.3.** for

structures. The apparent rate of reaction is 2 orders of magnitude greater for ethyl

thioglycolate than with the methyl 3-mercaptopropionate, indicating the obvious change

according to $pK_a$.

*The Effects of Solvent Polarity on Apparent Reaction Rate*

In a typical base catalyzed reaction, the thiol and base form ionic species as an

initial step in the formation of the reactive thiolate nucleophile. Ions exist freely or in

pairs, and the amount of each free ion or ion pair is greatly determined by the polarity, or

dielectric constant ($\varepsilon$) of the solvent. Solvents with low polarity, such as benzene ($\varepsilon$ at

25°C =2.3), produce more regions of distinct ion pairs in shielded clusters, which reduce

the availability, and therefore the apparent rate of reaction, of a thiolate anion to react

with a substrate.[44] Whereas, solvents with higher polarity, such as acetonitrile ($\varepsilon$ at 25°C

=38), produce well solvated ion pairs, which allow the thiolate anion to more easily react

with the substrate. Indeed, data in **Table 3.4.** shows an increase in the apparent rate of

reaction by a factor of ~2.5 of methyl 3-mercaptopropionate with hexyl acrylate in

benzene and acetonitrile as the solvent polarity increases.

*Effect of Electron Withdrawing Group on Reaction Rate*

The conjugate addition of thiols has broad applicability to a range of electron

deficient double bonds. For example, quantitative yields of thio-Michael adducts can be

obtained with maleimides, fumarates, maleates, acrylamides, acrylonitrile and acrylates

under hexylamine catalysis, see **Table 3.5.** and **Chart 3.4.** for structures. However, some

substituted $\alpha,\beta$-unsaturated esters, such as methacrylates, crotonates, and cinnamates,

show decreased activity. In comparing the methacrylate with the crotonate, methyl

substitution at the $\alpha$ or $\beta$-carbon will make the carbon-carbon double bond less

electrophilic and data in **Table 3.5.** shows a decrease in the rates of both thiol addition reactions. However, substitution at the α-carbon greatly reduces the final yield of the conjugate addition product when hexylamine is used as the catalyst. In the nucleophile catalyzed reaction, the enolate anion produced on a methacrylate will be destabilized with the methyl group substitution in the α-carbon, which decreases the probability of enolate formation causing a general overall decrease in reactivity. The crotonate with methyl substitution in the β-carbon of the double bond shows a decrease in the overall kinetics due to steric hindrance in the thiolate addition step; however, final yields indicate that methyl substitution at the β-carbon does not have as a great an affect. For example in **Table 3.5.**, near quantitative yields of product formed in the conjugate addition of hexanethiol to ethyl crotonate in 12 hours, whereas, only 25% of double bond of the methacrylate has reacted in the same time period. Steric hinderance in the α-carbon decreases the rate of addition of *either* the initial step of the nucleophilic catalyst attack or a subsequent thiolate attack on the acrylate, which decreases the overall reaction rate. Indeed, destabilization of the enolate in either of these two steps will result in a decrease in kinetics.

## Summary and Conclusions

The nucleophile catalyzed thio-Michael reaction shows exceptional versatility as a sister reaction to the radical-mediated thiol-ene click reaction due to low catalyst concentrations, applicability to a wide range of substrates, commercially and inexpensive benign catalysts, and ease of use. The rates of the nucleophile catalyze reaction are comparable to that of the photoinitiated thiol-ene reaction and provide near quantitative

yield within seconds. Results reported, herein, suggest the nucleophilic catalyzed thio-Michael addition follows an anionic chain mechanism with rates $>10^3$ faster than typical tertiary amine catalysts.

References

1. Dondoni, A. *Angew. Chem. Int. Ed.* **2008**, 47, 2–5.

2. Becer, C.R.; Hoogenboom, R.; Schubert, U.S. *Angew. Chem. Int. Ed.* **2009**, 48(27), 4900-4908.

3. Hoyle, C.E.; Lee, T.Y.; Roper, T. *J. Polym. Sci. Part A: Polym. Chem.* **2004**, 42, 5301.

4. Morgan, C. R.; Magnotta, F.; Ketley, A. D. *J. Polym. Sci., Polym. Chem. Ed.* **1977**, 15, 627–45.

5. Jacobine, A. F. In *Radiation Curing in Polymer Science and Technology III, Polymerisation Mechanisms*, Fouassier, J. D., Rabek, J. F., Eds.; Elsevier Applied Science: London, 1993; Vol. 3, p. 219.

6. Cramer, N.B.; J. Scott, P.; Bowman, C.N. *Macromolecules* **2002**, 35(14), 5361–5365.

7. Cramer, N.B.; Davies, T.; O'Brien, A.K.; Bowman, C.N. *Macromolecules*, **2003**, 36(12), 4631–4636.

8. Tibbitt, M.W.; Anseth, K.S. *Biotech. Bioeng.* **2009**, 103(4), 655-663.

9. Rissing C.; Son, D.Y. *Organometallics*, **2009**, 28(11), 3167–3172.

10. Killops, K.L.; Campos, L.M.; Hawker, C.J. *J. Am. Chem. Soc.* **2008**, 130(15), 5062–5064.

11. Campos, L.M.; Meinel, I.; Guino, R.G.; Schierhorn, M.; Gupta, N.; Stucky, G.D.; Hawker, C.J. *Adv. Mater.* **2008**, 20, 3728–3733.

12. Khire, V.S.; Yi, Y.; Clark, N.A. Bowman, C.N. *Adv. Mater.* **2008**, 20(17), 3308-3313.

13. Hagberg, E.C.; Malkoch, M.; Ling, Y.; Hawker, C.J.; Carter, K.R. *Nano Lett.*, 2007, 7(2), 233–237.

14. Smythe, E.J.; Dickey, M.D.; Whitesides, G.M.; Capasso, F. *ACS Nano* **2009**, 3(1), 59–65.

15. Dickey, M.D.; Collister, E.; Raines, A.; Tsiartas, P.; Holcombe, T.; Sreenivasan, S.V.; Bonnecaze, R.T.; Willson, C.G. *Chem. Mater.* **2006**, 18(8), 2043–2049.

16. Moran, I.W.; Briseno, A.L.; Loser, S.; Carter, K.R. *Chem. Mater.* **2008**, 20(14), 4595–4601.

17. Lub, J.; Broer, D.J.; van den Broek, N. *Annalen* **1997**, 11, 2281 – 2288.

18. Natarajan, L.V.; Shepherd, C.K.; Brandelik, D.M.; Sutherland, R.L.; Chandra, S.; Tondiglia, V.P.; Tomlin, D.; Bunning, T.J. *Chem. Mater.* **2003**, 15(12), 2477–2484.

19. White, T.J.; Natarajan, L.V.; Tondiglia, V.P.; Lloyd, P.F.; Bunning, T.J.; Guymon, C.A. *Macromolecules* **2007**, 40(4), 1121–1127.

20. Kilambi, H.; Reddy, S.K.; Beckel, E.R.; Stansbury, J.W.; Bowman, C.N. *Chem. Mater.* **2007**, 29(4), 641-643.

21. Jonkheijm, P.; Weinrich, D.; Köhn, M.; Engelkamp; H.; Christianen, P.C.M.; Kuhlmann, J.; Maan, J.C.; Nüsse, D.; Schroeder, H.; Wacker, R.; Breinbauer, R.; Niemeyer, C.M.; Waldmann, H. *Angew. Chem. Int. Ed.* **2008**, 47(23), 4421-4424

22. Senyurt, A.F.; Wei, H.; Hoyle, C.E.; Piland, S.G.; Gould, T.E. *Macromolecules* **2007**, 40(14), 4901–4909.

23. Chan, J.W.; Wei, H.; Zhou, H.; Hoyle, C.E.; *Eur. Polym. J.* **2009**, 45, 2717–2725.

24. Kilambi, H.; Stansbury, J.W.; Bowman, C.N. *J. Polym. Sci., Part A: Polym. Chem.* **2008**, 46, 3452–3458.

25. Mather, B. D.; Viswanathan, K.; Miller, K.M.,; Long, T.E. *Prog. Polym. Sci.* **2006**, 31, 487-531.

26. Li. M.; De, P.; Gondi, S.R; Sumerlin, B.S. *J. Polym. Sci., Part A: Polym. Chem.* **2008**, 46, 5093-5100.

27. Bae, J.W.; Lee, E.; Park, K.M.; Park, K.D. *Macromolecules* **2009**, 42(10), 3437–3442.

28. White, J.E. *Ind. Eng. Chem. Prod. Res. Dev.* **1986**, 25, 395-400.

29. Patai, S.; *The Chemistry of the Thiol Group, Parts 1-2*, John Wiley and Sons, Inc., New York, 1974.

30. Menow-Garw, D. *J. Org. Chem.* **1972**, 37(24), 3797-3803.

31. Nebioglu, A.; Leon, J.A.; Khudyakov, I.V. *Ind. Eng. Chem. Res.* **2008**, 47, 2155-2159.

32. Elbert, D.L.; Hubbell, J.A. *Biomacromolecules* **2001**, 2(2), 430-441.

33. Heggli, M.; Tirelli, N.; Zisch, A.; Hubbell, J.A. *Bioconjugate Chem.* **2003**, 14, 967-973.

34. Lutolf, M.P.; Lauer-Fields, J.L.; Schmoekel, H.G.; Metters, A.T.; Wber, F.E.; Fields, G.B.; Hubbell, J.A., *Proc. Nat. Acad. Sci.* **2003**, 100(9), 5413-5418.

35. Lutolf, M. P.; Tirelli, N.; Cerritelli, S.; Cavalli, L.; Hubbell, J. A. *Bioconjugate Chem.* **2001**, 12, 1051.

36 Pratt, A.B.; Weber, F.E.; Schmoekel, H.G.; Mueller, R.; Hubbell, J.A. *Biotech. Bioeng.* **2004**, 86(1), 27-36.

37. Liu, Y.; Bingfeng, S. Wang, B.; Wakem, M.; Deng, L. *J. Am. Chem. Soc.* **2009**, 131, 418-419.

38. Chan, J.W.; Hoyle, C.E.; Lowe, A.B. *J. Am. Chem. Soc.* **2009**, 131(16), 5751-5753.

39. Chan, J.W.; Yu, B.; Hoyle, C.E.; Lowe, A.B. *Chem. Commun.* **2008**, 4959-4961.

40. Shin, J.; Matsushima, H.; Chan, J.W.; Hoyle, C.E *Macromolecules* **2009**, 42(9), 3294-3301.

41. Nurmiab, L.; Lindqvistb, J.; Randevb, R.; Syrettb, J.; Haddleton, D.H. *Chem. Commun.* **2009**, 2727-2729.

42. Yu, B.; Chan, J.W.; Hoyle, C.E.; Lowe, A.B. *J. Polym. Sci., Part A: Polym. Chem.* **2009**, 47(14), 3544-3557.

43. Friedman, M.; Cavins, J.F.; Wall, J.S. *J. Am. Chem. Soc.* **1965**, 87(16) 3672-3682.

44. Ignatov, V.A.; et. al. *Izvestiya Vysshikh Uchebnykh Zavedenii, Khimiya I Khimicheskaya Tekhnologiya* **1980**, 23(11), 1350-1355.

45. Hurd, Charles D.; Gershbein, Leon L. *J. Am. Chem. Soc.* **1947**, 69, 2328-35.

46. Bruice, P.Y. *Organic Chemistry, 3$^{rd}$ Ed.*, Prentice Hall, Upper Saddle River, NJ, USA, 2001.

47. Smith, M.B.; March, J.; *March's Advanced Organic Chemistry: Reactions, Mechanisms, Structure, 5$^{th}$ Ed.*, John Wiley and Sons, Inc., New York, 2001.

48. Serjeant, E.P.; Dempsey, B.; *Ionisation Constants of Organic Acids in Aqueous Solution.* Pergamon Press Inc., New York, 1979.

49. H.K. Hall, Jr. *J. Am. Chem. Soc.* **1957**, 79, 5441-5444

50. P. Neta; Schuler, R.H.; *J. Phys. Chem.* **1972**, 76(19), 2673-2679.

51. Bordwell, F.G. *Acc. Chem. Res.* **1988**, 21, 456-463.

52. Matthews, W.S.; Bares, J.E.; Bartmess, J.E.; Bordwell, F.G.; Cornforth, F.J.; Drucker, G.E.; Margolin, Z.; McCallum, R.J.; McCollum, G.J.; Vanier, N.R. *J. Am. Chem. Soc.* **1975**, 97(24), 7006-14.

53. Bernasconi, C.F. *Acc. Chem. Res.* **1987**, 20, 301-308.

54. Bernasconi, C.F. *Acc. Chem. Res.* **1992**, 25, 9-16.

55. Bernasconi, C.F.; Paschalis, P.; *J. Am. Chem. Soc.* **1986**, 108, 2969-2977.

56. Bernasconi, C.F.; Hibdon, S.A. *J. Am. Chem. Soc.* **1983**, 105, 4343-4348.

57. Bernasconi, C.F. *Tetrahedron* **1989**, 45(13), 4017-4090.

58. Bernasconi, C.F.; Killion, Jr., R.B. *J. Am. Chem. Soc.* **1988**, *110*, 7506-7512.

59. Bensa, D.; Rodriguez, J. *Syn. Commun.* **2004**, 34(8), 1515–1533.

60. Baidya, M.; Mayr, H. *Chem. Commun.* **2008** (15), 1792–1794.

61. Reed, R.R.; Réau, R.; Dahan, R.; Bertrand, G. *Angew. Chem. Int. Ed.* **1993**, 32(3) 399-401.

62. Jost, M.; Greie, J.-C.; Stemmer, N.; Wilking, S.D.; Altendorf, K.; Sewald, N. *Angew. Chem. Int. Ed.* **2002**, 41(22), 4267-4269.

63. Kumagai, N.; Matsunaga, S.; Shibasaki, M. *Angew. Chem. Int. Ed.* **2004**, 43, 478-482.

64. Margetic, D. In *Superbases for Organic Synthesis: Guanidines, Amidines, Phosphazenes and Related Organocatalysts*, Ishikawa, T., Ed.; John Wiley & Sons Ltd, West Sussex, 2009; p. 9.

65. Makinsky, A.A.; Kritzyn, A.M.; Uljanova, E.A.; Zakharova O.D.; Nevinsky, G.A. *Rus. J. Bioorg.Chem.* **2000**, 26(10), 662-668.

66. Danehy. J.P.; Noel, C.J. *J. Am. Chem. Soc.* **1960**, 82, 2511-2515.

67. psp pka

68. Stewart, I.C., Bergman, R.G., and Toste, F.D. *J. Am. Chem. Soc.* **2003**, 125, 8696-8697.

69. Nising, C.F., Stefan, Bräse, *Chem. Soc. Rev.* **2008**, 37, 1218–1228.

70. Gimbert, C.; Lumbierres, M.; Marchi, C.; Moreno-Mañas, M.; Sebastián, R.M.; Vallribera, A. *Tetrahedron* **2005,** 61, 8598–8605.

71. Klemarczyk, P. *Polymer* **2001**, 42(7), 2837-2848.

72. Henderson, Jr., W.A.; Streult, C. A. *J. Am. Chem. Soc.* **1960**, 82, 5791-5794.

73. Henderson, Jr., W.A.; Buckler, S.A. *J. Am. Chem. Soc.* **1960**, 82, 5794-5800.

74. Weston, Jr., R.; Bigeleisen, J. *J. Am. Chem. Soc.* **1954**, 76, 3074-3078.

75. Darensbourg, D.J.; Zimmer, M.S.; Rainey, P.; Larkins, D.L. *Inorg. Chem.* **2000**, 39, 1578-1585.

76. Hupe, D.J.; Jencks, W.P. *J. Am. Chem. Soc.* **1977**, 99(2), 451-464.

77. Dmuchovsky, B.; Bineyard, B.D.; Zienty, F.B. *J. Am. Chem. Soc.* 1964, 86, 2874-2877.
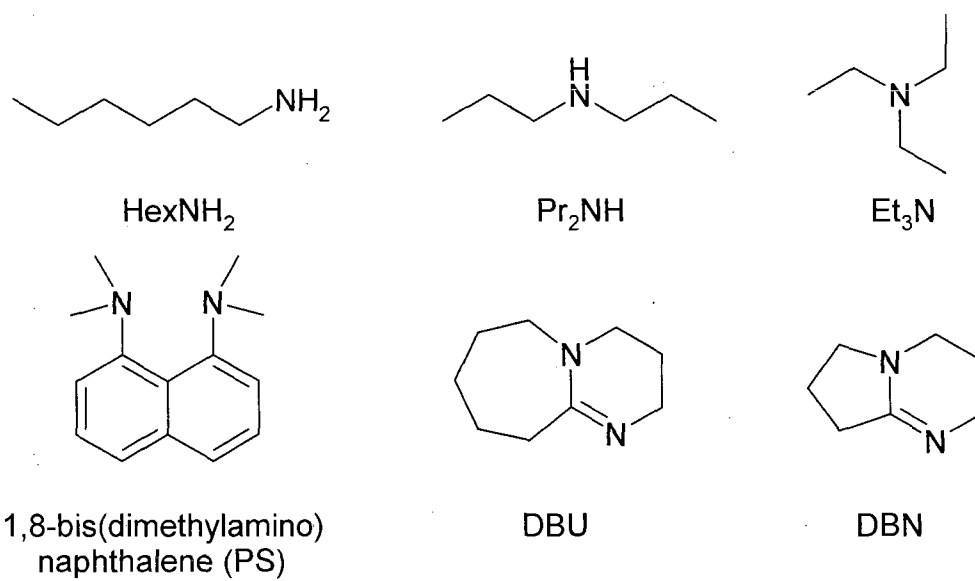
**Chart 3.1.** Structures of amine catalysts.
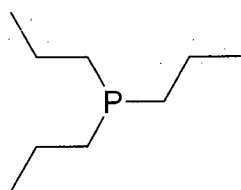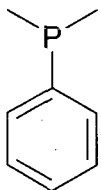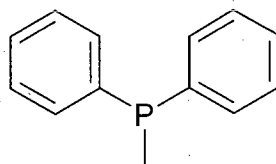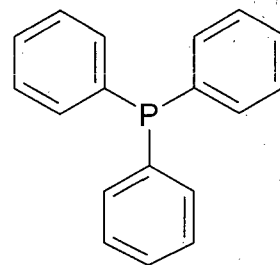
**Chart 3.2.** Structures of nucleophilic phosphine catalysts.
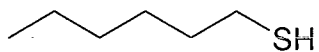
hexane thiol

(HT)
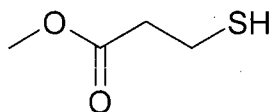
methyl 3-mercaptopropionate

(M3M)
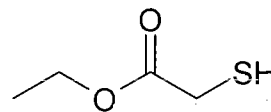
ethyl thioglycolate

(ETG)

**Chart 3.3.** Structures of thiols.
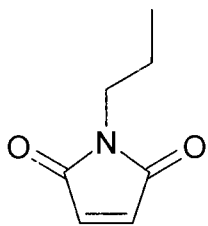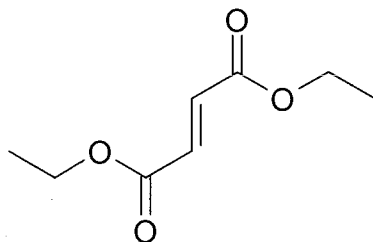
| | | |
|---|---|---|
| Propyl Maleimide | Diethyl Fumarate | Diethyl Maleate |
| Hexyl Acrylate | Ethyl Methacrylate | Ethyl Crotonate |
| Ethyl Cinnamate | Dimethyl Acrylamide | Acrylonitrile |
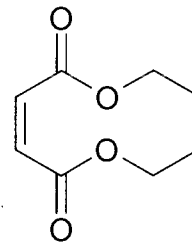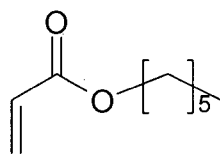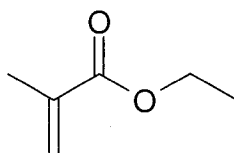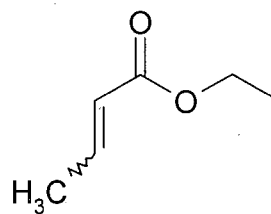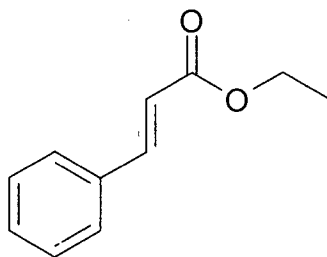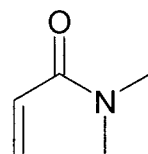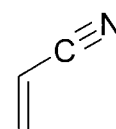
**Chart 3.4.** Structures of electron poor enes.

Initiation
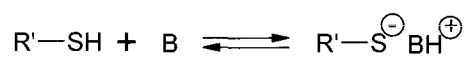


Propagation (polar solvent)
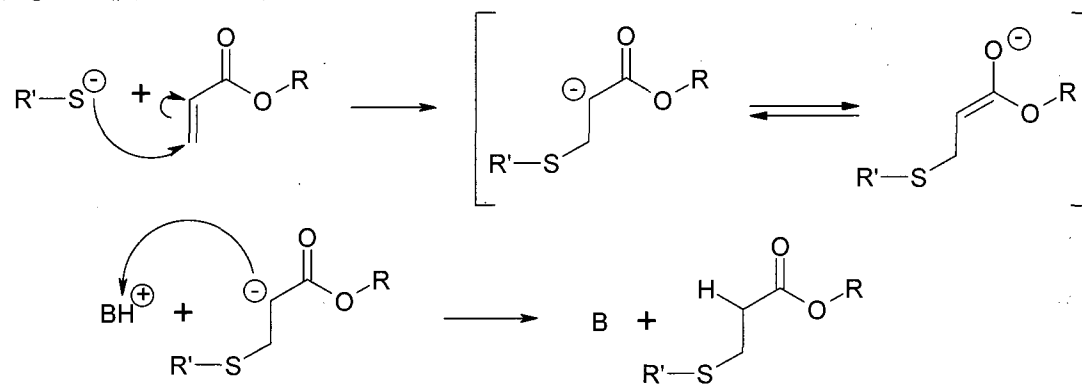


Propagation (non-polar solvent)
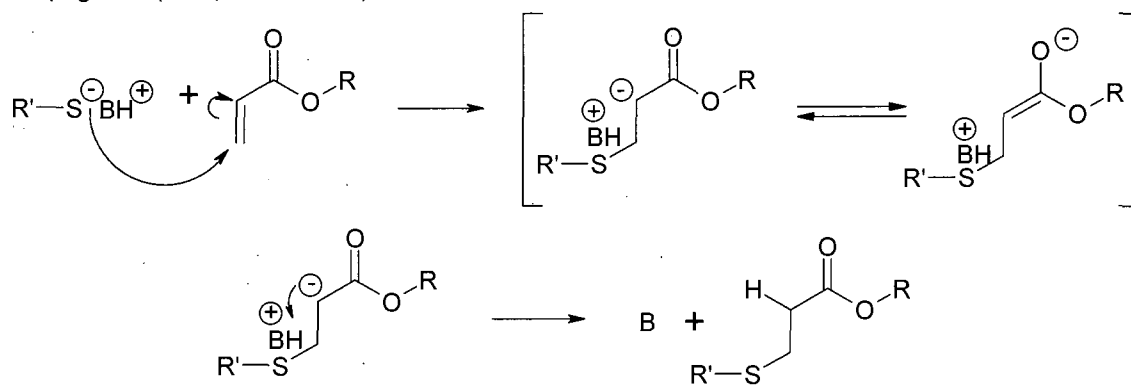


**Scheme 3.1.** Base catalyzed thio-Michael conjugate addition reaction.

Initiation
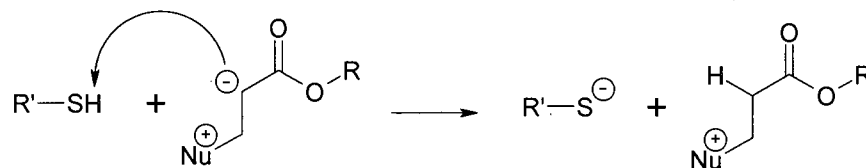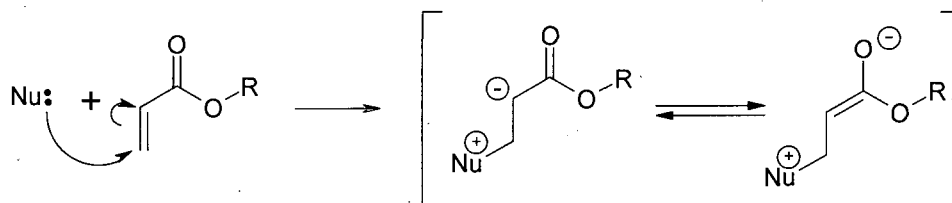


Propagation
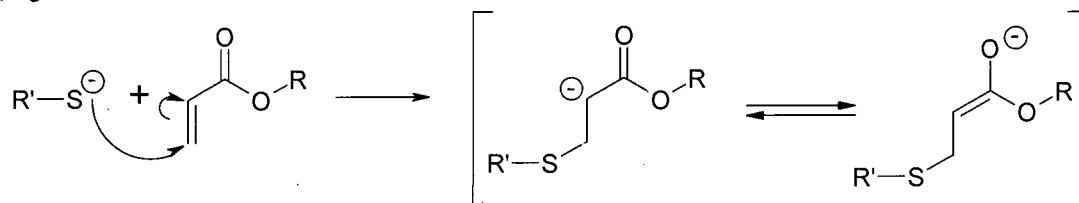


**Scheme 3.2.** Proposed nucleophile catalyzed thio-Michael conjugate addition reaction.

**Table 3.1.** Effect of amine catalyst ($pK_a$ values) on apparent rate constant.

| Thiol | Ene | Catalyst | $pK_a$ | M (mol*L$^{-1}$) | $k_{app}/10^{-4}$ (mol*L$^{-1}$*s$^{-1}$)[b] |
|-------|-----|----------|--------|------------------|-----------------------------------------------|
| HT | Hexylacrylate | HexNH$_2$ | 10.6 | 0.43 | 53.4 |
| | | Pr$_2$NH | 11.00 | 0.43 | 8.02 |
| | | Et$_3$N | 10.75 | 0.43 | 0.028[c] |

5mmole hexane thiol mixed with (0.43M) catalyst, 5mmole hexylacrylate added just before RTIR measurement; [a] HT $pK_a$ = 10.3; [b] rate constant taken at 30% conversion unless otherwise noted, [c] rate constant taken over 500 secs.

**Table 3.2.** Effect of amine catalyst (pK$_a$ values) on apparent rate constant.

| Thiol | Ene | Catalyst | pK$_a$ | M (mol*L$^{-1}$) | k$_{app}$/10$^{-4}$ (mol*L$^{-1}$*s$^{-1}$)[b] |
|-------|-----|----------|--------|------------------|-------------|
| HT | Hexylacrylate | PS | 12.1 | 0.4 | 0.020[c] |
| HT | Hexylacrylate | DBU | 11.6 | 0.4 | Too fast |
| | | | | 0.004 | 5.24 |
| HT | Hexylacrylate | DBN | 13.5 | 0.004 | 54.9 |

5mmole hexane thiol mixed with catalyst, 5mmole hexylacrylate added just before RTIR measurement; [a] HT pK$_a$ = 10.3; [b] rate constant taken at 30% conversion unless otherwise noted, [c] rate constant taken over 500 secs.; (PS=Proton sponge).

**Table 3.3.** Effect of phosphine catalyst on apparent rate constant.

| Thiol | Ene | Catalyst | M (mol*L$^{-1}$) | $k_{app}/10^{-4}$ (mol*L$^{-1}$*s$^{-1}$)[a] |
|-------|-----|----------|------------------|------------------------------------------------|
| HT | Hexyl acrylate | P($i$-Pr)$_3$ | 0.003 | 1811.9 |
| | | PMe$_2$Ph | 0.003 | 430.7 |
| | | PMePh$_2$ | 0.003 | 0.987 |
| | | PPh$_3$ | 0.003 | 0.01249[b] |

2M thiol mixed with (0.003M) catalyst in 45 wt% benzene, 2M hexylacrylate added just before RTIR measurement; [a] rate constant taken at 30% conversion unless otherwise noted, [b] rate constant taken at 500 seconds

**Table 3.4.** Effect of solvent and thiol $pK_a$ on apparent rate constant.

| Thiol | $pK_a$ (thiol) | Solvent[a] | Ene | Catalyst | M (mol*L$^{-1}$) | $k_{app}/10^{-4}$ (mol*L$^{-1}$*s$^{-1}$)[b] |
|-------|------|--------|-----|----------|-----|------|
| ETG | 7.95 | | Hexylacrylate | | | |
| | | Benzene | | TEA | 0.05 | 1.73[c] |
| | | Benzene | | HA | 0.05 | 162.4 |
| | | | | | | |
| | | Acetonitrile | | HA | 0.005 | Too fast |
| M3M | 9.33 | | Hexylacrylate | | | |
| | | Benzene | | HA | 0.05 | 6.90[c] |
| | | | | | | |
| | | Acetonitrile | | TEA | 0.05 | 2.88[c] |
| | | Acetonitrile | | HA | 0.05 | 17.3 |

2M thiol mixed with (0.05M) catalyst in solvent, 2M hexylacrylate added just before RTIR measurement; [a] 45 wt% solvent; [b] rate constant taken at 30% conversion unless otherwise noted, [c] rate constant taken at ~20% conversion.

**Table 3.5.** Effect of ene structure on conversion.

| Thiol | Ene | Conversion (%)[a] | Time (hours)[b] | $k_{app}/10^{-4}$ $(mol*L^{-1}*s^{-1})^c$ |
|-------|-----|------------------|-----------------|------------------------------------------|
| HT | Propyl maleimide | 99 | 3 | Very Fast |
| | Diethylfumarate | 99 | 3 | 40.0 |
| | Diethylmaleate | 99 | 3 | 28.5 |
| | $N,N$-dimethyl acrylamide | 99 | 3 | 18.6 |
| | Acrylonitrile | 99 | 3 | 0.67 |
| | Ethyl crotonate | 96 | 12 | 0.058[d] |
| | Ethyl cinnamate | 75 | 12 | 0.058[d] |
| | Ethyl methacrylate | 25 | 12 | 0.058[d] |

5mmole hexane thiol mixed with (0.2M) catalyst, 5mmole hexylacrylate and allowed to react at 25°C without stirring; [a] measured by ^{1}H NMR using $CDCl_3$ as solvent; [b] products were analyzed by ^{1}H NMR at 3 and 12 hours, final conversion may have been reached in shorter time. [c] rate constant taken at 30% conversion unless otherwise noted, [d] rate constant taken over 500 secs.
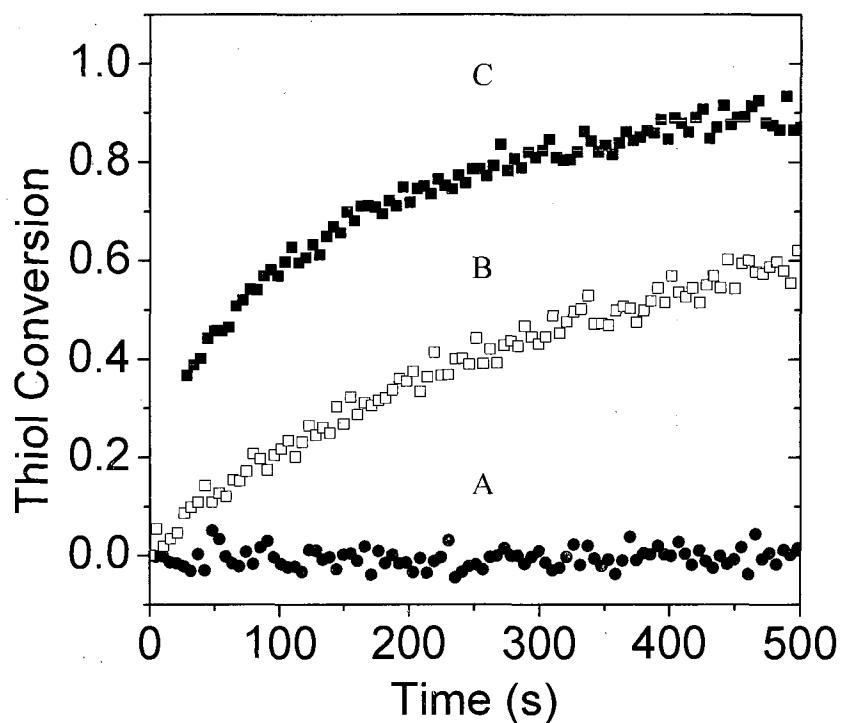
**Figure 3.1.** Thiol conversion vs. time kinetic profiles using amine catalysts. 5mmoles hexane thiol with 5mmoles hexyl amine with 0.4M catalyst: (■) hexylamine, (□) di-*n*-propylamine, and (●) triethylamine. (RTIR conversion of 2570 cm$^{-1}$)
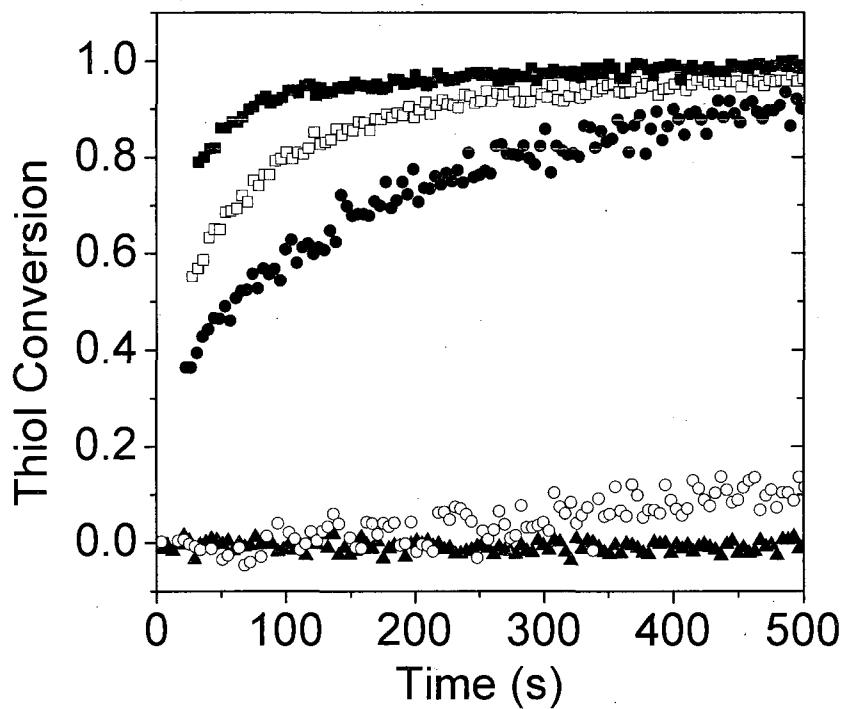
**Figure 3.2.** Thiol conversion vs. time kinetic profiles. 5mmoles hexanethiol with 5mmoles hexyl acrylate with (▲) 0M, (○) 0.05M, (●) 0.54M, (□) 0.54M, and (■) 0.75M hexylamine catalyst. (RTIR conversion of 2570 cm$^{-1}$)
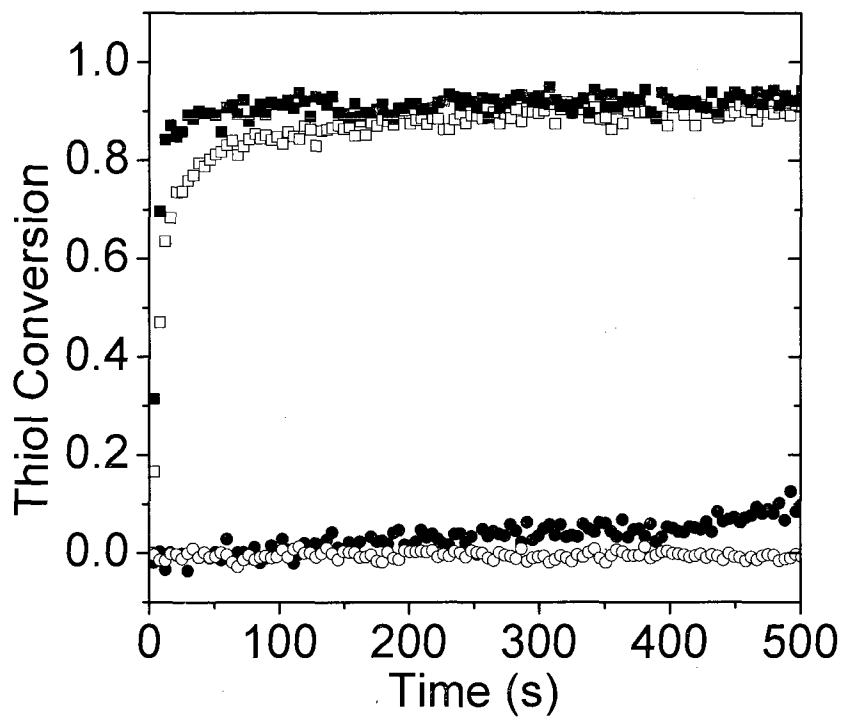
**Figure 3.3.** Thiol conversion vs. time kinetic profiles using phosphine catalysts. 2M hexane thiol with 2M hexyl acrylate with 0.003M catalyst: (■) P($n$-Pr)$_3$, (□) PMe$_2$Ph, (●) PMePh$_2$, and (○) PPh$_3$. (RTIR conversion of 2570 cm$^{-1}$)

# CHAPTER IV

## EFFECTS OF PRIMARY AMINE CATALYZED THIO-ACRYLATE MICHAEL REACTION ON THE KINETICS, MECHANICAL AND PHYSICAL PROPERTIES OF THIO-ACRYLATE NETWORKS

Abstract

Thio-acrylate networks were prepared using two methods. The first method involved the in-situ photopolymerization of a multifunctional thiol mixed with a multifunctional acrylate in the presence of a photoinitiator (photo-cure only), while the second method utilized an extremely efficient thio-acrylate Michael reaction followed by the photopolymerization of unreacted acrylate functional groups (amine catalysis/photo- cure). The thio-acrylate Michael reaction was catalyzed by a primary amine that promoted a rapid 1-to-1 Michael addition reaction of thiol to acrylate. Kinetic analysis via real-time infrared (RTIR) spectroscopy verified the 1-to-1 addition, the rates of the thio-acrylate Michael reaction and the total incorporation of the thiol into the networks at various concentrations when the amine catalyst was used. Differential scanning calorimetry (DSC) and dynamic mechanical thermal analysis (DMTA) data show very narrow glass transition temperatures for the networks prepared when the amine catalysis/photo-cure sequence was used. The two step sequential process can be used to target network films that can be tailored to have high energy damping properties at a given temperature, e.g. room temperature. Finally, in all cases, whether the photo-cure only or the amine catalysis/photo-cure process was used, the glass transition temperature increased with the initial acrylate feed concentration.

Introduction

Photoinitiated polymerization processes involving multi-(meth)acrylate

monomers are used in many applications including protective coatings, optical and

electronic components, and 3D structures.[1-4] The chain growth mechanism involved

in (meth)acrylate radical polymerization results in films with micro-domain structures

through formation of highly dense localized areas and inhomogenous networks.[5-7]

The inhomogeneity leads to broad glass transitions and incomplete monomer

conversions.[6-7]

An alternative to photopolymerization of simple (meth)acrylates and mixtures

of (meth)acrylates involves thiol-ene polymerization which has recently experienced a

resurgence.[3-5,8-19] Thiol-ene photoinitiated polymerizations, as opposed to simple

(meth)acrylates, proceed rapidly to high conversions in air by a free-radical step

growth process wherein thiols are added across ene double bonds to form sulfides.

The network structures formed are extremely uniform and exhibit physical and

mechanical properties that simply cannot be duplicated by other polymerization

systems.[11-19] For example, meth(acrylate) photopolymerized network systems are

brittle and show less adhesion than thio-acrylate systems.[8,9] Since thiols have the

ability to add across virtually any type of ene double bond, many different

combinations of binary thiol-ene and ternary thiol-ene-ene or thiol-ene-(meth)acrylate

systems have been investigated.[12-16] Because of the wide availability of monomers

with different ene groups, it is possible to tailor the physical and mechanical

properties of binary and ternary network structures to meet a diversity of

applications.[20-31] Binary thiol-ene reactions consist of two types. The first type

involves the free-radical step-growth chain reaction of a multifunctional thiol and a

multifunctional ene that does not otherwise undergo homopolymerization. The second type, shown in **Figure 4.1.**, involves two simultaneous radical chain processes, the addition of a multifunctional thiol to a multifunctional ene such as a (meth)acrylate and the simultaneous homopolymerization of the meth(acrylate).[4,13,17-19] Such dual radical processes lead to unique networks, but in certain cases they are difficult to control and can lead to networks with broadened mechanical energy loss transition regions when the (meth)acrylate concentration is high.

Recently, it has been shown that the Michael addition reaction involving the addition of thiols to electron deficient double bonds such as (meth)acrylates can be achieved by the use of primary amine or secondary amine catalysts.[32-39] Such systems proceed by a nucleophilic initiated anionic chain process that results in much faster rates that can be achieved using traditional amines such as trialkyl amines, which are thought to function as base catalysts that are relatively inefficient in the formation of thiolate anions. Accordingly, primary and secondary amines in catalytic amounts (<2 wt%) produce a 1-to-1 reaction of thiol with acrylate leading to high conversions (>95%) in short time periods (2-3 minutes or less).

Herein, we report two different protocols for curing the same trithiol-triacrylate mixture. In the first case, the trithiol-triacrylate mixture is initially reacted by addition of a nucleophilic amine catalyst that induces an efficient thio-acrylate Michael reaction (**Figure 4.1.a**). This amine catalyzed reaction leads to high conversions, and when an excess of acrylate groups is present initially, all of the thiol will be consumed by the Michael reaction with acrylate leaving excess acrylate groups, which can be subsequently photo-cured by an efficient acrylate homopolymerization process. In the second case (photo-cure only), the thio-acrylate

mixture is exposed to light with no prior thio-acrylate Michael reaction and only the

reactions in **Figure 4.1.b** occur, i.e., the initial amine catalyzed thio-acrylate Michael

reaction in **Figure 4.1.a** does not occur. Herein, we clearly show that by varying the

thiol:acrylate molar functional group ratio and the protocol for curing (amine

catalysis/photo-cure or photo-cure only), it is possible to control the final network

structure. A general methodology for tailoring the mechanical and performance

properties of networks formed from the same starting materials simply by changing

curing protocol will be clearly demonstrated, this opens up the way for a wide variety

of applications such as energy absorbing thermosets, protective coatings, and

advanced optical devices.

<div align="center">Experimental</div>

*Materials*

Trimethylol propane triacrylate (TMPTA) and trimethylol propane tris(3-

mercaptopropionate) (trithiol) were obtained from Sartomer Chemical and Bruno

Bock, respectively, and used without further purification. The chemical structure of

TMPTA and trithiol used in this study are shown in **Figure 4.2**. Irgacure® 651, $\alpha,\alpha$-

dimethoxy-$\alpha$-phenylacetophenone, was obtained from Ciba Specialty Chemicals.

Hexyl amine was obtained from Aldrich Chemical Co. and used without further

purification. Trithiol-TMPTA mixtures were prepared by blending the trithiol into the

TMPTA based on molar functional group concentration. The amount of UV initiator

used was 2 wt%. The amount of amine catalyst, when used, was 1 weight %. Films on

glass plates (200 μm) were photo-cure on a Fusion curing line (10 passes) with a D

bulb (belt speed of 10 feet/min, 3.1 W/cm$^2$ irradiance). Films cure with amine catalyst

were allowed to react for 24 hours before irradiating with UV light, although the thio-acrylate Michael reaction reactions were essentially complete in only a few minutes.

*Characterization*

Real-time FTIR was used to determine the kinetics of the reaction using a modified Bruker 88 spectrometer. UV light from an Oriel lamp system equipped with a 200 W high pressure mercury-xenon bulb was channeled through an electric shutter and fiber optic cable in the sample chamber. Photopolymerizations were conducted in a cell prepared by sandwiching the samples between two sodium chloride salt plates at a thickness of ~20 μm using a light intensity of 0.55 mW/cm$^2$ measured with an IL-1400 calibrated radiometer from International Light. IR absorption spectra were obtained under continuous UV irradiation at a scanning rate of 5 scans per second. The characteristic IR absorbance bands used to monitor the disappearance of the reactant and monomer during the photoreactions were ene: 812 cm$^{-1}$ and thiol: 2570 cm$^{-1}$. The reactant conversions were calculated by integrating the peak areas as a function of time.

Differential scanning calorimetry (DSC) was used to determine the $T_g$ of cure samples on a TA Instrument DSC Q1000. All measurements were conducted under nitrogen at 10 °C/min heating and cooling rates. All samples were heated to ~50 °C above the $T_g$ to remove thermal history before the analysis. Dynamic mechanical thermal analysis (DMTA) was used to determine the thermal transitions and mechanical properties of cure samples on a Rheometric Scientific DMTA V. Persoz pendulum hardness (ASTM D-4366 using a BYK-Gardner pendulum hardness tester with a square frame pendulum) values are the average of 6 measurements.

*Film Preparation*

Two types of films were prepared. In the first case, trithiol was mixed with 2 wt% Irgacure® 651 and/or 1 wt% hexyl amine in the sonicator for 10 minutes in a scintillation vial. The solution was then mixed with TMPTA until no bubbles remained in the vial. Films (either 500 or 300 micron thick depending upon whether used for DMTA or other analysis) made between glass plates with spacers were allowed to cure at room temperature for 24 hours. The samples were then photo-cure on a Fusion curing line (10 passes) with a D bulb (belt speed of 10 feet/min, 3.1 W/cm$^2$ irradiance). In the second case, films prepared in the absence of amine were immediately photo-cure on the same Fusion line system.

## Results and Discussion

Results of the two types of methodologies for polymerization of several binary combinations of trimethylol propane triacrylate (TMPTA) and trimethylol propane tris(3-mercaptopropionate) (trithiol) are presented and direct comparisons are made with respect to kinetics and thermal/mechanical properties of the polymerized networks. The two monomers were chosen to exemplify the strategy of using the amine catalyzed thio-acrylate Michael reaction to set up the gel structure followed by a subsequent free-radical photopolymerization process to produce a final cure network. The reaction kinetics and subsequent thermal scanning and dynamic mechanical analysis of the cure films are presented. The rationale for conducting sequential amine catalysis and photo-curing will be clearly and succinctly established. Before proceeding, it should be noted that the light irradiance used for the real-time infrared (RTIR) kinetic analysis is much lower than that used for photo-curing the

samples for materials analysis. The latter process uses a very high irradiance source with multiple exposure sequences in order to attain high, essentially quantitative conversion.

*Kinetics of Photo-Cure Only Systems*

In order to establish a basis for comparison with the sequential processing method for producing films from mixtures of TMPTA and trithiol, photopolymerization in the absence of the amine catalyzed step was first performed. **Figure 4.3.** shows the results for samples that were only exposed to the light source (photo-cure only). All compositions are defined as listed in **Table 4.1.** on a functional group mol% basis where the sum of acrylate functional groups plus the thiol functional groups is taken as 100 mol% of functional groups; both TMPTA and trithiol have three functional groups each. Since we will ultimately be concerned with the total functional groups left unconverted, all kinetic and conversion results presented (with the exception of the results in **Figure 4.7.a**) are based on 100 mol% representing the combination of all the thiol and acrylate functional groups added together. In other words, in a 50:50 mol% initial system if half of the thiol groups were converted (i.e. 50% of the thiol functional groups reacted) the conversion would be listed as 25 mol%. Concomitantly, kinetic plots of conversion versus time are also presented in terms of the mol% of either thiol or acrylate functional groups reacted assuming 100 mol% to be the sum of the thiol functional groups plus the acrylate functional groups. From the photopolymerization RTIR results in **Figure 4.3.** for thiol (**Figure 4.3.a**) and TMPTA (**Figure 4.3.b**), mol% functional group conversion versus time plots of samples containing 50-100 mol% acrylate functional groups in the initial feed, it is apparent that the rate of free-radical acrylate homopolymerization

induced by UV light is faster than that of the thio-acrylate free-radical chain process. This has been demonstrated in numerous papers and is only presented herein to provide a direct comparison for the samples polymerized by the two step amine catalysis/photo-cure curing sequence [13,17-19]. The final mol% conversions for all samples are given in **Table 4.1.** for comparison. For samples with greater than 20 mol% acrylate functional groups in the initial feed, a significant amount of unreacted thiol groups was found in each system under the light intensity conditions employed. For a 50:50 mol% ratio of thiol to acrylate, the total amount of thiol incorporated into the networks is only 21.5 mol% while all (i.e., 50 mol%) of the acrylate reacts. At a 50:50 mol% ratio the thiol does not attain high conversion since the acrylate homopolymerization is much faster. This leaves substantial unconverted thiol in the final matrix. As the ratio of acrylate to thiol concentration increases, the network crosslink density increases. The results in **Table 4.1.** show that a maximum amount of thiol groups incorporated into the network occurs when the thiol to acrylate mol% functional group ratio is 40:60. Even though the amount of thiol in the feed sample decreases from the 50:50 mol% thiol:acrylate mixture, the amount of thiol incorporated into the network attains a maximum for the 40:60 mol% thiol:acrylate mixture. **Figure 4.4.** clearly shows that the total combined amount of unreacted mol% acrylate plus unreacted mol% thiol reaches a minimum for the 30:70 mol% system, and hence the highest combined mol% conversion of thiol plus acrylate groups in any of the photo-cure only systems.

*Amine Catalysis/Photo-Cure Kinetics*

**Figure 4.5.** demonstrates the efficacy of the primary amine as a nucleophilic catalyst for thio-acrylate network formation. Each mixture shows a 1-to-1 conversion

of acrylate to thiol with 1 wt% hexyl amine as the catalyst. It has been reported that primary amines lead to very fast thio-acrylate Michael reaction rates.[37,38] It is noted that use of triethyl amine with essentially the same pKa as hexyl amine requires very long reaction times to attain the same thio-acrylate conversions shown in **Figure 4.5.** This is suggestive that the primary amine is functioning as an efficient nucleophilic catalyst to initiate a fast anionic chain type reaction comparable to that which has been reported for the addition of aliphatic alcohols and acrylates.[40] Because the thiol $pK_a$ is much lower than that of a comparable alcohol (by a factor of ~5 orders of magnitude), the thio-acrylate Michael reaction is a much more efficient and rapid reaction. The complete kinetic analysis of primary amines as nucleophilic catalysts for thio-acrylate Michael reactions will be reported in a separate paper. One particularly noteworthy facet about the results in **Figure 4.5.** is that the conversions are presented only for the first 1100 seconds after mixing. In all cases the conversion for the thiols is essentially quantitative, i.e., in each case even though a crosslinked matrix forms, all of the thiol reacts if enough time is allowed, leaving only unreacted acrylate. This means that 20 mol% thiol and 20 mol% acrylate conversion (based on 100 total mol% of the sum of thiol plus acrylate functional groups) will be attained for the thiol:acrylate 20:80 mol% mixture, 30 mol% thiol and 30 mol% acrylate conversion will be attained for the thio-acrylate 30:70 mol% mixture, and so forth. (**Figure 4.6.** expands the time scale of the results in **Figure 4.5.** of a 50:50 mol% thiol:acrylate showing near complete conversion of both thiol and acrylate in ~2hours using 1 wt% hexyl amine catalyst.) At a higher amine concentration and/or higher temperatures full conversion of thiol and acrylate occurs in a much shorter amount of time.

The results in **Figure 4.7.** deal with the photo-cure conversion of the subsequent homopolymerization of acrylate that was not consumed in the amine catalyzed thio-acrylate Michael reaction. Therefore, for the 40:60 mol% thiol:acrylate mixture, 20 mol% unreacted acrylate remains. The plots in **Figure 4.7.** show the additional mol% conversion of unreacted acrylate by the photo-cure after the amine catalyzed cure, i.e., the curve labeled 40:60 shows that 19 mol% of the 20 mol% of unreacted acrylate remaining after the amine catalyzed cure reacts in the photo-cure step. The conversions in **Figure 4.7.** which are collected in numerical format in **Table 4.2.** clearly demonstrate that the unreacted acrylate groups (remaining after the initial thio-acrylate amine catalyzed thio-acrylate Michael reaction) converted by homopolymerization in the photo-cure step decreased as the initial mol% of acrylate in the mixture (or the amount of unreacted acrylate present prior to the photopolymerization step) increased. RTIR results confirm the supposition that for each mixture in **Tables 4.1.** and **4.2.** (50-100 mol% acrylate) the amine catalyzed curing results in reaction of all thiol groups prior to exposure to the UV light source. The results in **Figure 4.8.** and **Tables 4.1.** and **4.2.** clearly indicate the rationale for employing the amine catalysis/photo-cure reaction sequence, a processing strategy based upon first reacting all of the thiol functional groups with acrylate groups via a thio-acrylate Michael reaction process followed by the photopolymerization process to convert unreacted acrylate. The two step sequence certainly ensures that no unreacted thiol groups exist in the final cure networks.

*DSC and DMTA Analysis*

DSC analysis of each cure system (both amine catalysis/photo-cure and photo-cure only) was conducted to identify thermal transitions. In **Figure 4.9.a**, the $T_g$ of

the amine catalysis/photo-cure 50:50 mol% thiol:acrylate mixture shows the narrowest glass transition region of all of the systems investigated. As the amount of acrylate increases the glass transition region broadens and the glass transition temperature increases, as expected for incorporation of acrylate homopolymer which is known to lead to inhomogenous structures with higher glass transition temperatures.[14-16] In **Figure 4.9.b** a similar trend is seen for samples obtained by simply photo-curing with no initial amine catalyzed thio-acrylate Michael reaction, i.e., according to the protocol used to produce the samples in **Table 4.1**. In these cases, the glass transition temperature range for each mixture is broader and higher than the corresponding systems that were amine catalyzed prior to photo-curing.

In order to substantiate the results in **Figure 4.9.** obtained by DSC, DMTA scans of each system, both with and without the amine catalyzed curing step, were obtained in the tensile mode. Tan δ vs. temperature and E' vs. temperature plots are given in **Figures 4.10.** and **4.11**. In each case in **Figure 4.11.**, the E' values in the rubbery phase increased as the acrylate concentration increased. In accordance with the results in **Figure 4.9.**, for amine catalysis/photo-cure samples, the Tan δ plots in **Figure 4.10.** had peak maxima at much lower temperatures and the transitions were narrower as indicated by the full-width half-maximum (FWHM) values for the samples with 60-100 mol% acrylate. This certainly substantiates that the amine catalysis/photo-cure networks are much more uniform. We note that the photo-cure only sample with 50 mol% acrylate had a similar Tan δ maximum and FWHM value as the completely amine catalyzed sample. This low temperature transition maximum results from substantial concentrations of unreacted thiol groups. **Table 4.1.** shows that 57 % [(50 mol%-21.5 mol%)/100 mol%] of the thiols are unreacted for the 50:50

thiol:acrylate molar mixtures. In fact, as shown in **Table 4.3.** for the collected Tan

$\delta$ peak maxima temperatures ($T_{max}$) and FWHM values for each sample in **Figure**

**4.10.**, one notes a direct correlation between the differences, $\Delta T$, in $T_{max}$ values

between the amine catalysis/photo-cure and photo-cure only samples and the percent

of unreacted thiol values from **Table 4.1**. And, as already noted, for the 50:50 mol%

thiol:acrylate systems, the $T_g$s of both the amine catalysis/photo-cure and photo-cure

only samples have about the same values. Apparently, the lower $T_g$ afforded by the

large concentration of flexible sulfide units in the amine catalysis/photo-cure sample

is influenced by having a large concentration of dangling unreacted thiol groups

which effectively plasticize the matrix.

Next more traditional physical damping and pencil hardness measurements

were conducted on all of the films, both amine catalysis/photo-cure and photo-cure

only. The evaluations were all conducted at room temperature. First, consider the

results in **Table 4.4.** for the photo-cure only samples. It is obvious that there is a

marked increase in the pencil hardness for the sample with 60 mol% acrylate where

according to **Table 4.1.**, the actual percentage of unreacted thiol decreased from 35%

to 57% (note %, not mol%) for the sample with 50 mol% acrylate. The pencil

hardness accordingly remained high for the samples with greater than 60 mol%

acrylate. Next consider the Persoz hardness which is a measure of energy damping

and is heavily influenced by the energy loss which occurs at mechanical transitions,

i.e., $T_g$. Consider first the amine catalysis/photo-cure samples where the

measurements were all made at room temperature. It can be seen from **Figure 4.10.**

that the Tan $\delta$ versus temperature plots for the 60 % and 70 % acrylate samples

indicate substantial energy loss with corresponding low damping times (42 and 48

secs) at room temperature. For the samples with 50 mol% and 80 mol% acrylate, there is less energy loss at room temperature, consistent with the higher damping times (73 and 72 secs) which indicate less damping. Next consider the photo-cure only samples. The damping times for the 50 mol% and 60 mol% acrylate based films exhibit Persoz damping times reflective of their Tan δ values at room temperature. The damping times for the 70 mol% and 80 mol% acrylate based films are extremely high (235 and 262 secs) corresponding to the very low Tan δ values at room temperature in **Figure 4.10.** for the 70 mol% and 80 mol% acrylate based samples. The final result is that networks can be produced at room temperature that have very high energy damping, and yet exhibit excellent pencil hardness, i.e., excellent scratch resistance.

## Summary and Conclusions

Two processes have been used to cure a thiol:acrylate system, a standard photo-curing (photo-cure only) reaction and an amine catalyzed thio-acrylate Michael reaction followed by the photocuring of any unreacted acrylate (amine catalysis/photo-cure). The resultant physical, thermal and mechanical properties of the films were characterized. In both cases, increasing the amount of acrylate in the thiol:acrylate mixture increased and broadened the glass transition of the resultant network. DMTA and DSC analysis indicated the formation of highly uniform networks, i.e. narrow glass transition regions, for all of the amine catalysis/photo-cure and photo-cure only networks. The sequential amine catalysis/photo-cure produced films exhibited narrowed glass transition temperature regions at lower temperatures. Both DMTA and Persoz analysis indicated that amine catalysis/photo-cure films

produced with higher acrylate content (70 % and 80 %) had higher energy damping ability than the corresponding photo-cure films. Pencil hardness measurements were not apparently a function of the curing process, thus allowing films with simultaneous high energy damping and excellent hardness to be obtained. Finally, it is noted that although long times were used in the present study for the amine cure reactions in order to ensure high conversion after gelation for the 1:1 molar system, in general the amine cure reaction can be achieved in 1-2 minutes for most of the mixtures if higher amine concentrations are used. This makes the overall two sequence process quite viable for many applications which would benefit from tuning the properties of films produced from thiol:acrylate mixtures by use of a controlled dual processing methodology.

## Acknowledgments

References

1. Hoyle, C.E.; Cole, M.; Bachemin, M.; Kuang, W.; Viswanathan, K.; Jonsson S. ACS Symposium Series **2003**, 847, (Photoinitiated Polymerization), 52-64.

2. Cole, M.C.; Bachemin, M.; Nguyen, C.K.; Viswanathan, K.; Hoyle, C.E.; Jonsson, S. Hall HK Experience the World of UV/EB RadTech 2000, The Premier UV/EB Conference & Exhibition Technical Conference Proceedings Baltimore, MD, United States, Apr 9-12, **2000**, 211-220.

3. Roper, T.M.; Hoyle, C.E.; Magers, D.H. *Photochemistry and UV Curing* **2006**, 253-264.

4. Hoyle, C.E.; Lee, T.Y.; Roper, T. *J. Polym. Sci., Part A: Polym. Chem.* **2004**, 42(21), 5301-5338.

5. Bowman, C.N.; Okay, O.; Redy, S. *Macromolecules* **2005**, 38, 4501-4511.

6. Bowman, C.N.; Anseth, K.S. *Chem. Eng. Sci.* **1994**, 48(14), 2207-2217.

7. Peppas, N.; et al. *Polym. Bull.* **1993**, 31, 229-233.

8. Bunel, C.; Youssef, B.; et al. *Polymer* **2007**, 42, 2727-2736.

9. Morgan, C.R.; Ketly, A.D. *J. Polym. Sci. Part C: Polym. Lett.* **1978**, 16, 75.

10. Jacobine, A.F. in: Fouassier, J.B.; Rabek, J.F. *Radiation Curing in Polymer Science and Technology* vol. 3 New York: Elsevier, **1993**, 219.

11. Cramer, N.B.; Bowman, C.N. *Macromolecules* **2002**, 35, 5361.

12. Lee, T.Y.; Kaung, W.; Jonsson, E.S.; Lowery, K.; Guymon, C.A.; Hoyle, C.E. *J. Polym. Sci., Part A: Polym. Chem.* **2004**, 42(17), 4424-4436.

13. Rydholm, A.E.; Held, N.L.; Benoit, D.S.W.; Bowman, C.N.; Anseth, K.S. *J. Biomed.Mater. Res. Part A.* **2008**, 86A(1), 23-30.

14. Senyurt, A.F.; Wei, H.; Phillips, B.; Cole, M.; Nazarenko, S.I.; Hoyle, C.E.; Piland, S.G.; Gould, T.E. *Macromolecules* **2006**, 39(19), 6315-6317.

15. Wei. H.; Senyurt, A.F.; Jonsson, S.; Hoyle, C.E. *J. Polym. Sci., Part A: Polym. Chem.* **2007**, 45(5), 822-829.

16. Senyurt, A.F.; Wei, H.; Hoyle, C.E.; Piland, S.G.; Gould, T.E. *Macromolecules* **2007**, 40(14), 4901-4909.

17. Rydholm, A.E.; Reddy, S.K.; Anseth, K.S.; Bowman, C.N. *Biomacromolecules* **2006**, 7(10), 2827-2836.

18. Cramer, N.B.; Bowman, C.N. *J. Polym. Sci., Part A: Polym. Chem.* **2001**, 39(19), 3311-3319.

19. Johnson, P.M.; Stansbury, J.W.; Bowman, C.N. *J. Polym. Sci., Part A: Polym. Chem.* **2008**, 46(4), 1502-1509.

20. Senyurt, A.F.; Warren, G.; Whitehead, J.B.; Hoyle, C.E. *Polymer* **2006**, 47(8), 2741–2749.

21. Beckel, E.R.; Cramer, N.B.; Harant, A.W.; Bowman, C.N. *Liq. Cryst.* **2003**, 30(11), 1343–1350.

22. Cramer, N.B.; Beckel, E.R.; Harant, A.W.; Davies, T.; Williamson, D.L.; Bowman, C.N. *Liq. Cryst.* **2002**, 29(10), 1291–1296.

23. Wutticharoenwong, K.; Soucek, M.D. *Macromol. Mater. Eng.* **2008**, 293, 45- 56.

24. Carioscia, J.A.; Lu, H.; Stansbury, J.W.; Bowman, C.N. *Dent. Mater.* **2005**, 21(12), 1137–1143.

25. Lu, H.; Carioscia, J.A.; Stansbury, J.W.; Bowman, C.N. *Dent. Mater.* **2005**, 21(12), 1129–1136.

26. Hagberg, E.C.; Malkoch, M.; Ling, Y.B.; Hawker, C.J.; Carter, K.R. *Nano. Lett.* **2007**, 7(2), 233–237.

27. Khire, V.S.; Yi, Y.; Clark, N.A.; Bowman, C.N. *Adv. Mater.* **2008**, 20(17), 3308-3313.

28. Campos, L.M.; Meinel, I.; Guino, R.G.; Schierhorn, M.; Gupta, N.; Stucky, G. D.; Hawker, C.J. *J. Adv. Mater.* **2008**, 20(19), 3728-3733.

29. Natarajan, L.V.; Brown, D.P.; Wofford, J.M.; Tondiglia, V.P.; Sutherland, R.L.; Lloyd, P.F.; Bunning, T.J. *Polymer* **2006**, 47(12), 4411–4420.

30. Natarajan, L.V.; Shepherd, C.K.; Brandelik, D.M.; Sutherland, R.L.; Chandra, S.; Tondiglia, V.P.; Tomlin, D.; Bunning, T.J. *Chem. Mater.* **2003**, 15(12), 2477–2484.

31. White, T.J.; Natarajan, L.V.; Tondiglia, V.P.; Lloyd, P.F.; Bunning, T.J.; Guymon, C.A. *Macromolecules* **2007**, 40(4), 1121-1127.

32. Khire, V.S.; Lee, T.Y.; Bowman, C.N. *Macromolecules* **2007**, 40(16), 5669-5677.

33. Khire, V.S.; Kloxin, A.M.; Couch, C.L.; Anseth, K.S.; Bowman, C.N. *J. Polym. Sci., Part A: Polym. Chem.* **2008**, 46(20), 6896-6906.

34. Khire, V.S.; Lee, T.Y.; Bowman, C.N. *Macromolecules* **2008**, 41(20), 7440-7447.

35. Shin, J.; Matsushima, H.; Chan, J.W.; Hoyle, C.E. *Macromolecules* **2009**, 42(9), 3294-3301.

36. Li, M.; De, P.; Gondi, S.R.; Sumerlin, B.S. J. Polym. Sci., Part A: Polym. *Chem.* **2008**, 46, 5093.

37. Sanui, K.; Ogata, N. *Bull. Chem. Soc. Jpn.* **1967**, 40, 1727.

38. Chan, J.W.; Yu, B.; Hoyle, C.E.; Lowe, A.B. *Chem. Comm.* **2008**, 40, 4959-4961.

39. Qiu, X.P.; Winnik, F.M. *Macromol. Rapid. Comm.* **2006**, 27(19), 1648-1653.

40. Stewart, I.C.; Bergman, R.G.; Toste, F.D. *J. Am. Chem. Soc.* **2003**, 125, 8696.

**Table 4.1.** Feed ratios, acrylate homopolymerization and thiol-acrylate co-polymerization for photo-cured only systems. Light intensity: 18.7 mW/cm$^{-2}$ with 1 wt% α,α-dimethoxy-α-phenylacetophenone (Irgacure® 651) as photoinitiator.*

| Initial Acrylate Feed (mol%) | Initial Thiol Feed (mol%) | Thiol Conversion (mol%) | Acrylate Conversion (mol%) | Total Reacted Thiol + Acrylate (mol%) | Total Unreacted Thiol + Acrylate (mol%) |
|---|---|---|---|---|---|
| 50 | 50 | 21.5 | 50 | 71.5 | 28.5 |
| 60 | 40 | 26 | 59.4 | 85.4 | 14.6 |
| 70 | 30 | 24 | 65.1 | 89.1 | 10.9 |
| 80 | 20 | 16.6 | 70.4 | 87 | 13.0 |
| 90 | 10 | 9.6 | 67.5 | 77.1 | 22.9 |
| 100 | 0 | -- | 71 | 71 | 29 |

*Sum of acrylate functional groups plus thiol functional groups taken as 100 mol% of functional groups.

**Table 4.2.** Feed ratios, acrylate homopolymerization and thiol-acrylate co-polymerization for amine catalysis/photo-cure systems. 1 wt% hexyl amine and light intensity: 18.7 mW/cm$^{-2}$ with 2 wt% α,α-dimethoxy-α-phenylacetophenone (Irgacure® 651) as a photoinitiator.*

| Initial Acrylate Feed (mol%) | Initial Thiol Feed (mol%) | Acrylate Remaining after Amine Catalysis (mol%) | Acrylate Conversion with Photocure after Amine Catalysis (mol%) | Acrylate (Total) Conversion (mol%) | Thiol Conversion (mol%) | Total Reacted Thiol + Acrylate (mol%) |
|---|---|---|---|---|---|---|
| 50 | 50 | 0 | 0 | 50 | 50 | 100 |
| 60 | 40 | 20 | 19 | 59 | 40 | 99 |
| 70 | 30 | 40 | 35 | 65 | 30 | 95 |
| 80 | 20 | 60 | 46 | 66 | 20 | 88 |
| 100 | 0 | 100 | 71 | 71 | 0 | 71 |

*Sum of acrylate functional groups plus thiol functional groups taken as 100 mol% of functional groups.

**Table 4.3.** Temperature at tan $\delta$ peak maximum ($T_{max}$) and temperature difference ($\Delta T$) between different peak maxima temperatures for systems cured with photo-cure only and amine catalysis/photo-cure processes.

| Initial Acrylate Feed (mol%) | $T_{max}$ (°C)* | FWHM (°C)* | $T_{max}$ (°C)** | FWHM (°C)** | $\Delta T$ (°C) |
|---|---|---|---|---|---|
| 50 | 2 | 25 | 5 | 28 | -3 |
| 60 | 33 | 28 | 10 | 21 | 23 |
| 70 | 95 | 55 | 37 | 44 | 58 |
| 80 | 142 | 110 | 82 | 105 | 60 |

* photo-cure only
** amine catalysis/photo-cure

**Table 4.4.** Persoz and pencil hardness measurements of films prepared.

| Initial Acrylate Feed (mol%) | Persoz* | Pencil Hardness** | Persoz* | Pencil Hardness** |
|---|---|---|---|---|
| 50 | 74 ± 4 | HB | 73 ± 3 | HB |
| 60 | 56 ± 2 | 8H | 42 ± 2 | 8H |
| 70 | 235 ± 3 | 8H | 48 ± 4 | 8H-9H |
| 80 | 262 ± 3 | 9H+ | 72 ± 2 | 9H+ |

\* photo-cure only
\*\* amine catalysis/photo-cure
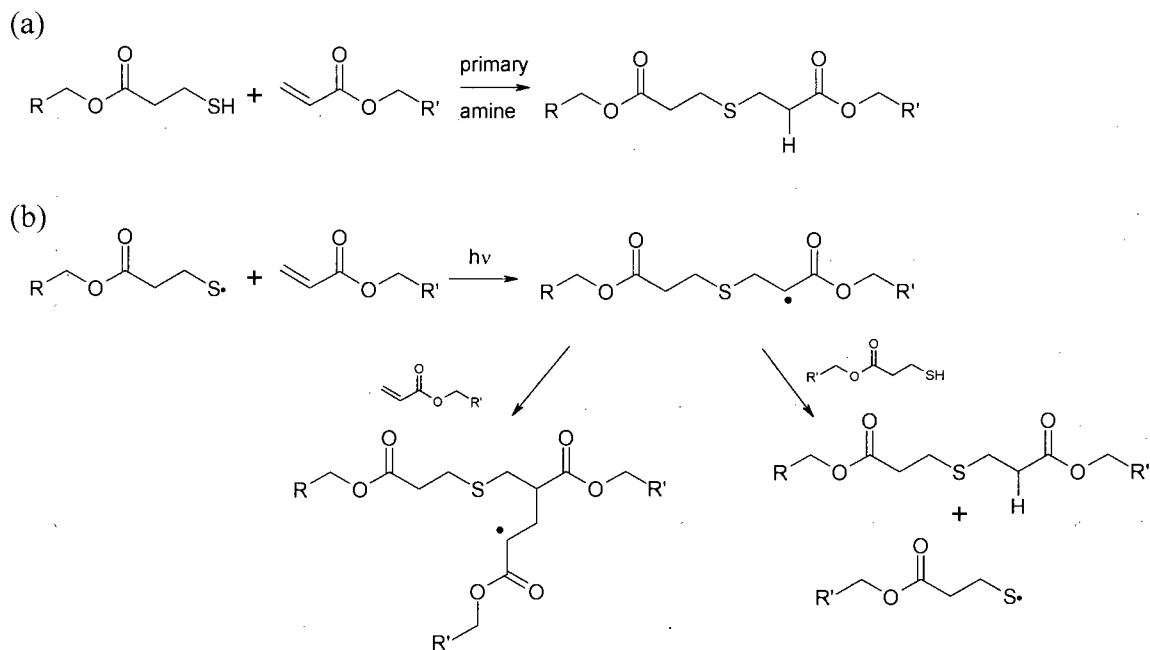
**Figure 4.1.** Basic mechanistic pathways for thiol-acrylate reactions with (a) an amine catalyst and (b) photo-cure. The photo-cure process only involves the two reactions in (b), while the amine catalysis/photo-cure process involves the amine catalyzed reaction followed by the photo-induced polymerization (photo-cure) of acrylate groups unreacted in (a).
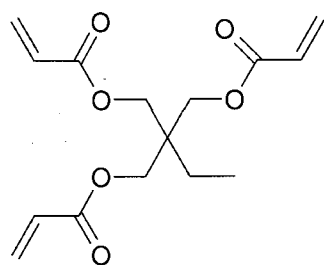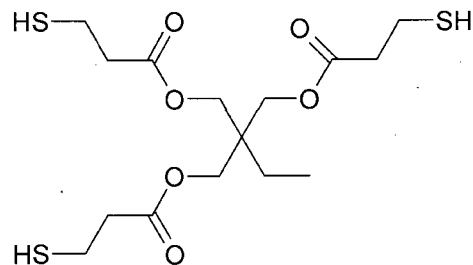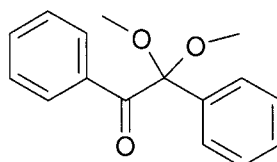
**Figure 4.2.** Structures of TMPTA, trithiol, and photoinitiator.
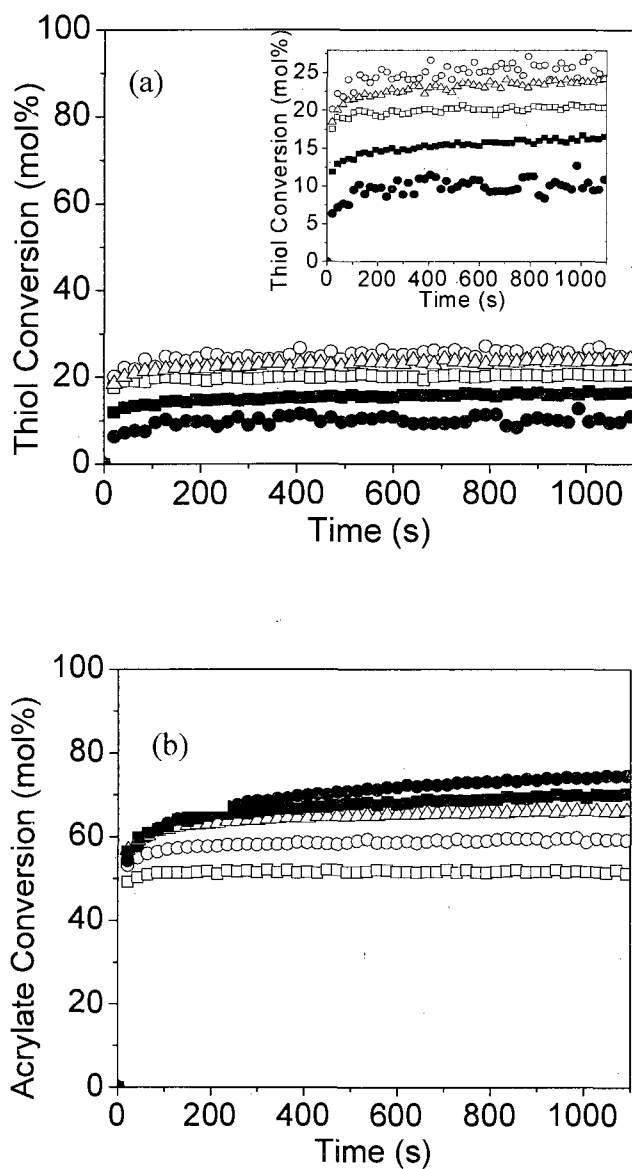
**Figure 4.3.** (a) Thiol and (b) acrylate conversions in photo-cure only systems. [Thiol:acrylate (mol %) 50:50 (□), 40:60 (○), 30:70 (Δ), 20:80 (■), and 10:90 (●)] Light intensity: 18.7 mW/cm$^{-2}$ with 2 wt% α,α-dimethoxy-α-phenylacetophenone (DMPA) as a photoinitiator.

**Figure 4.4.** Total thiol + acrylate mol % unreacted as a function of acrylate mol % feed in a photo-cure only system. (Compiled from results in **Figure 4.3.**)
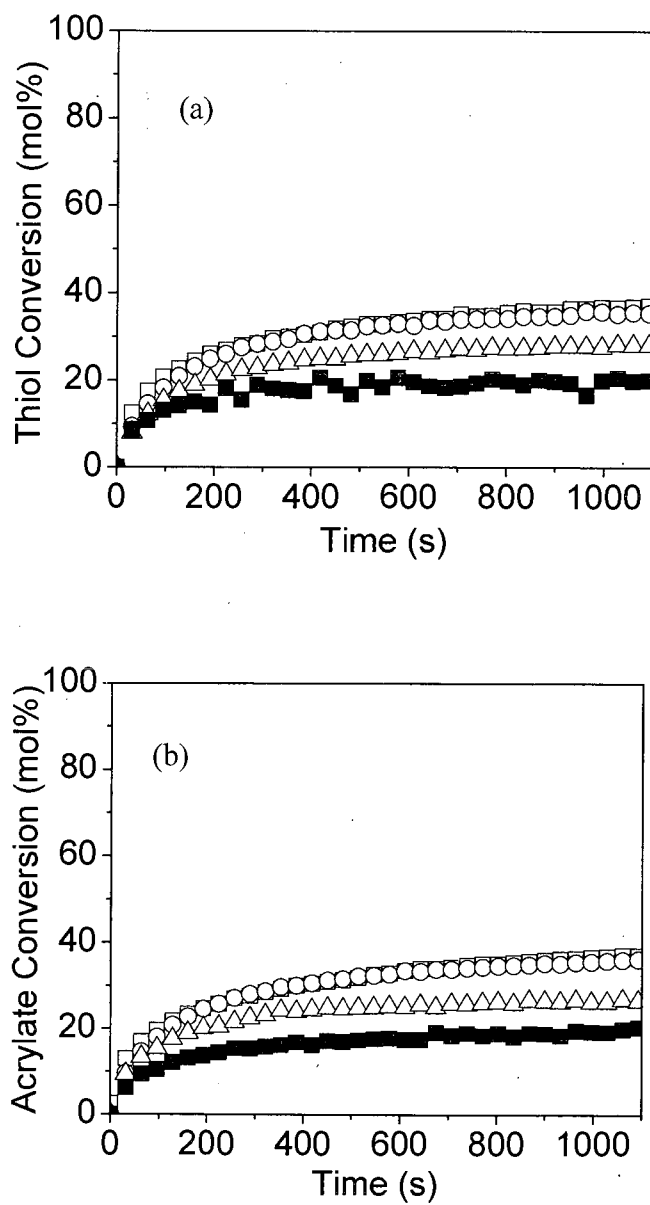
**Figure 4.5.** (a) Thiol and (b) acrylate mol % conversions. [Thiol:acrylate (mol %) 50:50 (□), 40:60 (○), 30:70 (△), and 20:80 (■)] Each system amine cured using 1 wt% hexyl amine.
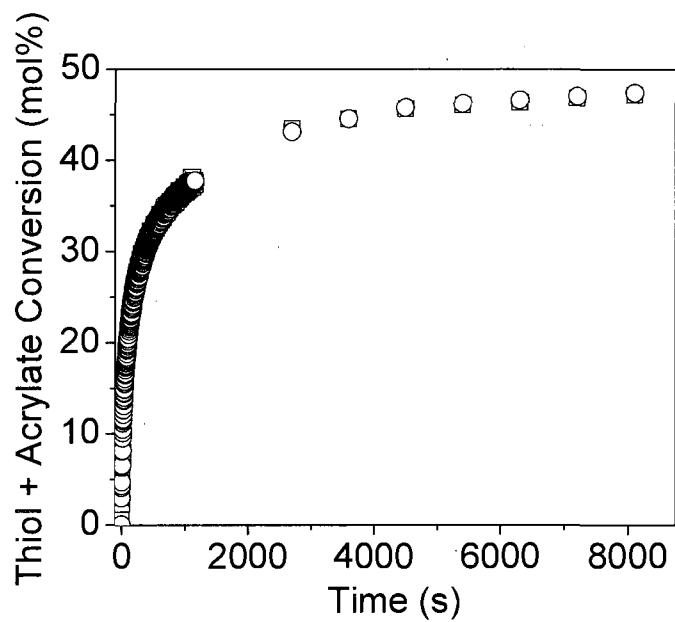
**Figure 4.6.** Thiol and acrylate mol % conversion vs. time using 1 wt% hexyl amine; reaction monitored to near 98% conversion of each component.
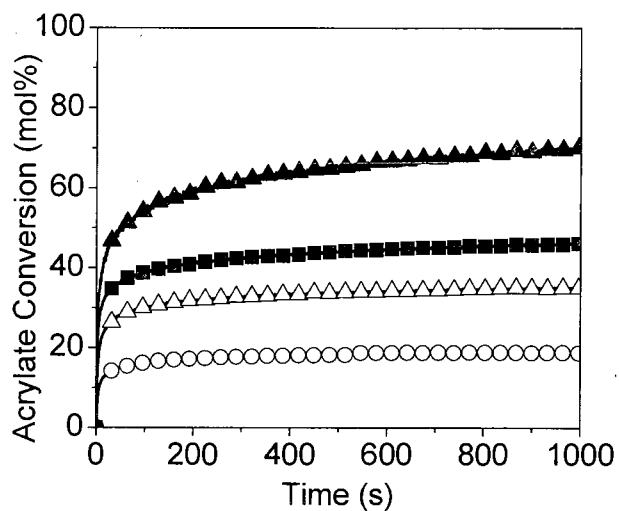
**Figure 4.7.** Acrylate mol % conversion of photo-cure only following the amine catalysis shown in **Figure 4.5**. [Thiol:acrylate (mol %) 40:60 (○), 30:70 (Δ), and 20:80 (■)] Light intensity: 18.7 mW/cm$^{-2}$ with 2 wt% α,α-dimethoxy-α-phenylacetophenone (DMPA) as a photoinitiator.

**Figure 4.8.** Sum of thiol + acrylate mol % unreacted as a function of acrylate mol % feed in an amine catalysis/photo-cure system.
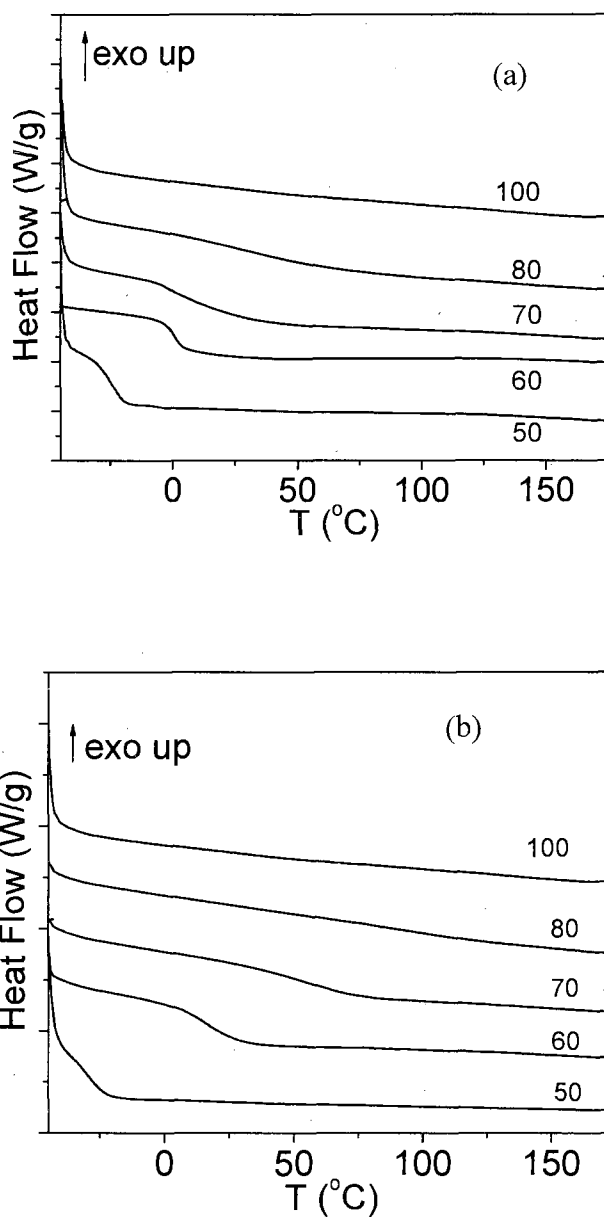
**Figure 4.9.** DSC scans of networks prepared by (a) amine catalysis/photo-cure and (b) photo-cure only. Fusion high intensity lamp, D bulb (400-W/in. input), line speed = 12.2 m/min and irradiance of 3.0 W/cm$^2$ with 2 wt% $\alpha,\alpha$-dimethoxy-$\alpha$ -phenylacetophenone (DMPA) as a photoinitiator. The mol % of acrylate in the feed indicated above each scan.
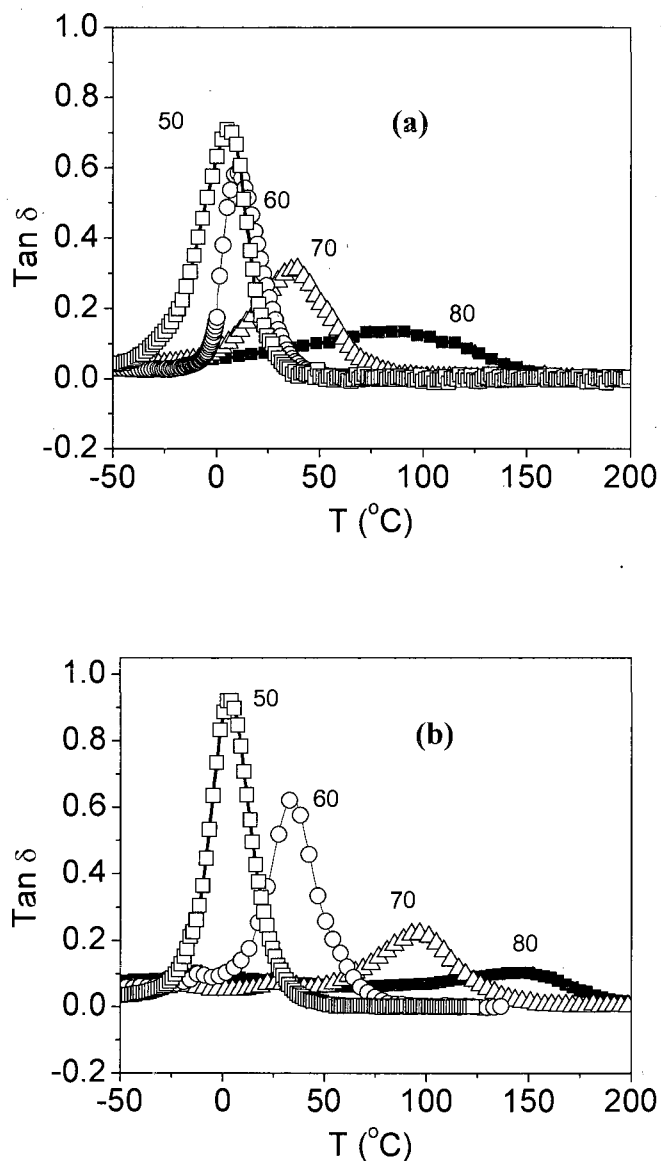
**Figure 4.10.** Tan δ analyzed by DMTA networks prepared by (a) amine catalysis/photo-cure and (b) photo-cure only. [Thiol:acrylate (mol %) 50:50 (□), 40:60 (○), 30:70 (Δ), and 20:80 (■)] Fusion high intensity lamp, D bulb (400-W/in. input), line speed= 12.2 m/min and irradiance of 3.0 W/cm² with 2 wt% α,α-dimethoxy-α-phenylacetophenone (DMPA) as a photoinitiator. The mol % of acrylate in the feed indicated on each plot.
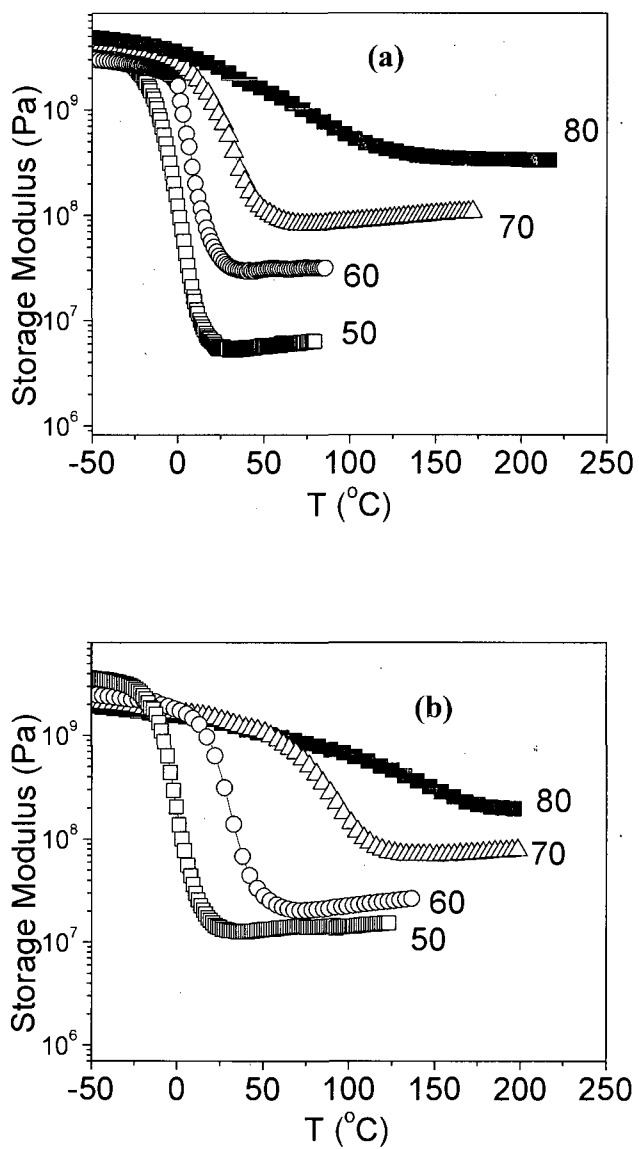
**Figure 4.11.** Storage moduli (E') analyzed by DMTA networks prepared by (a) amine catalysis/photo-cure and (b) photo-cure only. [Thiol:acrylate 50:50 (□), 40:60 (○), 30:70 (Δ), and 20:80 (■)] Fusion high intensity lamp, D bulb (400-W/in. input), line speed= 12.2 m/min and irradiance of 3.0 W/cm² with 2 wt% α,α-dimethoxy-α-phenylacetophenone (DMPA) as a photoinitiator. The mol % of acrylate in the feed indicated on each plot.

CHAPTER V

THE NUCLEOPHILIC, PHOSPHINE-CATALYZED THIOL–ENE CLICK
REACTION AND CONVERGENT STAR SYNTHESIS WITH RAFT-PREPARED
HOMOPOLYMERS

Abstract

The synthesis of 3-arm star polymers from reversible addition–fragmentation chain transfer (RAFT)-prepared precursor homopolymers in combination with thiol–ene click chemistry is described. Homopolymers of $n$-butyl acrylate and $N,N$-diethylacrylamide were prepared with 1-cyano-1-methylethyl dithiobenzoate and 2,20-azobis(2-methylpropionitrile) yielding materials with polydispersity indices (Mw/Mn)$\leq$1.18 and controlled molecular weights as determined by a combination of NMR spectroscopy, size exclusion chromatography (SEC), and matrix assisted laser desorption ionization time-of-flight mass spectrometry (MALDI-TOF MS). Subsequent one-pot reaction of homopolymer, hexylamine (HexAM), dimethylphenylphosphine (DMPP), and trimethylolpropane triacrylate (TMPTA) results in cleavage of the thiocarbonylthiol end-group (by HexAM) of the homopolymer yielding a macromolecular thiol that undergoes DMPP-initiated thiol-Michael addition to TMPTA yielding 3-arm star polymers. The presence of DMPP is demonstrated to serve an important second role in effectively suppressing the presence of any polymeric disulfide as determined by SEC. Such phosphine-mediated thiol–ene reactions are shown to be extremely rapid, as verified by a combination of FTIR and NMR spectroscopies, with complete consumption of the C=C bonds occurring in a matter of min. MALDI-TOF MS and SEC were used to verify the

formation of 3-arm stars. A broadening in the molecular weight distribution (Mw/Mn~1.35) was observed by SEC that was attributed to the presence of residual homopolymer and possibly 2-arm stars formed from trimethylolpropane diacrylate impurity. Interestingly, the MALDI analysis also indicated the presence of 1- and 2-arm species most likely formed from the fragmentation of the parent 3-arm star during analysis. Finally, a control experiment verified that the consumption of C=C bonds does not occur via a radical pathway.

## Introduction

The thiol–ene reaction is, simply, the hydrothiolation of a C=C bond whose origins can be traced to the turn of the 20th century. Importantly, from a synthetic standpoint, one key advantage of the thiol–ene reaction is its broad applicability and wide range of experimental conditions under which it can be conducted. For example, such reactions can be performed under radical,[1] nucleophilic catalyzed,[2] and amino acid catalyzed,[3] conditions in a regioselective manner to yield exclusively Markovnikov or anti- Markovnikov products with virtually any ene substrate. Historically, the thiol–ene reaction has been evaluated primarily as a means of preparing perfect networks. For example, commercially available tri and tetra functional thiols polymerize with multifunctional enes via a two-step radical step-growth process to yield high density networks.[1,4–9] These radical polymerization reactions proceed readily in the presence of water and/or oxygen, and the final networks have very narrow glass transition regions, on the range of 10–15°C full width at half maximum, and thus are ideal for tuning their tan δ damping absorption maxima to ensure high energy absorption upon high energy impact.[6,7] Since radical

thiol–ene reactions take place rapidly and proceed to high conversion using essentially any terminal electron rich or electron poor ene there is tremendous latitude in designing systems for applications ranging from holographic diffraction gratings[8] to dental restoratives,[9] the latter benefitting from low volume shrinkage and stress buildup during network formation.

The term 'click chemistry'– or 'click reaction' – was coined by Sharpless and co-workers in 2001 to describe an approach to building complex molecules from a few, straightforward, thermodynamically favorable reactions, commonly involving the construction of carbon atom–heteroatom linkages.[10] To be classified as a click reaction Sharpless et al. outlined simple criteria that a reaction must meet. For example, the reaction must be modular, broad in scope, give (near) quantitative yields, generate inoffensive byproducts, and be stereospecific.[10] Examples of reactions that fulfill these criteria include the Cu(I) catalyzed reaction between an alkyne and an azide, Diels–Alder reactions in general, C=C bond additions, non-Aldol carbonyl chemistry, and nucleophilic ring opening reactions, especially involving epoxides. Currently, the accepted 'gold standard' of such reactions, the Cu(I)-mediated reaction between an alkyne and azide has been exploited in applications ranging from small molecule organic synthesis, drug discovery, and materials science.[11–13] Recent examples include the ATRP of 3-azidopropyl methacrylate followed by post-polymerization reaction of the pendent azide groups with a variety of functional alkynes,[14] the "click" polymerization of monomers bearing both azide and alkyne groups,[15] the synthesis of layer-by-layer dendritic films,[16] and the preparation of 3-miktoarm stars and 1st generation dendritic copolymers employing a combination of ATRP and alkyne/azide click chemistry.

Recently the thiol–ene reaction has been evaluated as a click reaction in alternative areas of materials synthesis. For example, Killops, Campos and Hawker[17] reported the synthesis of 4th-generation thioether-based dendrimers in which a key building step was the radical mediated click thiol–ene reaction between 1-thioglycerol and the starting 2,4,6-triallyloxy-1,3,5-triazone core followed by additional reactions between 1-thioglycerol and ene bonds introduced via the esterification of peripheral OH groups with 4-pentenoic anhydride. Such reactions were shown to be extremely high yielding and facile. Gress, Völkel, and Schlaad[18] described the synthesis and controlled cationic isomerization polymerization of 2-(3-butenyl)-2-oxazoline to yield well-defined (co)polymers with pendent ene functionality. Subsequently, the ene groups were reacted by a thiol-click process, quantitatively, under radical conditions with a range of small molecular thiols including methyl-3-mercaptopropionate, 1-thiolglycerol, and the protected sugar 2,3,4,6-tetra-O-acetyl-1-thio-b-D-glucopyranose to yield the corresponding side-chain modified (co)polymers.

Reversible addition–fragmentation chain transfer (RAFT) radical polymerization[19–24] is a controlled synthesis technique that employs thiocarbonylthio compounds as degenerative chain transfer agents. Particularly impressive with RAFT is the ease with which it is executed as well as its broad versatility with respect to substrate choice and polymerization conditions. However, in the context of the work reported herein it is important to highlight that (co)polymers prepared via this route bear a single thiocarbonylthio functionality at the chain terminus that is available for post-polymerization reaction. Indeed, such thiocarbonylthio end-groups can be readily reduced to other reactive or non-reactive functionality. For example, Lowe et al.[25] demonstrated the facile $NaBH_4$ cleavage, in aqueous media, of dithioester-

terminated (co)polymers to yield the corresponding thiolate terminal materials. When performed in the presence of a gold sol, such reactions resulted in sequential dithioester end-group cleavage followed by covalent attachment/stabilization of the gold sol. Such a sequence of reactions has also been employed for the modification of planar gold surfaces[26] and gold nanorods.[27] Indeed, this facile approach has been adopted by numerous research groups using both $NaBH_4$[28] as well as other hydride reducing agents. Scales, Convertine and McCormick reported the synthesis of fluorescently tagged poly(N-isopropylacrylamide) via sequential $NaBH_4$ cleavage of the trithiocarbonate end-group followed by a 24 h treatment of triscarboxyethyl phosphine prior to reaction with $N$-(1-pyrenyl)-maleimide.[29] Alternatively, the thiocarbonylthio functionality is known to be easily cleaved using primary and secondary amines to yield thiols, and has been employed in the thioacylation of proteins.[30-33] The treatment of thiocarbonylthio groups with amines has also been examined in the materials arena, especially with RAFT prepared (co)polymers. Quiz, Tanaka and Winnie recently described the aqueous phase behavior of cyclic poly($N$-isopropylacrylamide)s that were prepared in a multi-step process, one step of which involved the cleavage of trithiocarbonate end-groups with butylamine.[34] Li and co-workers[35] reported the synthesis of functional telechelics based on RAFT-prepared poly($N$-isopropylacrylamide) in which the trithiocarbonate end-group was cleaved to a thiol using 2-ethanolamine yielding the free thiol functional species that was subsequently employed in additional modification reactions.

Star (co)polymers are the simplest examples of branched polymers with all branches (arms) extending from a single point. Star (co)polymers can be prepared via one of three general routes: 1) the arm first (convergent) approach, 2) employing a

multifunctional initiator (divergent approach), and 3) the microgel approach in which a small amount of multifunctional cross-linking agent is added at the end of a polymerization process. Each of these approaches has associated advantages and disadvantages. The convergent approach allows for a thorough characterization of the arms prior to star formation aiding in the subsequent characterization of the star materials. However, to favor star formation an excess of 'arms' is often required which will exist as an impurity in the final product. Additionally, extended reaction times are often needed to achieve acceptable yields. The divergent approach requires that all initiation sites possess the same reactivity and that all are activated simultaneously, at least if well-defined stars are desired. The microgel approach is the simplest approach to making stars, but it is very difficult to control the number of arms per star. Recently, we reported our initial results regarding the use of a RAFT-prepared homopolymer of $N,N$-diethylacrylamide (DEAm) that served as a masked macromolecular secondary thiol in the convergent synthesis of 3-arm star polymers via a macromolecular thiol–ene reaction.[36] The sequential hexylamine-mediated cleavage of the dithioester end-group followed by Dimethylphenylphosphine catalyzed thiol-Michael addition to trimethylolpropane triacrylate resulted in a rapid convergent synthesis of 3-arm star polymers. It should be noted that while star polymers have been previously prepared via RAFT by all three of the methods noted above,[37–43] the convergent approach we described had not previously been employed. Indeed, such an approach specifically takes advantage of RAFT-prepared (co)polymers and the click nature of the thiol–ene reaction. Expanding on this initial disclosure we describe herein a more detailed investigation of such convergent star syntheses, further highlighting the versatility of the method for star polymer synthesis

and reiterating the synthetic utility of the nucleophilic thiol–ene reaction in polymer/materials chemistry.

## Experimental

*Materials*

All reagents were purchased from the Aldrich Chemical Company at the highest available purity and used as received unless noted otherwise. Trimethylolpropane triacrylate (TMPTA) (>83% pure) was provided by Sartomer. *N,N*-Diethylacrylamide was purchased from PolySciences and purified by vacuum distillation. *n*-Butyl acrylate was purified by passage over a column of basic alumina. 1-Cyano-1-methylethyl dithiobenzoate (CPDB) was prepared according to a literature procedure[44]. 2,2-Azobis(2-methylpropionitrile) (AIBN) was recrystallized from methanol and stored in a freezer prior to use.

*RAFT Homopolymerization of N,N-diethylacrylamide (DEAm)*

A mixture of DEAm (11.0 g, 86.5 mmol), CPDB (569 mg, 2.57 mmol), AIBN (84.4 mg, 0.514 mmol), and DMF (11.0 g) was added to a Schlenk flask equipped with a magnetic stirring bar. The mixture was stirred for at least 30 min in an ice bath to ensure complete dissolution of all components. The flask was then purged by repeatedly evacuating and refilling with $N_2$ at least 3 times and subsequently immersed in a preheated oil bath at 70°C. After 11 h the reaction was quenched by rapid cooling in liquid $N_2$ and exposure to air. The polymer was isolated by precipitation into a large excess of hexanes. The polymer was then dissolved in water and isolated by lyophilization yielding 9.53 g of polymer.

*RAFT Homopolymerization of n-Butyl Acrylate*

The homopolymerization of n-butyl acrylate was accomplished following the procedure detailed above except that the reaction was left for 22.5 h at 70°C. The residual *n*-butyl acrylate monomer was removed in vacuo at ~1 mbar.

*Model Reaction between Ethyl 2-Mercaptopropionate and TMPTA*

Ethyl-2-mercaptopropionate (1.8 mL, $1.4 \times 10^{-5}$ moles, 1.5 molar excess based on acrylate functional groups) was added to a scintillation vial (20 mL capacity) along with 0.5 g THF. To this solution were then added TMPTA (2.5 mL, $8.3 \times 10^{-6}$ moles) and Dimethylphenylphosphine (DMPP) (10.0 mL, 0.11 M). The reaction was allowed to proceed for 5 min prior to NMR analysis.

*Preparation of 3-arm Stars (1.5:1 Molar Ratio of –SH:Ene) with Poly(n-Butyl Acrylate) or Poly(N,N-Diethylacrylamide)*

Dithioester-terminated poly(*n*-butyl acrylate) (0.15 g, $1.4 \times 10^{-5}$ moles, molar mass ~3700, ~1.5 molar excess based on acrylate functional groups) was dissolved in 0.5 g of THF in a scintillation vial (20 mL capacity). To this solution were added TMPTA (2.5 mL, $8.3 \times 10^{-6}$ moles), dimethylphenylphosphine (10.0 mL, 0.11 M), and hexylamine (20.0 mL, 0.35 M, 4 X excess based on [SH] groups). The solution was allowed to react for 5 min prior to analysis by NMR spectroscopy. Dithioester-terminated poly(*N,N*-diethylacrylamide) (0.78 g) was dissolved in THF (2.0 g) in a scintillation vial. After dissolution,14 mL of TMPTA was added followed by 29 mL of DMPP. The solution was stirred under nitrogen for 5 min to ensure complete homogeneity. Hexylamine (35 mL) was then added to this solution and the mixture allowed to stir overnight. The polymer was subsequently purified by precipitation into hexanes, followed by drying in vacuo overnight.

*Reaction of TMPTA, Dimethylphenylphosphine, and Hexylamine*

This control experiment was performed to confirm that the phosphine was not catalyzing the addition of the primary amine across the ene double bonds, i.e. catalyzing an aza-Michael addition reaction. TMPTA (2.5 mL, $8.3 \times 10^{-6}$ moles) was dissolved in 0.5 g of THF in a scintillation vial (20 mL capacity). To this were added dimethylphenylphosphine (10 mL, 0.11 M) and hexylamine (20 mL, 0.35 M). The reaction was allowed to proceed for 5 min prior to NMR analysis.

*Reaction of TMPTA, Dithioester-terminated Polymer, Dimethylphenylphosphine, Hexylamine in the Presence of TEMPO*

This control experiment was conducted to verify that the consumption of ene was not proceeding via a free radical pathway. Dithioester-terminated poly(*n*-butyl acrylate) ($1.4 \times 10^{-5}$ moles, Mw~3500, ~1.5 molar excess based on ene functional groups) was dissolved in 0.5 g of THF in a scintillation vial (20 mL capacity). TEMPO (0.01 g, 2 wt%) was then added to the solution. To this solution were added TMPTA (2.5 mL, $8.3 \times 10^{-6}$ moles), dimethylphenylphosphine (10.0 mL, 0.11 M), and hexylamine (20.0 mL, 0.35 M, 4 X excess based on [SH] groups). The solution was allowed to react for 5 min prior to analysis by NMR spectroscopy.

*Characterization*

MALDI-TOF mass spectrometry (MALDI-TOF MS) was performed on a Bruker Reflex III Instrument equipped with a 337 nm $N_2$ laser in the reflector mode and 20 kV acceleration voltage. a-Cyano-4- hydroxycinnamic acid (CHCA) was used as a matrix for molecular weight determination of the poly(N,N-diethylacrylamide) polymers before and after star formation. NMR spectra were recorded on either a 300 (Bruker 300 53 mm) or 500 MHz NMR spectrometer. Specifically, in the case of the

500 MHz spectrometer: ^{13}C NMR characterization: All spectra were acquired on a Varian UNITYINOVA spectrometer operating at a frequency of 125 MHz for carbon and using a standard 5 mm two channel probe. A 90° pulse width of 5.75 ms was used. The acquisition time was 1.5 s with no recycle delay, making the time between scans 1.5 s. Proton decoupling was implemented during data acquisition to remove [1]H–[13]C scalar coupling. Samples were dissolved in THF, with sealed capillaries filled with DMSO-$d_6$ used for deuterium shimming and locking. ^{1}H NMR characterization: All spectra were acquired on a Varian UNITYINOVA spectrometer operating at a frequency of 499.8 MHz for proton and using a standard 5 mm two channel probe. A 90° pulse width of 15.25 ms and acquisition time of 1.9 s were used. Typically 64–96 scans were acquired for each sample, with a recycle delay of 4.1 s making the overall time between scans 6 s. Samples were dissolved in $D_2O$ or directly in non-deuterated THF with sealed capillaries filled with DMSO-$d_6$ used for deuterium shimming and locking. Organic SEC was conducted on a Waters system comprised of a Waters 515 HPLC pump, Waters 2487 Dual l absorbance detector, Waters 2410 RI detector with a PolymerLabs PLgel 5 mm guard column and a PolymerLabs PLgel 5 mm MIXED-C column, in THF stabilized with 281 ppm BHT at a flow rate of 1.0 mL/min. The column was calibrated with a series of narrow molecular mass distribution poly(methyl methacrylate) standards. FTIR spectra were recorded using a modified Bruker 88 spectrometer equipped, with an MCT detector, over the range 4000–400 cm$^{-1}$ at a resolution of 4.0 cm$^{-1}$. Samples were sandwiched between two sodium chloride salt plates at a thickness of ~20 mm. Each spectrum was collected over 32 scans. The data were analyzed with the Bruker OPUS/IR Version 4.0 software.

## Results and Discussion

RAFT-prepared (co)polymers serve as convenient precursors to reactive thiol/thiolate-terminal materials that can be used for subsequent post-polymerization reactions. Given the current, and growing, interest in click chemistry we examined the application of RAFT-synthesized homopolymers of $N,N$-diethylacrylamide (DEAm) and $n$-butyl acrylate (BA) as dithioester-terminal precursors in the convergent synthesis of 3-arm star polymers via a nucleophilic, phosphine-catalyzed macromolecular thiol–ene reaction with the trifunctional coupling agent trimethylolpropane triacrylate (TMPTA). The general synthetic approach is outlined in **Scheme 5.1**.

Precursor homopolymers of polyDEAm (PDEAm) and polyBA (PBA) were prepared under typical RAFT conditions employing 1-cyano-1-methylethyl dithiobenzoate (CPDB, **Scheme 5.1.**) as the RAFT chain transfer agent (CTA) in conjunction with AIBN as the source of primary radicals, at 70°C in DMF. **Table 5.1.** summarizes the molecular characteristics of the resulting homopolymers ($Mn_{theory}$, $Mn_{exptGPC}$, $Mn_{exptNMR}$, Mp (the peak maximum molecular weight, see Discussion later in manuscript), and Mw/Mn).

Entirely consistent with homopolymers prepared by RAFT, the resulting materials possess narrow molecular mass distributions with the polydispersity indices (Mw/Mn) being $\leq 1.18$. The observed difference in the measured Mn by SEC and the theoretical Mn is a direct result of the fact that the SEC instrument was calibrated with narrow molecular mass distribution poly(methyl methacrylate) standards which are not ideal standards for the synthesized homopolymers. However, the Mn as determined by via end-group analysis using $^1$H NMR spectroscopy is entirely

consistent with the targeted Mn based on the degree of conversion. As a representative example, **Figure 5.1.** shows the $^1$H NMR spectrum, SEC trace (RI signal – shown inset) and MALDI-TOF MS trace for the PDEAm1 homopolymer. Several points are worth noting. Given the low-targeted Mn of the PDEAm and PBA homopolymers of 4500 at quantitative conversion their absolute molecular mass can be readily determined by end-group analysis using NMR spectroscopy. **Figure 5.1.A** shows the $^1$H NMR spectrum of the PDEAm1 homopolymer recorded in D$_2$O. The protons associated with the phenyl end-group group are clearly visible at ~7.6–7.8 ppm and are labeled b. A simple ratio of the integrals associated with b versus the resonance labeled a, which is assigned to the methylene protons directly bonded to the nitrogen atom of the amide side-group, yields a calculated absolute Mn of 3800. In contrast, the Mn determined by SEC was 2800 (see inset). Supporting the end-group calculations is the MALDI-TOF MS data. **Figure 5.1.B** shows the MALDI-TOF MS trace for the PDEAm1 homopolymer along with an expansion between 3000 and 4000 a.m.u. shown inset. The major distribution is centered at ca. 3800 a.m.u., a value identical to that calculated by end-group analysis. The difference in atomic mass between the major peaks is 127.86 a.m.u., very close to the atomic mass of the DEAm monomer of 127.10 a.m.u. Similar data were obtained for the PBA homopolymer. For example, **Figure 5.2.** shows the $^1$H NMR spectrum of the PBA homopolymer, again demonstrating the ability to perform accurate endgroup analysis.

With the well-defined homopolymers in-hand the convergent synthesis of 3-arm star polymers via a macromolecular thiol–ene click reaction employing trimethylolpropane triacrylate (TMPTA) as the coupling reagent under phosphine-catalyzed conditions was examined in greater detail. To reiterate, the nucleophile

catalyzed thiol-Michael reaction can be conducted using a primary or secondary amine although, as noted recently,[36] dimethylphenylphosphine (DMPP) serves as an extremely potent catalyst for such reactions. The convergent star synthesis was accomplished by employing a combination of primary amine (hexylamine (HexAM)) and DMPP. The HexAM was added to specifically serve as the cleaving agent of the dithioester end-groups on the PDEAm/PBA homopolymers while the DMPP was employed to catalyze the subsequent macromolecular thiol–ene reaction. Previously, it was noted[36] that the presence of the phosphine, aside from serving as an extremely effective catalyst for the thiol-Michael reaction, served an equally important role in eliminating the presence of disulfide, formed from the reaction between the reduced RAFT homopolymers, a reaction that can occur readily in the presence of only amine. The application of phosphines as reducing agents for disulfides is well documented. For example, Scales et al. reported the treatment of PNIPAm, containing significant polymeric disulfide after $NaBH_4$ end-group reduction, with triscarboxyethyl phosphine.[29] However, in this report the authors reported the need for extended reaction times (24 h) and the use of a large excess of phosphine (150 molar excess based on thiol functionality) to achieve the desired reduction. In contrast, performing the dithioester endgroup reduction in the presence of phosphine serves the same function, although such extended reaction times or high concentrations are not required.[36] To further highlight this beneficial effect, **Figure 5.3.** shows the MALDI-TOF MS traces for the PBA homopolymer (absolute Mn of 3300 as determined by $^1H$ NMR end-group analysis) in which the dithioester group was cleaved with HexAM in the absence (**Figure 5.3.A**) and presence of DMPP (**Figure 5.3.B**). When the cleavage reaction is performed with only HexAM under a normal air atmosphere, the

MALDI-TOF MS trace clearly shows that in addition to the desired thiol-terminated

product, the reaction also results in the formation of the corresponding disulfide as

evidenced by the presence of a second distribution centered at about ca. 6700 a.m.u.

In contrast, when the reaction is performed with the HexAM/DMPP combination, the

MALDI-TOF MS trace indicates the absence of any disulfide. Clearly, such an

approach is more convenient than the sequential approach reported previously for

obtaining thiol-terminated RAFT-prepared (co)polymers. The exact role of the DMPP

is not, however, clear and its exact mode of action has not been elucidated at this

time. However, it is presumably acting in one of two possible ways. Disulfide

formation is a direct result of the aerial oxidation of the thiol-terminated

homopolymers. Therefore, DMPP is either inhibiting the aerial oxidation process or,

as reported previously, is serving as a reducing agent for disulfide that may be formed

during the end-group reduction.

The beneficial effect of the added DMPP was also verified by SEC. **Figure

5.4.** shows the chromatograms (RI signal) for the PDEAm1 homopolymer after

cleavage of the dithioester end-groups performed in the presence and absence of

DMPP. When conducted in the absence of DMPP, the SEC trace shows the presence

of a higher molecular mass species as evidenced by the bimodal distribution –there is

a clear shoulder centered at a retention time of ~8.1 min on the main distribution. In

contrast, but entirely consistent with the MALDI-TOF MS results for the PBA

homopolymer, when the reduction is performed in the presence of DMPP the

resulting distribution is symmetric and unimodal with no evidence of any higher

molecular mass species resulting from the formation of disulfide.

Having demonstrated the well-defined nature of the precursor homopolymers and the clearly beneficial nature of the DMPP not only serving as a potent nucleophilic catalyst for the macromolecular thiol–ene reaction but also acting as an effective reagent for preventing/reducing disulfide formation, a more detailed examination of the actual star-forming reaction was conducted.

As demonstrated previously, real-time FTIR[1,5] is an extremely effective means of monitoring thiol–ene reactions. Indeed, for reactions between small molecule thiols and enes, absorption bands associated with both functional groups can be monitored readily in real time. Specifically, the ene presents distinct IR bands that can be monitored at ~1600 (C=C stretch) and 810 cm$^{-1}$ (the C–H bend in C=C–H), whereas the consumption of the thiol can be followed by following the disappearance of the weak band at 2575 cm$^{-1}$. Unfortunately, given the polymeric nature of the thiol in these convergent star syntheses it was not possible to directly monitor the band associated with the thiol due to its low concentration. However, the consumption of the ene could be readily followed. As a representative example, **Figure 5.5.A** shows the IR spectrum, plotted between 900 and 780 cm$^{-1}$, for the reaction of PDEAm1 with TMPTA/DMPP before and 5 min after the addition of HexAM. The band of interest at 810 cm$^{-1}$ (the C–H bend in C=C–H) is clearly visible as a shoulder on the more intense band at ca. 790 cm$^{-1}$ in the spectrum (solid line) of PDEAm1, TMPTA and DMPP. A second spectrum recorded approximately 5 min after the addition of HexAM is also shown in **Figure 5.5.A** (dotted line), and indicates close to complete conversion after this short period of time. This highlights the fact that the macromolecular thiol–ene reaction is rapid which while not common for convergent

star syntheses is entirely consistent with the thiol–ene reaction in general. Similar observations were made in the case of the PBA homopolymer (**Figure 5.5.B**).

The rapid consumption of C=C bonds was also confirmed by $^1$H NMR spectroscopy. **Figure 5.6.A** shows the $^1$H NMR spectrum, recorded in THF with a DMSO-d$_6$ inset, plotted between δ=6.5 and 5.5 ppm for dithioester-terminal PBA and TMPTA highlighting the presence of the vinylic functional groups on TMPTA as evidenced by the resonances at ~6.3, 6.05–6.1, and 5.8 ppm all associated with the hydrogen atoms on the C=C bonds. Following the acquisition of this spectrum, the sample tube was removed from the spectrometer, the required volumes of DMPP and HexAM added, the tube reinserted in the spectrometer, the sample locked/shimmed and a second spectrum recorded, **Figure 5.6.B**. Consistent with the FTIR spectroscopic results, the C=C bonds are completely consumed within this short period of time with absolutely no evidence of any vinylic H's present in the $^1$H NMR spectrum.

While both the FTIR and $^1$H NMR spectroscopic data demonstrate that the C=C bonds are consumed extremely rapidly in the presence of dithioester-terminal polymer, HexAM and DMPP, neither technique proves unequivocally that the consumption of ene bonds is due to the desired thiol–ene reaction. In an attempt to verify that the disappearance of the C=C bonds was due to the macromolecular thiol-Michael reaction $^{13}$C NMR spectroscopy was used to identify the original vinylic carbon atoms after reaction with the macromolecular thiols. To aid with structural verification a small molecule model reaction was first conducted. Specifically, the DMPP catalyzed reaction between ethyl-2-mercaptopropanoate, a small molecule model for the polymeric ester/amide, and TMPTA was conducted and the product

characterized with respect to specifically identifying the chemical shifts of the saturated carbon atoms labeled a and b in **Figure 5.7.A**, i.e., those that were originally the vinylic carbon atoms of TMPTA. In this small molecule model reaction the key resonances were clearly visible at $\delta$=34.59 (carbon atom alpha to the C=O group) and 26.52 (carbon atom directly bonded to S) ppm. Having successfully identified the region and resonances of interest the same analysis was performed on the polymeric star products. **Figure 5.7.B** shows the ^{13}C NMR spectrum, plotted between $\delta$=35 and 26 ppm for the reaction between PDEAm1 and TMPTA with DMPP as catalyst and HexAM as endgroup cleaving agent. Obviously, such ^{13}C NMR analysis on a moderate-to-high molecular mass 3-arm star polymer is not as straightforward; however, the resonances of interest are observed at $\delta$=34.59 and 26.68 ppm. These ^{13}C NMR spectroscopic results confirm that the results obtained by FTIR and ^{1}H NMR spectroscopies result from a macromolecular thiol–ene reaction.

Additional indirect evidence for the macromolecular thiol–ene reaction was obtained via a simple control experiment in which TMPTA, HexAM, and DMPP were mixed in an NMR tube in THF at concentrations consistent with the 3-arm star syntheses (**Figure 5.8.**). As demonstrated previously, the C=C bonds in the presence of polymer are consumed very rapidly. However, in the absence of the thiol-terminated polymer the C=C bonds are clearly visible after only 5 min of 'reaction' indicating that their consumption is a direct result of reaction with thiol functional groups.

In addition to verifying that consumption of ene bonds occurs only in the presence of thiol-terminated polymer, this control experiment additionally confirms that DMPP does not catalyze the aza-Michael reaction, i.e. the addition of HexAM

across the C=C bonds. Mechanistically, it is reasonable to propose that the DMPP

catalyzed thiol–ene reaction proceeds via an ionic chain reaction in which addition of

phosphine to an activated ene results in the formation of an intermediate, resonance

stabilized carbon-centered enolate zwitterion. Such an intermediate has indeed been

proposed for the phosphine-catalyzed addition of alcohols[45] and various carbon-

centered nucleophiles to a range of electron deficient enes[46] including acrylates. This

strong base intermediate subsequently abstracts a proton from a thiol, yielding a

thiolate that is a potent nucleophile capable of undergoing direct Michael addition to

an activated ene forming an intermediate enolate which abstracts another proton from

additional thiol, resulting in chain propagation, **Scheme 5.2.**

Clearly, the intermediate carbon-centered enolate anion must be a sufficiently

strong base to abstract a proton from a thiol molecule to induce the subsequent chain

reaction. In the case of thiols, the intermediate enolate is sufficiently powerful to

facilitate the deprotonation reaction ($pK_a$ of the thiol functional group is typically ~8–

9). However, for DMPP to catalyze the addition of HexAM across the C]C bonds the

intermediate base must be strong enough to deprotonate the primary amine, which has

a $pK_a$~40. There is no question that the intermediate enolate is not sufficiently strong

to deprotonate HexAM, i.e. the weaker acid/base pair is not formed.

As previously demonstrated,[36] MALDI-TOF MS serves as a convenient

method for verifying 3-arm star formation. **Figure 5.9.** shows the experimentally

determined MALDI-TOF MS spectrum of the product obtained from the reaction of

PDEAm1 ($Mn$ =3800 via end-group analysis) with TMPTA, DMPP and HexAM

employing CHCA as the MALDI-TOF MS matrix. The observed mass spectrum

clearly confirms the presence of the 3-arm star products with a major distribution

centered at ~11,000 a.m.u. However, in addition to the 3-arm star products there are

clearly distributions that are due to the presence of both 2- and 1-arm species. There

are at least two possible sources for these products. Firstly, it should be reiterated that

commercially available TMPTA has a listed purity of 83–100% with the major

contaminants being trimethylolpropane diacrylate and trimethylolpropane

monoacrylate. Given that TMPTA was used as received these impurities will clearly

result in the formation of the 1- and 2-arm star products. A second source of 1- and 2-

arm fragments is a direct result of the MALDI-TOF MS experiment, i.e. the MALDI-

TOF MS-induced fragmentation of high-arm stars to lower-arm stars.[47] This is not

uncommon and fragmentation of analyte under MALDI-TOF MS experimental

conditions is well documented and is known to be dependent on variables including

the nature of the matrix and the laser pulse energy. Evidence for such fragmentation

can be extracted from the MALDI-TOF MS trace in **Figure 5.9**. For example, **Figure

5.10.A** shows an expansion in the 3-arm star region highlighting a peak with m/z =

11,500. From this peak we can estimate the average molecular mass of each arm since

we know the exact molecular weight of the core fragment and the likely cationic

species. Since no specific cationizing species was added we assume that the ionized

species is either [3-arm star + H]$^+$, [3-arm star + Na]$^+$, or [3-arm star + K]$^+$. Based on

our previous observations, PDEAm is known to readily form adducts with Na$^+$, and

so the peak with m/z = 11,500 is likely due to [3-arm star + Na]$^+$. Therefore, the

molecular weight of the 3-arm star is 11,500 - 23 = 11,477 g/mol. Given that the core

fragment has a molecular mass of 296 g/mol then the average molecular mass of each

arm can be calculated to be 3727 g/mol. For the purpose of analysis and the

identification of 1- and 2-arm fragments derived from fragmentation in the instrument

we are assuming that the fragmentation can occur at the points indicated in **Figure 5.10.A** (a, b, and c). These may not be the only fragmentation points but are the only positions we will consider here. In the case of the 3-arm star, fragmentation could occur at one, two or all three distinct positions yielding 1- and 2-arm products. Cleavage of the C–O bonds (a) yields a polymer chain that is terminated with a carboxylate group; in this case the cleaved product will be PDEAm1–S–CH$_2$–CH$_2$–CO$_2^-$ +H$^+$. Based on the calculated average molecular mass of an arm, as noted above, plus the CH$_2$–CH$_2$–CO$_2^-$ +H$^+$ portion gives a species with a molecular weight of 3800 g/mol. **Figure 5.10.B** shows an expansion of **Figure 5.9.** in the region m/z = 3790–3900. The major peak in this region has an m/z value of 3801 which agrees almost exactly with the predicted value. In addition, peaks are observed at +16 and +32m/z that may be due to the sulfoxide and sulfone respectively formed from the oxidation of the thioether functionality in the polymer chains. Analysis of the m/z = 7670–7800 region, **Figure 5.10.C**, indicates the presence of products that can be assigned to 2-arm stars with molecular masses consistent with species formed by fragmentation of the corresponding 3-arm stars at all three of the indicated points shown in **Figure 5.10.A**. **Table 5.2.** shows the chemical structures of the major 2-arm star fragments in this region as well as the measured and theoretical molecular weights associated with H$^+$, Na$^+$, and K$^+$ each species. For each of the theoretical m/z values calculated (based on the assumption that we are dealing with fragmentation of the [3-arm star + Na]$^+$ species with an m/z = 11,500) then it is possible to identify a major peak in this range that is within several units of the theoretical value. It should be noted that the observed peak centered around m/z = 7735 could also be due to 2-arm species formed by the addition of the thiol-terminated homopolymer to trimethylolpropane diacrylate

as well as to 2-arm star formed by the fragmentation of a 3-arm star at one of the points indicated in green. Supporting the MALDI-TOF MS data, the SEC traces in **Figure 5.11**. qualitatively indicate the successful formation of the star polymers. The trace at higher retention volume (solid line) is for the PDEAm1 homopolymer while the second chromatogram (dotted line) represents the resulting star polymer. Several points are worth highlighting. While the chromatogram for the precursor homopolymer is symmetrical and narrow (Mw/Mn = 1.15) the trace for the 3-arm star polymer is distinctly non-symmetric, somewhat broad (Mw/Mn = 1.35) and has an Mp (peak maximum molecular weight) that is not 3 X that of the homopolymer. Each of these points is readily explained. The non-symmetric nature of the chromatogram, i.e. tailing to higher retention volume, is due to both the excess of PDEAm homopolymer initially added and the presence of some '2-arm' star products. This is not a result of incomplete reaction, with the acrylate groups in the TMPTA since we demonstrated above (**Figure 5.6.**) that there are no detectable double bonds after reaction, but most likely due to the presence of the diacrylate impurity in TMPTA. Indeed, as noted above the TMPTA is not pure with the di-acrylate and mono-acrylates being the major impurities. The disagreement between the Mp values for the DEAm homopolymer and the 3-arm star product is also expected based on the known hydrodynamic properties of linear versus star polymers. Specifically, star polymers have higher densities than their linear counterparts and thus smaller hydrodynamic volumes for identical molecular masses, a feature that is borne out in the SEC results. Having verified successful 3-arm star formation using a combination of FTIR spectroscopy, $^1$H/$^{13}$C NMR spectroscopy, MALDI-TOF MS, and SEC in the presence of HexAM and DMPP a control experiment was performed to eliminate the

possibility of consumption of the C=C bonds in TMPTA via a radical process. An NMR experiment was set-up with PBA under exactly the same conditions as noted previously (see **Figure 5.6.**) except that 2 wt% TEMPO was also added. If the consumption of C=C bonds occurred via a radical pathway then the presence of TEMPO would, presumably, completely inhibit consumption by serving as a radical trap, or at least have a very significant effect on the reaction rate and yields. **Figure 5.12.** shows the $^1$H NMR spectrum of the reaction recorded after 5 min with the vinylic region shown inset. There is little/no evidence of any vinylic hydrogens confirming that the C=C bonds are not consumed via a radical pathway.

## Summary and Conclusions

Described herein is a detailed examination of a convergent synthetic approach to 3-arm star polymers via a macromolecular thiol–ene click reaction. Well-defined precursor homopolymers of N,N-diethylacrylamide (DEAm), and n-butyl acrylate (BA) were prepared via RAFT using 1-cyano-1-methylethyl dithiobenzoate as the RAFT agent and AIBN as the source of primary radicals. Key to this approach is the specific use of RAFT-synthesized (co)polymers since such materials serve as convenient masked terminal thiol bearing materials capable of undergoing post-polymerization reactions. When the hexylamine-mediated cleavage of the dithioester endgroups is conducted in the presence of dimethylphenylphosphine (DMPP) and trimethylolpropane triacrylate, sequential cleavage/thiol–ene reactions occur to yield the target 3-arm star polymers as verified by a combination of $^1$H/$^{13}$C NMR spectroscopy, FTIR spectroscopy, size exclusion chromatography, and MALDI-TOF MS. DMPP is demonstrated to serve two important roles. Firstly, it acts as an

extremely potent nucleophilic catalyst for the macromolecular thiol–ene reaction, which is proposed to propagate by a very reactive ionic carbon-centered enolate chain process that is not inhibited by any water that may be present. Secondly, it serves to prevent/inhibit disulfide formation between thiol-terminated polymers that can be a problem when the end-group reduction is performed only in the presence of amine. Control experiments confirmed that the ene bonds are only consumed in the presence of thiol and that the reaction does not proceed via a radical pathway.

## Acknowledgments

References

1. Hoyle, C.E.; Lee, T.Y.; Roper, T.; *J. Polym. Sci. Part A Polym. Chem.* **2004**; 42: 5301–38.

2. Gimbert, C.; Lumbierres, M.; Marchi, C.; Moreno-Mañas, M.; Sebastián, R.M.; Vallribera, A.; *Tetrahedron* **2005**; 61: 8598–605.

3. Kumar, A.; Akanksha; *Tetrahedron* **2007**; 63: 11086–92.

4. Khire, V.S.; Benoit, D.S.W.; Anseth, K.S.; Bowman, C.N.; *J. Polym. Sci. Part A: Polym. Chem.* **2006**; 44: 7027–39.

5. Simpson, N.; Takwa, M.; Hult, K.; Johansson, M.; Martinelle, M.; Malmstroem, E.; *Macromolecules* **2008**; 41: 3613–9.

6. Senyurt, A.F.; Hoyle, C.E.; Wei, H.; Piland, S.G.; Gould, T.E.; *Macromolecules* **2007**; 40: 3174–82.

7. Senyurt, A.F.; Wei, H.; Hoyle, C.E.; Piland, S.G.; Gould, T.E.; *Macromolecules* **2007**; 40: 4901–9.

8. White, T.J.; Natarajan, L.V.; Tondiglia, V.P.; Lloyd, P.F.; Bunning, T.J.; Guymon, C.A.; *Macromolecules* **2007**; 40: 1121–7.

9. Carioscia, J.A.; Schneidewind, L.; O'Brien, C.; Ely, R.; Fesser, C.; Cramer, N., Bowman, C.N.; *J. Polym. Sci. Part A: Polym. Chem.* **2007**; 45: 5686–96.

10. Kolb, H.C.; Finn, M.G.; Sharpless, K.B.; *Angew. Chem. Int. Ed.* **2001**; 40: 2004–21.

11. Fournier, D.; Hoogenboom, R.; Schubert, U.S.; *Chem. Soc. Rev.* **2007**; 36: 1369–80.

12. Binder, W.H.; Sachsenhofer, R.; *Macromol. Rapid Commun.* **2007**; 28: 15–54.

13. Evans, R.A.; *Aust. J. Chem.* **2007**; 60: 384–95.

14. Sumerlin, B.S.; Tsarevsky, N.V.; Louche, G.; Lee, R.Y.; Matyjaszewski, K.; *Macromolecules* **2005**; 38: 7540–5.

15. Kobayashi, S.; Itomi, K.; Morino, K.; Lida, H.; Yashima, E.; *Chem. Commun.* **2008**: 3019–21.

16. Vestberg, R.; Malkoch, M.; Kade, M.; Wu, P.; Fokin, V.V.; Sharpless, K.B.; *J. Polym. Sci. Part A: Polym. Chem.* **2007**; 45: 2835–46.

17. Killops, K.L.; Campos, L.M.; Hawker, C.J.; *J. Am. Chem. Soc.* **2008**; 130: 5062–4.

18. Gress, A.; Völkel, A.; Schlaad, H.; *Macromolecules* **2007**; 40: 7928–33.

19. Chiefari, J.; Chong, Y.K.; Ercole, F.; Krstina, J.; Jeffery, J.; Le, T.P.T.; et al.; *Macromolecules* **1998**; 31: 5559–62.

20. Moad, G.; Rizzardo, E.; Thang, S.H.; *Aust. J. Chem.* **2005**; 58: 379–410.

21. Lowe, A.B.; McCormick, C.L.; *Prog. Polym. Sci.* **2007**; 32: 283–351.

22. Perrier, S.; Takolpuckdee, P.; *J. Polym. Sci. Part A: Polym. Chem.* **2005**; 43: 5347–93.

23. Favier, A.; Charreyre, M.-T.; *Macromol. Rapid Commun.* **2006**; 27: 653–92.

24. Stenzel, M.H.; *Chem. Commun.* **2008**: 3486–503.

25. Lowe, A.B.; Sumerlin, B.S.; Donovan, M.S.; McCormick, C.L.; *J. Am. Chem. Soc.* **2002**; 124: 11562–3.

26. Sumerlin, B.S.; Lowe, A.B.; Stroud, P.A.; Urban, M.W.; McCormick, C.L.; *Langmuir* **2003**; 19: 5559–62.

27. Hotchkiss, J.W.; Lowe, A.B.; Boyes, S.G.; *Chem. Mater.* **2007**; 9: 6–13.

28. Spain, S.G.; Albertin, L.; Cameron, N.R.; *Chem. Commun.* **2006**: 4198–200.

29. Scales, C.W.; Convertine, A.J.; McCormick, C.L.; *Biomacromolecules* **2006**; 7: 1389–92.

30. Souppe, J.; Urrutigoity, M.; Levesque, G.; *Biochim. Biophys. Acta.* **1998**, 957: 254–7.

31. Delêtre, M.; Levesque, G.; *Macromolecules* **1990**; 23: 4733–41.

32. Levesque, G.; Arsène, P.; Fanneau-Bellenger, V.; Pham, T.-N.; *Biomacromolecules* **2000**; 1: 387–99.

33. Levesque, G.; Arsène, P.; Fanneau-Bellenger, V.; Pham, T.-N.; *Biomacromolecules* **2000**; 1: 400–6.

34. Qiu, X.-P.; Tanaka, F.; Winnik, F.M.; *Macromolecules* **2007**; 40: 7069–71.

35. Li, M.; De, P.; Gondi, S.R.; Sumerlin, B.S.; *J. Polym. Sci. Part A: Polym. Chem.* **2008**; 46: 5093–100.

36. Chan, J.W.; Yu, B.; Hoyle, C.E.; Lowe, A.B.; *Chem. Commun.* **2008**: 4959–61.

37. Mayadunne, R.T.A.; Jeffery, J.; Moad, G.; Rizzardo, E.; *Macromolecules* **2003**; 36: 1505–13.

38. Duréault, A.; Taton, D.; Destarac, M.; Leising, F.; Gnanou, Y.; *Macromolecules* **2004**; 37: 5513–9.

39. Bernard, J.; Favier, A.; Zhang, L.; Nilasaroya, A.; Davis, T.P.; Barner-Kowollik, C.; et al.; *Macromolecules* **2005**; 38: 5475–84.

40. Mori, H.; Ookuma, H.; Endo, T.; *Macromolecules* **2008**; 41: 6925–34.

41. Plummer, R.; Hill, D.J.T.; Whittaker, A.K.; *Macromolecules* **2006**; 39: 8379–88.

42. Feng, X.-S.; Pan, C.-Y.; *Macromolecules* **2002**; 35: 4888–93.

43. Inglis, A.J.; Sinnwell, S.; Davis, T.P.; Barner-Kowollik, C.; Stenzel, M.H.; *Macromolecules* **2008**; 41: 4120–6.

44. Moad, G.; Chiefari, J,; Chong, Y.K.; Krstina, J.; Mayadunne, R.T.A.; Postma, A.; et al.; *Polym. Int.* **2000**; 49: 993–1001.

45. Stewart, I.C.; Bergman, R.G.; Toste, F.D.; *J. Am. Chem. Soc.* **2003**; 125: 8696–7.

46. Methot, J.L.; Roush, W.R.; *Adv. Synth. Catal.* **2004**; 346: 1035–50.

47. Subbi, J.; Aguraiuja, R.; Tanner, R.; Allikmaa, V.; Lopp, M.; *Eur. Polym. J.* **2005**; 41: 2552–8.
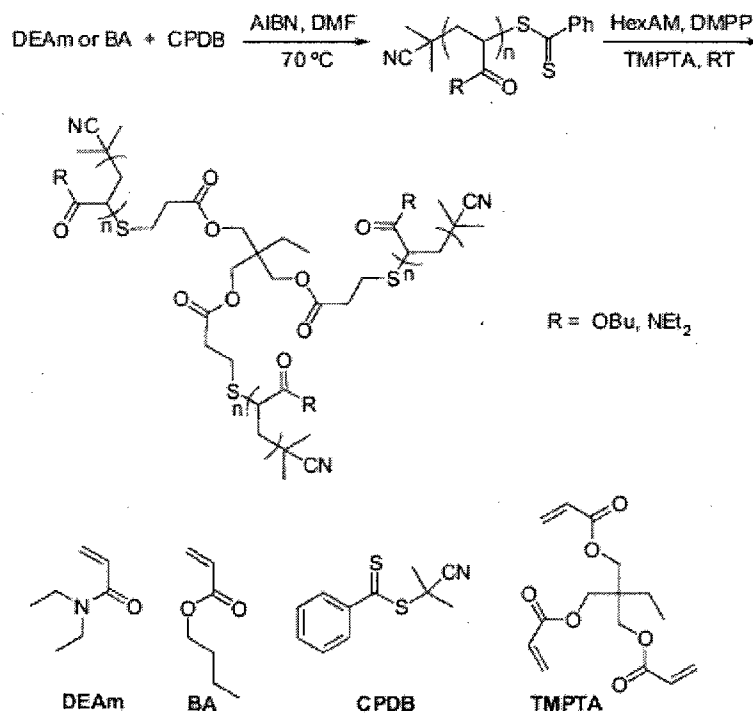
**Scheme 5.1.** Synthetic outline for the convergent approach to 3-arm star polymers under nucleophilic phosphine-catalyzed conditions using RAFT-prepared precursor homopolymers.
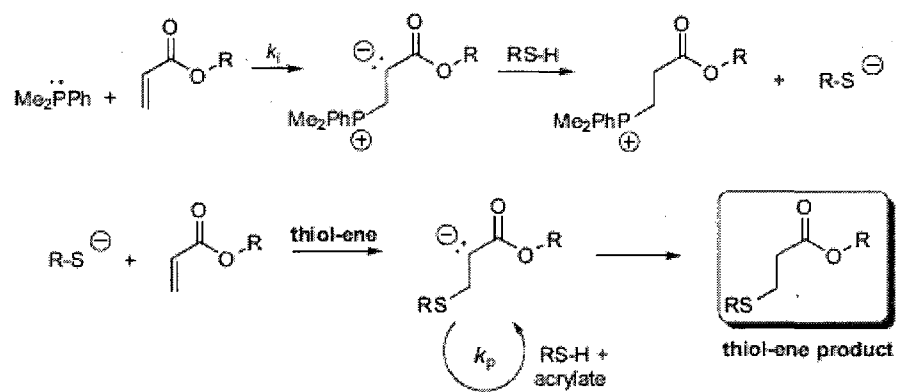
**Scheme 5.2.** Proposed anionic (enolate) chain mechanism for the phosphine-catalyzed addition of a thiol to an activated acrylic double bond.
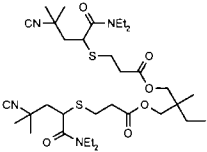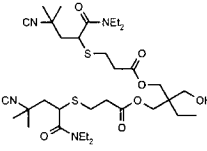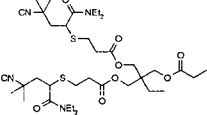
**Table 5.1.** Summary of homopolymer characteristics.

| Homopolymer | $M_n$ theory[a] | $M_n$ by SEC [b] | $M_n$ by NMR | $M_p$ by SEC | $M_w/M_n$ [b] |
|---|---|---|---|---|---|
| PDEAm1 | 4500 | 2800 | 3800 | 3400 | 1.15 |
| PDEAm2 | 4500 | 2900 | 4400 | 3600 | 1.18 |
| PnBA | 4500 | 3600 | 3300 | 4300 | 1.18 |

[a] At quantitative conversion.
[b] Determined in THF, relative to poly(methyl methacrylate) standards.

**Table 5.2.** Proposed structures of possible two-arm stars formed via fragmentation reactions along with the theoretical and measured m/z values for the H⁺, Na⁺, and K⁺ adducts.

| 2-Arm species | $H^+$, m/z theory | $H^+$, m/z observed | $Na^+$, m/z theory | $Na^+$, m/z observed | $K^+$, m/z theory | $K^+$, m/z observed |
|---|---|---|---|---|---|---|
|  | 7681 | 7679 | 7703 | 7703 | - | - |
|  | - | - | - | - | 7739 | 7735 |
|  | 7754 | 7751 | 7776 | 7774 | 7795 | 7794 |
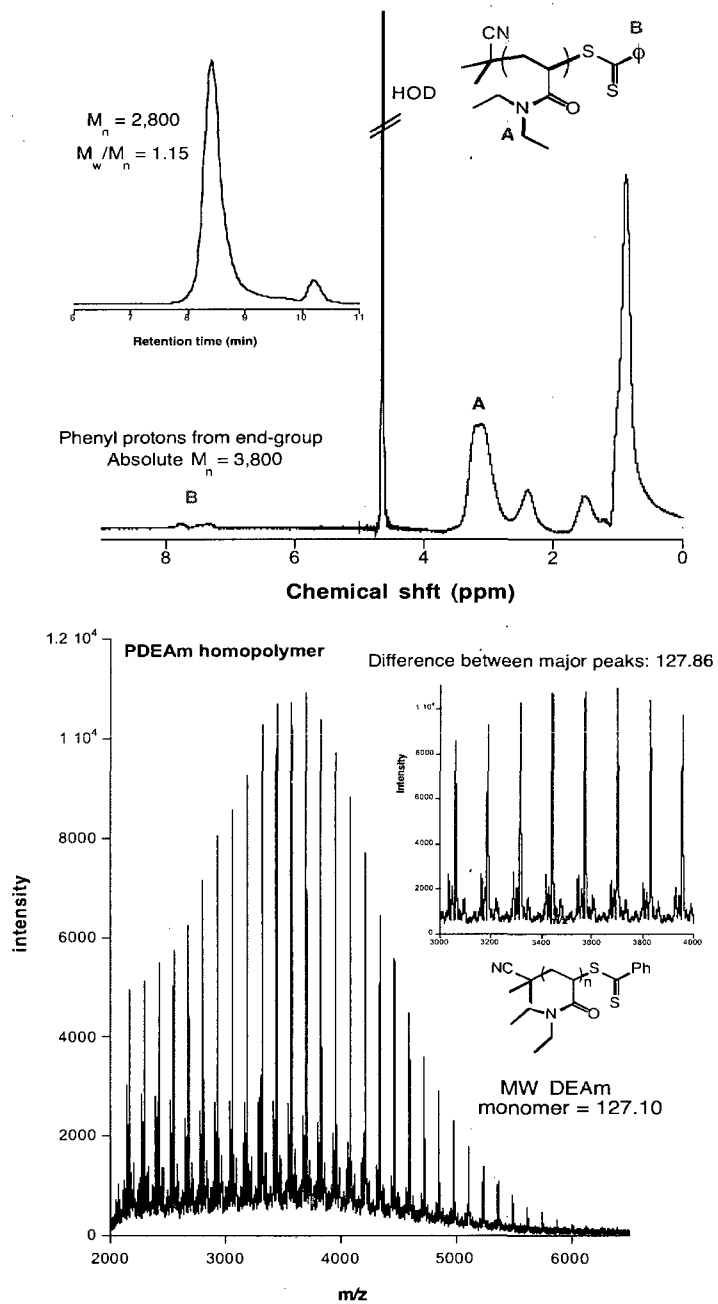
**Figure 5.1.** (A) $^1$H NMR spectrum, recorded in D$_2$O, of PDEAm2 demonstrating the ability to conduct end-group analysis with the SEC trace (RI signal) shown inset, and (B) the MALDI-TOF MS trace of the same homopolymer with an expansion between 3000 and 4000 a.m.u. shown inset.
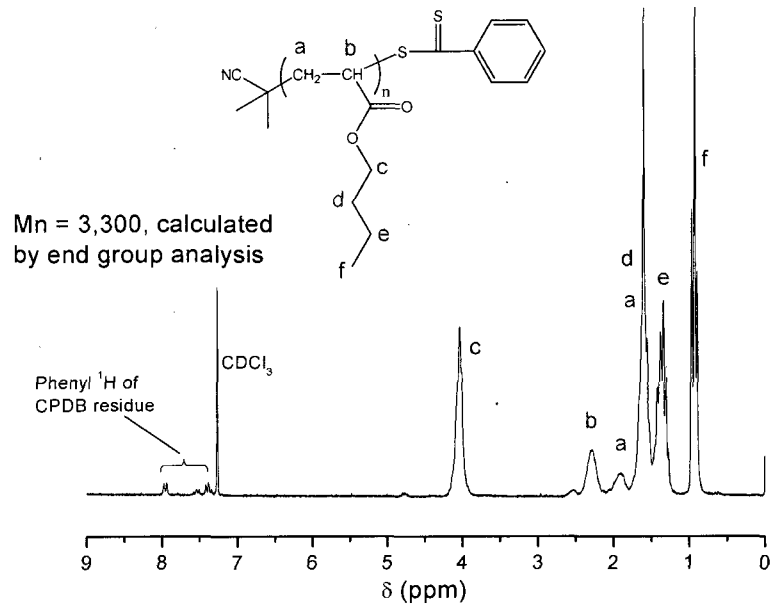
**Figure 5.2.** $^1$H NMR spectrum, recorded in CDCl$_3$, of PBA with end-group analysis.
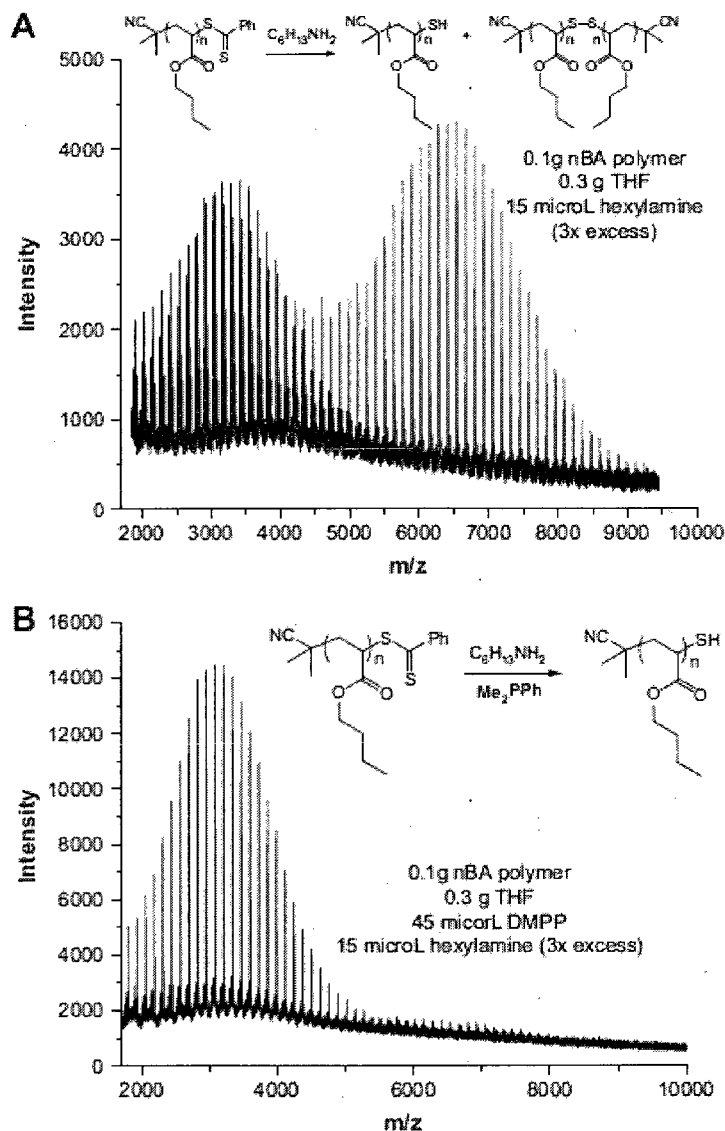
**Figure 5.3.** (A) MALDI-TOF MS trace of the products obtained after dithioester end-group reduction of PBA performed in the presence of only hexylamine (0.1 g BA homopolymer in 0.3 g THF with 15 mL of hexylamine), and (B) MALDI-TOF MS trace of the same homopolymer after end-group reduction in the presence of hexylamine and dimethylphenylphosphine (0.1 g BA homopolymer in 0.3 g THF, 45 mL of dimethylphenylphosphine, and 15 mL of hexylamine).
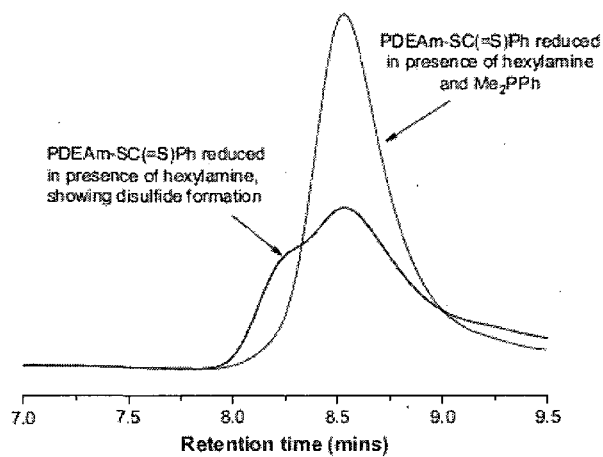
**Figure 5.4.** SEC traces (RI signal) of the products obtained after end-group cleavage with hexylamine of PDEAm1 in the presence and absence of dimethylphenylphosphine demonstrating the beneficial effect of phosphine in reducing/eliminating the presence of polymeric disulfide.
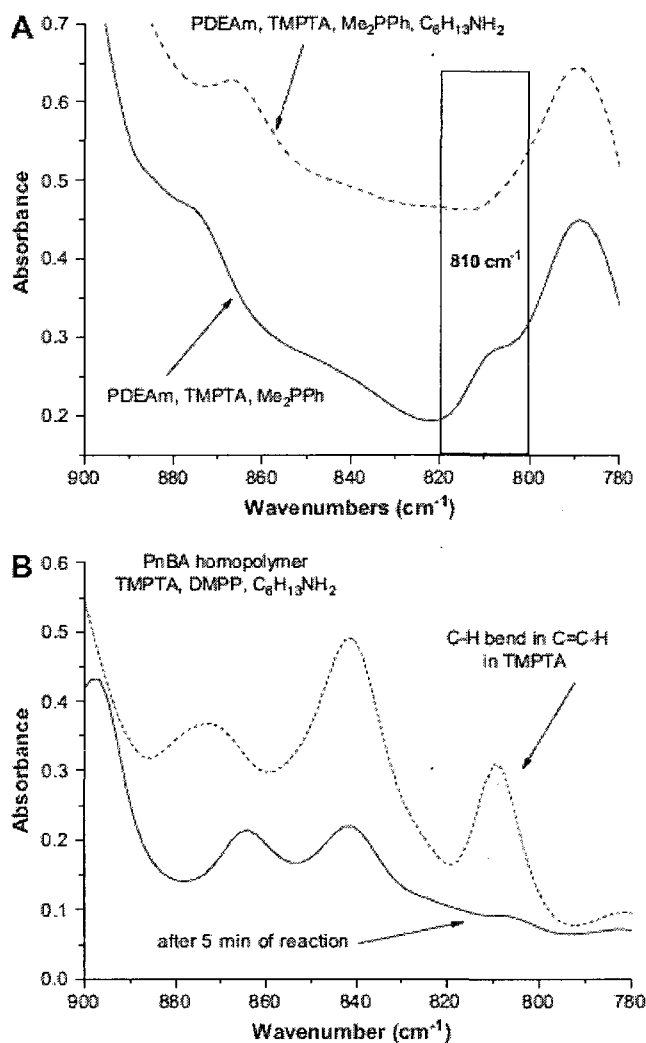
**Figure 5.5.** (A) FTIR spectroscopic trace for PDEAm2, TMPTA, and dimethylphenylphosphine before and after the addition of hexylamine highlighting the rapid consumption of C=C bonds as evidenced by the disappearance of the band at 810 cm$^{-1}$ associated with the C–H bend in C=C–H of TMPTA, and (B) same experimental data for the corresponding PBA homopolymer.
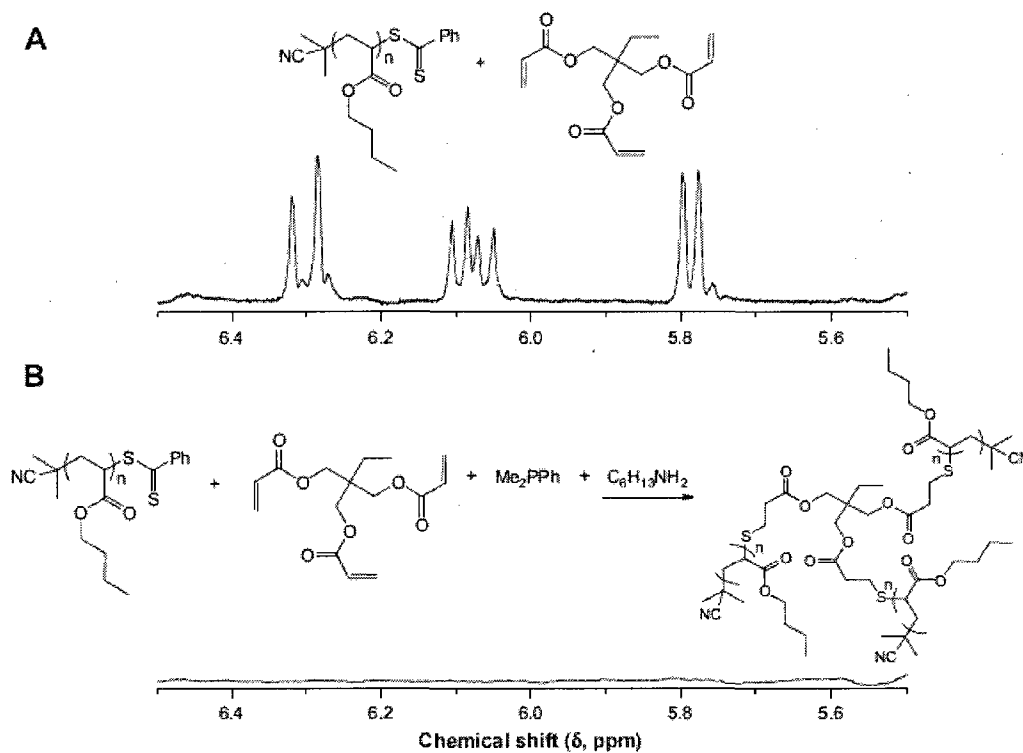
**Figure 5.6.** (A) $^1$H NMR spectrum of PBA+TMPTA, recorded in CDCl$_3$, highlighting the presence of the vinylic hydrogens in TMPTA, and (B) the $^1$H NMR spectrum of the same solution recorded approximately 5 min after the addition of hexylamine and dimethylphenylphosphine highlighting the complete absence of C=C bonds (NB – y scale ranges are identical).
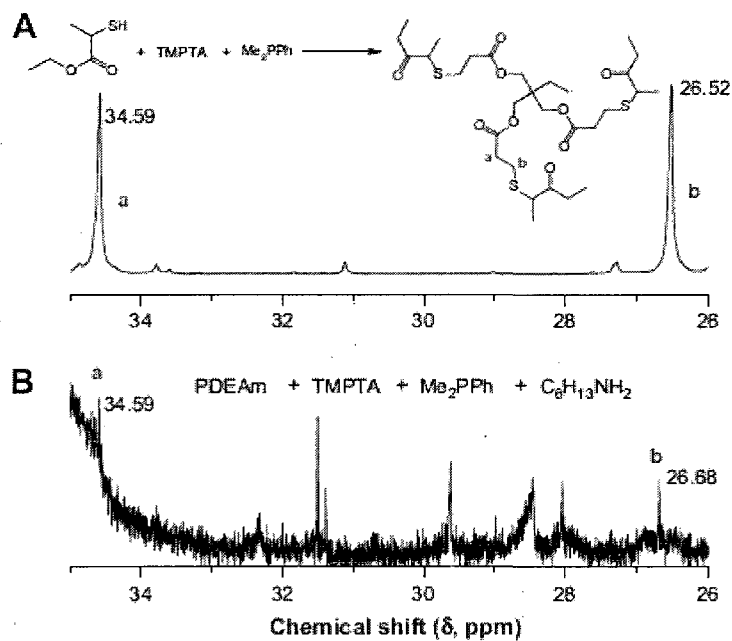
**Figure 5.7.** (A) $^{13}$C NMR spectrum plotted between 35 and 26 ppm for the model reaction between ethyl-2-mercaptopropionate (1.8 mL, 1.4 X 10$^{-5}$ moles) and TMPTA (2.5 mL, 8.3 X 10$^{-6}$ moles) catalyzed by dimethylphenylphosphine (10.0 mL, 0.11 M), recorded after 5 min of reaction highlighting the resonances associated with successful thiol–ene reaction, and (B) the $^{13}$C NMR spectrum, plotted over the same range, for the polymeric version with PDEAm2 with added hexylamine (20.0 mL, 0.35 M) to cleave the dithioester end-groups.
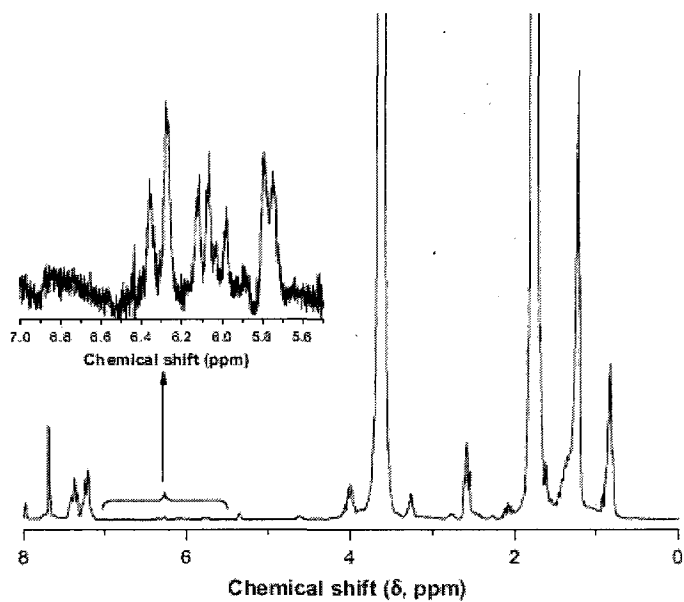
**Figure 5.8.** $^1$H NMR spectrum, recorded in CDCl$_3$, of a mixture of TMPTA, hexylamine, and dimethylphenylphosphine with an expansion of the vinylic region shown inset demonstrating the retention of C=C bonds in the absence of thiol.
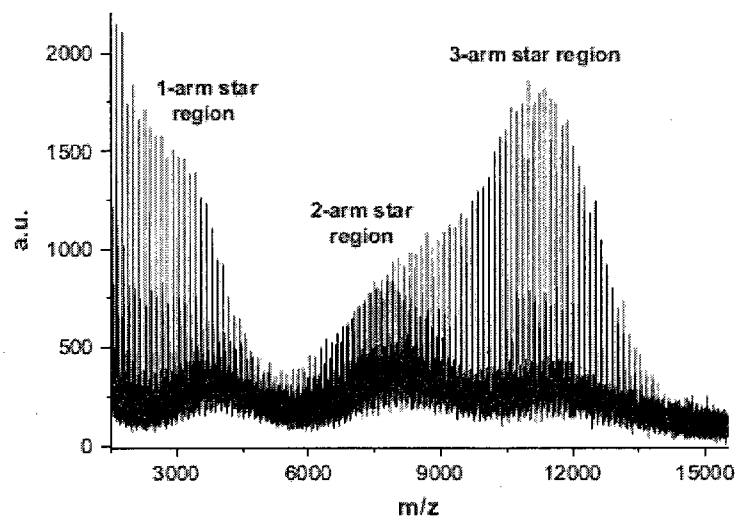
**Figure 5.9.** MALDI-TOF MS trace of the PDEAm1 star product, plotted between m/z = 1500 and 15,500 highlighting the presence of the desired 3-arm star product along with the presence of 2- and 1-arm species.
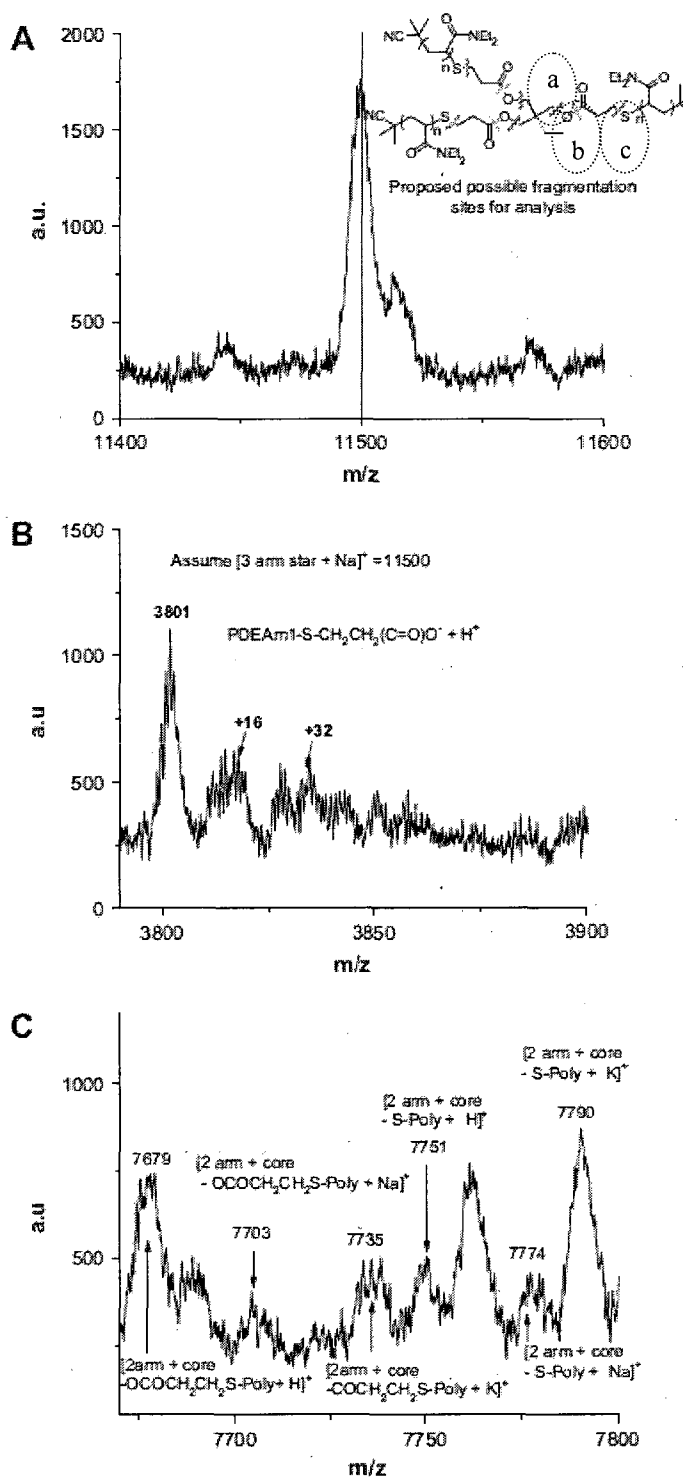
**Figure 5.10.** (A) MALDI-TOF MS trace plotted between m/z = 11,400 and 11,600 highlighting the presence of a 3-arm star based on PDEAm1 with an m/z = 11,500 (assumed to be [3-arm PDEAm + Na]$^+$). Shown inset is the generic structure of a PDEAm-based 3-arm star with possible fragmentation sites noted, (B) the same MALDI-TOF MS trace plotted between m/z = 3790 and 3900 (part of the 1-arm star region) showing the presence of a species with m/z = 3801 which corresponds to a

star arm formed by MALDI-induced fragmentation (structure shown inset), along with the presence of peaks at m/z = 3801 + 16 and 3801 + 32 that may species associated with oxidized sulfur atoms, and (C) the same MALDI-TOF MS trace plotted between m/z =7670 and 7800 (part of the 2-arm region) showing the presence of a series of peaks assigned to various 2-arm species formed via fragmentation reactions of the 3-arm star.
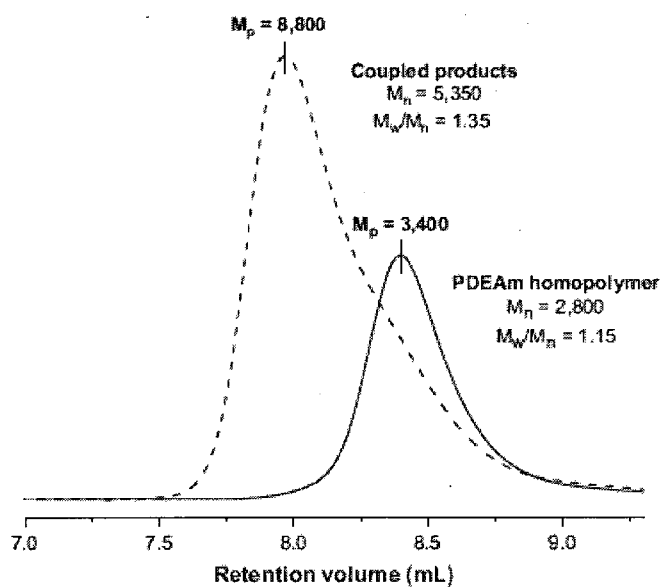
**Figure 5.11.** SEC traces (RI signal) of the PDEAm1 homopolymer and the corresponding 3- arm star polymer with the Mn, Mp, and Mw/Mn values listed.
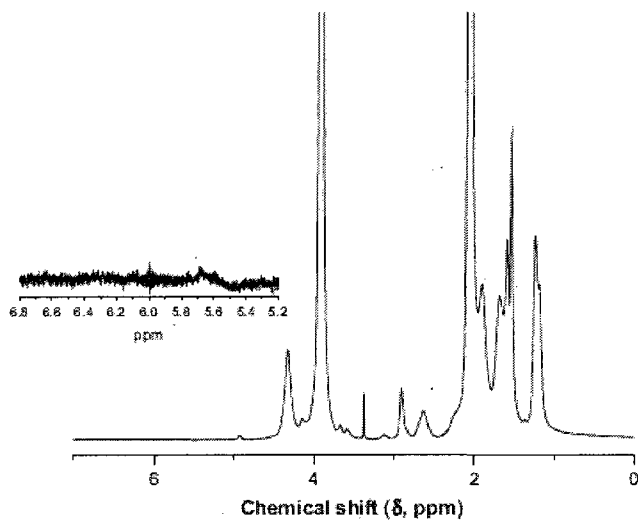
**Figure 5.12.** $^1$H NMR spectrum, recorded in CDCl3, after 5 min of reaction between PBA, TMPTA, dimethylphenylphosphine, hexylamine, and TEMPO demonstrating the complete disappearance of C=C bonds (the vinylic region is expanded in the inset), verifying that the reaction does not proceed via a radical process.

CHAPTER VI

SEQUENTIAL PHOSPHINE-CATALYZED, NUCLEOPHILIC THIOL-

ENE/RADICAL-MEDIATED THIOL-YNE REACTIONS AND THE FACILE

ORTHOGONAL SYNTHESIS OF POLYFUNCTIONAL MATERIALS

Abstract

A series of polyfunctional branched materials were prepared by the

photoinitiated reaction addition of thiols across the triple bonds of alkynes resulting in

quantitative loss of thiol and alkyne groups. Tetrafunctional alkynes were

quantitatively prepared by the rapid, solvent-less nucleophile catalyzed thio-Michael

addition reaction of a tetrafunctional thiol with propargyl acrylate. Exact molecular

weights of the polyfunctional materials were determined MALDI-TOF MS. Kinetics

of the reactions were analyzed by real-time FTIR (RTIR) and products were

characterized spectroscopically by $^1$H and $^{13}$C NMR.

Introduction

The thiol-ene reaction has recently attracted significant attention in the

materials arena,[1] as it displays many of the attributes of click chemistry.[2] Hawker and

co-workers[3] have highlighted its application in dendrimer synthesis, while Lowe et

al.[4] have described a macromolecular version in convergent star synthesis. Dove and

coworkers[5] described its use in preparing functional biodegradable polylactides, and

Schlaad and co-workers[6] utilized it to modify side chains of poly[2-(3-butenyl)-2-

oxazoline], while Rissing and Son[7] detailed the synthesis of branched organosilanes

with a range of functional thiols. Importantly, it should be noted that the thiol-ene

reaction proceeds under a variety of experimental conditions, including acid/base catalysis,[8] nucleophilic catalysis,[9] radical mediation (most commonly under photochemical conditions),[1] and via a solvent-promoted process.[10]

The real strength of the thiol-ene reaction is the broad range of ene substrates that readily undergo hydrothiolation, including activated and nonactivated species.[1] The reaction between a thiol and an yne has been widely studied.[11] As with the thiol-ene reaction, the thiol-yne reaction proceeds rapidly under a variety of experimental conditions, selectively yielding the mono- or bis-addition products. While the thiol-yne reaction is well-documented in the fields of organic[12] and organometallic[13] chemistry, it has been essentially overlooked in the polymer/materials area, with very few examples detailing its application appearing in the literature. However, recent reports have appeared from Fairbanks and coworkers[14] and Hoyle and coworkers.[15] The latter described the straightforward synthesis of high-refractive-index materials derived from the radical-mediated reaction of alkylthiols and simple diynes and is covered in the later chapter of this manuscript. It is important to note that the radical thiol-yne reaction possesses characteristics virtually identical to those of the radical thiol-ene reaction. However, the reaction of 2 equiv of thiol with the alkyne is itself a two-step process. The first step involves the addition of thiol to the C≡C bond to yield an intermediate vinyl thioether that subsequently undergoes a second, formally thiol-ene, reaction with additional thiol, yielding the 1,2 double-addition species as the sole product in quantitative yield.[16]

Experimental

*Materials*

Propargyl acrylate, adamantane-1-thiol, 6-mercapto hexanol, thioglycerol, 3-mercaptopropionic acid, mercaptosuccinic acid, captopril, 3-(trimethoxysilyl) propanethiol, α-cyano-4-hydroxycinnamic acid (CHCA), trans-indole acrylic acid (IAA), dimethylphenylphosphine, benzene, dichloromethane, and methanol were purchased from Aldrich Chemical Co. and used as received. The photoinitiator, α,α-dimethoxy-α-phenylacetophenone (Irgacure 651), was obtained from Ciba Specialty Chemicals. 3-mercaptopropyl polyhedral oligomeric silsesquioxane [POSS] was obtained from Hybrid Plastics and pentaerithrytol tetra(3-mercaptopropionate) [4-thiol] was obtained from Bruno Bock Chemicals.

*Synthesis of the 4-Functional Alkyne (14)*

Pentaerythritol tetra (3-mercaptoprionate) (2.44 g, 5 mmol) was mixed with 2 X $10^{-3}$ M Me$_2$PPh. To this mixture was added propargyl acrylate (2.20 g, 20 mmol). The reaction was left for 1 hr to ensure complete reaction. The reaction was monitored by IR and NMR spectroscopies.

*Synthesis of 16-Functional Alcohol*

**14** (0.116 g, 0.125 mmol) was mixed with thioglycerol (0.108 g, 1 mmol) and 2 wt% α,α-dimethoxy-α-phenylacetophenone in a 20mL glass scintillation vial. Samples were irradiated using a medium pressure Hg lamp (light intensity 9.25mW/cm$^2$) until thiol and yne were completely converted as determined by RTIR spectroscopy.

*Synthesis of 16-Functional Acid*

**14** (0.116 g, 0.125 mmol) in 2g of a 50:50 mixture of dichloromethane/methanol was mixed with mercaptosuccinic acid (0.150 g, 1 mmol) and 2 wt% α,α-dimethoxy-α-phenylacetophenone in a 20 mL glass scintillation vial. Samples were irradiated using a medium pressure Hg lamp (light intensity 9.25mW/cm$^2$) until thiol and yne were completely converted as determined by RTIR spectroscopy.

*Synthesis of 8-Functional Alcohol*

**14** (0.116 g, 0.125 mmol) was mixed with 6-mercapto-1-hexanol (0.134 g, 1 mmol) and 2 wt% α,α-dimethoxy-α-phenylacetophenone in a 20 mL glass scintillation vial. Samples were irradiated using a medium pressure Hg lamp (light intensity 9.25mW/cm$^2$) until thiol and yne were completely converted as determined by RTIR spectroscopy.

*Synthesis of 8-Functional Acid*

**14** (0.116 g, 0.125 mmol) was mixed with 3-mercaptopropionic acid (0.162 g, 1 mmol) and 2 wt% α,α-dimethoxy-α-phenylacetophenone in a 20 mL glass scintillation vial. Samples were irradiated using a medium pressure Hg lamp (light intensity 9.25mW/cm$^2$) until thiol and yne were completely converted as determined by RTIR spectroscopy.

*Synthesis of 8-Functional Captopril*

**14** (0.116 g, 0.125 mmol) in 2g of a 50:50 mixture of dichloromethane/methanol was mixed with captopril (0.217 g, 1 mmol) and 2 wt% α,α-dimethoxy-α-phenylacetophenone in a 20 mL glass scintillation vial. Samples were irradiated using a medium pressure Hg lamp (light intensity 9.25mW/cm$^2$) until thiol and yne were completely converted as determined by RTIR spectroscopy.

*Synthesis of 8-Functional POSS*

**14** (0.116 g, 0.125 mmol) in 2g of a benzene was mixed with mercaptopropyl isobutyl POSS® (0.891 g, 1 mmol) and 2 wt% $\alpha,\alpha$-dimethoxy-$\alpha$-phenylacetophenone in a 20 mL glass scintillation vial. Samples were irradiated using a medium pressure Hg lamp (light intensity 9.25mW/cm$^2$) until thiol and yne were completely converted as determined by RTIR spectroscopy.

*Synthesis of 8-Functional Adamantane*

**14** (0.116 g, 0.125 mmol) in 2g of a benzene was mixed with 1-adamantanethiol (0.163 g, 1 mmol) and 2 wt% $\alpha,\alpha$-dimethoxy-$\alpha$-phenylacetophenone in a 20 mL glass scintillation vial. Samples were irradiated using a medium pressure Hg lamp (light intensity 9.25mW/cm2) until thiol and yne were completely converted as determined by RTIR spectroscopy.

*Characterization*

*Kinetics.* Modification of 4-thiol with propargyl acrylate was formulated in a 1:1 molar ratio of thiol to acrylate with ~2 × 10-3 M Me$_2$PPh catalyst. All samples were 2:1 thiol to alkyne molar ratios, or 1:1 functional group ratios, taking the alkyne to be tetrafunctional using 2 wt% $\alpha,\alpha$-dimethoxy-$\alpha$-phenylacetophenone (Irgacure 651). Sample thicknesses were approximately 200 microns. RTIR was used to monitor the loss of thiol (2570 cm$^{-1}$), acrylate (810 cm$^{-1}$), and yne (2120 cm$^{-1}$) functional groups. The light intensity of the high pressure mercury lamp delivered to the sample via a light pipe was ~ 20 mW/cm$^2$ for photoinduced reactions.

*Measurements and instrumentation.* FT-IR spectra were recorded using a modified Bruker 88 spectrometer. Samples were sandwiched between two sodium

chloride salt plates at a thickness of ~20 micron. Each spectrum was collected over 32 scans. The data were analyzed with the Bruker OPUS/IR Version 4.0 software.

MALDI-TOF mass spectrometry (MALDI-TOF MS) was performed on a Bruker Reflex III Instrument equipped with a 337 nm $N_2$ laser in the reflector mode using both positive and negative modes and 20kV acceleration voltage. α-Cyano-4-hydroxycinnamic acid (CHCA) and trans-indole acrylic acid (IAA) were used as matrices for molecular weight determination.

NMR spectra were recorded on a Bruker 300 (53 mm). $^{13}$C NMR characterization and $^1$H NMR characterization with samples (10%v/v) dissolved in $d_6$-benzene, DMSO-$d_6$, methanol-$d_4$ or CDCl$_3$ used for deuterium shimming and locking.

## Results and Discussions

In this chapter, the first example of sequential thiol-ene/thiol-yne reactions that proceed in an orthogonal fashion, as a means of preparing highly functional materials under facile conditions (i.e., at ambient temperature and humidity under an air atmosphere) are highlighted. We specifically take advantage of the extremely rapid and quantitative reaction of a thiol with an activated ene under nucleophile-initiated conditions (a thiol-Michael reaction), employing dimethylphenylphosphine (Me$_2$PPh) as the initiator, in conjunction with the radical-mediated thiol-yne reaction, which proceeds rapidly to yield the 1,2-addition product exclusively[16] and quantitatively. Initially, a model reaction was examined to determine the general reaction kinetics and to establish the feasibility of the proposed sequential approach to a range of multifunctional materials. The 1:1 reaction of the mercaptoethylester 1

with propargyl acrylate (2) at ambient temperature under bulk conditions in the

presence of ~2 × 10-3 M Me$_2$PPh resulted in the rapid, selective addition of the thiol

group across the activated ene to yield the propargyl thioether diester 3 in 100% yield.

(**Figure 6.1.A**). Even at such a low concentration of Me$_2$PPh, the reaction reached

>90% conversion within ~2.5 min and was complete after ~17 min. Increasing the

concentration of Me$_2$PPh significantly enhanced the rate to the extent that the reaction

was complete in less than 1 min. The impressive rate of these phosphine-mediated

reactions is attributed to the anionic chain mechanism, (**Scheme 6.1.**) in which the

powerful nucleophile Me$_2$PPh is employed to generate a strong enolate base. Gimbert

et al.[17] previously proposed such a mechanism for phosphine-mediated thio-Michael

addition reactions, and Stewart et al.[18] highlighted the same mechanism for the

phosphine-catalyzed oxa-Michael addition of water and alcohols to activated enes.

However, this is the first time it has been proposed for the nucleophilic thiol- Michael

reaction. It should be highlighted that a key feature of this combination of reagents,

namely, the low pKa of the thiol coupled with the high reactivity of the thiolate anion

toward conjugate addition, enables this reaction to be performed with 100%

efficiency even in the presence of other protic species such as water. Subsequently,

the terminal propargyl group in 3 was reacted with 2 equiv of thioglycerol (4) in the

presence of 2 wt % α,α-dimethoxy-α-phenylacetophenone at 365 nm under a normal

air atmosphere at ambient temperature and humidity. The thiol-yne reaction can be

readily followed using real-time RTIR spectroscopy (**Figure 6.1.B**) by recording the

disappearance of the peak at 2120 cm$^{-1}$ associated with the yne and that at 2570 cm$^{-1}$

associated with the thiol. Under these experimental conditions, >90% conversion was

observed within ~1.5 min, and complete consumption of both functional species

occurred within ~10 min, yielding the tetra-alcohol **5** quantitatively. The structure of product **5** was confirmed unambiguously via $^1$H and $^{13}$C NMR spectroscopy. **Figure 6.1.C** shows the $^1$H NMR spectrum of 5, with peak assignments. After this demonstration of the feasibility of conducting sequential thiol-ene/thiol-yne reactions in an orthogonal manner, the methodology was applied to the synthesis of a series of polyfunctional structures employing a range of functional thiols, including examples recently highlighted by Hawker et al.,[19] to demonstrate the broad utility of the thiol-yne reaction and also the sequential thiol-ene/thiol-yne process. Specifically, in addition to **4**, we examined mercaptosuccinic acid **(6)**, a secondary thiol; captopril **(7)**, an angiotensin converting enzyme (ACE) inhibitor; 3-(trimethoxysilyl) propanethiol **(8)**; the 3-mercaptopropyl polyhedral oligomeric silsesquioxane [POSS] **(9)**; adamantane-1-thiol **(10)**, a tertiary thiol; 3-mercaptopropionic acid **(11)**; and 6-mercaptohexanol **(12)** **(Figure 6.2.)**. The synthetic approach was identical to that highlighted above, except that the tetrathiol pentaerithrytol tetra(3-mercaptopropionate) **(13)** was used in place of 1 in the initial thiol-ene reaction with **2** **(Scheme 6.2.)**. Where possible, the reactions were conducted neat, but in the case of **6, 7, 9,** and **10**, solvents were required, see Experimental section for details. In all instances, the resulting multifunctional materials required no cleanup or were easily purified by simple washing/extraction. The products were characterized by a combination of NMR spectroscopy and matrix-assisted laser desorption ionization time-of-flight mass spectrometry (MALDI-TOF MS). For example, **Figure 6.3.A** shows the $^1$H NMR and **Figure 6.3.B** MALDI-TOF MS trace for the 16-functional polyol obtained from reaction of **14** with R-SH **(4)**. With the assumption of quantitative reaction for both the thiol-ene and thiol-yne reactions, which is

reasonable given the results for the model reaction, the resulting 16-functional polyol would have an expected molecular mass of 1794.4 Da. The MALDI-TOF MS trace indicates a primary peak at m/z = 1816.4 that is due to the Na+-cationized 16-functional polyol, i.e., [16-functional polyol + Na]+. The **Figure 6.3.B** inset shows the measured (black line), and calculated (gray line) isotopic distributions associated with [16-functional polyol + Na]+. These agree perfectly with each other and further serve to confirm the quantitative nature of these sequential thiol based click reactions. (It should be noted that it is also possible to observe a lower-molecular-weight peak due to products derived from the trithiol impurity in **(14)**, see **Figure 6.4**. Additional MALDI-TOF MS plots and isotopic splitting patterns are given in **Figures 6.5-6.8** and representative $^1$H NMR spectra are given in **Figures 6.9** and **6.10**. **Table 6.1.** summarizes the experimentally determined molecular masses, with the major m/z peak listed along with the theoretical molecular masses of the H+- and Na+-cationized products calculated by assuming that quantitative conversion was obtained, from the reactions of **14** with **4, 6-8, 11,** and **12**. In all instances, the major observed MALDI-TOF MS peak corresponds to either the H+- or Na+-cationized species. The agreement between the theoretical molecular masses based on quantitative conversion for the thiol-ene/ thiol-yne sequence and the experimentally determined values is excellent, generally within 1-2 Da. Such agreement further highlights the broad utility and quantitative nature of these sequential thiol-based reactions. Unfortunately, the products derived from the reactions of **14** with **9** and **10** could not be successfully analyzed by MALDI TOF MS. However, FTIR and $^1$H NMR spectroscopic monitoring of these reactions indicated complete consumption of both the thiol and

yne components, consistent with the results of the reactions of the other thiols with **14,** see **Figures 6.11-6.14**.

## Summary and Conclusions

In summary, we have presented the first examples of sequential thiol-ene/thiol-yne reactions for the facile synthesis of polyfunctional materials using a range of commercially available thiols, including examples having potential biomedical significance. We have highlighted the radical-mediated thiol-yne reaction and demonstrated its versatility in advanced materials synthesis. In view of the combination of yield, orthogonality, and rate, it is expected that the phosphine-mediated thiol-ene reaction, the radical mediated thiol-yne reaction, and the tandem thiol-ene/thiol-yne sequence will be employed in a plethora of applications ranging across the chemical, materials, optical, electronic, and biomolecular fields.

References

1. Hoyle, C. E.; Lee, T. Y.; Roper, T. *J. Polym. Sci., Part A: Polym. Chem.* **2004**, *42*, 5301.

2. Kolb, H. C.; Finn, M. G.; Sharpless, K. B. *Angew. Chem., Int. Ed.* **2001**, *40*, 2004.

3. Killops, K. L.; Campos, L. M.; Hawker, C. J. *J. Am. Chem. Soc.* **2008**, *130*, 5062.

4. Chan, J. W.; Yu, B.; Hoyle, C. E.; Lowe, A. B. *Chem. Commun.* **2008**, 4959.

5. Pounder, R. J.; Stanford, M. J.; Brooks, P.; Richards, S. P.; Dove, A. P. *Chem. Commun.* **2008**, 5158.

6. Gress, A.; Volkel, A.; Schlaad, H. *Macromolecules* **2007**, *40*, 7928.

7. Rissing, C.; Son, D. Y. *Organometallics* **2008**, *27*, 5394.

8. Li, M.; De, P.; Gondi, S. R.; Sumerlin, B. S. *J. Polym. Sci., Part A: Polym. Chem.* **2008**, *46*, 5093.

9. Sanui, K.; Ogata, N. *Bull. Chem. Soc. Jpn.* **1967**, *40*, 1727.

10. Tolstyka, Z. P.; Kopping, J. T.; Maynard, H. D. *Macromolecules* **2008**, *41*, 599.

11. Rutledge, T. F. *Acetylenes and Allenes*: Reinhold Book Corporation: New York, 1969.

12. See, for example: Yadav, J. S.; Subba Reddy, B. V.; Raju, A.; Ravindar, K.; Baishya, G. *Chem. Lett.* **2007**, *36*, 1474.

13. See, for example: Ogawa, A.; Ikeda, T.; Kimura, K.; Hirao, T. *J. Am. Chem. Soc.* **1999**, *121*, 5108.

14. Fairbanks, B. D.; Scott, T. F.; Kloxin, C. J.; Anseth, K. S.; Bowman, C. N. *Macromolecules* **2009**, *42*, 211.

15. Chan, J. W.; Zhou, H.; Hoyle, C. W.; Lowe, A. B. *Chem. Mater.* **2008**, *21*(8), 1579-1585.

16. Sauer, J. C. *J. Am. Chem. Soc.* **1957**, *79*, 5314.

17. Gimbert, C.; Lumbierres, M.; Marchi, C.; Moreno-Manas, M.; Sebastian, R. M.; Vallribera, A. *Tetrahedron* **2005**, *61*, 8598.

18. Stewart, I. C.; Bergman, R. G.; Toste, F. D. *J. Am. Chem. Soc.* **2003**, *125*, 8696.

19. Campos, L. M.; Killops, K. L.; Sakai, R.; Paulusse, J. M. J.; Damiron, D.;Drockenmuller, E.; Messmore, B. W.; Hawker, C. J. *Macromolecules* **2008**, *41*, 7063.
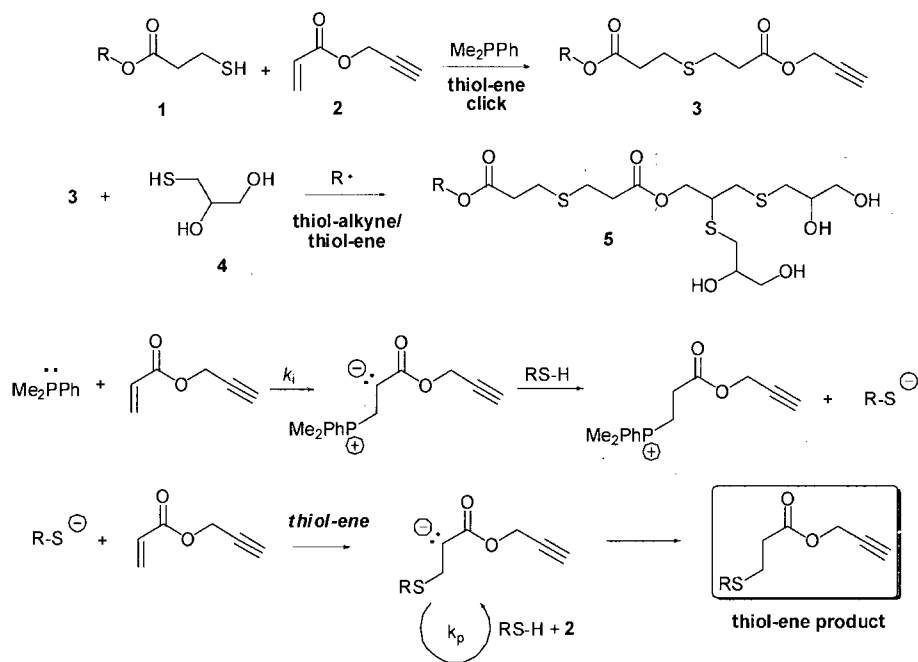
**Scheme 6.1.** Sequential thiol-ene/thiol-yne reactions[a] and the proposed anionic chain mechanism for the Me₂PPh-initiated thiol-ene reaction to an activated ene

[a] (i) Dimethylphenylphosphine (Me2PPh) (~2 × 10⁻³ M), **1** (1 equiv), **2** (1 equiv); (ii) **3** (1 equiv), **4** (2 equiv), 2 wt % α,α-dimethoxy-α-phenylacetophenone, 365 nm (reaction rate depends on sample thickness).
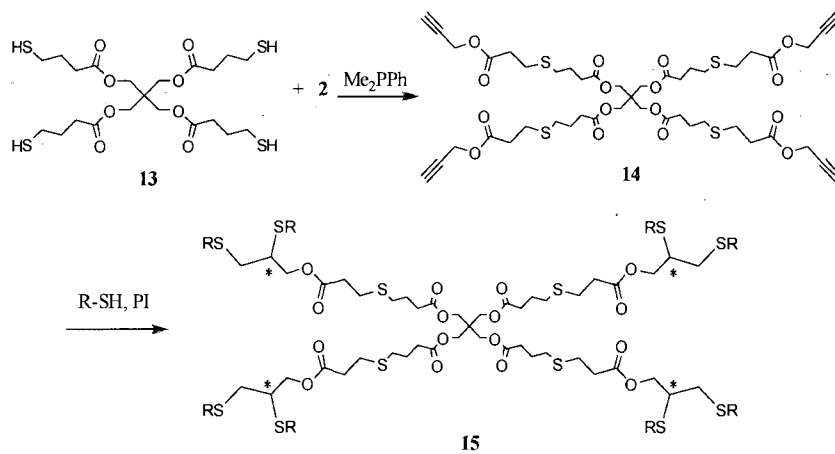
**Scheme 6.2.** Synthesis of multifunctional thioethers via sequential thiol-ene/thiol-yne reactions (generated stereocenters denoted by *)

**Table 6.1.** Summary of measured molecular masses of the thioether-based polyfunctional products.

| target molecule | theoretical molecular mass (Da) | | major MALDI-TOF MS peak (m/z) |
|---|---|---|---|
| | H+ | Na+ | |
| 16-alcohol (4 +14) | 1794.4 | 1817.4 | 1816 |
| 16-acid (6 + 14) | 2130.4 | 2153.3 | 2128.5 |
| 8-alcohol (12 + 14) | 2003.1 | 2026 | 2025 |
| 8-acid (11 + 14) | 1778.3 | 1801.3 | 1799 |
| 8-captopril (7 + 14) | 2667.4 | 2690.4 | 2666.5 |
| 8-silane (8 + 14) | 2499.9 | 2522.9 | 2519 |

**A**
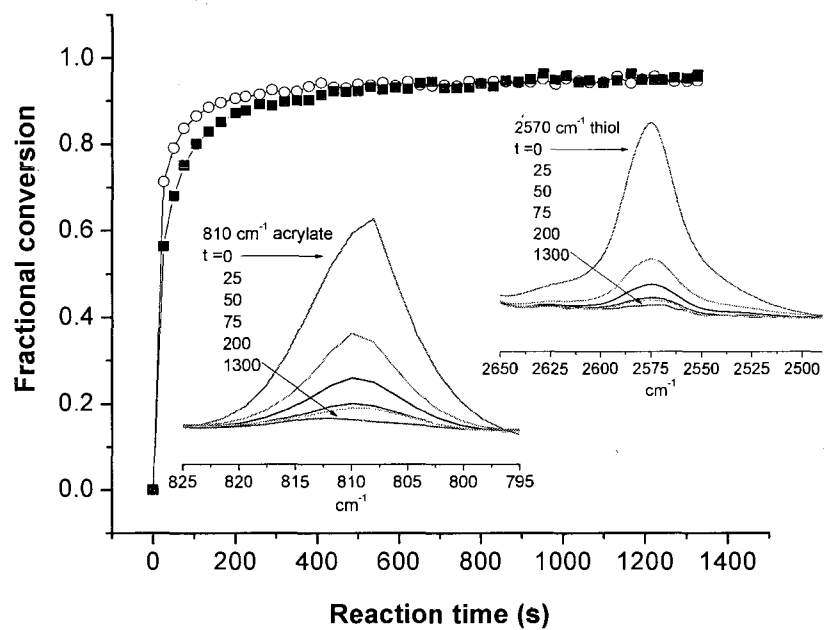


**B**
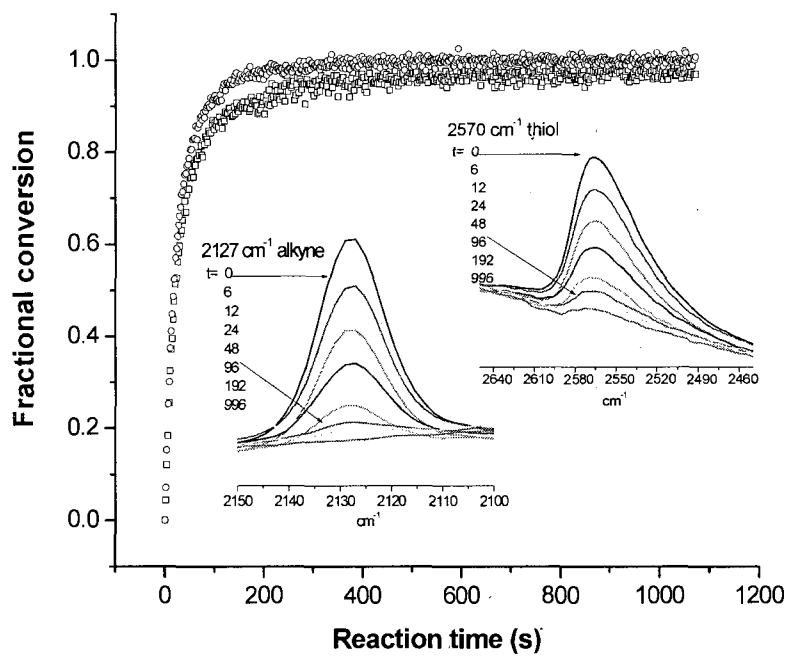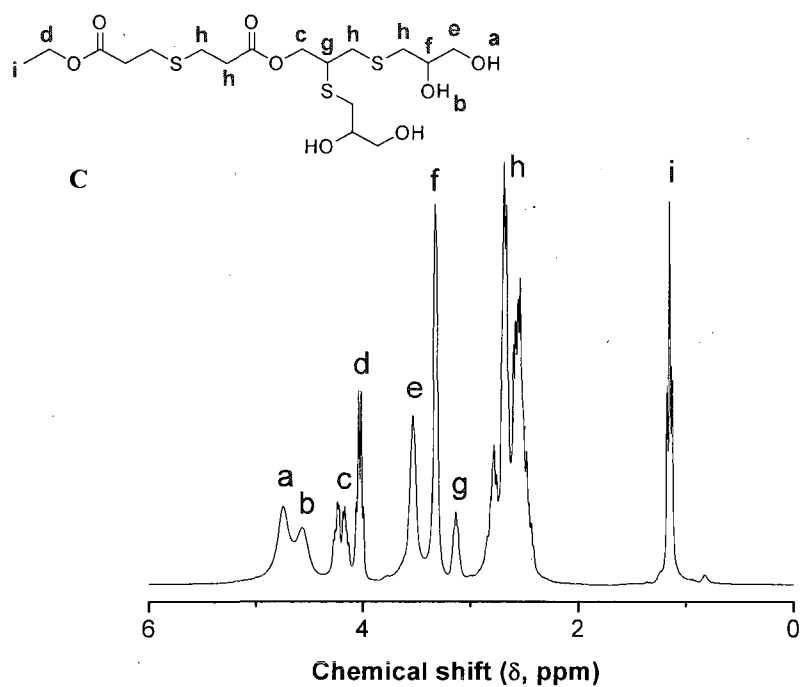
**Figure 6.1.** (A) RT-FTIR monitoring of the reaction between **1** (R=CH$_2$CH$_3$) and **2**: (○) thiol peak area at 2570 cm$^{-1}$, and (■) acrylate peak area at 810 cm$^{-1}$. (B) RT-FTIR monitoring of the photochemical reaction between **3** (R=CH2CH3) and **4**: (□) thiol peak area at 2570 cm$^{-1}$ and (○) yne peak height at 2127 cm$^{-1}$. (C) $^1$H NMR spectrum recorded in $d_6$-DMSO, with relevant peak assignments, confirming the structure of **5** (R=CH$_2$CH$_3$).
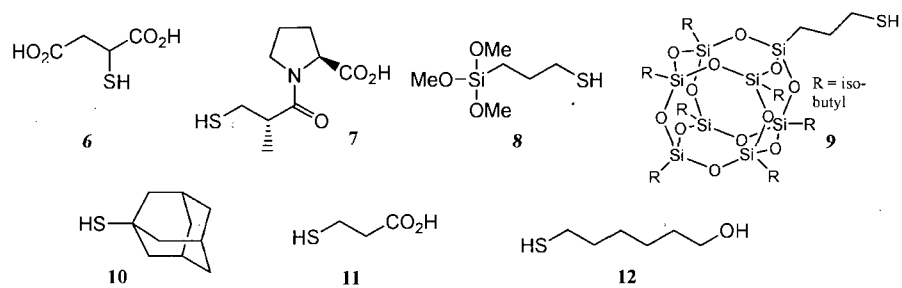
**Figure 6.2.** Chemical structures of commercially available functional thiols employed for the synthesis of polyfunctional materials.
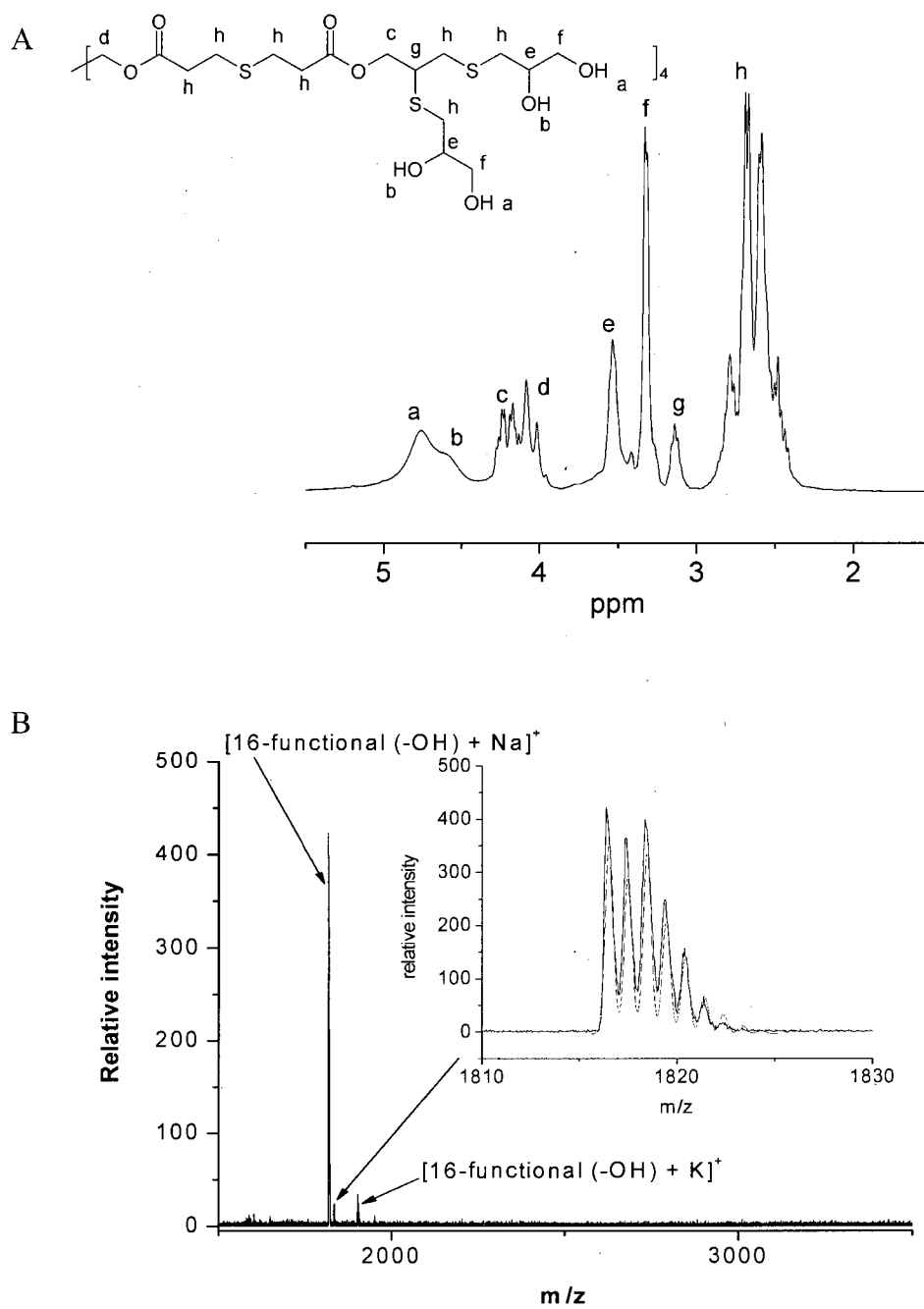
**Figure 6.3.** (A) Chemical structure and $^1$H NMR spectrum of the 16-functional alcohol $^1$H NMR ($d_6$-DMSO), δ (ppm): 2.32-2.92 (56H, broad m), 3.06-3.20 (4H, broad t), 3.20-3.44 (16H, broad d), 3.44-3.60 (8H, broad t), 3.88-4.33 (16H, m), 4.35-5.16 (16H) (B) MALDI-TOF MS trace of the 16-functional polyol derived from the thiol-yne reaction of **4** with **14** under photochemical conditions.
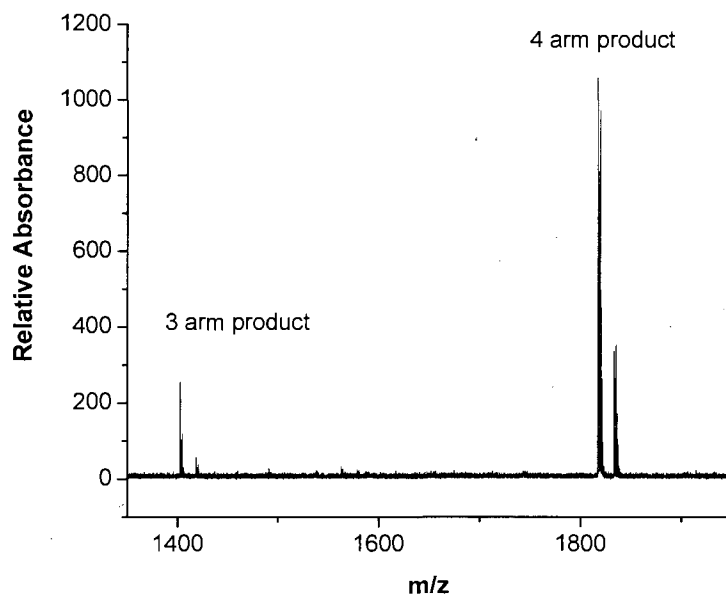
**Figure 6.4.** MALDI-TOF MS spectrum of the 16-functional alcohol highlighting the presence of 3-arm products.
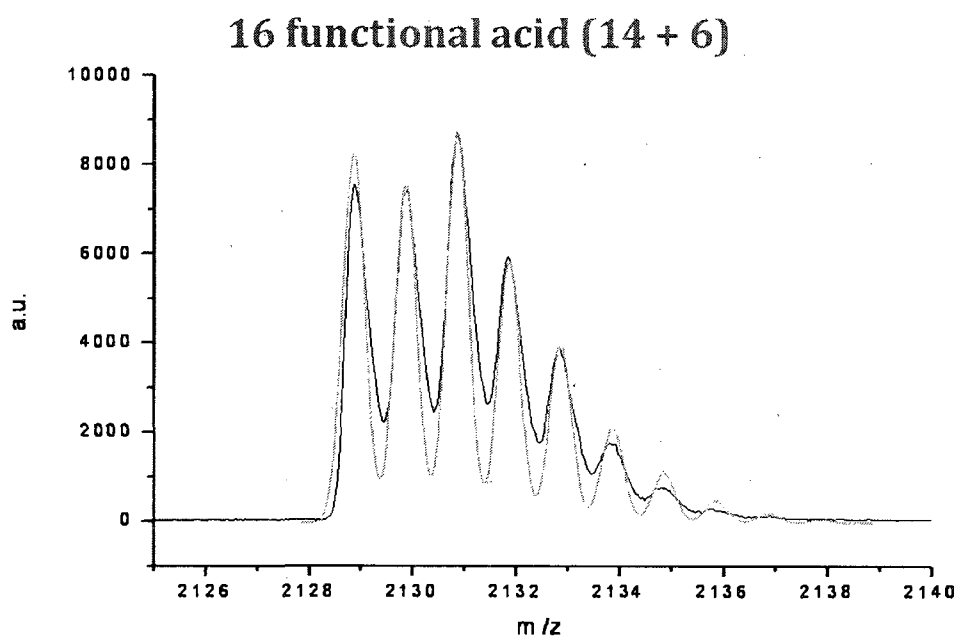
**Figure 6.5.** Measured (black) and predicted (gray) isotopic mass distributions for the products from the reaction of **14** with **6**.
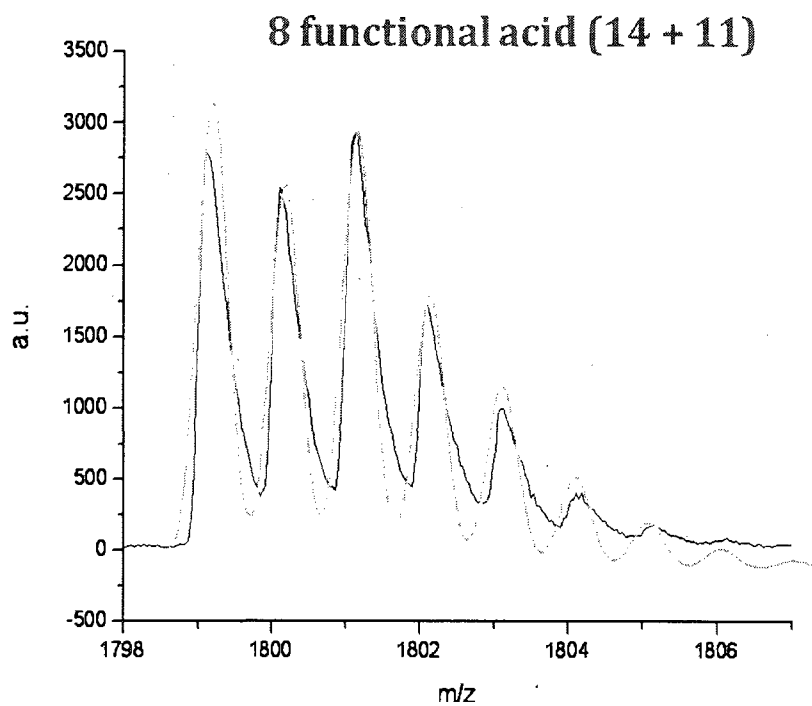
**Figure 6.6.** Measured (black) and predicted (gray) isotopic mass distributions for the products from the reaction of **14** with **11.**
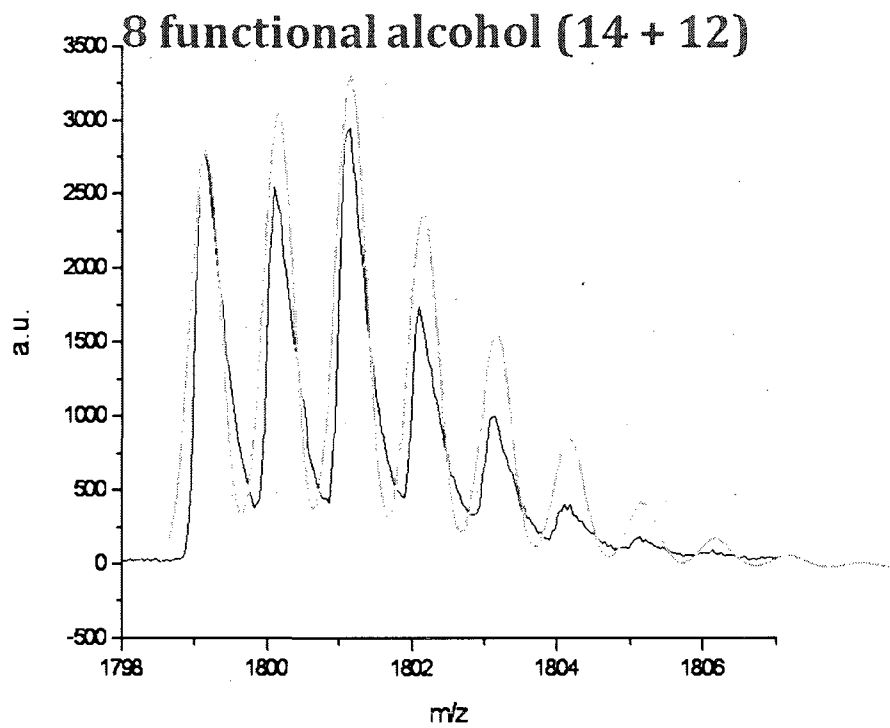
**Figure 6.7.** Measured (black) and predicted (gray) isotopic mass distributions for the products from the reaction of **14** with **12**.
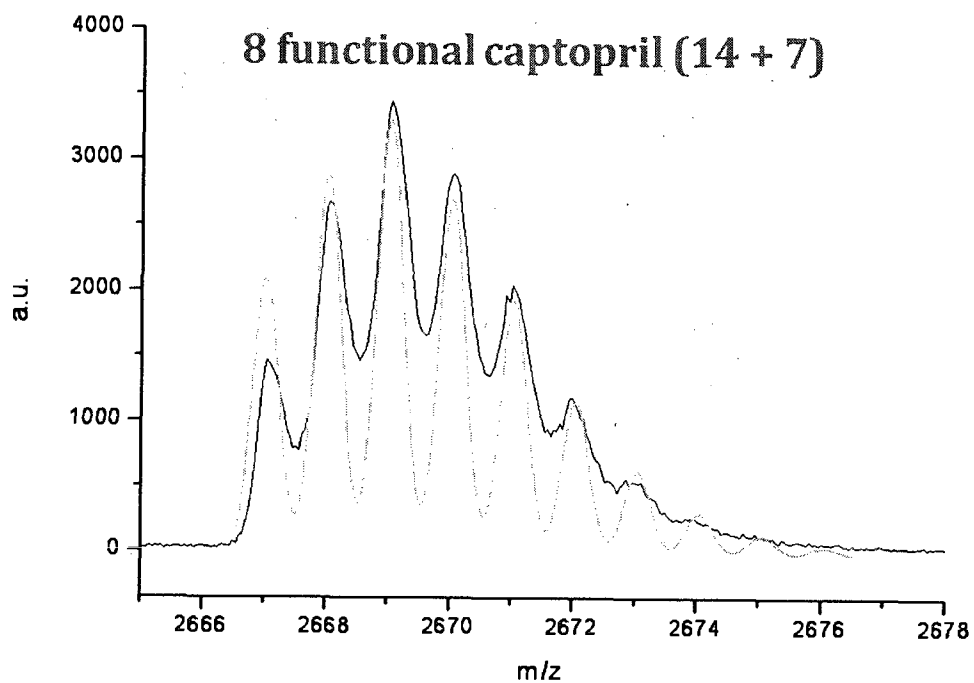
**Figure 6.8.** Measured (black) and predicted (gray) isotopic mass distributions for the products from the reaction of **14** with **7**.
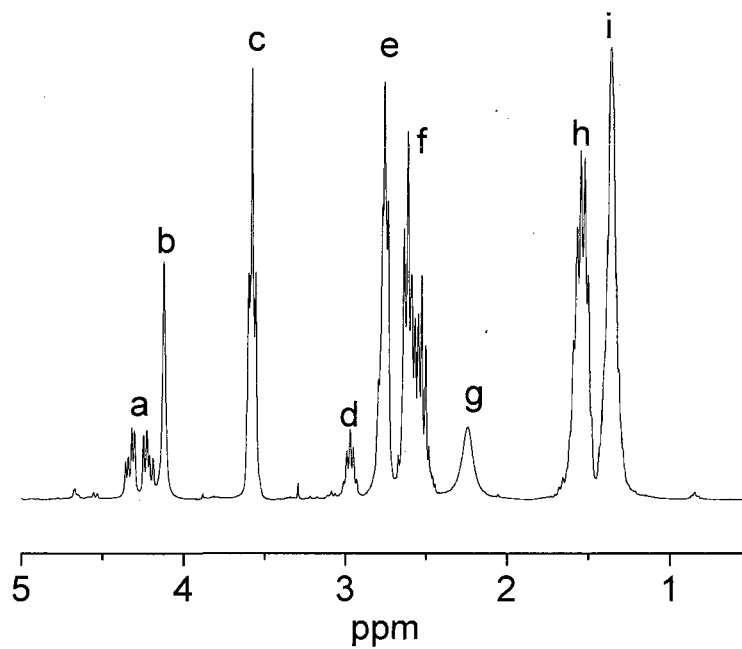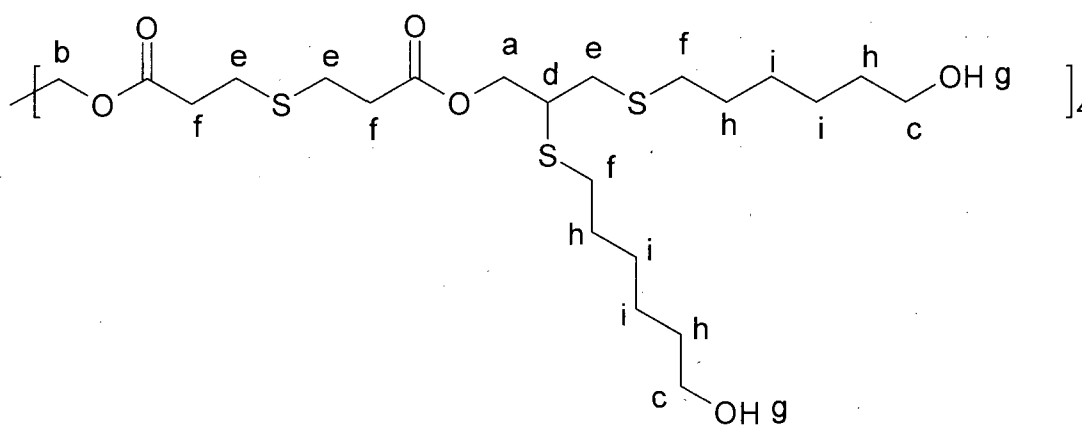
**Figure 6.9.** Chemical structure and $^1$H NMR spectrum of the 8-functional alcohol. $^1$H NMR (CDCl$_3$), δ (ppm): 4.427-4.159 8H m, 4.165-4.055 8H s, 3.660-3.496 16H m, 3.042-2.896 4H m, 2.870-2.685 24H m, 2.687-2.446 32H m, 2.428-2.052 8H (9H) broad s, 1.620-1.420 32H m, 1.450-1.250 32H (36H) broad s.

**Figure 6.10.** Chemical structure and $^1$H NMR spectrum of the 8-functional acid. $^1$H NMR (d$_4$-methanol), δ (ppm): 4.12-4.50 (16H, a+b, m), 3.10-3.22 (4H, c, t), 2.50-3.02 (40H, m), 2.76-2.49 (32H, m).
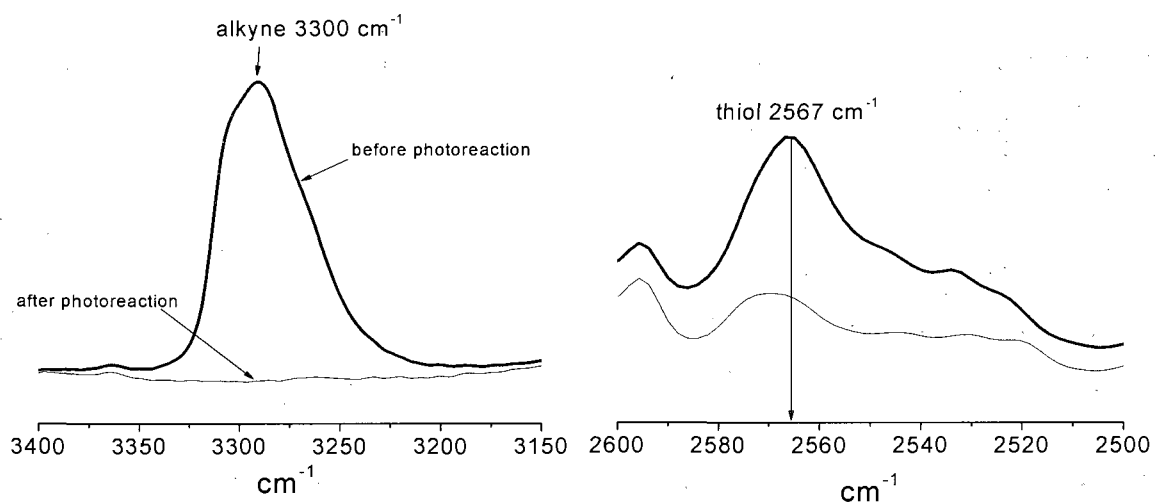
**Figure 6.11.** (a) FTIR spectra demonstrating the consumption of alkyne functional groups for the reaction between **14** and 1-adamantanethiol and (b) FTIR spectra for the same reaction demonstrating the consumption of thiol functional groups for the reaction between **14** and 1-adamantanethiol ($2567 \ cm^{-1}$ completely disappears and broad signal at $2572 \ cm^{-1}$ is not associated with thiol).
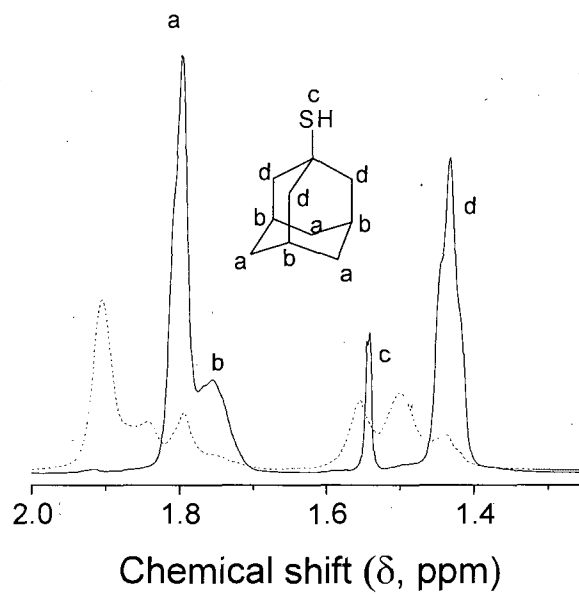
**Figure 6.12.** $^1$H NMR before (solid) and after (dashed) reaction of 1-adamantanethiol and **14**. Note the overall shift and the disappearance of the strong peak associated the thiol proton (1.53 ppm).
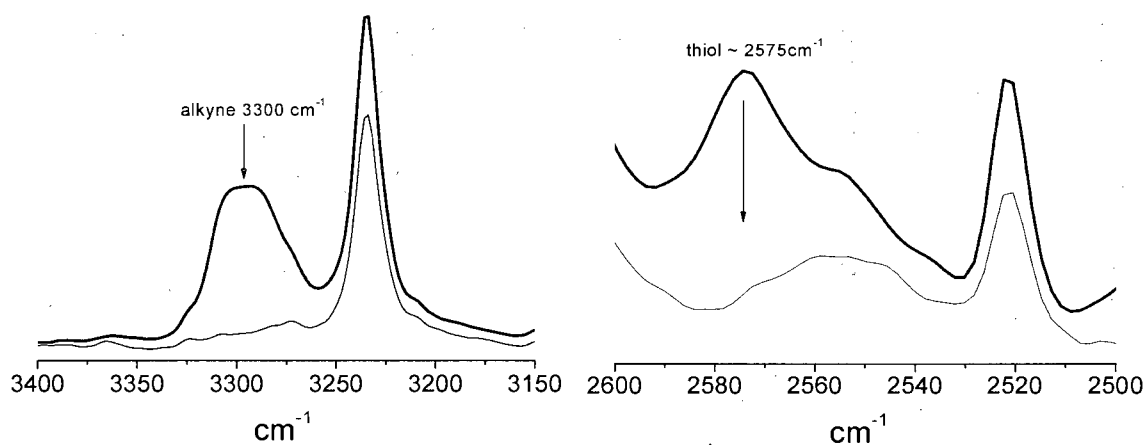
**Figure 6.13.** (A) FTIR spectra demonstrating the consumption of alkyne functional groups for the reaction between **14** and 3-mercaptopropylisobutyl POSS and (B) FTIR spectra for the same reaction demonstrating the consumption of thiol functional groups for the reaction between **14** and with 3-mercaptopropylisobutyl POSS.
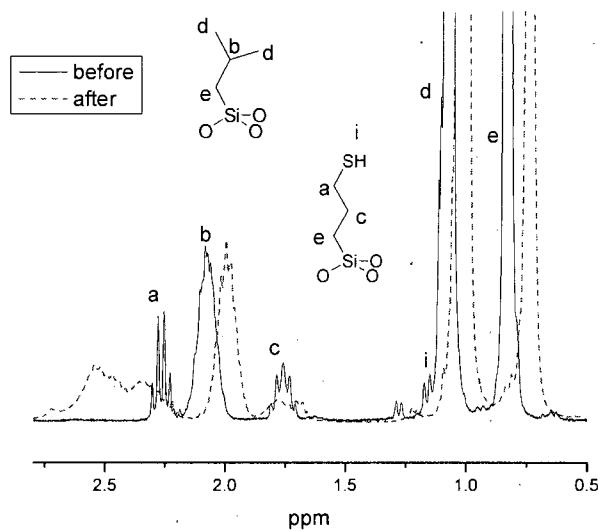
**Figure 6.14.** $^1$H NMR before (solid) and after (dashed) reaction of thiol-POSS and **14**. Note the overall shift and the disappearance of the strong peaks associated with carbons adjacent to thiol.

CHAPTER VII

SYNTHESIS AND THIOL-YNE PHOTOPOLYMERIZATION OF NOVEL

MULTIFUNCTIONAL ALKYNES

Abstract

Multifunctional alkynes (functionality = 4, 6, and 8) were prepared utilizing the nucleophile catalyzed thio-Michael addition reaction from commercially available multifunctional thiols (functionality = 2, 3, and 4) and propargyl acrylate. Real-time FTIR (RTIR) and NMR spectroscopies indicate that the conjugate addition under these conditions proceeded to high conversions within seconds using the nucleophilic catalyst dimethylphenylphosphine, in the absence of solvent, at room temperature, and with no side products. A family of networks was prepared by the photoinitiated thiol-yne reaction employing a 2:1 ratio of thiol to alkyne resulting in uniform crosslinked materials of increasing crosslink density. Photopolymerization profiles indicate that all of the thiol-yne reactions proceed rapidly to high conversion with conversions decreasing with increasing functionality of the thiol and/or alkyne groups. Differential scanning calorimetry (DSC) and dynamic mechanical thermal analysis (DMTA) results clearly show that the $T_g$ increases as the overall crosslink density increases (from -10 to 42°C by DMTA). DMTA also indicates an increase in rubbery modulus (from 6 to 23MPa at 70°C) with a decrease in the molecular weight between crosslinks.

## Introduction

The photoinitiated thiol-ene radical step-growth reaction of thiol across electron rich ene double bonds proceeds rapidly, with little-to-no side products, in the presence of oxygen or water, without photoinitiator, and in the absence of solvents.[1-19] This reaction has been recently highlighted in a variety of synthetic methods demonstrating its use as a highly efficient process for chemical and materials synthesis and modification.[20-28] The thiol-ene reaction can be initiated using a photointiator (and light), light alone, or a thermal initiator (and heat) to generate primary radicals. Polymeric networks can be prepared if the average functionalities of either or both the thiol and electron rich ene monomers are greater than 2. In a typical case where the thiol and ene are tri or tetra functional, highly uniform densely cross-linked networks with few unreacted functional groups are formed. One of the salient kinetic features of thiol-ene polymerization is the absence of any significant side product formation since the only undesirable side products are the result of radical coupling reactions. The networks are held together by sulfide linkages that connect the chemical structures associated with the thiol and electron rich ene monomers. These networks are characterized by dynamic mechanical thermal analysis (DMTA) tan δ versus temperature plots and are analyzed to have relatively low full width half maximum (FWHM) temperatures (~10 °C) at the network glass transition.[2,4]

It has been reported that small molecule monofunctional alkyl thiols in solution undergo a two-step sequential reaction with terminal alkynes to produce 1,2-dithioethers essentially identical to that reported for thiol-enes.[2,29-31] However, despite reports of the basic free radical thiol-yne reaction,[29-31] this reaction was not

used for materials preparation until Bowman and coworkers reported that a tetrafunctional thiol readily co-polymerizes with a dialkyne in a photoinduced radical step-growth process (Scheme 1).[5,32] Each alkyne was reported to react with two thiol groups with the initial intermediate thio-vinyl ether product being approximately three times more reactive than the alkyne towards thiol addition. The reaction proceeds at high rates under ambient humidity and atmospheric oxygen conditions to high conversion, thereby providing an extremely efficient methodology for fabricating high performance networks and films. Additionally, reports have been made using the thiol-yne reaction for the preparation of high refractive index materials comprised of only sulfur and hydrocarbon. Chan et al. reported the reaction of a series of dialkynes (functionality = 4) and dithiols to rapidly produce highly crosslinked networks with the resulting refractive index values directly dependent on the sulfur content and independent of cross-linking density.[36] Additionally, it was reported that the glass transition temperature ($T_g$) values increased in systems where a tetra-functional thiol was reacted with a tetra-functional di-alkyne (2:1 ratio) in comparison to a di-functional di-alkene whereby both the di-alkyne and di-alkene had similar chemical compositions. These results indicate that the unique thiol-yne reaction produces networks with increased crosslink density as indicated by a substantial increase in $T_g$.[32]

The $T_g$ is affected by 2 factors: the degree of crosslinking and the composition of the backbone. Previous reports describe methods of increasing $T_g$ by altering the composition, or rigidity, of the backbone of thiol-ene networks by incorporating esters, isocyanurates, and triazines, for example. Additionally, $T_g$ values have been shown to increase by increasing the functionality of either the thiol or ene component

from 4 > functionality > 2 and keeping the functionality of the other component (thiol or ene) constant. Additionally, reports indicated the increase, or control, over $T_g$ in thiol-ene systems by adding acrylate moieties which were subsequently photopolymerized. Multi-acrylates are known to have high $T_g$ values; however the resulting FWHM values of tan δ provided from DMTA analysis are broad and can span over 100°C, reducing the control and tailorability of final networks.[2,4,13,34] The incorporation of thiols into multi-acrylate systems increases control over final mechanical and physical properties; however, in thiol-acrylate systems, many reactive sites remain unconverted which can lead to dangling chains, a loss in network uniformity, extractable monomer, and changes in mechanical and physical properties over time.[2,6,34] Other reports demonstrate that oligomerization (functionality > 4) of thiols shows relatively no change in $T_g$ or modulus of final networks.[6,35] In these reports, monomers were conjugated by some linking group to increase the average functionality. It was determined that systems with functionalities of either thiol or ene monomer greater than 4 do not correlate the predicted gel point with rates and conversions.[2,6,35]

Networks designed using methods described herein show control over $T_g$ solely by increasing the degree of crosslinking without changing the chemical composition or network uniformity. We purport to build a series of highly uniform crosslinked networks that are comprised of starting materials containing nearly exact chemical compositions (similar degrees of backbone flexibility) and varying degrees of branching to investigate the effects of crosslink density on mechanical and physical properties. These networks are formed by an efficient manner amenable to rapid fabrication under ambient conditions using light to initiate the process.

Herein, difunctional, trifunctional, and tetrafunctional thiols are used to prepare difunctional, trifunctional and tetrafunctional alkynes with functionalities of 4, 6, and 8, respectively, using the highly efficient nucleophile catalyzed thio-Michael addition reaction. It will be empirically demonstrated that there is a distinct correlation between network crosslink density and mechanical properties within these systems. By controlling the structure of the multifunctional alkynes, a series of networks were prepared with multi-functional thiols in a 2:1 (thiol:alkyne) ratio with control over the rigidity of the network backbones while changing the degree of branching. Polymerization kinetics were used to determine trends in polymerization profiles and correlate them to physical and mechanical properties. Differential scanning calorimetry (DSC) was used to establish the changes in $T_g$ values while monitoring the $\Delta c_p$, which directly correlates to crosslink density. Dynamic mechanical thermal analysis (DMTA) was used to verify the DSC $T_g$ data and establish changes of homogeneity within each network. Additionally, DMTA was used to determine the storage modulus values of each network and correlate these values with calculated gel points and molecular weight between crosslink values.

## Experimental

*Materials*

Propargyl acrylate and dimethylphenylphosphine (Me$_2$PPh) were purchased at the highest purity from Aldrich Chemical Company and used as received. Ethylene glycol di(3-mercaptopropionate), trimethylolpropane tris(3-mercaptopropionate) and pentaerythritol tetra(3-mercaptopropionate) were obtained from Bruno Bock

Chemical Company. α,α-Dimethoxy-α-phenylacetophenone (Irgacure 651) was obtained from Ciba Chemical Company.

*Synthesis of 2YNE*

Ethylene glycol di(3-mercaptoprionate) (**2THIOL**) (2.38 g, 10 mmol) was mixed with $2 \times 10^{-3}$ M Me$_2$PPh. To this mixture was added propargyl acrylate (2.20 g, 20 mmol). The reaction was left for 1 hr to ensure complete reaction. The reaction was monitored by RTIR spectroscopy.

*Synthesis of 3YNE*

Trimethylolpropane tris(3-mercaptoprionate) (**3THIOL**) (2.98 g, 10 mmol) was mixed with $2 \times 10^{-3}$ M Me$_2$PPh. To this mixture was added propargyl acrylate (3.30 g, 30 mmol). The reaction was left for 1 hr to ensure complete reaction. The reaction was monitored by RTIR spectroscopy. $^1$H NMR (300MHz, CDCl$_3$) δ4.667(6H), δ4.006(6H), δ3.128(3H), δ2.713- δ2.610(m, 24H), δ1.439(m, 2H), and δ0.848(m, 3H).

*Synthesis of 4YNE*

Pentaerythritol tetra(3-mercaptoprionate) (**4THIOL**) (2.44 g, 5 mmol) was mixed with $2 \times 10^{-3}$ M Me$_2$PPh. To this mixture was added propargyl acrylate (2.20 g, 20 mmol). The reaction was left for 1 hr to ensure complete reaction. The reaction was monitored by RTIR spectroscopy. $^1$H NMR (300MHz, CDCl$_3$) δ4.676(8H), δ4.115(8H), δ3.333(4H), and δ2.721- δ2.621(m, 32H).

*Kinetics*

Modification of **2THIOL**, **3THIOL** and **4THIOL** with propargyl acrylate was formulated in a 1:1 molar ratio of thiol to acrylate with ~$2 \times 10^{-3}$ M Me$_2$PPh serving as the nucleophilic catalyst. Samples with thicknesses of 250 microns were

sandwiched between NaCl plates with glass spacers. RTIR was used to monitor the loss of thiol and acrylate functional groups at 2570 $cm^{-1}$ (-S-H stretch) at 1640 $cm^{-1}$ (-C=C- stretch), respectively.

*Film Synthesis and Kinetics*

Photocured samples were 2:1 thiol to alkyne molar ratios, or 1:1 functional group ratios, taking each alkyne to be difunctional using 2 wt% α,α-dimethoxy-α-phenylacetophenone (Irgacure 651). Samples were prepared with thicknesses of 250 microns sandwiched between NaCl plates with glass spacers. RTIR was used to monitor the loss of thiol at 2570 $cm^{-1}$ and alkyne at 2120 $cm^{-1}$ (-C≡C- stretch) functional groups. The light intensity of the high pressure mercury lamp delivered to the sample via a light pipe was ~ 35.4 $mW/cm^2$ for photoinduced reactions.

*Film Preparation for Mechanical and Physical Testing*

All samples were prepared in a 1:1 molar functional group ratio (or 2:1 thiol to alkyne) with 1% Irgacure 651. Samples (500 microns thick) were cured in silicone molds with dimensions 25mm X 5mm X 0.5mm and covered with glass slides. The samples were photo-cured on a Fusion curing line (12 passes) with a D bulb (belt speed of 10 feet/min, 3.1 $W/cm^2$ irradiance). All samples were allowed to remain at 60°C for 72 hours before any measurements were made.

*Measurements and Instrumentation*

NMR spectra were recorded on a Bruker 300 (53 mm) spectrometer. All spectra were recorded in $CDCl_3$ at 10%v/v, unless noted otherwise.

Real-time FTIR (RTIR) was used to determine the kinetics of the reaction using a modified Bruker 88 spectrometer. UV light from an Oriel lamp system equipped with a 200 W high pressure mercury-xenon bulb was channeled through an

electric shutter and fiber optic cable in the sample chamber. Photopolymerizations were conducted using a light intensity of 35.4 mW/cm$^2$ measured with an IL-1400 calibrated radiometer from International Light. IR absorption spectra were obtained under continuous UV irradiation at a scanning rate of 5 scans per second.

Thermal transitions were monitored by a TA Instrument DSC Q1000. All samples were heated to 120 °C for 5 minutes at 10°C/min to erase thermal history. Samples were then cooled to -80 °C at 10°C/min and then heated at 10°C/min to 150°C. DSC data from the second heating scan are reported in W/g.

Modulus and tan δ measurements were performed on a Rheometric Scientific DMTA V at 2°C/min from -60°C to 100°C. The $T_g$ was determined as the temperature at the peak max in the tan δ curve. Storage moduli (E') are reported in Pa.

## Results and Discussion

*Synthesis and Kinetics of Multifunctional Alkynes*

Three multifunctional thiols (**2THIOL, 3THIOL**, and **4THIOL, Figure 7.1**) were modified with propargyl acrylate in a *nucleophile catalyzed* reaction via a thio-Michael process resulting in **2YNE, 3YNE**, and **4YNE**, respectively, **Figure 7.1.**, while the base (triethylamine) catalyzed Michael addition of thiols to electron deficient alkenes is a common reaction in organic synthesis; the use of the nucleophile (primary amines and trialkyl phosphines) catalyzed conditions is less commonly employed.[34,35,37] The nucleophile catalyzed reaction significantly reduces the amount of catalyst required, can be carried out in the absence of solvent, exhibits rapid quantitative conversions dependant on catalyst concentration (in as little as a

few seconds), and produces no side products. The kinetics of thio-Michael reaction were monitored by RTIR, and results have been previously reported in the literature,[37] and show near quantitative conversion of both the thiol and acrylate functional groups in a few minutes.

*Kinetic Study of Networks Prepared from Multifunctional Thiols and Novel Multifunctional Alkynes*

These newly prepared multifunctional alkynes, **2YNE**, **3YNE**, and **4YNE**, and multifunctional thiols, **2THIOL**, **3THIOL**, and **4THIOL**, were then used to prepare a series of nine networks having variation in network densities but nearly identical chemical compositions. Films were prepared by mixing a multifunctional alkyne (YNE) with a multifunctional THIOL and 1 wt% photoinitiator. The kinetics of each reaction were monitored by RTIR using 250 micron thick samples sandwiched between NaCl plates and irradiated with full arc UV light at 35.4 mW/cm$^2$. (Note the sample thickness and intensity of light of the RTIR films differs of that of films used for mechanical testing.) **Figure 7.2.** shows the conversion vs. time plot of the photoinitiated reaction of 3THIOL with 3YNE with 1% Irgacure 651 in a 250 micron thick sample, as an example. The data in **Figure 7.2** illustrates the high conversion of thiol with yne (final conversion post-cure was greater than 95% of both thiol and yne). The data shows a slight increase in yne conversion rate and final percent conversion (at 500s). When an alkyne reacts with a thiyl radical in a typical photoinitiated network system, a thio-vinyl ether radical is produced, see **Scheme 7.1.** This radical then abstracts a hydrogen from another thiol, yielding a thio-vinyl ether that subsequently reacts in a typical thiol-ene reaction. The high reactivity of the intermediate vinylthioether towards further thiyl radical addition thus facilitates the

formation of the double addition product. Bowman and coworkers determined that the rate of thiol addition to the thio-vinyl ether is ~3 times greater than the reaction of the thiol with the parent alkyne in a stoichiometric formulation of 4THIOL with decadiyne.[32] The difference in reactivity of the alkyne and the intermediate thio-vinyl ether was determined to be the cause of the difference in apparent rates of thiol and alkyne conversions.

The RTIR data in **Figure 7.3.** shows a decrease in the rate of the thiol-yne reaction as the functionality of the monomers increases. This is inconsistent with reports of model thiol-ene systems where there is no change in the rate of conversion based on the functionality of the monomers greater than 4.[2,35] For example, Clark and coworkers report an initial decrease in apparent reaction rate upon increasing thiol functionality from 2 to 3 to 4, which correlates with the prediction by gel point theory. The rates, however, plateau or seem unaffected in systems where the thiols have functionalities greater than 4 (i.e., 6, 9, or 12). Furthermore, the photoinitiated reaction of a hyperbranched 16-functional thiol and trifunctional ene (pentaerythritol triallylether) has been reported to have the same rates and conversions as a tri-functional thiol (trimethylolpropane tris(3-mercaptopropionate)) and the same trifunctional ene, noting the large difference in crosslinking gel point theoretical calculations (18% for the former and 50% for the latter).[2] In **Table 7.1.**, the theoretical calculated gel points for networks prepared in this study are listed using the classical equation, usually applied for thiol-ene systems:

$$p_c = \sqrt{\frac{1}{r(1-f_1)(1-f_2)}}$$
  Equation 1

where $p_c$ is the gel point, $r$ is the ratio of thiol to ene, $f_1$ is the functionality of the thiol and $f_2$ is the functionality of the ene. From the kinetic data shown in **Figure 7.3.**, it is evident that the apparent rate and conversion of the thiol-yne reaction decreases as the functionality of the monomers and crosslink density of the networks increases. This behavior can be explained by the unequal reactivity of the alkyne and the thio-vinyl ether moieties. Since, it has been established that the radical-mediated reaction of thiols with a thio-vinyl ether groups is faster than that of a thiols with alkyne groups, the differing reactivity rates alter the kinetics traditionally expected from thiol-ene systems with monomers of functionality less than 4.[33] Hence, as the functionality of the either the alkyne or the thiol increases, the gel point decreases and the rate and conversion both decrease.

$$\rho_x = \frac{E}{3RT}$$

*Mechanical and Physical Analysis of Networks Prepared from Multifunctional Thiols and Novel Multifunctional Alkynes*

The mechanical and physical properties of networks prepared from multifunctional thiols and multifunctional alkynes were analyzed by DSC and DMTA. All films were prepared at 500 microns in silicone molds and covered with glass slides while curing. **Figure 7.4.** shows the DSC scans of all nine films divided into sets grouped by the multifunctional thiol for clarity. In each case, as the alkyne functionality increases from 2-4 (or the total functionality of each monomer increases

from 4 - 8), the $T_g$ increases, **Table 7.2.** Additionally, the $T_g$ range is narrow for all systems due to the uniform network structure which is common in most thiol-ene systems regardless of network density. By examining the DSC $T_g$ data further, one notices an increase in $T_g$ by ~10°C as the functionality of thiol increases from 2 to 3 to 4 when copolymerized with a given alkyne. For example, the $T_g$s of 2THIOL-2YNE, 3THIOL-2YNE, and 4THIOL-2YNE are -20, -10, and -1, respectively. Specific control over $T_g$ in network systems has not been demonstrated in previous work solely by increasing the monomer functionality. Additional evidence for the differences in the network structures of the nine thiol-alkyne systems can be suggested by calculating heat capacity at constant pressure at $T_g$ for the DSC heating scans in **Figure 7.4.** $c_{p,glass}$ is primarily determined by the vibrational degree of freedom, which is the characteristic of solid-like behavior at temperatures above $T_g$, $c_{p,rubber}$, in addition to the translational degree of freedom which is the characteristic of liquid-like behavior and associated to network density. Thus, the jump in heat capacity at $T_g$ ($\Delta c_p$ at $T_g$) decreases as network density increases.

**Figure 7.5.** shows the tan δ values for all multifunctional thiol and multifunctional alkyne network systems grouped according to each multifunctional alkyne. Tan δ values, listed in **Table 7.2.**, show an increase in $T_g$ as the crosslink density increases, consistent with the DSC measurements. Additionally, the narrow FWHM values, which are expected of thiol-ene systems, slightly increase as the crosslink density of each system increases. Narrow FWHM values have been shown to correlate with homogeneity in network structure.[2] Systems based on starting materials (monomers) with lower functionality such as those in **Figure 7.5.a** exhibit very narrow FWHM values ~11°C. As the functionality of the systems increase, the

FWHM value increases indicating that there is loss in homogeneity of the systems. Because the double addition of thiol to alkyne is a sequential reaction (thiol with alkyne and then thiol with thio-vinyl ether), non-regiospecific products and the possibility of chain cyclization potentially cause less homogeneous network structure formation.[29,32,33,36] However, FWHM values demonstrated with thiol-alkyne highly crosslinked networks are still very narrow compared to highly crosslinked multi-acrylates systems. [2,32,35,36] Storage moduli vs. temperature plots are shown in **Figure 7.6**. This data shows an apparent increase in moduli (E') value in the rubber state based on crosslink density, which corresponds to the ideal rubber theory according to the equation

$$E' = \frac{\rho RT}{M_c} \qquad\qquad \text{Equation 2}$$

where $\rho$ is density, R is the ideal gas constant, T is the absolute temperature, and $M_c$ is the molecular weight between crosslinks. Data in **Table 7.1** .show the relationship between rubber moduli, calculated crosslink density, and calculated gel points.

Thiol-yne photopolymerizations can be used to tailor mechanical and physical properties of highly crosslinked networks. Rapid and clean synthesis of multifunctional alkynes by the nucleophile catalyzed thio-Michael addition reaction and commercially available thiols. Networks can be prepared with minimal changes in monomer rigidity while increasing crosslink density. High conversions of both thiol and alkyne show promise for these materials and this method for a wide variety of fundamental investigations and applications.

Summary and Conclusions

The nucleophile catalyzed thio-Michael addition reaction was used to prepare multifunctional alkynes with that proceeded to high conversions, rapidly, without purification or isolation steps, and with little side product formation. A series of networks with thioether linking groups were prepared by a rapid step-growth radical mediated photopolymerization process. According to narrow thermal and mechanical transitions obtained by DSC and DMTA analysis, the network structures prepared were analyzed to have uniformity in chemical structure. FWHM values for tan $\delta$ versus temperature plots were greater than that for thiol-ene networks but were narrow compared to multi-acrylate networks prepared by photopolymerization. Highly crosslinked networks were then tailored with increasing $T_g$, from -10 to 42°C, as determined by DMTA. This data was confirmed by DSC. Additionally, elastic moduli increased with increasing crosslink density from 6 to 23MPa. The results presented herein demonstrate that thiol-yne chemistry can successfully be employed as a rapid high-throughput technique to prepare network materials to analyze structure property relationships. In his study, systems based on higher functionalities of (yne) ene functionality are shown to increase $T_g$ and E' values in a rapid, controlled step growth photopolymerization under ambient conditions.

## Acknowledgments

References

1.  Jacobine, A. F. In *Radiation Curing in Polymer Science and Technology III, Polymerisation Mechanisms*, Fouassier, J. D., Rabek, J. F., Eds.; Elsevier Applied Science: London, 1993; Vol. 3, p. 219.

2. Hoyle, C. E.; Lee, T. Y.; Roper, T. *J. Polym. Sci., Part A: Polym. Chem.* **2004**, *42*, 5301.

3. Reddy, S. K.; Cramer, N. B.; Kalvaitas, M.; Lee, T.; Bowman, C. N. *Aust. J. Chem.* **2006**, *59*, 586.

4. Senyurt, A. F.; Wei, H.; Hoyle, C. E.; Piland, S. G.; Gould, T. E. *Macromolecules* **2007**, *40*, 4901.

5. Bowman, C. N.; Carioscia, J.; Lu, H,; Stansbury, J. W.; PCT Int. Appl., 2005, 34 pp.

6. Carioscia, J. A.; Lu, H.; Stansbury, J. W.; Bowman, C. N. *Dent. Mater.* **2005**, *21*, 1137.

7. Reddy, S. K.; Cramer, N. B.; Bowman, C. N., *Macromolecules* **2006**, *39*, 3681.

8. Wei, H. Y.; Li, Q.; Ojelade, M.; Madbouly, S.; Otaigbe, J. U.; Hoyle, C. E. *Macromolecules* **2007**, *40*, 8788.

9. Cook, W. D.; Chausson, S.; Chen, F.; Le Pluart, L.; Bowman, C. N.; Scott, T. F. *Polym. Int.* **2008**, *57*, 469.

10.  Johnson, P. M.; Stansbury, J. W.; Bowman, C. N. *J. Polym. Sci., Part A: Polym. Chem.* **2008**, *46*, 1502.

11.  Nilsson, C.; Simpson, N.; Malkoch, M.; Johansson, M.; Malmstrom, E. *J. Polym. Sci., Part A: Polym. Chem.* **2008**, *46*, 1339.

12. White, T. J.; Natarajan, L. V.; Tondiglia, V. P.; Lloyd, P. F.; Bunning, T. J.; Guymon, C. A. *Polymer* **2007**, *48*, 5979.

13. Senyurt, A. F.; Hoyle, C. E.; Wei, H. Y.; Piland S. G.; Gould, T. E. *Macromolecules* **2007**, *40*, 3174.

14. Carioscia, J. A.; Stansbury, J. W.; Bowman, C. N. *Polymer* **2007**, *48*, 1526.

15. Wei, H. Y.; Senyurt, A. F.; Jonsson, S.; Hoyle, C. E. *Macromolecules* **2007**, 822.

16. Sangermano, M.; Gross, S.; Priola, A.; Rizza, G.; Sada, C. *Macromol. Chem. Phys.* **2007**, *208*, 2560.

17. Carioscia, J. A.; Schneidewind, L.; O'Brien, C.; Ely, R.; Feeser, C.; Cramer, N.; Bowman, C. N. *J. Polym. Sci., Part A: Polym. Chem.* **2007**, *45*, 5686.

18. Cook, W. D.; Chen, F.; Pattison, D. W.; Hopson, P.; Beaujon, M. *Polym. Int.* **2007**, *56*, 1572.

19. Ortiz, R. A.; Urbina, B. A. P.; Valdez, L. V. C.; Duarte, L. B.; Santos, R. G.; Valdez, A. E. G.; Soucek, M. D. *J. Polym. Sci., Part A: Polym. Chem.* **2007**, *45*, 4829.

20. Killops, K.L.; Campos, L.M.; Hawker, C.J. *J. Am. Chem. Soc.* **2008**, *13*, 5062.

21. Campos, L. M.; Killops, K. L.; Sakai, R.; Paulusse, J. M. J.; Damiron, D.; Drockenmuller, E.; Messmore, B. W.; Hawker, C. J. *Macromolecules* **2008**, *41*, 7063.

22. Voets, I.K.; de Keizer, A.; Stuart, M.A.C.; Justynska, J.; Schlaad, H.; *Macromolecules* **2007**, *40*, 2158.

23. Lutz, J. F.; Schlaad, H. *Polymer* **2008**, *49*, 817.

24. Gress, A.; Volkel, A.; Schlaad, H. *Macromolecules* **2007**, *40*, 7928.

25. Hordyjewicz-Baran, Z.; You, L. C.; Smarsly, B.; Sigel, R.; Schlaad, H. *Macromolecules* **2007**, *40*, 3901.

26. Brummelhuis, N.; Diehl, C.; Schlaad, H. *Macromolecules* **2008**, *41*, 9946.

27. Dondoni, A. *Angew. Chem. Int. Ed.* **2008**, *47*, 8995.

28. Roper, T. M.; Guymon, C. A.; Jonsson, E. S.; Hoyle, C. E. *J. Polym. Sci., Part A: Polym. Chem.* **2004**, *42*, 6283.

29. Blomquist, A. T.; Wolinsky, J.; *J. Org. Chem.* **1958**, *23*, 551.

30. Griesbaum, K.; *Angew. Chem. Internat. Ed.,* **1970**, 9(4), 273-287.

31. Behringer, H.; *Annalen,* **1949**, *564*, 219.

32. Fairbanks, B. D.; Scott, T. F.; Kloxin, C. J.; Anseth, K. S.; Bowman, C. N. *Macromolecules* **2008**, *42*, 211.

33. Okay, O.; Bowman, C. N.; *Macromol. Theory Simul.,* **2005**, *14*, 267.

34. Chan, J.W.; Wei, H.; Zhou, H.; Hoyle, C.E.; *Eur. Polym. J.,* **2009**, 45, 2717–2725.

35. Clark, T.; Kwisnek, L.; Hoyle, C.E.; Nazarenko, S.; *J. Polym. Sci., Part A: Polym. Chem.* **2008**, 47(1), 14-24.

36. Chan, J.W.; Zhou, H.; Hoyle, C.E.; Lowe, A.B.; *Chem. Mater.,* **2009**, 21(8), 1579-1585.

37. Chan, J.W.; Hoyle, C.E.; Lowe A.B.; *J. Am. Chem. Soc.,* **2009**, 131(16), 5751-5753.
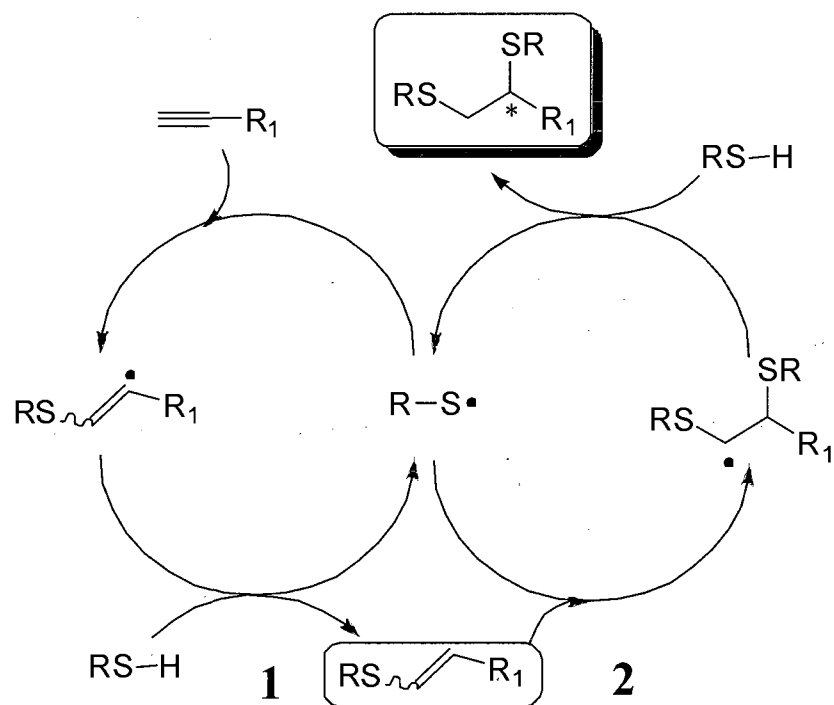
**Scheme 7.1.** Proposed mechanism of the thiol-yne reaction.

**Table 7.1.** Functionality of monomers, predicted gel point, measured storage modulus reported at 70°C, and calculated cross-link density.

| Thiol | Alkyne | $f_1$ (thiol) | $f_2$ (alkyne) | $p_c$ (gel point) | E' at 70°C (MPa) | Calculated cross-link density (M) |
|---|---|---|---|---|---|---|
| 2THIOL | 2YNE | 2 | 4 | 57.7 | 6.3 | 0.74 |
| | 3YNE | 2 | 6 | 44.7 | 13 | 1.52 |
| | 4YNE | 2 | 8 | 37.8 | 13.7 | 1.60 |
| 3THIOL | 2YNE | 3 | 4 | 40.8 | 12.2 | 1.43 |
| | 3YNE | 3 | 6 | 31.6 | 15.6 | 1.82 |
| | 4YNE | 3 | 8 | 26.7 | 16.6 | 1.94 |
| 4THIOL | 2YNE | 4 | 4 | 33.3 | 14 | 1.64 |
| | 3YNE | 4 | 6 | 25.8 | 16.7 | 1.95 |
| | 4YNE | 4 | 8 | 21.8 | 23 | 2.69 |

**Table 7.2.** $T_g$ and $\Delta c_p$ values determined by DSC; $T_g$ and FWHM values determined by DMTA.

| Thiol | Alkyne | DSC $T_g$ ($^{o}$C) | $\Delta c_p$ (J/g/$^{o}$C) | DMTA $T_g$ ($^{o}$C) | DMTA FWHM ($^{o}$C) |
|-------|--------|---------|---------|---------|---------|
| 2THIOL | 2YNE | -20 | 0.5456 | -10 | 11 |
|  | 3YNE | -11 | 0.4823 | 5 | 11 |
|  | 4YNE | -3 | 0.4813 | 11 | 12 |
| 3THIOL | 2YNE | -10 | 0.4236 | 9 | 12 |
|  | 3YNE | 0 | 0.4790 | 20 | 14 |
|  | 4YNE | 5 | 0.4716 | 27 | 16 |
| 4THIOL | 2YNE | -1 | 0.4859 | 17 | 20 |
|  | 3YNE | 11 | 0.4654 | 27 | 20 |
|  | 4YNE | 14 | 0.4313 | 42 | 21 |
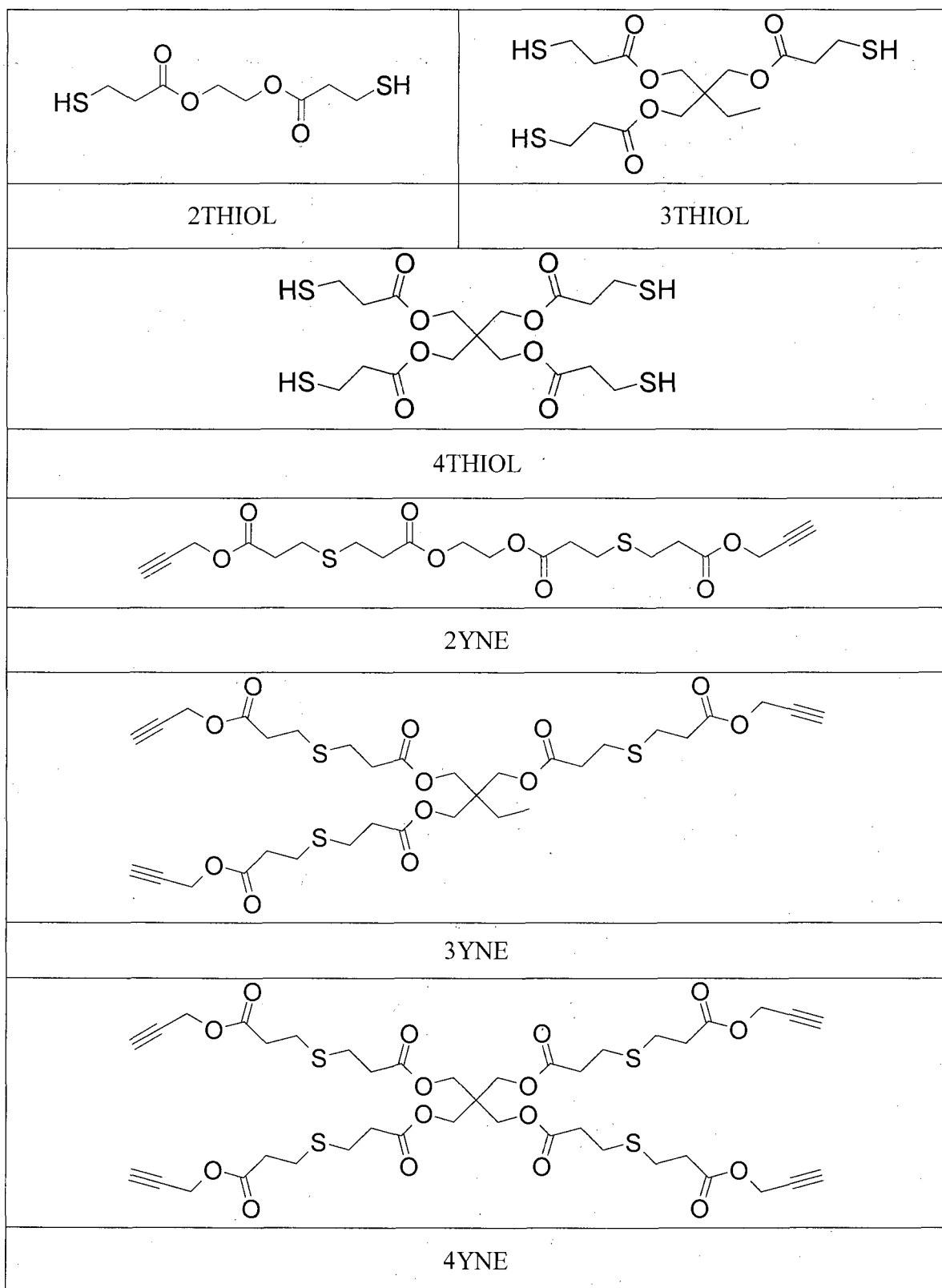
**Figure 7.1.** Structures and acronyms for multifunctional thiols and alkynes.
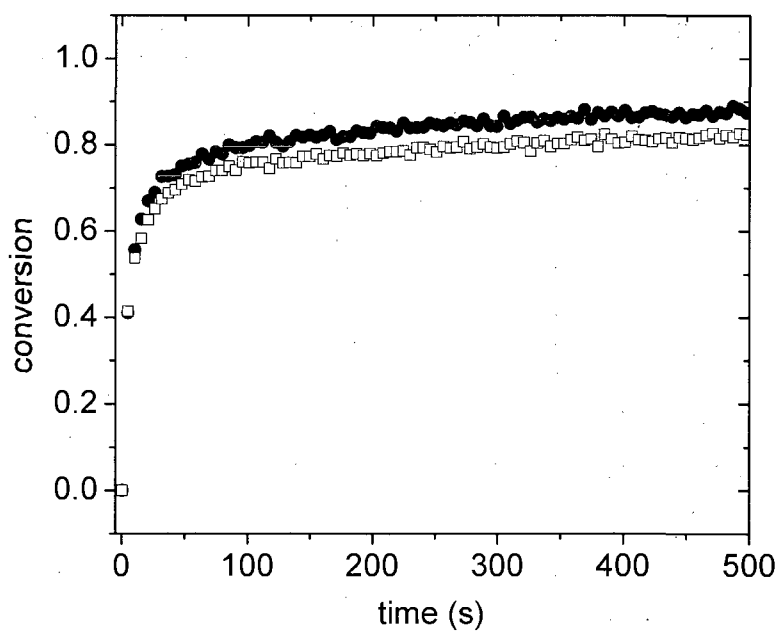
**Figure 7.2.** RT-FTIR based percent conversion time plots for 2:1 molar ratios of (□) thiol and (●) alkyne reactive groups for 3THIOL-3YNE thick film formulation. (250 micron thick films, 1 wt% Irgacure 651, light intensity: 53.4 mW/cm$^{-2}$)
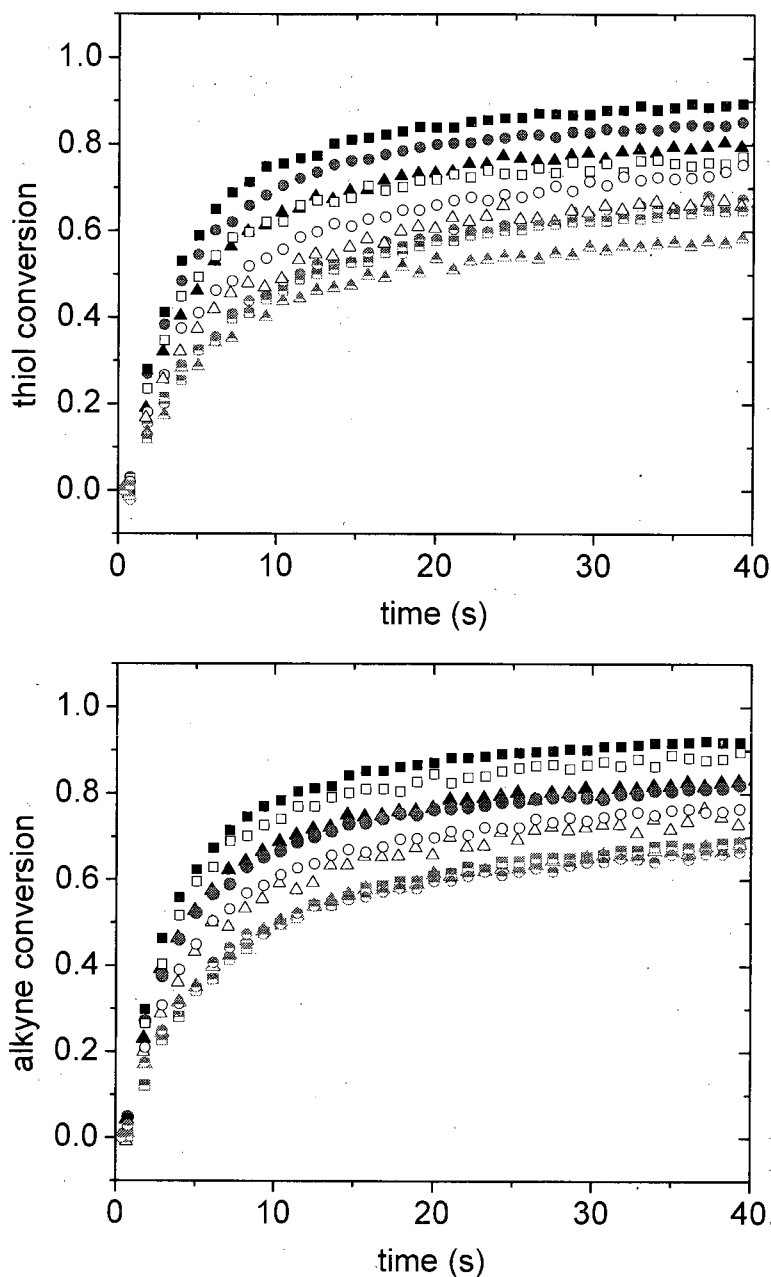
**Figure 7.3.** RTIR based percent conversion time plots for 2:1 molar ratios of (top) thio and (bottom) alkyne reactive groups for (■) 2THIOL-2YNE, (●) 3THIOL-2YNE, (▲) 4THIOL-2YNE, (□) 2THIOL-3YNE, (○) 3THIOL-3YNE, (△) 4THIOL-3YNE, (◨) 2THIOL-4YNE, (◓) 3THIOL-4YNE, (▲) 4THIOL-4YNE thick film formulation. (250 micron thick films, 1 wt% Irgacure 651, light intensity: 53.4 mW/cm$^{-2}$)
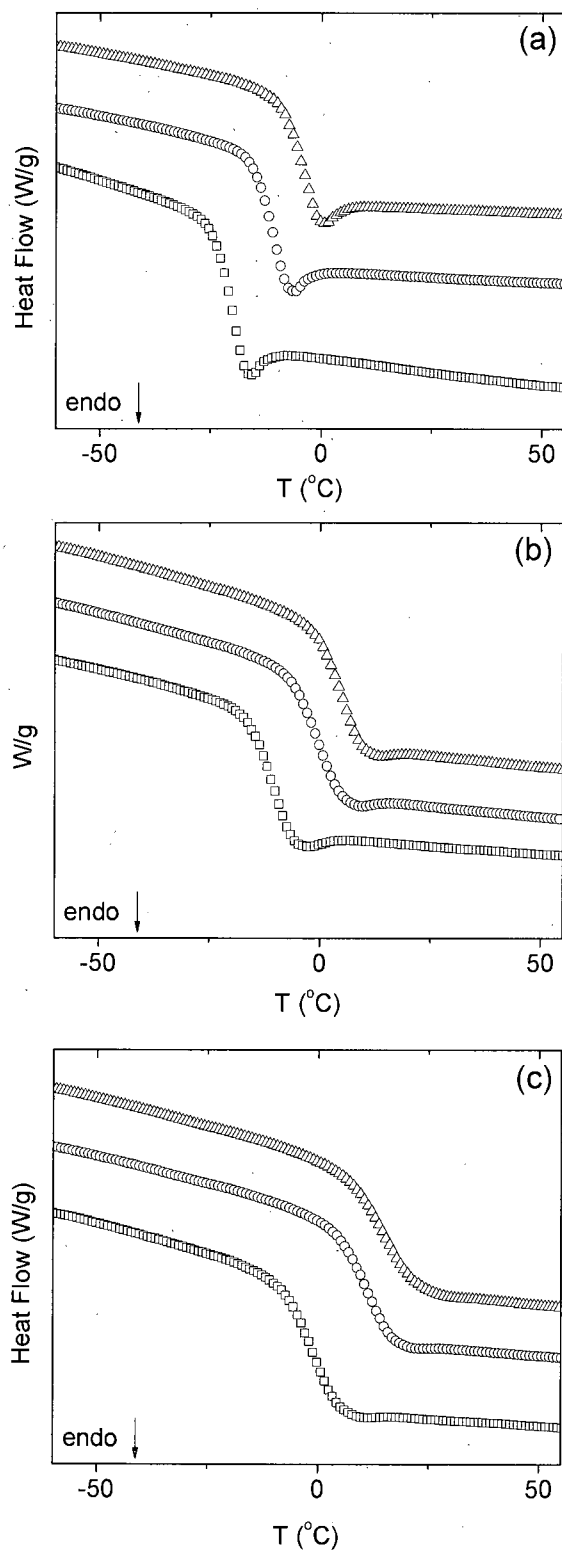
**Figure 7.4.** DSC vs. temperature of DMA E' plots for photopolymerized networks formed from 2:1 thiol:alkyne mixtures: (a) 2THIOL with (□○▲□) 2YNE, (○) 3YNE, and (△) 4YNE; (b) 3THIOL with (□) 2YNE, (○) 3YNE, and (△) 4YNE; and (c) 4THIOL with (□) 2YNE, (○) 3YNE, and (△) 4YNE.
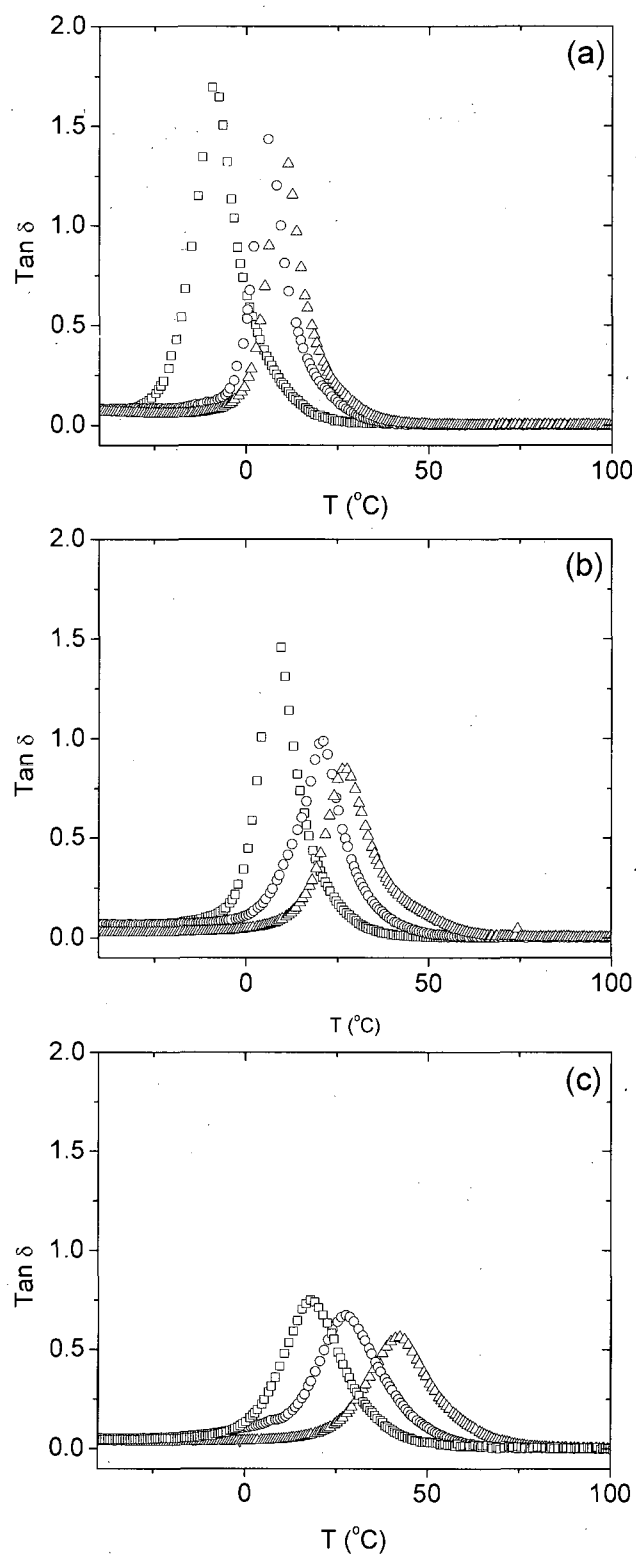
**Figure 7.5.** Tan δ plots vs. temperature of DMA E' plots for photopolymerized networks formed from 2:1 thiol:alkyne mixtures: (a) 2THIOL with (□) 2YNE, (○) 3YNE, and (△) 4YNE; (b) 3THIOL with (□) 2YNE, (○) 3YNE, and (△) 4YNE; and (c) 4THIOL with (□) 2YNE, (○) 3YNE, and (△) 4YNE.

**Figure 7.6**. Elastic modulus plots vs. temperature of DMA E' plots for photopolymerized networks formed from 2:1 thiol:alkyne mixtures: (a) 2THIOL with (□) 2YNE, (○ ) 3YNE, and (△) 4YNE; (b) 3THIOL with (□) 2YNE, (○) 3YNE, and (△) 4YNE; and (c) 4THIOL with (□) 2YNE, (○) 3YNE, and (△) 4YNE.

# CHAPTER VIII

# PHOTOPOLYMERIZATION OF THIOL-ALKYNES: POLYSULFIDE NETWORKS

## Abstract

A series of photoinitiated reactions involving radical chain addition of dithiols across the triple bonds of dialkynes results in quantitative loss of all of the thiol and alkyne groups in 1:1 molar functional group neat mixtures. The reactions proceed rapidly to give uniform networks with relatively narrow differential scanning calorimetry (DSC) and dynamic mechanical analysis (DMA) glass transition ranges. The glass transitions of the network films are directly related to the network structure and range from below 0 °C to about 40 °C as determined by DMA. The thiol-alkyne based hydrocarbon networks with sulfide linking groups have refractive index values which extend as high as 1.66. There is a linear relationship between the network density and the refractive index, both of which increase linearly with weight percent sulfur.

## Introduction

The radical step growth reaction for thiol addition across ene double bonds proceeds rapidly in the presence of oxygen or water with few side products.[1-19] Recently the efficiency and quantitative nature of the thiol-ene reaction, has been used in a variety of synthetic processes that delineate and define its use as a highly efficient reaction for chemical and materials synthesis.[20-27] The thiol-ene reaction is generally initiated by using either a photointiator (and light) or a thermal initiator (and heat) to generate radicals. Alternatively, light alone can be used to produce a

lysis of the sulfur-hydrogen bond to produce thiyl radicals capable of initiating the chain growth process. Linear polymers are produced if the thiol and enes have functionalities of 2, and network polymers are produced if the average functionalities of the thiol and ene are greater than 2. In the typical case where the thiol and ene are tri or tetra functional, densely linked networks which are highly uniform with little unreacted functional groups are formed. These networks are characterized by dynamic mechanical tan δ versus temperature plots at the network glass transition that have full width half maximum (FWHM) temperatures of 10-15 °C,[2,4] depending upon the actual structure of the thiol and ene components. This means that the networks are extremely uniform since such FWHM values are typically characteristic of linear polymers with low polydispersity. The corresponding DSC scans of thiol-ene networks are characterized by extremely narrow glass transition ranges consistent with the DMA results.

One of the salient kinetic features of thiol-ene polymerization is the absence of any significant side product formation since the only real side products are a result of radical coupling processes. The networks are held together by sulfide linkages that connect the chemical structures associated with the thiol and ene monomers. To date, most of the thiols used in forming thiol-ene networks have ester linkages comprised of carbon and oxygen carboxylate esters. There have been reports of multifunctional (e.g. trifunctional) alkenes used to make thiol-ene networks.[28] However, due to limited availability of alkyl thiols and hydrocarbon enes with functionalities greater than two, thiol-ene polymerizations that lead to networks with only carbon, hydrogen and sulfur are limited.

One of the factors that has not been explored to any great extent in thiol-ene systems is the tailoring of network films that have high refractive index and density while maintaining network structures with high uniformity. This is unfortunate since the inclusion of sulfur in a variety of molecular formats into polymer matrices continues to attract a significant amount of attention.[29-33] Many potential applications exist for relatively high refractive index materials where the refractive index can be controlled over a range of values. Since sulfur has a high atomic refraction[33] compared to typical organic atoms such as oxygen, carbon, nitrogen, and hydrogen, there is interest in being able to incorporate sulfur into hydrocarbon networks while maintaining control over the mechanical and thermal properties. Toward this end, consider first a hypothetical uniform thermoset hydrocarbon network comprised of only hydrogen and carbon. The refractive index of such networks would be very low and independent of how the network structure was linked since the inherent refraction of saturated molecular structures containing only carbon and hydrogen is very low. Starting from this consideration, we purport to build a family of uniform hydrocarbon thermoset networks that would contain sulfide linkages that are formed by an efficient manner amenable to rapid fabrication under ambient conditions using light to initiate the process. This would of course lend itself to photocuring of thin network films or thick thermoset plastics, opening up a whole array of potential applications in the optics field. Such networks will be designed to contain a variation in sulfur content and crosslink density to allow for a clear correlation between sulfur weight percent and the network refractive index.

Herein, we report the use of difunctional alkynes and a series of end functionalized dithiolalkanes. It will be shown that the use of thiol-yne chemistry to

fabricate materials represents a sister process to the thiol-ene reactions already discussed.[1-27] Indeed, in the past, it has been reported that small molecule monofunctional alkyl thiols in solution undergo a two-step sequential reaction with terminal alkynes to give high yields of 1,2-dithioethers essentially identical to that reported for thiol-enes.[2,34-36] The radical reaction of thiol-enes which were originally reported in 1905[37] and received considerable attention in the chemical literature up until 1975 when Morgan and Ketly introduced the first photoinitiated thiol-ene radical processes for industrial films and coating applications.[1,2] To date thiol-yne reactions have not been used for making new materials. Moreover, from the conditions originally reported for the thiol-yne reactions, it was not possible to tell how fast and efficient they really were, and if they could be employed for materials synthesis.[34-36] In other words, while the thiol-yne reactions were reported over 50 years ago to be facile processes, there has been little effort to capitalize on what could be an exceptional opportunity for materials fabrication. Just as the Huisgen reaction involving the alkyne-azide 1,3-dipolar cycloaddition reaction process, originally reported in 1967,[38] had new life for materials synthesis breathed into it by the recognition by Kolb, Finn and Sharpless[39] that the reaction possessed exceptional qualities including rapid, high yield reactions that proceeded under ambient conditions, the potential for the thiol-yne radical reaction sequence purports to be a facile method for the rapid fabrication of new materials. Toward this end, Bowman et al. recently showed (**Scheme 8.1.**) that a tetrafunctional thiol readily polymerizes with dialkynes via a photoinduced radical step growth process identical to that for traditional thiol-enes.[40] The reaction was reported to proceed at high rates under ambient humidity and atmospheric oxygen conditions to high conversion, thereby

providing for an extremely efficient methodology for fabricating high performance networks and films. By extending this to the reaction of difunctional alkane thiols with dialkynes, which are technically tetrafunctional with respect to the addition of thiols, we have produced highly crosslinked hydrocarbon networks comprised of only carbon, hydrogen and sulfur with relatively high refractive indices. The reactions are rapid, proceed to essentially quantitative conversion and by choice of the methylene chain length separating the yne and thiol end groups, it is possible to systematically vary the sulfur content in the network and the crosslink density. Herein, it will be demonstrated that there is a linear relationship between not only the sulfur weight percent in the network and the refractive index, which can be as high as 1.66, but also the network density: note that we discuss both the network density (g/mL) and the network crosslink density as two separate items.

The synthetic approach presented herein demonstrates the ability to prepare in a rapid one step synthetic approach polymer crosslinked networks composed of only sulfur and hydrocarbon exhibiting relatively high refractive indices with commercially available starting materials. It produces no side products, has no other heteroatons than sulfur, requires no material clean up, and does not use solvents or high temperatures to process films.

<div align="center">Experimental</div>

*Materials*

All thiols and alkynes, whose structures and names are given in **Figure 8.1.**, were purchased from Aldrich Chemical Co. and used as received. The photoinitiator,

1-hydroxy-cyclohexyl-phenyl-ketone or Irgacure 184, was obtained from Ciba Specialty Chemicals.

*Kinetics*

All samples were 2:1 thiol to alkyne molar ratios, or 1:1 functional group ratios, taking the dialkyne to be tetrafunctional using 2 wt% 1-hydroxy-cyclohexyl phenyl ketone (Irgacure 184). Sample thicknesses were approximately 200 microns. Real-time FTIR was used to monitor the loss of thiol (2570 cm$^{-1}$) and yne (2120 cm$^{-1}$) functional groups. The light intensity of the high pressure mercury lamp delivered to the sample via a light pipe was ~ 20 mW/cm$^2$.

*Network Preparation for Mechanical, Thermal and Optical Property Analysis*

Samples ~1mm thickness were placed between glass plates and irradiated using a medium pressure Hg lamp (light intensity 9.25mW/cm$^2$) for 30 minutes. All samples were prepared from nominally 1:1 molar functional group ratios and allowed to remain at room temperature for at least 2 days before any measurements were made.

*Measurements and Instrumentation*

Thermal transitions were monitored by a TA Instrument DSC Q1000 DSC. All samples were heated to 150 °C for 5 minutes at 10 °C/min to erase thermal history. Samples were then cooled to -75 °C at 5 °C/min and then heated at 10 °C/min. DSC data are reported in W/g from the second heating scan. Modulus and tan delta measurements were monitored by a Rheometric Scientific DMTA V. Storage moduli (E') are reported in Pa. Refractive index measurements were recorded on a Bausch and Lomb Abbe 3L Refractometer at ~25 °C using bromo-naphthalene and an unfiltered white light source. The refractive index values are

essentially comparable to isolated 589 nm D line values. Density measurements were recorded using the XS104 Mettler Toledo micro-balance equipped with a density determination kit at ~22 °C in water.

## Results and Discussion

The four dithiols and three dialkynes in **Figure 8.1.** were used to prepare a series of networks that contain only sulfur, carbon and hydrogen. These networks, in addition to having variation in the network crosslinking density, are characterized by an increasing sulfur content. The results will first focus on a brief consideration of the polymerization profiles of the thiol-yne systems followed by an evaluation of the physical, mechanical, and optical properties of the resulting films.

### Kinetics

In the kinetic analysis, each terminal yne group is considered to be difunctional making each dialkyne tetrafunctional with respect to the radical reaction with thiol. As an example of the kinetic results that were obtained for all of the possible combinations of the dithiols and dialkynes in **Figure 8.1.**, the real-time infrared based conversions for the thiol (2570 cm$^{-1}$) and yne (2120 cm$^{-1}$) peaks for 1:1 functional group molar mixtures of ODY and HDT are shown in **Figure 8.2.a** for the first 50 seconds of exposure to the unfiltered output of the high pressure mercury lamp. The disappearance of both the thiol and yne groups is rapid under the conditions employed (200 microns and 20 mW/cm$^2$), with the percent conversion of functional groups at a given photolysis time being slightly greater for the yne than the thiol. This is reflective of the reaction of the alkyl vinyl sulfide that was formed by the initial thiol-yne reaction (**Scheme 8.1.**). According to Bowman et al.,[40] the slower

reaction is the addition of thiol to yne, i.e., the thiol-yne reaction leading to formation of the alkyl vinyl sulfide is approximately three times slower than the reaction between thiol and alkyl vinyl sulfide. The overall result is to have a low concentration of the alkyl vinyl sulfide intermediate product forming but disappearing as thiol reacts with the alkyl vinyl sulfide. For a detailed kinetic analysis of the thiol-alkyne radical step-growth process in **Scheme 8.1.**, the interested reader is referred to reference 40. The results for the EDT-ODY photopolymerization shown in **Figure 8.2.b** show a trend similar to that for the EDT-ODY photopolymerization, i.e., the yne percent conversion rate is greater than that of the thiol. Although not shown, the conversion rate for the thiol and yne components for the BDT-ODY photopolymerization is intermediate between the HDT-ODY and EDT-ODY photopolymerizations. This is consistent with the restrictions in mobility as the alkane unit length becomes shorter, resulting in a reduction in the reaction rate. Such observations have been made for thiol-ene systems where the rates have decreased modestly as the thiol and ene functionalities have increased.[2] Similar results (not shown) obtained for the other dithiol-dialkyne combinations exhibit the same trends with respect to thiol-alkyne conversions, i.e., lower rates for the EDT systems compared to the HDT systems under the same exposure conditions.

Summarizing, rapid rates and conversions approaching 100% of each functional group are achieved under the relatively mild photolysis under ambient conditions used for the real time IR measurements. Actually, real-time IR based conversions for all combinations in **Figure 8.2.** for several minutes, have been recorded and all achieve essentially 100% conversions within our ability to record IR peaks at the high conversions. As shown in **Table 8.1.**, the weight percent of sulfur,

calculated from the weight of the individual thiol and ene components, in the network approaches 46 % in the case of the photopolymerized $H_{pt}DY$ and EDT system. Questions dealing with the mechanical and thermal properties and relationship between the refractive index of the polymerized network and the sulfur content will be evaluated next.

*Thermal and Dynamic Mechanical Analysis*

Having demonstrated that the thiol and alkyne components in the 1:1 thiol-alkyne molar functional group mixtures are effectively photopolymerized to high conversion, DSC scans and DMA storage modulus and tan δ plots for all nine of the thiol-alkyne networks are given in **Figures 8.3., 8.4.,** and **8.5**. To ensure high conversion of all samples, as we have already mentioned in the previous section and as detailed in the Experimental, samples were exposed to high light intensities and doses. Consider first the DSC scans. In each case for a given dialkyne, the resulting network glass transition temperature increases as the dithiol molecular weight decreases. This is consistent with an expected increase in the glass transition temperature with an increase in network crosslink density. The DSC glass transition temperatures from **Figure 8.2.** recorded in **Table 8.1.** extend from -15 °C to 14 °C depending on the particular dithiol-dialkyne combination used to prepare the network. It is noted that the samples prepared from EDT have consistently greater DSC or DMA glass transition values than the samples prepared from BDT and HDT since the number of methylene spacer groups doubles and triples on going from EDT to BDT to HDT. One particularly important point about all of the networks is the rather narrow range for the glass transition region, which is typical of thiol-ene networks.[2,4] The supposition that the dithiol-dialkyne networks are uniform is confirmed by the

DMA results in **Figures 8.4.** and **8.5.** where the storage modulus, E', and the tan δ energy damping exhibit narrow temperature transitions. The transitions in **Figures 8.4.** and **8.5.**, as quantified by the FWHM values of the tan δ versus temperature plots in **Figure 8.4.** listed in **Table 8.1.**, are clearly very narrow compared to FWHM values for photopolymerized multifunctional (meth)acrylate transitions which can be up to 200 °C.[2] This indicates that the dithiol-dialkyne networks are relatively uniform. However, the FWHM values for thiol-yne reactions (**Table 8.1.**) are ~20-25 °C while the thiol-ene networks evaluated under the same conditions are typically near 10 °C.[2, 4] The kinetics of the sequential polymerization process no doubt effects the formation of cyclic rings which form. Specifically, it has been reported that the formation of cyclic rings in thiol-ene polymerization results from the intramolecular addition of thiyl radicals to ene double bonds on the same oligomeric molecule.[41] The resulting ring structures vary in size, and hence their distribution influences the mechanical properties of the thiol-ene network. Accordingly, the ring structure size distribution in thiol-yne networks might be expected to be different from that of traditional thiol-enes due to the two sequential regiospecific reactions, yielding two non-identical sulfide linkages, that comprises the overall thiol-yne reaction process.[34]

*Density and Refractive Index*

Two important physical and optical properties associated with the dithiol-dialkyne networks, density and refractive index, were measured. The results in **Table 8.1.** clearly show that the dithiol-dialkyne networks have high refractive index values spanning a 0.08 range from approximately 1.58 to 1.66. These very high refractive indices are the direct result of incorporating sulfur into the hydrocarbon network in the form of sulfide linkages as seen by comparing the refractive index values with the

percentage of sulfur in the network (the last column in **Table 8.1.**). Concomitantly, as shown in **Table 8.1.**, the densities of the networks also increase with sulfur content. The plots in **Figures 8.6.** and **8.7.** show that both the refractive index and the density increase linearly with the sulfur content. This is certainly expected from the high atomic refraction and density inherent to sulfur. **Figure 8.8.** shows structures and acronyms of several traditional thiol and ene components used to form thiol-ene networks for comparison with the dithiol-dialkyne networks in **Table 8.1.** The densities and refractive index values for the photopolymerized thiol-ene networks produced from the components in **Figure 8.8.** are given in **Table 8.2.** A comparison of refractive index for the thiol-ene networks and thiol-yne networks cannot be made based strictly on sulfur content, since the thiol-ene systems have other heteroatoms present including oxygen and nitrogen. Nonetheless, it is important to show that the refractive index values of the dithiol-dialkyne networks are much higher than for the traditional thiol-ene networks. Of course, both the thiol-ene and thiol-yne networks have high densities due to the high crosslink density which results from the step-growth nature of the thiol-ene and thiol-yne reactions. The refractive index values for these thiol-ene systems, where there are other heteroatoms present (oxygen and nitrogen) but the sulfur contents are relatively small, exhibit lower refractive index values than for any of the thiol-yne based networks due to the latter's high sulfur content. The refractive index is obviously influenced heavily by the percent sulfur in the network. Note that even the 4T-TTT based network with the highest network density only has a refractive index of ~1.56.

Finally, in order to delineate the effect of crosslink density versus sulfur content on all of the parameters including thermal/mechanical transitions, density and

refractive index, films were made using the dithiol TEDT (see **Figure 8.1.**) and H$_{pt}$DY. This network is particularly interesting since the molecular weight of the linking chain between the two terminal thiols is greater than for EDT and approximately equivalent to that for HDT. The result is a decrease in the crosslink density of the network film compared to the EDT-H$_{pt}$DY film with corresponding decrease in the glass transitions measured by both DSC and DMA (see **Table 8.1.**). Nonetheless, both the density and the refractive index increase with the percent increase in sulfur obtained when TEDT is used. Importantly, both the refractive index and density for the TEDT-H$_{pt}$DY network in **Figures 8.6.** and **8.7.** clearly fit on the linear plots versus sulfur weight percent for the other dithiol-dialkyne networks, in agreement with the well known high atomic refraction and density of sulfur.

## Summary and Conclusions

Ten hydrocarbon networks with sulfur linking groups were made by a rapid step-growth radical photopolymerization process. According to narrow thermal and mechanical transitions obtained by DSC and DMA analysis, the network structures were very uniform. However, the FWHM values for tan δ versus temperature plots are somewhat greater than for thiol-ene networks. High weight percentages of sulfide linkages approaching 50% were incorporated into the network. It was found that both the refractive index and the density are linearly proportional to the sulfur content in the network. The results presented herein demonstrate that high concentrations of sulfur can be incorporated into highly uniform hydrocarbon thermoset networks by a rapid photopolymerization process under ambient conditions. This demonstrates the importance of the two regioselective *thiol-yne* reactions as a useful reaction bearing

many of the characteristics of, and providing an interesting correlation between the *thiol*-ene[20-27] and alk*yne*-azide[38,39] type reactions.

## Acknowledgments

References

1. Jacobine, A. F. In *Radiation Curing in Polymer Science and Technology III, Polymerisation Mechanisms*, Fouassier, J. D., Rabek, J. F., Eds.; Elsevier Applied Science: London, **1993**; Vol. 3, p. 219.

2. Hoyle, C. E.; Lee, T. Y.; Roper, T. *J. Polym. Sci., Part A: Polym. Chem.* **2004**, *42*, 5301.

3. Reddy, S. K.; Cramer, N. B.; Kalvaitas, M.; Lee, T.; Bowman, C. N. *Aust. J. Chem.* **2006**, *59*, 586.

4. Senyurt, A. F.; Wei, H.; Hoyle, C. E.; Piland, S. G.; Gould, T. E. *Macromolecules* **2007**, *40*, 4901.

5. Bowman, C. N.; Carioscia, J.; Lu, H,; Stansbury, J. W. PCT Int. Appl., 2005, 34 pp.

6. Carioscia, J. A.; Lu, H.; Stansbury, J. W.; Bowman, C. N. *Dent. Mater.* **2005**, *21*, 1137.

7. Reddy, S. K.; Cramer, N. B.; Bowman, C. N., *Macromolecules* **2006**, *39*, 3681.

8. Wei, H. Y.; Li, Q.; Ojelade, M.; Madbouly, S.; Otaigbe, J. U.; Hoyle, C. E. *Macromolecules* **2007**, *40*, 8788.

9. Cook, W. D.; Chausson, S.; Chen, F.; Le Pluart, L.; Bowman, C. N.; Scott, T. F. *Polym. Int.* **2008**, *57*, 469.

10. Johnson, P. M.; Stansbury, J. W.; Bowman, C. N. *J. Polym. Sci., Part A: Polym. Chem.* **2008**, *46*, 1502.

11. Nilsson, C.; Simpson, N.; Malkoch, M.; Johansson, M.; Malmstrom, E. *J. Polym. Sci., Part A: Polym. Chem.* **2008**, *46*, 1339. .

12. White, T. J.; Natarajan, L. V.; Tondiglia, V. P.; Lloyd, P. F.; Bunning, T. J.; Guymon, C. A. *Polymer* **2007**, *48*, 5979.

13. Senyurt, A. F.; Hoyle, C. E.; Wei, H. Y.; Piland S. G.; Gould, T. E. *Macromolecules* **2007**, *40*, 3174.

14. Carioscia, J. A.; Stansbury, J. W.; Bowman, C. N. *Polymer* **2007**, *48*, 1526.

15. Wei, H. Y.; Senyurt, A. F.; Jonsson, S.; Hoyle, C. E. *Macromolecules* **2007**, 822.

16. Sangermano, M.; Gross, S.; Priola, A.; Rizza, G.; Sada, C. *Macromol. Chem. Phys.* **2007**, *208*, 2560.

17. Carioscia, J. A.; Schneidewind, L.; O'Brien, C.; Ely, R.; Feeser, C.; Cramer, N.; Bowman, C. N. *J. Polym. Sci., Part A: Polym. Chem.* **2007**, *45*, 5686.

18. Cook, W. D.; Chen, F.; Pattison, D. W.; Hopson, P.; Beaujon, M. *Polym. Int.* **2007**, *56*, 1572.

19. Ortiz, R. A.; Urbina, B. A. P.; Valdez, L. V. C.; Duarte, L. B.; Santos, R. G.; Valdez, A. E. G.; Soucek, M. D. *J. Polym. Sci., Part A: Polym. Chem.* **2007**, *45*, 4829.

20. Killops, K.L.; Campos, L.M.; Hawker, C.J. *J. Am. Chem. Soc.* **2008**, *13*, 5062.

21. Campos, L. M.; Killops, K. L.; Sakai, R.; Paulusse, J. M. J.; Damiron, D.; Drockenmuller, E.; Messmore, B. W.; Hawker, C. J. *Macromolecules* **2008**, *41*, 7063.

22. Voets, I.K.; de Keizer, A.; Stuart, M.A.C.; Justynska, J.; Schlaad, H.; *Macromolecules* **2007**, *40*, 2158.

23. Lutz, J. F.; Schlaad, H. *Polymer* **2008**, *49*, 817.

24. Gress, A.; Volkel, A.; Schlaad, H. *Macromolecules* **2007**, *40*, 7928.

25. Hordyjewicz-Baran, Z.; You, L. C.; Smarsly, B.; Sigel, R.; Schlaad, H. *Macromolecules* **2007**, *40*, 3901.

26. Brummelhuis, N.; Diehl, C.; Schlaad, H. *Macromolecules* **2008**, *41*, 9946.

27. Dondoni, A. *Angew. Chem. Int. Ed.* **2008**, *47*, 8995.

28. Roper, T. M.; Guymon, C. A.; Jonsson, E. S.; Hoyle, C. E. *J. Polym. Sci., Part A: Polym. Chem.* **2004**, *42*, 6283.

29. Matsuda, T.; Funae, Y.; Yoshida, M.; Yamamoto, T.; Takaya, T. *J. Appl. Polym. Sci.* **2000**, *76*, 45.

30. Okutsu, R.; Ando, S.; Ueda, M. *Chem. Mater.* **2008**, *20*, 4017.

31. Okutsu, R.; Suzuki, Y.; Ando, S.; Ueda, M. *Macromolecules* **2008**, *41*, 6165.

32. Berti, C.; Pilati, F.; Manaresi, P.; Guaita, M.; Chiantore, O. *Polymer* **1994**, *35*, 1564.

33. Matsumoto K., Costner, E.A.; Nishimura, I.; Ueda, M.; Willson, C.G. *Macromolecules* **2008**, *41*, 5674.

34. Blomquist, A. T.; Wolinsky, J. *J. Org. Chem.* **1958**, *23*, 551.

35. Griesbaum *Angew. Chem. Internat. Edit.* **1965**, *9*, 273.

36. Behringer, H. *Annalen* **1949**, *564*, 219.

37. Posner, T. *Ber. Chem. Ges.* **1905**, *38*, 646.

38. Huisgen, R.; Szeimes, G.; Mobius, L. *Chem. Ber.* **1967**, *100*, 2494.

39. Kolb, H. C.; Finn, M. G.; Sharpless, K. B. *Angew. Chem. Int. Ed.* **2001**, *40*, 2004.

40. Fairbanks, B. D.; Scott, T. F.; Kloxin, C. J.; Anseth, K. S.; Bowman, C. N. *Macromolecules* **2008**, *42*, 211.

41. Okay, O.; Bowman, C. N. *Macromol. Theory Simul.* **2005**, *14*, 267.
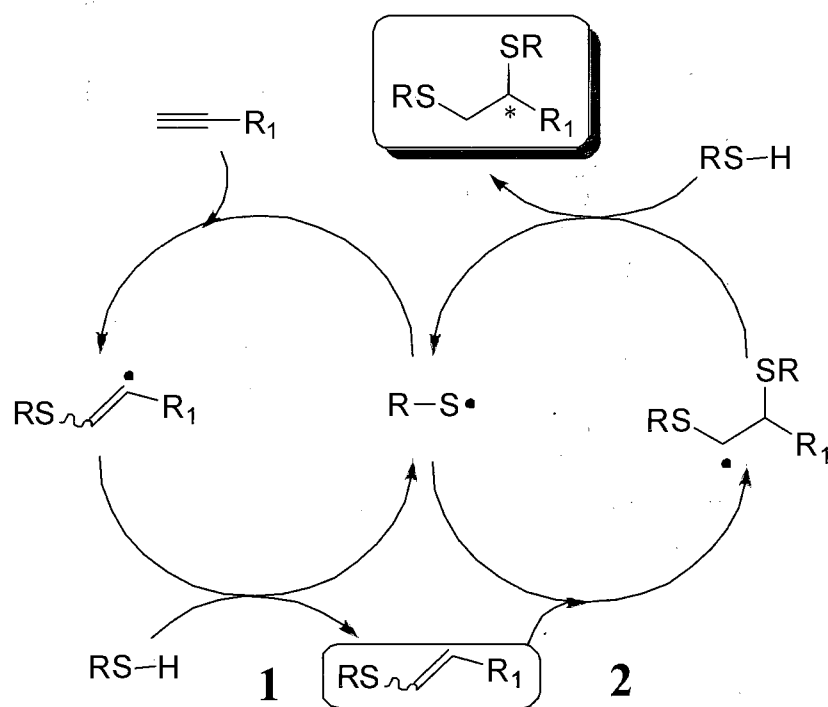
**Scheme 8.1.** Proposed thiol-yne chain reaction mechanism

**Table 8.1.** Physical and optical data for thiol-alkyne networks

| Dithiol | Diyne | Density (g/mL) | RI | DSC $T_g$ (°C) | DMA $T_g$ (°C) | DMA FWHM (°C) | Wt% S |
|---------|-------|----------------|-----|----------------|----------------|----------------|-------|
| TEDT | $H_{pt}DY$ | 1.280 | 1.6575 | -14 | 16 | 15 | 48.00 |
| EDT | $H_{pt}DY$ | 1.250 | 1.6540 | 14 | 38 | 21 | 45.72 |
| | ODY | 1.210 | 1.6381 | 9 | 33 | 19 | 43.54 |
| | NDY | 1.202 | 1.6265 | 9 | 30 | 21 | 41.56 |
| BDT | $H_{pt}DY$ | 1.172 | 1.6081 | -5 | 15 | 21 | 38.1 |
| | ODY | 1.147 | 1.6024 | -4 | 20 | 24 | 36.57 |
| | NDY | 1.139 | 1.5995 | -5 | 22 | 20 | 35.17 |
| HDT | $H_{pt}DY$ | 1.105 | 1.5820 | -15 | 5 | 23 | 32.66 |
| | ODY | 1.096 | 1.5792 | -11 | 5 | 20 | 31.53 |
| | NDY | 1.089 | 1.5755 | -10 | 10 | 19 | 30.48 |

**Table 8.2.** Refractive index (RI) values and densities of several thiol-ene networks

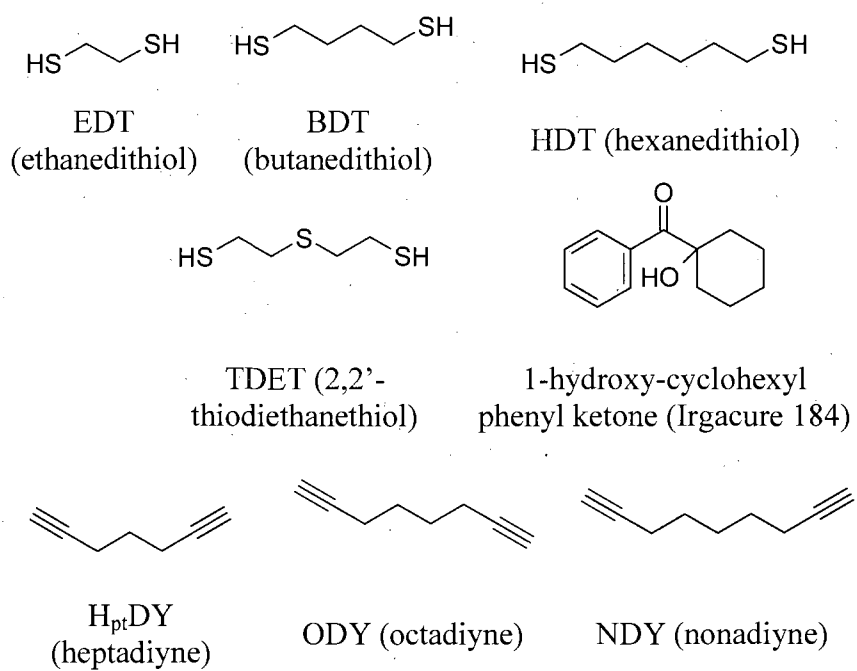| | Ene | Density (g/mL) | RI | wt% S |
|----|------|------|------|------|
| 4T | APE | 1.261 | 1.5350 | 15.44 |
| | TEGDVE | 1.252 | 1.5215 | 14.36 |
| | TTT | 1.382 | 1.5622 | 15.62 |

**Figure 8.1.** Structures and acronyms for alkyl dithiols and dialkynes.
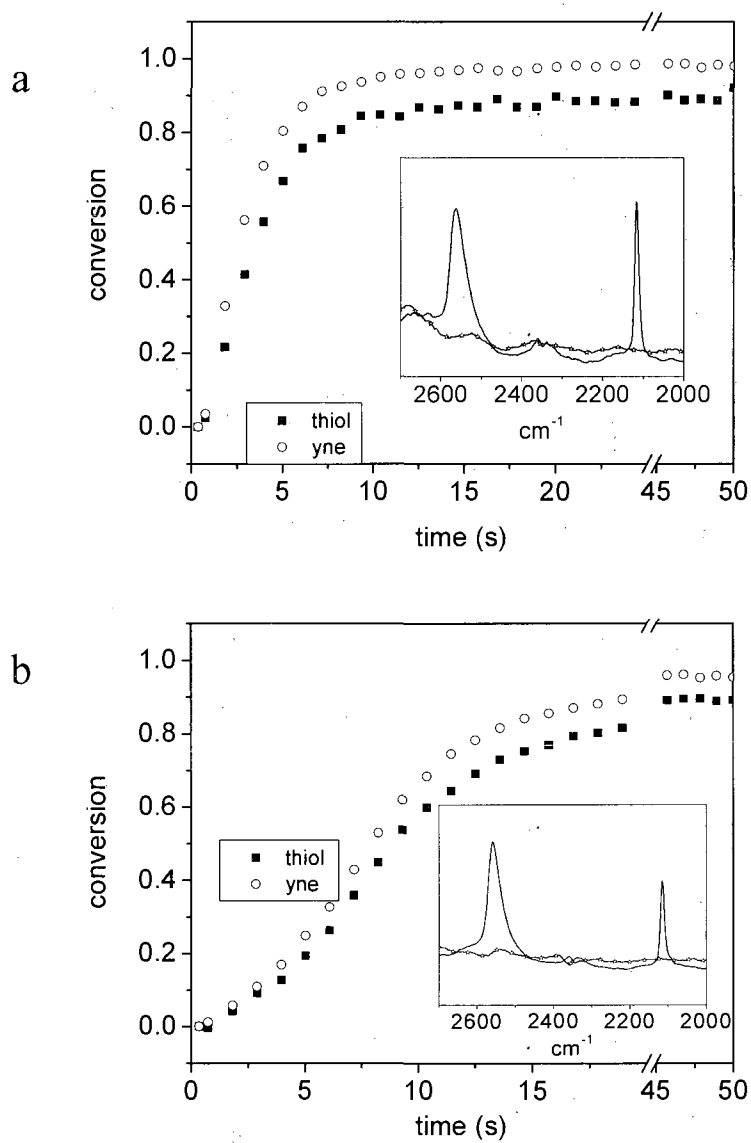
**Figure 8.2.** RT-FTIR based percent conversion time plots for 2:1 molar ratios of thiol:alkyne reactive groups for (a) hexanedithiol-octadiyne and (b) ethanedithiol-octadiyne.
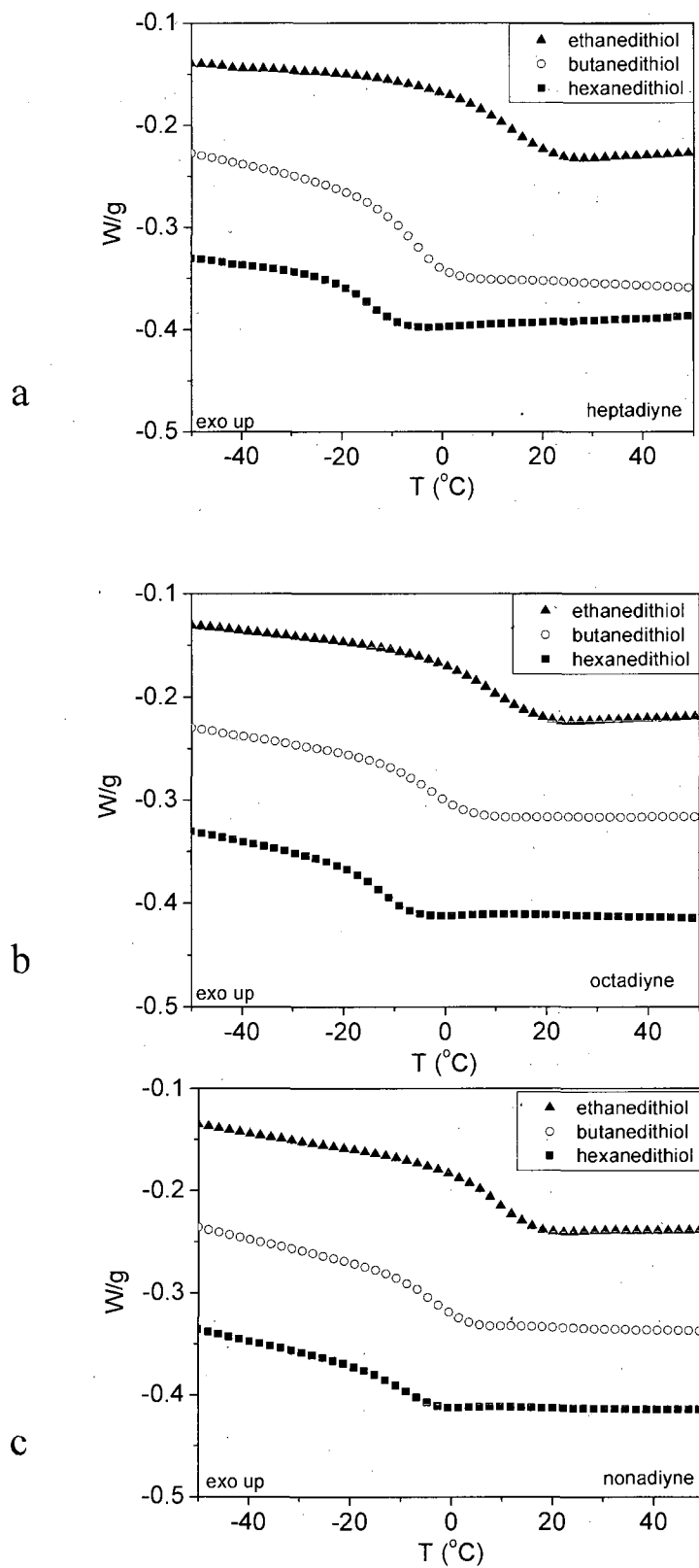
**Figure 8.3.** DSC scans for photopolymerized networks formed from 2:1 thiol:alkyne mixtures: (a) heptadiyne-dithiol, (b) octadiyne-dithiol, and (c) nonadiyne-dithiol.

**Figure 8.4.** DMA tan δ plots for photopolymerized networks formed from 2:1 thiol:alkyne mixtures: (a) heptadiyne-dithiol, (b) octadiyne-dithiol, and (c) nonadiyne-dithiol.

**Figure 8.5.** DMA E' plots for photopolymerized networks formed from 2:1 thiol:alkyne mixtures:   (a) heptadiyne-dithiol, (b) octadiyne-dithiol, and (c) nonadiyne-dithiol.
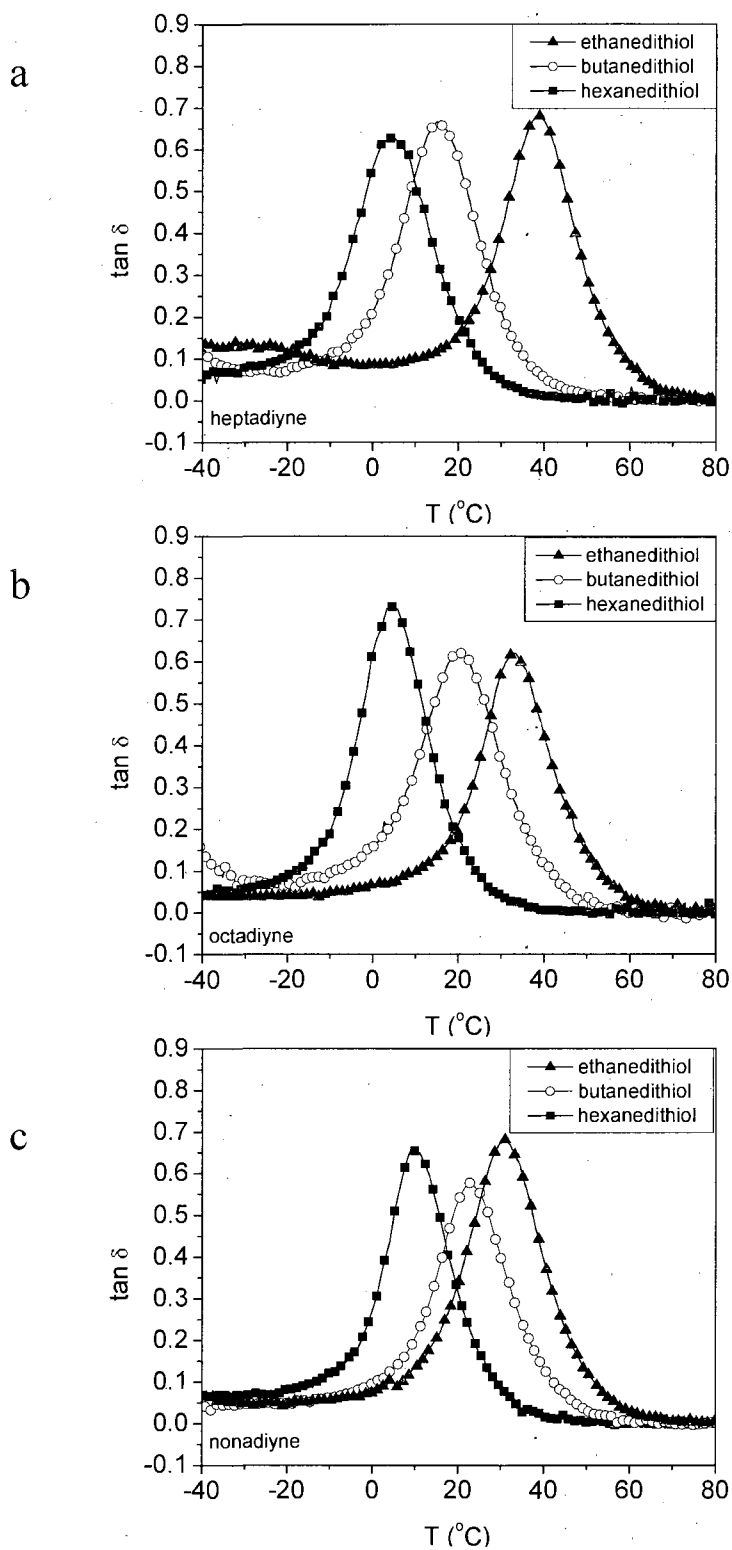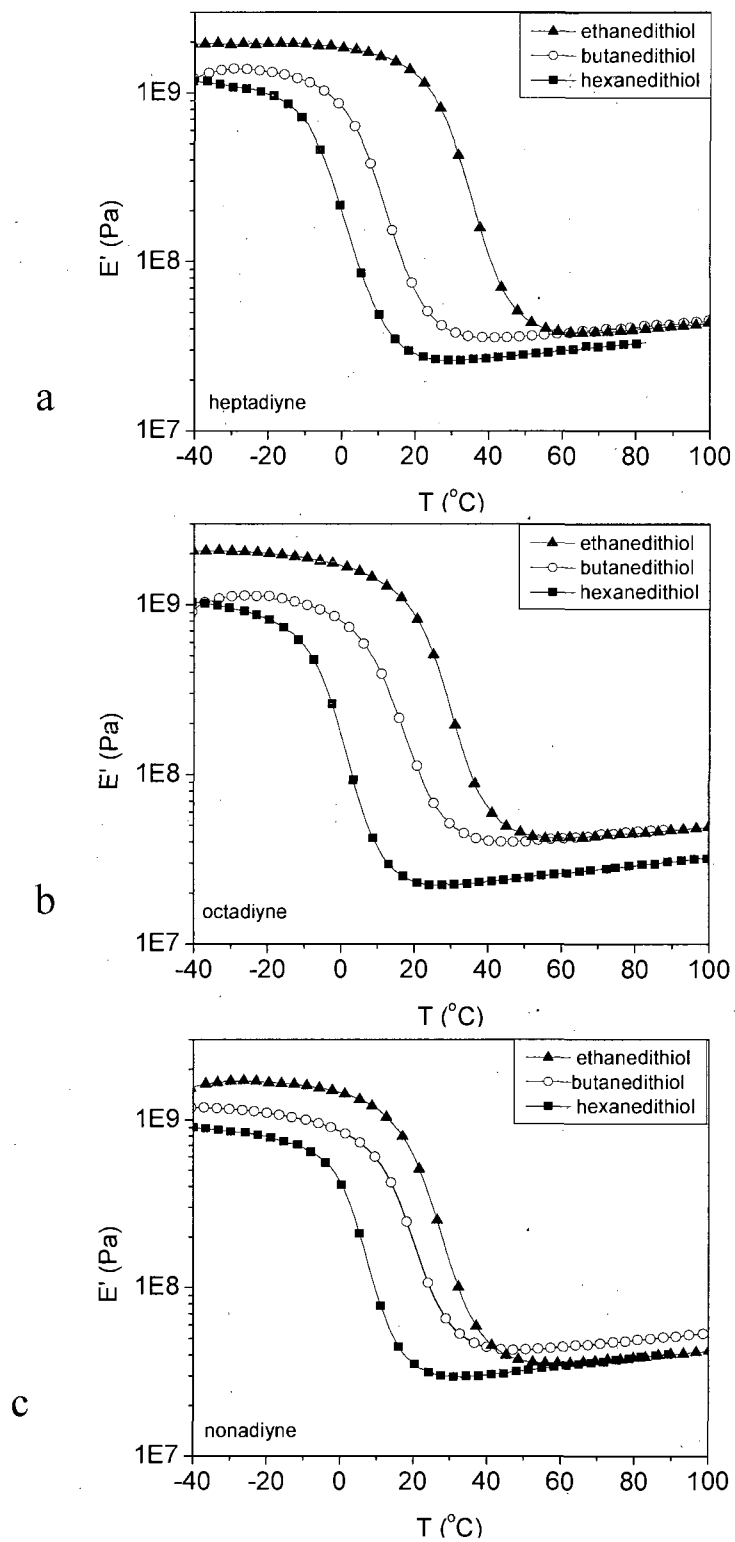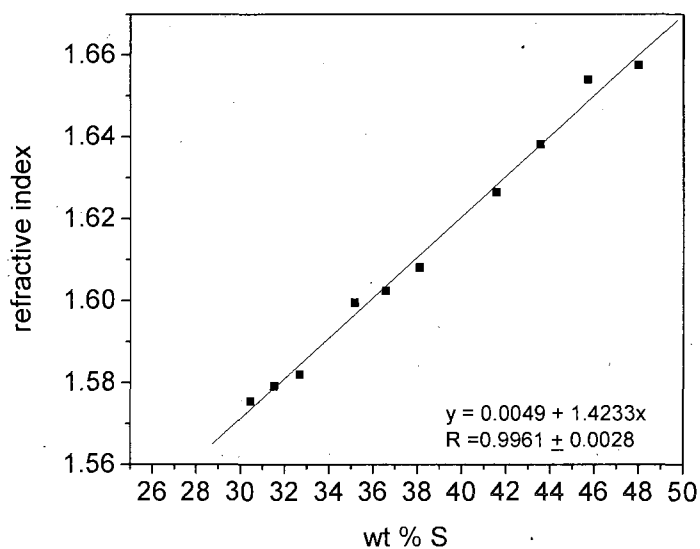
**Figure 8.6.** Refractive index verus weight percent sulfur plots for photopolymerized networks formed from 2:1 thiol:alkyne mixtures.
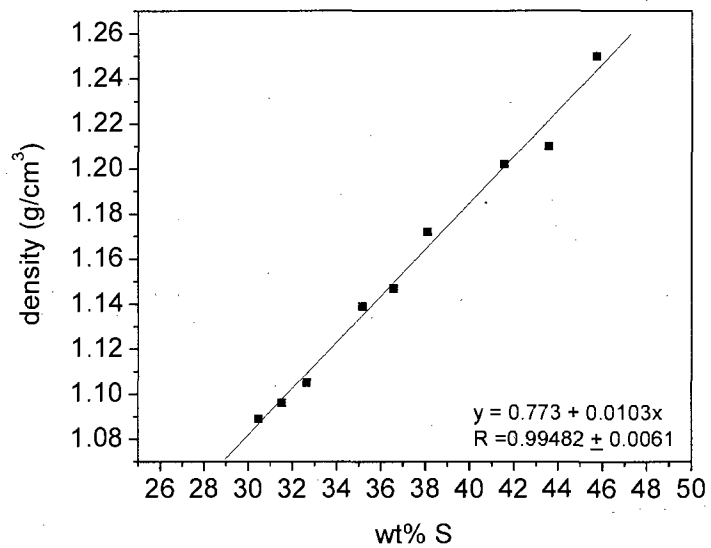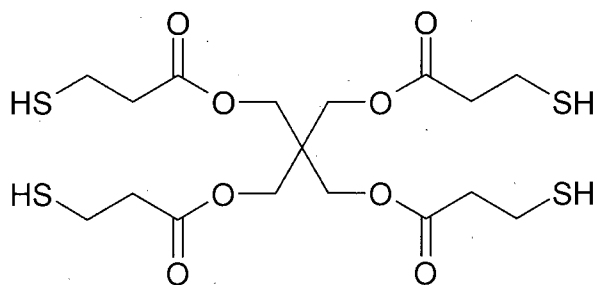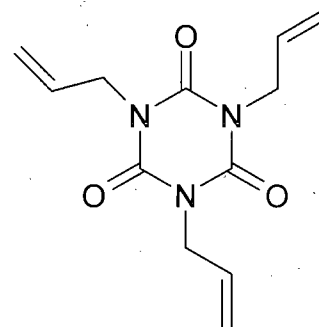
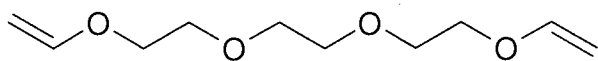**Figure 8.7.** Density versus weight percent sulfur for photopolymerized networks formed from 2:1 thiol:alkyne mixtures.
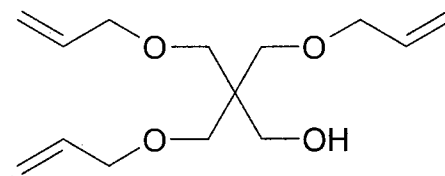
4T (Pentaerithrytol tetrakis(3-mercaptopropionate))

TTT (Triallyl triazine)

TEGDVE (Triethyleneglycol divinyl ether)

APE (Allyl pentaerithrytol allylether)

**Figure 8.8.** Structures and acronyms for tetrathiol and multialkenes.

# CHAPTER IX

## CONCLUSIONS AND RECOMMENDATIONS

The research presented in this dissertation discusses the mechanism and utility of the nucleophile catalyzed thio-Michael addition reaction as a novel thiol-ene click reaction and applications of the thio-alkyne photopolymerization reaction. The conclusions of each study are overviewed within the following paragraphs.

The mechanism of the nucleophile catalyzed thio-Michael addition reaction has been investigated and determined to differ from the traditionally accepted base catalyzed reaction, which requires longer reaction times and high catalyst concentrations to produce high conversions. The use of primary amines or tertiary phosphines, which are both superior nucleophiles in comparison to tertiary amines, significantly increases the apparent rates of reaction of several thio-Michael addition reactions and produces near quantitative conversion at low catalyst concentrations within minute(s). Tertiary phosphines, which are classified as poor Brønsted bases, show exceptional rates of hydrothiolation to electron deficient alkenes by initially activating an acrylate to produce an enolate anion, which is a very strong Brønsted base. The enolate anion is responsible for initiating an anionic chain mechanism, whereby the initiating enolate species abstracts a proton from a thiol, which forms a thiolate anion. In the propagation step, the thiolate anion then attacks the double bond of another acrylate substrate, which then forms another enolate anion of the acrylate substrate. This reaction continues until all thiol has reacted. Spectroscopic evaluation has determined that no side product formed in the systems described in this investigation. The overall rate of reaction is dependant on the

nucleophilicity and concentration of the catalyst, $pK_a$ and nucleophilicity of the thiol, and steric hindrance and electron density of the electron poor substrate.

The nucleophile catalyzed thio-Michael addition reaction in combination with the photo induced acrylate homopolymerization reaction was used to prepare crosslinked networks. The photopolymerization of multi-acrylates produces films of highly crosslinked, relatively inhomogeneous networks characterized by high, broad $T_g$ values indicated by DMTA tan δ measurements. Films with increasing concentration of thiol (0, 20, 30, 40, and 50 mol%) were formulated to prepare networks using two different methods: (1) first, the nucleophile catalyzed thio-Michael addition reaction was used to pre-react all thiol groups, followed by the photo-initiated curing to hompolymerize any of the remaining acrylate groups and (2) photo-cure only of the same formulations. In method 1, pre-reacting all of the thiol groups by the nucleophile catalyzed thio-Michael addition reaction converted all thiol groups and increased the amount of unreacted mol % acrylate as the amount of mol % thiol in each formulation decreased. In method 2, each system studied showed an increasing amount of unreacted mol% thiol as the mol% increased in the initial formulations. Additionally in method 2, a significant amount of acrylate remained unreacted. A minimum mol% of total unreacted groups (thiol and acrylate) was determined to be ~90% in the 30:70 mol% thiol:acrylate photo-cured only system. $T_g$ values determined by DSC and DMTA decreased in all systems as the feed of thiol increased. FWHM of tan δ values by DMTA broaden in a given formulation when using method 2, in comparison to method 1, indicating that networks were produced with a higher degree of inhomogeneity by not pre-reacting the thiol.

Star polymers were prepared by the nucleophile catalyzed thio-Michael addition reaction of polymers prepared by RAFT to a tri-acrylate core. RAFT polymerization utilizes chain transfer agents (CTA), such as dithioesters, which are easily reduced to thiol and disulfide groups by using simple reducing agents following polymerization. Dimethylphenylphosphine served a dual purpose: (1) to catalyze the addition of the terminal thiol to the tri-acrylate core and (2) to inhibit the formation of disulfide formation commonly seen in the reduction step of RAFT polymers. Quantitative conversion of acrylate was verified with spectroscopy. GPC and MALDI-TOF were used to confirm near quantitative conversion for the formation of 3-arm star polymers.

Using the nucleophile catalyzed thio-Michael addition reaction, tetra-functional alkynes were prepared by the conjugate addition of propargyl acrylate to a tetra-functional thiol. Subsequently, the radical mediated thiol-alkyne reaction was used to covalently attach various thiol containing molecules in a 2:1 ratio of thiol to alkyne. The reaction proceeded quantitatively, in the absence of solvent, rapidly, and with no side products. The efficiency of this reaction was confirmed by NMR, RTIR, and MALDI-TOF MS. This study showed the utility of the thiol-alkyne reaction for the preparation of monodisperse polyfunctional material (up to 16 functional groups) in a two step method without stringent purification or isolation steps for the first time.

Di-, tri-, and tetra-functional alkynes were prepared through the nucleophile catalyzed Michael addition reaction and photopolymerized with di-, tri-, and tetra-functional thiols to prepare a series (9) of networks. Increasing the functionality of the starting materials increased the $T_g$ and rubbery modulus of the resulting crosslinked materials. It was previously determined that monomer functionality, when greater than 4,

did not obey Flory's gel point theory; however, because of the unique thiol-yne reaction, it was determined that thiol-yne systems containing monomers with functionalities greater than 4 obey gel point theory; kinetic profiles indicate that as the monomer functionality increases, the gel point decreases and as monomer functionality increases, modulus and $T_g$ increase. This study demonstrated the utility of both the nucleophile catalyzed thio-Michael addition reaction and the radical mediated thiol-yne reaction for the tailoring of network materials. Additionally, this work highlights the high-throughput nature of thiol-ene chemistry as a facile, simple method of preparing libraries of compounds for rapid determination of structure property relationships.

The radical mediated thiol-yne reaction was utilized to determine the effects of sulfur composition on refractive index. It is well known that due to the high polarizability and atomic density of sulfur, materials containing high amounts of sulfur have high refractive index values. A series (10) of networks were prepared composed of hydrocarbon and sulfur via the radical mediated reaction of dialkynes and alkyl dithiols. These networks were designed to increase the wt% of sulfur by decreasing the hydrocarbon length between crosslinks. As the amount of sulfur to hydrocarbon increased, the refractive index of the resulting network increased. Additionally, network crosslink density was determined to not affect refractive index as greatly as overall sulfur content.

The research reported in this dissertation describes some novel applications of the nucleophile catalyzed thio-Michael addition reaction and the radical mediated thiol-yne reaction as sister reactions to the more common radical mediated thiol-ene as an effective

method of material synthesis and modification. Several suggestions for future work will be made in the following paragraphs.

During these investigations, there are decreased kinetic profiles and lower conversions in radical mediated thiol-ene systems containing amines (primary, secondary, or tertiary). Because of the difference in $pK_a$ values, it has been hypothesized that some thiols and amines form ionic pairs, which reduces the formation of the thiyl radical. Additionally, it is well understood that small amounts of acids are added to multifunctional thiol monomers for added stability. For future work, investigations can be designed to determine the effects of pH on the radical thiol-ene reaction or on systems containing moieties with high $pK_a$ values. It would be interesting to design systems that triggered the thiol-ene or thio-Michael reactions based on pH change.

Thiols have been well investigated in click type reactions with disulfides, electron rich and electron poor enes, nucleophilic substitution reactions with halides, and isocyanates. Fewer investigations have been made that focus on the reaction of thiols with three member cyclic monomers such as oxiranes, thiiranes, aziridines, and other cyclic monomers containing esters, amides, and anhydrides. Thiolate anions, such as those produced in the nucleophile catalyzed thio-Michael addition reaction, have great potential as strong nucleophiles that could easily undergo ring opening reactions in organic synthesis, polymerizations, or materials modification. Additionally, the reaction of thiols with isothiocyanates in the presence of a weak base shows evidence of rapid quantitative conversion without side product formation. Uniquely, the reaction product – dithiocarbamate - is susceptible to attack by other nucleophiles, such as simple primary amines. The attack by a primary amine results in the formation of the initial thiol and a

thiourea group. The subsequently formed- or recycled - thiol groups can react in another unique reaction.

Tailoring the $T_g$ of thiol-ene materials is one of the salient features of this highly efficient chemistry. In this dissertation, we have demonstrated that increasing the amount of acrylate homopolymerization increases the $T_g$ and that increasing the crosslink density in the thiol-yne networks also increases the $T_g$ in thiol-ene systems. Future studies to investigate the effect of thiol-yne/acrylate ternary systems would be of interest for producing materials with higher $T_g$ than thiol-yne systems while increasing the homogeneity of multi-acrylate systems.

The nucleophile catalyzed thio-Michael addition reaction and the radical mediated thiol-yne reactions have shown potential as comparable and complementary reactions to the typical radical mediated thiol-ene click reaction.